ROLE OF ELECTRICAL AND MIXED SYNAPSES IN THE MODULATION OF SPINAL CORD SENSORY REFLEXES

by

Wendy Diana Bautista Guzman

A Thesis submitted to the Faculty of Graduate Studies of

The University of Manitoba

in partial fulfillment of the Requirements for the degree of

Doctor of Philosophy

Department of Physiology

Univerisity of Manitoba

Winnipeg

Acknowledgements

I would like to acknowledge my mentor Dr. Dave McCrea for bringing me to Winnipeg, and giving me the opportunity to work in his lab, together we faced great challenges working in new ideas and new preparations. Overcoming these challenges had allowed me to learn and give the best of me every day. Thanks to his excellent guidance as a mentor and as a person I was able to complete this thesis until the end.

I also thank Dr. James Nagy for his mentorship and guidance throughout the thesis work,these five years working together was a great experience for me, I really enjoyed doing experiments in his lab. I thank him for all his time and effort spent on guiding me, his discussions always provided me with great insight.

I will always be in doubt with both my mentors for inspiring me and allowing me to learn the best of them.
I thank the supervising committee Dr. Brian Schmidt, Dr. Brian McNeil and Dr. Larry Jordan for their valuable suggestions on this thesis.

I dedicate this thesis to my husband Victor for his unconditional love and support in this journey, to my parents Eduardo and Lourdes for their love and moral support that had kept me motivated and inspired.

I also would like to thank to my friends Dolly Chisick, Ernie Chisick, Sam Minuk, Darlene and Peter Morgan for their great friendship and support along this journey.

I thank to the funding agency MHRC for providing me with a PhD scholarship.

Abstract

The first part of my thesis involves an investigation into mechanisms underlying the presynaptic regulation of transmitter release from myelinated hindlimb sensory afferents in rodents.

The central hypothesis is that in addition to chemical transmission in spinal neuronal networks, electrical synapses formed by connexins are critically involved in presynaptic inhibition of large diameter sensory afferents.

Subsequent sections of the thesis present a detailed examination of the distribution of connexins in the rodent spinal cord with a particular emphasis on the neuronal connexin, Cx36.

Connexin36 (Cx36) is widely believed to be the protein forming the neuronal gap junctions that create electrical synapses between mammalian neurons in many areas of the central nervous system (Condorelli et al 1998). The first part of thesis concerns a previously unknown role of neuronal connexins in interneurone pathways involved in presynaptic control of synaptic transmission in the lumbar spinal cord of rodents. As far as we are aware, the idea that electrical contacts between spinal neurones contribute to spinal presynaptic inhibition is a novel hypothesis. Evidence will be presented: 1) that Cx36 is present in regions of the spinal cord containing interneurones involved in presynaptic inhibition, 2) that the lack of Cx36 in Cx36-/- knockouts mice results in a severe impairment of presynaptic inhibition, and 3) that blocking gap junctions pharmacologically in wild type mice impairs presynaptic inhibition.

The exploration of this hypothesis will involve a combination of electrophysiological and immunohistochemical approaches in juvenile wild-type and knockout mice lacking Cx36, as well as immunohistochemical observations in adult rodents. This first section of the thesis begins with the development of a preparation in which several measures of presynaptic inhibition described in the *in vivo* adult cat preparation can be examined *in vitro* in young mice.

The following sections of the thesis describe the distribution and features of Cx36 on neurones in mice and rats of different ages in four parts. The first will show that Cx36 is the only connexin associated with spinal neurons and refutes claims in the literature about the existence of a variety of connexions on spinal neurons. The second part will show that while gap junctions between some spinal neurons are only a transient developmental phenomenon, they persist in abundance in adult animals. The third part will present evidence of a previously unsuspected

association of Cx36 gap junctions at the chemical synapse between muscle afferent fibres and motoneurones. Specifically, an association between Cx36 and the glutamate transporter used in primary afferents, Vglut1 will be described. To our knowledge these results are the first to suggest the existence of mixed (electrical and chemical) synapses between primary afferents and motoneurones in the mature mammalian spinal cord. The final part of the thesis will describe the presence of Cx36 gap junctions on adult sacral motoneurones involved in control of sexual, urinary and defecation functions in the rodent.

TABLE OF CONTENTS

List of figures

General introduction

Section 1

Section 2

Section 3

List of abbreviations

BAC	Bacterial artificial chromosome
CDP	Cord Dorsum Potential
Cx36	Connnexin 36
Cx32	Connnexin 32
Cx26	Connnexin 26
Cx43	Connnexin 43
Cx45	Connnexin 45
Chat	Acetylcholine transferase
DRP	Dorsal root potential
EGFP	Enhanced green fluorescence protein
GAD65	Glutamic acid decarboxylase isoform 65
KO	knockout
Mo5	Trigeminal motor nuclei
MSR	Monosynaptic reflex
PAD	Primary afferent depolarization
Vglut-1	Vesicular transporter 1
Vglut-2	Vesicular transporter 2
Wt	wild-type

General Introduction

The continuous processing of information from sensory receptors in the limbs is an essential component in the generation of movements. Although many levels of the CNS process this sensory information, the first and often primary site is in the spinal cord where activity from a wide variety of skin, joint and muscle receptors converges onto individual spinal cord interneurones. These first order neurones called dorsal root ganglia neurones contact second order neurones in the spinal cord and (i.e. those contacted by primary afferents) often receive sensory input from several limb regions and from several receptor types (for a general summary see Jankowska, 1991). These second order neurones are the initial stages for decoding activity of peripheral receptors into modalities such as muscle length, tension and skin deformation. The integrative and electrical properties of first order neurones can filter, amplify and gate sensory transmission before relaying the information to other spinal and supraspinal neurones. First, second and higher order neurones generate spinal reflexes and shape descending voluntary motor commands during movement. While most spinal reflexes involve at least one interneurone between the sensory afferents and motoneurones, type Ia muscle spindle afferents from muscle spindles, in addition to contacting spinal interneurones, make direct connections with spinal motoneurones. These monosynaptic Ia-motoneurone connections produce the shortest latency components of the stretch reflex.

Synaptic transmission from primary afferents in the spinal cord is subject to a process called presynaptic inhibition that regulates the amount of transmitter released from afferent fibre terminals onto spinal neurones. During "sensory-evoked" presynaptic inhibition, activity in primary afferents from first order order sensory neurones not only excites second order neurones involved in reflex pathways, but also excites the neurones that produce presynaptic inhibition. Consequently, activation of peripheral sensory receptors can regulate the degree to which spinal neurones in reflex pathways are activated by sensory input (Rudomin and Schmidt 1999, Rudomin, 2009). This sensory-evoked presynaptic inhibitory process is the subject of the first part of this thesis. Centrally evoked presynaptic inhibition involves the regulation of transmitter release from sensory afferents by spinal locomotor networks (See Rossignol et al, 2006) but will not be discussed here.

In the spinal cord, it is generally accepted that sensory-evoked presynaptic inhibition involves a two neuron pathway (Jankowska et al, 1981; Rudomin et al, 1987, Rudomin, 2009, Shreckengost et al 2010, Hochman et al, 2010) in which sensory afferents activate dorsal horn excitatory interneurones that then activate gabaergic interneurones (reviewed in Rudomin and Schmidt, 1999; Rudomin, 2009). These interneurones make axo-axonic synapses with afferent fibre terminals. Release of the inhibitory neurotransmitter, GABA, opens chloride channels in the presynaptic terminal. While chloride channel opening results in a hyperpolarization (i.e. Cl- entry) in most areas of the nervous system, the presynaptic terminals of primary afferents are depolarized through the actions of GABA. This is because the intracellular chloride concentration becomes high in primary afferents shortly after birth with a resulting depolarization of the terminal (chloride efflux) when the chloride channels are opened. A developmental change occurs in which the chloride transporter initially present in the terminals is replaced by another, KCC2 that operates preferentially in the reverse direction. This co-transporter is expressed in dorsal root ganglia neurones and results in chloride efflux. This Cl- efflux is replenished by the activity of the $Na^+ K^+ Cl^-$ cotransporter that allows entry of Cl- and accumulation of high intracellular concentration inside the terminal (Payne et al, 1996; Rivera et al, 1999).Opening of the chloride channels coupled to $GABA_A$ receptors thus results in depolarization of the terminal. This depolarization can also produce an opening of voltage-activated K^+ channels, which are known to be present in various vertebrate nerve terminals (Jankowska et al, 1977; Jack et al, 1981; Brigant and Mallart, 1982; Forsythe, 1994; Zhang and Jackson, 1995) with consequent K^+ efflux. If the depolarization is strong enough, presynaptic inhibition can create an action potential in the presynaptic terminal that propagates antidromically to the periphery, as the dorsal root reflex (DRR) (Willis, 2006).

There are at least three consequences of the back propagating potentials evoked from intraspinal terminal depolarization. One is that an antidromic action potential will collide with and prevent transmission of an orthodromic action potential coming from the peripheral receptor to the spinal cord. In the case of large mammals such as man, the conduction time from the lower leg to the cord of the fastest sensory afferents, the Ia afferents, is on the order 62-67m/s (Burke et al 1983). If an antidromic action potential in an afferent fibre was evoked centrally at the same time as an action potential was evoked in the periphery at the receptor, it would cancel sensory input from that receptor for about 30 ms (twice the conduction time plus the refractory period of

the action potential in the myelinated nerve fibre). In the case of the small rodents to be used in the present thesis, conduction times would be very much shorter (although conduction velocity is lower than in man) and hence the "clearing of sensory input" by dorsal root reflexes is likely to be less of a factor during presynaptic inhibition in smaller animals. The second consequence of dorsal root reflexes concerns the peripheral release of transmitters from sensory fibres (see Willis, 2001). This release of pro-inflammatory molecules from small myelinated and unmyelinated afferents is a key component of neurogenic inflammation that produces hyperalgesia and allodynia in a variety of pathological conditions (Willis, 2001). Consequently, a better understanding of the mechanisms underlying presynaptic inhibition might also lead to a better understanding of pathological pain states and other clinical conditions. The third effect of the depolarization during presynaptic inhibition generating intra-terminal action potentials is that transmitter would be released from the terminal to the target postsynaptic neurone. As such, these depolarizations would in effect make afferent terminals into "last order" neurones for intraspinal or descending axons (Verdier et al, 2004; Bos et al, 2011).

This thesis focuses on the activation of sensory afferents that, through a depolarization of primary afferent terminals, results in a reduction in the effectiveness of subsequent sensory transmission to first order neurones in reflex pathways. Although there is some controversy about the precise mechanism by which terminal depolarization reduces transmitter release (Zhang and Jackson, 1995) there is overwhelming evidence that GABA release results in a decrease in synaptic transmission from afferents to their target neurons. Once GABA is released, GABA will activate both $GABA_A$ and $GABA_B$ receptors present in primary afferent terminals. Unlike the opening of chloride channels by $GABA_A$ receptors, $GABA_B$ mediated presynaptic inhibition involves activation of G-protein coupled $GABA_B$ receptors that results in a reduction in Ca^{++} entry into the terminal and reduced transmitter release (Curtis, 1994; Castro et al, 2007).

Presynaptic inhibition is an important mechanism in the regulation of many reflexes and an integral component of reflex control during locomotion (Duenas et al, 1990; Perreault et al, 1999; Gosgnach et al, 2000; Menard et al, 2003; reviewed in Rossignol et al, 2006). An understanding of presynaptic inhibition is also critical for management of human conditions, notably spasticity following spinal cord lesions where there is strong evidence that presynaptic inhibitory systems are depressed (Bos et al, 2013). While much of our knowledge about spinal

presynaptic inhibition centres on mechanisms involving $GABA_A$ receptors, these receptors are an unlikely target for therapeutic intervention. This is because $GABA_A$ receptors also play an important role in postsynaptic inhibition in the cord. On the other hand, $GABA_B$ agonists such as baclofen augment presynaptic inhibition and are a mainstay in the treatment of spasticity in spinal cord injured humans.

Primary afferents in the spinal cord

Classes of primary afferents

Experiments in section 1 use electrical stimulation of dorsal roots to activate sensory afferents and evoke presynaptic inhibition in young rodent *in vitro* preparations. This section of the Introduction discusses the types of afferent fibres activated by electrical stimulation at various intensities with the activation of large diameter myelinated afferents being of greatest interest for the present work.

Primary afferents enter the spinal cord via dorsal root fibres. Each dorsal root fibre is the central process of a dorsal root ganglion neurone with a distal process that innervates a peripheral sensory receptor or is a free nerve ending. The dorsal roots contain myelinated and unmyelinated sensory fibres from muscles, skin, subcutaneous, deep tissues and viscera. Cutaneous, joint and visceral afferents are composed of myelinated A□, □ and unmyelinated A□ and C fibers. Afferent fibres from muscles are also myelinated A alpha and Beta (also called group I and II) and unmyelinated (group III and IV fibres). No efferent fibres have been shown to be present in the dorsal roots.

Group I afferents have the highest conduction velocities and lowest threshold to electrical stimulation of all sensory afferents. Group I afferents are myelinated large caliber fibers that include intrafusal muscle spindle primary afferents (type Ia afferents) detecting the velocity and the state of length change. The conduction velocities of these spindle primary afferents in the cat soleus range from 65 to 120 m/s (average 90 m/s) (Jack and Roberts 1978; Hunt, 1954; Matthews, 1963; Rack and Westbury, 1966). In the rat Ia muscle spindle conduction velocities range between 33 to 44 m/s (De-Doncker et al, 2003; Djouhri and Lawson, 2001), whereas in the mice conduction velocities are between 47.4 to 55.2 m/s (average of 52m/s) (Steffens and Schoumburg, 2012). Sensory afferents within the group I class also include fibers

innervating Golgi tendon organs that respond to changes in muscle tension. They have similar, but on average slightly slower conduction velocities and higher electrical thresholds than the Ia afferents (Jack and Roberts, 1978). In the cat triceps surae muscles, the electrical threshold for group Ia muscle spindle afferents is typically in 1 to 1.5 times the threshold for the most excitable afferents in the nerve (T) whereas the threshold for Ib afferents ranges from 1.3 – 1.8T (see Jankowska et al, 1981). Group Ia afferents are the only ones with substantial monosynaptic connections to hindlimb motoneurones (Eccles et al, 1959).

Muscle spindles also contain more slowly conducing fibers, the group II afferents or spindle secondaries that also respond to changes in muscle length but have a resting firing rate dependent upon static muscle length. They conduct on average at 72 m/s in the cat (Jack and Roberts, 1978) and at velocities of 20-30 m/s in the mouse (Steffens & Schomburg, 2012). While the most sensitive group II afferents in the cat are recruited at 1.5T, some are not recruited until the stimulus intensity is raised to more than 2T (Jack and Roberts 1978). Unlike spindle primaries, spindle secondaries make few and only weak monosynaptic connections with motoneurones (Munson et al, 1982). Spindle group II afferents can, however, evoke powerful and complex reflex actions in hind limb motoneurones such as inhibition of the extensors and facilitation of flexors (Eccles et al, 1957; Schoembourg et al, 1998; Schoemborug and Steffens, 1998) as well as more localized reflex actions (Eccles and Lundberg, 1959; Lundberg 1987). In addition group II afferents can activate interneurones mediating presynaptic inhibition of segmental afferents and ascending systems in Clarke's column (Jankowska 1992, Ridell et al, 1995).

Group III afferents are thinly myelinated and conduct impulses between 2.5 and 30 meters per second in dogs (Paintal, 1960) and 9-19 m/s in mice (Steffens and Schomburg, 2012) They are also referred to as A□fibres (Paintal 1960) group III endings located in the hindlimb muscles of dogs also respond to punctate pressure (Paintal, 1960). Group IV afferents are unmyelinated and conduct impulses at less than 2.5 m/s in cat (Franz and Mense, 1975), in mice group IV fibers conduct 0.8-0.9 m/s (Steffens and Schomburg, 2012). They are also referred to as C fibres. In many respects, group IV muscle afferents possess different discharge properties than do group III muscle afferents. In the mice > 5T recruits group III and cutaneous afferents (Steffens and Schomburg, 2012).

Distribution of primary afferents in the spinal cord

The earliest studies using Golgi methods (Ramon y Cajal, 1901; Szentagothai, 1964; Scheibel and Scheibel, 1968) and other methods showed that primary afferents have widespread and complex arborizations within the spinal cord. Although a full review of this literature is beyond the present scope, a brief mention of the termination sites of primary afferents will be made.

Much of our information about the projections and terminations of thick myelinated fibers comes from intra-axonal staining of physiologically identified single afferents using tracers such as HRP. In general, the large diameter cutaneous and muscle afferents project to deeper layers of the cord including deeper layers of the dorsal horn, the ventral horn, and deeper medial cord regions such as lamina IV and VIII (Grant and Ygge, 1981; Grant et al 1982; Smith, 1983). Primary afferents also have somatotopic patterns of innervation along the mediolateral axis in the dorsal horn (Grant and Ygge, 1981; Grant et al, 1982; Smith, 1983; Ygge and Grant, 1983).

A consideration of intraspinal terminations of large diameter muscle afferents is of importance for this thesis. Earlier morphological and anatomical studies in the cat have established the structural and functional correlations of the Ia-motoneurone system (Scheibel and Scheibel, 1968; Brown and Fyffe, 1978a, b; Ishizuka et al, 1979; Hongo et al, 1978; Burke et al, 1979; Redman and Wamsley, 1983). These studies have shown that Ia afferents bifurcate into ascending and descending branches. Once bifurcated, these branches enter deep dorsal laminae IV-VI and the ventral horn in lamina IX. Collaterals from these branches arise about every millimeter along the axon (Brown and Fyffe, 1978; Ishizuka et al, 1979). Ia afferents from triceps surae, hamstrings, plantaris, flexor digitorum longus, and flexor hallucis longus muscles have been studied in the cat hind limb. Ia afferent collateral branches penetrate into laminae V-VI before subdividing. Each collateral then distributes terminals to three main zones at or near the segment of entry of the parent fiber (Jankowska, 1992; Burke and Glenn, 1996): (1) to the medial half of lamina VI, (2) to the dorsolateral parts of lamina VII, and (3) to the motor cell columns in lamina IX. Two groups of Ia afferents have different or additional central projections at the segmental level i.e. hamstrings Ia fibers project mainly to the medial and ventral parts of lamina VII and flexor digitorum longus and flexor hallucis longus in lower lumbar segments L5-

L6 often have additional prominent arborizations in laminae IV and VI of the dorsal horn (Ishizuka et al, 1979). In the rat only few a studies have addressed the terminations of Ia fibres. According to Smith (1983), flame shaped arbors in the rat extend to lamina V-VI. Primary afferents also form a dense plexus in lamina IV mainly at thoracic levels (Smith, 1983), lamina V and VI receive the same pattern of afferent innervation as the cat (Craig and Mense, 1983; Alvarez et al, 2002). Motoneurone pool size and longitudinal distribution within the cord also determines the distribution of the collaterals of Ia afferents as does the location of the interneurones contacted by afferents from particular muscles (Ishizuka et al, 1979).

Extensive studies in the cat show that Ia afferent fibers projecting to lamina VI subdivide in several terminal branches, on average from 9 to 10, and form *en passsant* boutons before they end in terminal boutons (Brown and Fyffe, 1978a). Some of the boutons are located in the ventral part of lamina V or in the dorsomedial part of lamina VII, but they are mainly concentrated in lamina VI. In this region numerous Ia axo-somatic and axo-dendritic contacts have been observed (Ishizuka et al, 1979, Brown and Fyffe, 1978b).

Lamina VII projections from Ia afferents are formed by two or three thin branches. At least one of these branches bifurcates and also travels toward the motor nuclei. Collaterals in lamina VII have at least 10 fine branches in the dorsolateral part of lamina VII. These form sparse terminations forming juxtasomatic contacts on medium-size neurons in this region (Ishizuka et al 1979;Brown and Fyffe, 1978). Neurones in dorsolateral VII include the Ia inhibitory interneurones mediating reciprocal inhibition (Jankowska and Lindstrom, 1972). A similar organization is found in rat (Alvarez et al, 2004; Hugues et al, 2005)

The majority of Ia terminals in the ventral horn project to alpha motoneurones. Each Ia fiber projects to most (around 90%) of the motoneurones in the homonymous pool and to a smaller proportion (50-60%) of motoneurones in heteronymous or synergistic pools (Mendell and Henneman, 1971; Munson and Sypert, 1979; Watt et al, 1976; Smith, 1983). The great majority of Ia terminals end in motor nuclei in lamina IX and DCST neurons in lamina VI (Walmsley, 1991), although studies have also suggested that some of these Ia terminals end in the cells of origin of the ventral spinocerebellar tract in L6 or higher segments (Burke et al, 1971). Each Ia afferent fiber gives 100-200 boutons and makes multiple synaptic contacts with the motoneurone surface at proximal and distal sites of the dendritic arbor (Scheibel and Scheibel

1981, Mendell and Henneman, 1971). Dorsal Clarke column neurons receive group I and II afferents in the thoracolumbar regions in cat and rat spinal cord (see Walmsley, 1991; Brushart and Mesulam, 1980). In the mouse these cells also receive primary afferent innervation (Hantman and Jessell, 2010). Group I and Ib afferents also reach lamina VIII interneurones in the cat (Aoyama et al, 1988). Ia inhibitory interneurones are located within this area as well as other populations including propiospinal interneurones. Group II afferents also target commissural lamina VIII interneurones (Harrison et al, 1986).

Unmyelinated thin afferents enter the dorsal horn via the dorsolateral fasciculus (Lissauer's tract) to terminate in superficial laminae I and II of the dorsal horn in the rat (Jancso and Kiraly, 1980; Nagy and Hunt, 1983; Suczs et al, 2013). Some of the collaterals of thin unmyelinated fibers are also observed in laminae V, VII and X (Cervero et al, 1979; Schouenbourg, 1984; Sugiura et al, 1989; Mizumura et al, 1993; Li et al, 2000; Suczs et al, 2013). The majority of terminal branches of C-fibers of somatic and visceral origin are distributed mainly in laminae I and II in rat. Cutaneous nociceptive afferents terminate in laminae I and III (Maslany et al, 1992), whereas large A beta fibers from cutaneous mechanoreceptors terminate in laminae III to V (Woolf, 1987), visceral afferent fibers end in laminae I and V (Cervero and Connell, 1984; Sugiura et al, 1993) and these include the unmyelinated C fibers and thin myelinated A delta fibers, including a subset of small rapidly conducting myelinated fibers (Knuepfer and Schramm, 1987; Vera and Nadelhaft, 1990).

We will now briefly review some of the current knowledge concerning the Ia connection to motoneurones as this is relevant to the study of the inhibition of the monosynaptic reflex included in the first part of this thesis.

Monosynaptic reflex and Ia- motoneurone synapse

Ia afferent fibres make functional monosynaptic excitatory connections with both homonymous and heteronymous motoneurones producing an EPSP with an average amplitude of 2-5 mV in the *in vivo* cat (Eccles et al, 1957) and a intracellulary recorded latency of 0.8 – 1.2 ms in adult cat motoneurones (Eccles et al, 1957). The rise time of these EPSPs from onset to peak ranges from 0.8 to 2 ms. Together the range of latencies and times to peak result in 0.4 ms

to 1.1 ms interval (Watt et al, 1976; Burke et al, 1976) between the firing of the first and the last recruited motoneurones contributing to the monosynaptic reflex (Araki et al, 1960). In the mouse, *in vitro* latencies of the Ia EPSP *in vitro* are in the range of 1.5 to 2.5 ms with similar amplitudes as found in the cat (Zhang et al, 2008; Frank et al, 2009)**.** These values were used in the present study to establish reasonable values for the latencies and duration of the monosynaptic reflex recorded in the ventral root in the *in vitro* mouse preparation.

Early studies on spinal reflex pathways examined changes in the amplitude of the monosynaptic reflex as an assessment of whether stimulation of a particular nerve or descending pathway resulted in excitation or inhibition of a motoneurone pool. In these types of studies (e.g. Renshaw, 1940; Lloyd, 1941) a monosynaptic reflex is evoked by stimulation of a peripheral nerve or the dorsal root. The short-latency (i.e. monosynaptic) reflex discharge of motoneurones is recorded in the ventral root or in a peripheral nerve. This is called the test stimulus and is most often produced by a single shock stimulus. Stimulation of another nerve or descending tract, the conditioning stimulus, is delivered at various time intervals preceding the test stimulus and consists of a single or a brief train of shocks. If the monosynaptic reflex (test response) decreases in the presence of the conditioning stimulus, a net inhibition of the motoneurone pool is inferred. During the 1940s and early 50s this method was an important tool in revealing the organization of reflex input to spinal motoneurones. One problem with this approach is that is sometimes difficult to sort out the effect when there is a mixture of excitation and inhibition produced throughout the motor pool by multiple reflex pathways activated by the conditioning stimulation. The development of intracellular recordings allowed more detailed analysis of the synaptic input to motoneurones in animals (Baldissera et al, 1982). Interestingly, the greater precision did not change many of the main conclusions that had emerged from the experiments employing the monosynaptic reflex. This suggests that the monosynaptic reflex method can provide useful results.

Monosynaptic reflex testing also forms the basis of much of what we know about the organization of spinal reflex pathways in man. In human experiments a monosynaptic reflex is produced by transcutaneous stimulation of a peripheral nerve. The most common site of stimulation is in the popliteal fossa which activates the nerves to triceps surae muscles and produces a monosynaptic reflex in the soleus muscle. This is the H reflex named in honour of Dr.

Hoffman who first described it (Hoffman, 1918). In both human and animal studies, the apparent simplicity of the monosynaptic projection of Ia afferents to homonymous motoneurones has arguably made it the synapse most accessible to study in the CNS. However, we now know that the so called monosynaptic reflex is not as simple as was initially thought.

It is now clear that in addition to the monosynaptic excitation of homonymous and heteronymous motoneurones, Ia afferents produce short-latency inhibitory reflex effects through di and trisynaptic pathways via Ia inhibitory interneurones (Jankowska et al, 1981a, Jankowska and McCrea, 1983). In addition, muscle stretch can result in long latency excitation or facilitation of the motor pool mediated by both spinal and supraspinal pathways activated by group II in the majority of flexor motoneurones (Laporte and Lloyd, 1952; Eccles et al, 1957; Hongo et al, 1969; Jankowska et al, 1981c; Harrison et al, 1983; McCrea, 1986, Jankowska, 2000). The monosynaptic connection between Ia afferents and motoneurones is also subject to modulation by a system of presynaptic inhibition that regulates the amount of transmitter released from the Ia terminal onto motoneurones (discussed below).

Presynaptic inhibition of the monosynaptic reflex

Development of the concept of a presynaptic regulation of transmitter release began with the finding by Frank and Fuortes (1957) that conditioning stimulation of a peripheral nerve resulted in a depression of the amplitude of the monosynaptic Ia EPSP in the absence of any postsynaptic inhibition in the motoneurone. The interpretation of this finding was initially controversial. One hypothesis was that the Ia EPSP depression was a result of "remote" dendritic inhibition occurring at a site in the motoneurone not detectable from an intra-somatic microelectrode (Frank and Fuortes, 1957). Another was that the conditioning stimulation activated a neuronal pathway that altered the amount of transmitter released from the afferents. The explanation of Ia EPSP depression by remote dendritic inhibition has now been refuted in several studies (e.g.Eide et al, 1968; Kellerth, 1968; Cook and Cangiano, 1970).

The hypothesis of a presynaptic locus for EPSP depression emerged from a series of studies in Eccles' laboratory that were preceded by the observations made by Frank and Fuortes (1957) on the inhibition of Ia EPSP amplitude with no apparent changes in the properties of the motoneurone. Eccles and his colleagues established a paradigm that allowed detection of the

onset latency and the duration of this inhibition as well as the mechanisms that produced it. This approach is now used to measure presynaptic inhibitory effects of the monosynaptic reflex *in vitro* and *in vivo* preparations, as well as during voluntary movements in humans. The experimental paradigm consists of evoking a test monosynaptic reflex by stimulation of the Ia afferents in a dorsal root or nerve and applying conditioning stimulation from another peripheral nerve. Condition-test intervals between the conditioning and test stimuli are chosen to avoid the effects of short-latency postsynaptic inhibitory through pathways such as those involved in reciprocal inhibition. Accordingly, intervals longer than 15 ms should avoid any postsynaptic inhibition in the motoneurone, produced by Ia or Ib reciprocal inhibition (Eide et al, 1968; Eccles et al, 1962).

The inhibition produced by this condition-test paradigm was relatively small when a single conditioning volley in a muscle nerve was used, but became much larger when brief trains of high frequency conditioning stimuli of nerves to flexor muscles were employed (Eccles, 1961). Brief trains of volleys in group Ia and Ib afferent fibers of nerves to flexor muscles produced an inhibition of monosynaptic reflexes in both extensor and flexor motoneurones. The depression of the monosynaptic EPSP resulted in an inhibition of the monosynaptic reflex (Eccles et al. 1962). The time course of monosynaptic reflex inhibition was similar to that of EPSP depression (Eccles et al, 1959; Eccles et al, 1964). Maximum inhibition was reached at time intervals between 15-20 ms and lasted to 200 ms (Eccles et al, 1959; Eccles et al, 1961, 1962).

Presynaptic inhibition of flexors and extensors has not been found to be similar. For example, activation of group I afferents in nerves to flexor muscles produces a greater inhibition of extensor afferents, whereas extensor muscles and high threshold muscle afferents produce little presynaptic inhibition of monosynaptic reflexes (Eccles et al, 1962). A recent review (Rudomin and Schmidt, 1999) presents this material in detail.

Primary afferent depolarization and dorsal root potentials

It is well established that primary afferent terminals in the spinal cord dorsal horn are subject to presynaptic inhibition from descending systems or from segmental primary afferent input that results in reduced transmitter release from the terminals (Rudomin and Schmidt,

1999). In the case of the monosynaptic reflex (MSR), presynaptic inhibition reduces monosynaptic excitation of motoneurones from Ia muscle spindle afferents. This inhibition is achieved by afferent terminal depolarization recorded in afferent fibers as primary afferent depolarization (PAD) or extracellulary as the dorsal root potential (DRP).

By the late 1950's it became possible to reliably record intra-axonal potentials in the cat spinal cord. Direct recording from afferent fibres showed that the depolarization of the terminal, i.e. primary afferent depolarization or PAD, correlates well with the depression of the EPSP in the motoneurone (Eccles and Krnjevic, 1959; Eccles et al, 1961, 1962). The time course of PAD also correlates well with the time course of the dorsal root potential (DRP) (Barron and Matthews, 1935; Toennies, 1938, Eccles et al, 1961).

As described above, dorsal root reflexes (DRR's) result from the back propagation of an action potential in the afferent fibre when the PAD exceeds the threshold for action potential initiation in the fibre. These antidromic impulses can also be seen as small negative-going spikes on the rising phase of the extracellular DRP.

The dorsal root potential was first recognized by a study from Barron and Matthews in 1938, who observed the prolonged negative dorsal root potential (DRP) on arrival of an afferent volley and recorded its associated dorsal root reflex. This finding lead to at least two changes in the understanding of spinal reflex pathways. At the time the only accepted mechanism to generate a prolonged activity was by repetitive firing of action potentials. The prolonged DRP moved the time scale of synaptic events from several milliseconds to hundreds of milliseconds. The other major realization was that the synchronous depolarization of afferents was likely the result of a large scale and wide convergence of spinal systems producing the DRP onto the afferents. Subsequent studies by Laporte and Lloyd (1952) described the components of the DRP with the DRP V component being the prolonged negative wave. His studies distinguished the effects of incoming nerve impulses and neighbouring and distant passive axons. DRP V has been generally accepted as an indirect measure of PAD (Eccles and Magni, 1962, Eccles, 1964). The DRP is associated with a negative-positive cord dorsum potential (CDP) recorded from an electrode on the dorsal surface of the cord relative to a nearby reference electrode (Willis 2006). The correlation of DRPs with the gating of afferent impulses has been studied extensively for 40 years. However the interneurones responsible for generating the DRPs have not been fully

identified (Jankoswka, 1992). This difficulty arises from the fact that the inputs used to generate the DRPs fire many types of neurones, and it is not easy to identify separate those that generate DRPs from those active in circuits with other functions. This difficulty is increased by the finding that some interneurones appear to generate both postsynaptic actions on other interneurones and presynaptic actions on afferents (Rudomin et al, 1987).

There is general agreement that GABA plays a major role in the generation of the dorsal root potential, primary afferent depolarization, and presynaptic inhibition. The evidence comes from the marked decrease of all three phenomena when GABA antagonists such as bicuculline and picrotoxin are applied (Eccles, 1959; Curtis and Lacey, 1998). Furthermore the axo-axonic terminals on primary afferents which are presumed to be the origin of the primary afferent depolarization contain GABA (Todd and Spike, 1993). However, it must be pointed out that other agents are likely involved. Even very large doses of GABA antagonists reduce the height of the dorsal root potential by only 50% (Wall and Bennett 1994). In the spinal rat a DRP evoked from stimulation on L4 and recorded in L3 only showed a maximum decrease with picrotoxin of 55% (Thompson et al; 1999). The same also observed in the neonatal rat (Kremer and Lev-tov et al, 1998). These finding indicate that there are other components of the DRP that are not mediated by GABA. Other transmitters implicated in presynaptic inhibition include glycine since glycine antagonists enhances the DRP presumably by increasing the excitation of dorsal horn interneurones by afferent stimulation (Thompson et al, 1999). Narcotic antagonists such as naloxone produce a small increase in the DRP and also increase firing of many dorsal horn interneurones (Suzue and Jessell, 1980; Briggs and Barnes, 1987). Similarly, the 5-HT antagonist methysergide also produces a significant decrease 72% of the DRP amplitude, and the combination of picrotoxin and methylsergide reduce the DRP to a very low level (Thompson and Wall, 1996).

Presynaptic inhibition and PAD

Eccles, first studies of presynaptic inhibition of monosynaptic reflex suggested the presence of axo-axonic synapses making contact with the primary afferents (Eccles et al, 1959), even when morphological evidence was not available at that time. According to this view,

primary afferent terminals are depolarized by GABA that is released from interneurones making axo-axonic contacts with primary afferent terminals. In the following we will describe the most reliable methods to record presynaptic inhibition and how they culminated in the elucidation of some of the mechanisms.

Early experiments by Gasser and Graham (1933) provided evidence that stimulation of a dorsal root depolarizes the intraspinal terminals of afferent fibers in a neighbouring dorsal root. Later studies by Eccles suggested that this depolarization was the origin of presynaptic inhibition (Eccles et al, 1962). The approach Eccles used was to record PAD in the form of dorsal root potentials from dorsal roots and cord dorsum P waves from the surface of the spinal cord (Eccles et al, 1962). With this method depolarization of axons after stimulating flexor nerves with a brief train of stimuli could be observed. This depolarization resulted in the increase of the P wave in the cord dorsum potential (Eccles, 1962). Patrick Wall (1958) showed that intraspinal stimulation in an area close to the afferent terminals produced an antidromic volleys that could be recorded in a peripheral nerve. The size of this volley increased when the excitability of the intraspinal afferent terminals was changed by a conditioning volley. For example, conditioning stimulation using 1 or 2 shocks applied to the PBST nerve resulted in an increase in the size of the antidromic volleys recorded in the FDHL nerve that were produced by intraspinal stimulation in the FDHL motor nucleus. This technique of assessing changes in the excitability of intraspinal afferent terminals became known as the Wall technique and has been used extensively by several laboratories.

Mechanisms of presynaptic inhibition

As mentioned, the prevailing hypothesis about the cellular mechanisms of presynaptic inhibition is that GABA inhibits the release of neurotransmitter (glutamate) from primary axons by blocking action potential invasion into their terminals or by reducing the amplitude of a single propagated action potential (Graham and Redman, 1994; Zhang and Jackson, 1995) thereby blocking or reducing the Ca^{++} influx needed for transmitter release.

Presynaptic inhibition of the monosynaptic reflex is due to a cascade of events occurring at GABAergic presynaptic terminals that involve primary afferent fiber depolarization by a presynaptic inhibitory axon which release GABA. This phenomenon has been intensively

searched in many preparations. Difficulty in the access to presynaptic terminals in mammalian spinal cord renders proving this hypothesis difficult. GABA induced depolarizations have been reported elsewhere in dorsal root ganglia neurones, peptidergic pituitary terminals among others. Therefore, there was the need to develop different models in different species such as crayfish (Cattaert and El Manira, 1999) and other non spinal mammalian systems to aid in the understanding of the ionic mechanisms elicited by GABA in the terminals. In slices of rat pituitary gland for instance, it has been possible to visualize and make patch clamp recordings of identified pituitary presynaptic terminals due to their large size. These laborious studies by Zhang and Jackson (1995) demonstrated that, by visualizing structures smaller than neurones called "swellings" in pituitary slices, presynaptic terminals can be readily identified and recorded, confirmation of this was possible with the use of retrograde markers after these were recorded. According to these studies a GABA induced depolarization recorded through a whole terminal patch clamp recording with 25 mM Cl- in the patch pipette produced an average depolarization of 15.9 + 1.3 mV with a holding and membrane potential of -60 mV in these presynaptic terminals (Zhang and Jackson 1995).

The depolarization is due to Cl^- efflux through anion channels coupled to $GABA_A$ receptors. The magnitude of this depolarization is sufficient to produce opening of voltage-activated K^+channels, which are known to be present in various vertebrate nerve terminals (Jankowska et al, 1977; Jack et al, 1981; Brigant and Mallart 1982; Forsythe 1994; Zhang and Jackson, 1995) with consequent K^+ efflux. The restoration of Cl^- and K^+ via activation of Na^+ K^+ Cl^- cotransport implies Na^+ gain. The presence of the co-transport in the terminal also allows a reversal of the E_{Cl-} resulting in depolarization instead of hyperpolarization in the presynaptic terminal (Jackson, 1993). The Na^+ that entered to the cell is immediately extruded via the Na^+/K^+ pump, thereby keeping its intracellular concentration, at its constant level (Alvarez Leefmans et al, 1995). The sequence of events were possible to infer from *in vitro* experiments made in sympathetic dorsal root ganglion cells and frog motoneurones where repetitive electrical stimulation or application of excitatory amino acids resulted in cell shrinkage due to the loss of K^+ and Cl^- (Serve et al, 1988; Ballanyi and Grafe,1985). Expression of the Na^+K^+ Cl^- co-transporter has been found in the presynaptic terminals of primary afferents in the spinal cord (Alvarez-Leefmans, 2004). Interestingly, recent studies have also demonstrated that 5HT2a receptors can up regulate the expression of KCC2 cotransporters needed for maintaining E_{Cl-}

above the resting membrane potential, allowing Cl- entry and consequent hyperpolarization in motoneurones. Currently this mechanism is being explored as a potential target to lower spasticity after spinal cord injury (Bos et al, 2013).

Presynaptic inhibition also causes increases in the conductance of the presynaptic terminal, which may or may not accompanied by depolarization resulting in a net effect on the action potential propagation in the postsynaptic axon. If the conductance increase is sufficiently large compared to the input conductance at the terminal, activation of the axo-axonal synapse virtually clamps the voltage to the equilibrium potential (E_{Cl-}) of the synapse. Depending on the Cl- equilibrium potential, the conductance change associated with the presynaptic inhibition may result in a hyperpolarization or depolarization. A depolarizing inhibition can block propagation in two ways. First the presynaptic conductance changes tend to clamp the voltage at the terminal to $E_{Cl-.}$ Second the depolarization may inactivate the Na+ channels locally, raising the spike threshold. The second mechanism has been shown to operate at the secretory terminals in the posterior pituitary, limiting the invasion of action potentials into the terminal arborization (Zhang and Jackson, 1993).

Once GABA is released from interneurones to the primary afferent terminals, GABA will activate both $GABA_A$ and $GABA_B$ receptors present in primary afferent terminals. $GABA_B$ mediated presynaptic inhibition involves activation of G-protein coupled $GABA_B$ receptors that leads to closing Ca^{++} currents and opening of K+ channels that will result in a hyperpolarization of the terminal and therefore will reduce transmitter release (Dolphin, 1995). Baclofen is an agonist of the $GABA_B$ receptor and is used to treat spasticity in patients. Studies in cat spinal cord by Curtis and Lacey (1998) demonstrated that the $GABA_B$ receptor-mediated phenomenon has a longer time course than those associated with $GABA_A$ receptors, although these effects were only seen after high frequency tetanus stimulation of the primary afferents, where $GABA_B$ mediated presynaptic inhibition was found to produce a prolonged inhibition of extensor reflexes (Curtis and Lacey, 1998). $GABA_B$ receptors activated at the presynaptic terminal result in presynaptic inhibition of transmitter release and decrease in the activation of postsynaptic targets this is the result of prolonged neuronal hyperpolarization produced by an increased membrane K conductance in the presynaptic terminal (Curtis and Lacey, 1998).

Early knowledge on the mechanisms producing PAD established treatments for spasticity based on $GABA_A$ such as benzodiazepines (GABA antagonists). Benzodiazepines are currently been used in patients, but are not recommended due to their other CNS effects (Sunnerhagen et al, 2013). Although $GABA_B$ antagonist directed therapy with baclofen is a mainstay treatment of spasticity, non GABA agents have also been used. These include tizanidine, an alpha 2 adrenergic blocker, as well as gabapentin, dantrolene and botulinum toxin. Currently the paradigm to treat spasticity has been divided into pharmacological and non pharmacological strategies, this is because increasing evidence has opened our appreciation of the peripheral and central factors involved in this condition (Sunnerhagen et al, 2013).

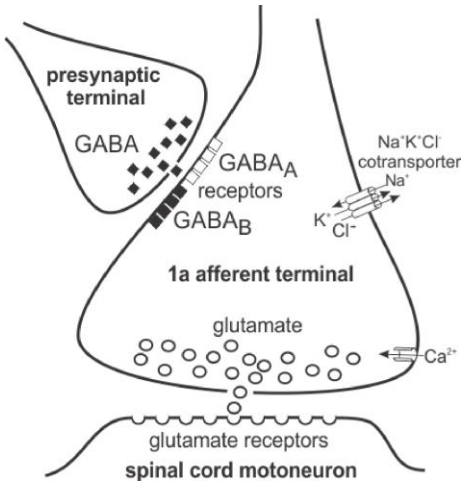

Figure 1. Schematic of the mechanisms of presynaptic inhibition in primary afferents. Diagram showing presynaptic modulation of monosynaptic reflex via axo-axonic synapses. Primary afferent terminals making monosynaptic contact with motoneurones receive axo-axonic synapses from gabaergic interneurones activated by antagonist nerve afferents.

P boutons

The anatomical substrate for presynaptic inhibition was not found until later developments in electron microscopy techniques were available. Axo-axonic synapses were first discovered by Gray (1962) in the spinal cord. Further studies using a variety of degeneration techniques by dorsal root section, Conradi (1969) allowed the identification of primary afferent terminals synaptically linked to the motoneurone membrane and themselves postsynaptic to another terminal. Their findings were later confirmed by the use of anterograde tracers on group Ia afferents by Maxwell (1983). The conclusion from the anatomical data was that presynaptic contacts onto primary afferents occur through axo-axonic connections, but dendroaxonic contacts also exist. Presynaptic contacts preferentially target a very specific element of dorsal horn afferent terminals. The number of axo-axonic and dendro-axonic connections received by the central terminals of different primary afferents varies widely. In a study by Pierce and Mendell (1993), it was reported in the cat, that 90% of Ia afferent terminals ending in lamina IV-VI receive axo-axonic contacts.

Presynaptic terminals contain tightly packed flattened and pleomorphic vesicles and establish a symmetric synapse onto primary afferent terminals, usually a unique small active zone (0.5 um). In classical electron microscopy studies they were usually referred to as P for presynaptic. This termed was first used by Conradi in (1969) or F terminals for flattened vesicles (Ralston, 1979). Another presynaptic element was also identified: presynaptic terminals contacting the primary afferent postsynaptic targets, forming synaptic arrangements known as "triads", these terminals would allow both pre and postsynaptic inhibition. These arrangements were found to occur frequently in the terminals presynaptic to Ia afferents, where a total of 66% of the terminals presented triadic arrangements (Pierce and Mendell, 1993).

The neurochemical content of the presynaptic elements was described in quantitative studies using immunoreactivity against GABA or the GABA producing enzyme GAD. These studies revealed that a very high proportion of terminals contacting primary afferent terminals contain GAD or GABA; 79% of terminals presynaptic to glomerular afferent terminals, found in lamina II and III terminals (Todd and Lochead, 1990, Gerke and Plenderleith, 2004) and 100% of terminals presynaptic to Ia fibres, hair follicle fibres, and A delta fibres (Maxwell and Noble, 1987; Maxwell et al, 1990, Alvarez et al, 1992) are believed to be gabaergic. These results agree

with the early physiological work discussed above that proposed a dominant role for GABA in presynaptic inhibition.

Spinal interneurones mediating PAD

The first attempt to identify subpopulations of interneurones involved in mediating PAD was be electrophysiological investigations of interneurone responses at mono or disynaptic latencies to group I strength stimulation (Eccles et al, 1962). Some interneurones had discharges that would outlast the inhibition of the monosynaptic reflex. This was considered as a feature that could explain the long duration of the PAD. Subsequent studies, however, suggest that the prolonged duration of PAD is not necessarily due to a sustained interneuronal activity, but may rather reflect the slow dynamics of GABA release and/or uptake (Rudomin and Munoz Martinez, 1969; Nicoll and Alger, 1979). Further studies using spike triggered averaging demonstrated that there were interneurones that were activated in phase to the DRP and to an inhibitory component in the ventral root potential, i.e., produce IPSPs in motoneurones. These interneurones were classified as class I and class II depending on their sensitivity to the $GABA_A$ antagonist picrotoxin, or strychnine, an antagonist of glycine (Rudomin and Jimenez, 1987). Class I interneurones were thought to be involved in the DRP which was also decreased by picrotoxin (Rudomin and Jimenez, 1987).

It is believed that the population of last order interneurones mediating PAD is distributed over long distances in the spinal cord. Lidierth and Wall (1996) demonstrated in the rat spinal cord that spontaneous DRP's recorded over widely separated lumbar are temporally synchronized. Furthermore these DRP's are associated with PAD and presynaptic inhibition (Lidierth, 2006). This has also been reported in early studies in the cat, where neurons in particular spinal cord laminae thought to mediate presynaptic inhibition were observed to exhibit some degree of synchronous activity (Rudomin, 2009).

The prevailing view is that presynaptic inhibition is mediated by GABAergic spinal interneurons that are located in lamina V-VI and that form axo-axonic synapses make on muscle and cutaneous afferent terminals (Maxwell et al, 1990; Rudomin, 2009). The study of gabaergic neurons and their targets led to the identification of an enzyme that synthetize GABA, Glutamic

Acid Decarboxylase (GAD). Two isoforms, GAD65 and GAD67, have been identified according to the molecular weight. Terminals differentially labelled with either one of the isoforms suggested that the two isoforms occur in different populations of gabaergic interneurones. The physiological significance of the different expression in interneurones difference has not been established, but is suggested to be related to factors such as afferent terminal GABA release mechanisms or 'tonic' versus 'phasic' firing properties of single neurones (Soghomonian and Martin, 1998). In the rat dorsal horn, GAD65 immunoreactivity is abundant in superficial laminae with decreasing amounts localized to the deeper laminae (Mackie et al, 2003). It is estimated that about 30% of neurones in laminae I–II are GABAergic (Todd and Sullivan, 1990) and these can induce either pre- or postsynaptic inhibition (Barber et al, 1978). In dorsal horn, there appears to be specific patterns of postsynaptic targeting mediated by classes of GABAergic neurones (Puskar et al, 2001), presumably to shape the output to other laminae or projection pathways. $GABA_A$ and $GABA_B$ receptors are localized to primary afferents, where they act to modulate glutamate and peptidergic transmitter release (Malcangio and Bowery, 1996). Inhibitory neurones in the dorsal horn are activated by noxious stimuli, as evidenced by enhanced expression of the immediate early gene c-*fos* in GABA-immunoreactive neurones (Todd et al, 1994), however, it is unknown whether this is mainly within the GAD65 or GAD67 interneurone population. GAD67 immunoreactive profiles are concentrated within laminae I–III, with moderate amounts also in laminae IV–VI (Mackie et al, 2003).

Of particular relevance to the present investigations are the results using a transgenic strain of mice encoding green fluorescent protein encoding for the GAD65 promoter. They show the existence of a subpopulation of GAD65-EGFP positive neurons in lamina IV-VI that form P boutons in lamina IX (Hugues et al, 2005). These interneurones have been found to project to lamina IX and form axo-axonic presynaptic terminals on Ia afferents (P boutons). Retrograde labelling of these neurons shows that the cells of origin of these terminals are located in laminae V-VI in adult mouse and rat. These results elegantly confirm previous studies made in the cat spinal cord on the likely location of interneurones mediating presynaptic inhibition of group I muscle fibre afferents (see Hugues et al, 2005).

Interneurones involved in the modulation of reflexes

Spinal interneurones involved in the activation of PAD

Spinal reflexes are modulated by diverse populations of interneurones located mainly in the deep dorsal laminae and lamina VII of the spinal cord. Their distribution and their phenotype have been used to classify them into different functions. Interneurones in laminae IV-VI receive monosynaptic contacts from tendon organs (group Ib afferents), muscle spindle secondary endings (group II afferents) and muscle spindle primary endings (Ia afferents) (Matthews, 1972). Cutaneous input is mainly processed initially by interneurones in more superficial laminae. Extensive investigation throughout the years has found that almost all interneurones receive input from multiple classes of afferents. For example, many of the interneurones with strong Ib input are also effectively activated by group Ia afferents (Fetz et al, 1979; Czarkowska et al, 1981, Jankowska et al, 1981, Harrison and Jankowska, 1985). The convergence of multiple afferent (and descending) systems to individual interneurones makes classification into distinct populations difficult. Interneurones that were once thought of as being "Ib interneurones", are now seen as part of a larger set of premotor interneurones that can integrate information from group II, Ia, and group Ib afferents. The majority of these have found throughout laminae V-VII (Jankowska et al, 2008, Jankowska et al, 2010). Intermingled subpopulations of neurons with more selective input from group II afferents and group I afferents are located in laminae VI-VII (Edgley and Jankowska, 1987). This system is often considered as the "non-reciprocal" inhibition system (Jankowska et al, 1981, Rudomin and Schmidt, 1999) in order to distinguish its actions from those of the interneurones that are activated primarily by Ia afferents and produce disynaptic inhibition of antagonist motoneurones (i.e. reciprocal inhibition). Reciprocal inhibition is mediated by Ia inhibitory interneurones located in ventral lamina VII and the border of lamina VIII and produce postsynaptic inhibition on motoneurones (Jankowska and Roberts, 1972). Non reciprocal inhibition is produced mainly by the activation of gabergic interneurones located in deep dorsal horn between lamina IV-VI (Jankowska et al, 1981, Rudomin and Schmidt, 1999). Intermingled in these areas are the gabaergic interneurones mentioned above that produce presynaptic inhibition in the afferent terminals, as well as interneurones involved in both pre and postsynaptic inhibition (Rudomin et al, 1987, Rudomin, 2009).

On average, interneurones projecting to motor nuclei represent 54% of the total population of intermediate zone interneurones. Of these, 47% have monosynaptic Ia and 62%

group II monosynaptic input from which 41% have both Ia and Ib excitatory inputs (Jankowska et al, 1981a). Descending rubrospinal, corticospinal and reticulospinal projections also converge on these interneurones. In the cat, there is a roughly rostro-caudal distribution of input to these interneurones with the more rostrally located populations receiving more group II input than the caudal populations. Unfortunately, this type of information is unavailable in the mouse.

In the cat spinal cord, recently a series of detailed studies identified the phenotype of a subpopulation of interneurones co-excited by group I and II afferents by injecting neurobiotin intracellularly in interneurones identified by their input, output and location. These interneurones were antidromically activated from the motor nucleus, and then by inmunocytochemistry, their reconstructed terminals were labeled by the vesicular transporter vglut-2 for the case of excitatory neurons and gephyrin and glutamic acid decarboxilase was used to detect glycinergic and gabaergic inhibitory neurons (Bannatyne et al, 2009). These studies revealed a mixture of gabaergic, glycinergic and glutamatergic neurons.

These excitatory and inhibitory interneurones are intermingled with the ones mentioned above mediating non reciprocal presynaptic inhibition, suggesting that not only gabaergic inhibitory interneurones are involved but also glutamatergic excitatory interneurones. This recent evidence adds to and confirms a previous classification (Rudomin et al, 1987).

Descending pathways modulating reflex actions

Modulation of spinal reflexes is also achieved by descending monoaminergic neuronal systems. For example, stimulation of the locus coeruleus-subcoeroleaus almost abolishes IPSPs evoked by stimulation of group II afferents, but has a negligible effect on IPSPs evoked by stimulation of group Ib afferents. These differential effects could be explained by increase in the amount of presynaptic inhibition been received by the group II activated interneurones (Riddell et al, 1993). Noradrenaline and 5-HT are known to modulate transmission from group II afferents to dorsal horn and intermediate zone interneurones (Jankowska and Edgley, 2005). Monoamines also exert inhibitory effects on group II afferents, as has been observed after DOPA administration on the FRA reflex. However the focus in this thesis only includes a consideration of presynaptic inhibition from primary afferents.

Discovery of chemical and electrical transmission

Throughout the first half of the twentieth century, there was a debate on whether synaptic transmission in the vertebrate central nervous system is mediated by electrical or chemical processes, as reviewed in detail by Eccles (1982). Chemical transmission was discovered in the endplate potentials at the neuromuscular junction by Gopfert and Schaefer (1938), who discovered that the action potential in the presynaptic fiber does not lead directly to the initiation of an action potential in the postsynaptic muscle fiber. This finding was later confirmed by Eccles and O'Connor (1939), who observed an action potential preceded by a slow transitional potential; when the action potential is present, this slow potential can disappear, but is readily unmasked by the presence of curare. It was clear that the nerve impulse in the presynaptic axon sets up a local depolarization at the muscle endplate, which was earlier thought by Eccles et al. (1941) to be though an electronic potential.

It seemed that the issue was resolved in favour of chemical transmission with the advent of motoneurone intracellular recordings in the early 1950's. Subsequent studies then demonstrated that graded potentials were present in cat sympathetic ganglia, squid stellate ganglion and spinal motoneurones in frog, cat and rat, respectively (Elfvin, 1963; Dermietzel, 1974; Tamarind and Quilliam, 1971; Gabella, 1981; Watanabe and Burnstock, 1976; Sotelo and Taxi, 1979; Shapovalov, 1981; Fulton and Navarrete, 1981). In each case, excitation of the presynaptic axons was found to give rise, with a measurable delay, to a slow depolarization of the postsynaptic cell. By the late 1940's, effects of acetylcholine were first described at the neuromuscular junction, indicating that grade potentials originated from transmitter release. Eccles postulated the existence of electrical transmission in the spinal cord and central nervous system, despite recognizing that this was not the case in the neuromuscular junction. He hypothesized that the phenomena of electrical transmission might occur in regions of the CNS where acetylcholine is not a neurotransmitter, and led him to propose the idea that electrical interaction between motoneurones and type II Golgi cells would result in an inhibition (Eccles and Brooks, 1947). By the 1950's, the implementation of electrophysiological techniques, such as intracellular recording, allowed Eccles and collegues to test all of his previous hypothesis. To his surprise, he found that the inhibition that he had proposed to occur was mediated by chemical synapses, for which later he was awarded a Nobel Prize, together with Hodgkin and Huxley (1963). Interestingly, all of studies in which he attempted to prove his hypothesis on electrical transmission led him to be even more convinced about chemical transmission, and led him to the

discovery of presynaptic inhibition a few years later (Eccles, 1959, 1961; Eccles and Magni, 1962). The majority of the papers published soon thereafter referred to chemical transmission in higher vertebrates and mammals.

However, the question of electrical transmission reappeared shortly thereafter. Some investigators at the time still assumed the existence of electrical interaction, and that this was as important as the chemical transmission. This arose from the finding of the first example of electrical synapses in the motor endplate of the crayfish (Furshpan and Potter, 1957). Support for electrical transmission was provided by electron microscopic evidence in a few systems (Bennett et al, 1963; Robertson, 1961) for what are now called gap junctions. A notable example is gap junctions between large myelinated club endings of eighth nerve afferents and the lateral dendrite of the Mauthner cell in fish, which was interpreted by Robertson et al, (1963) as being suggestive of electrical transmission.

Gap junctions and connexins

In initial electron microscopic descriptions of gap junctions, the extracellular space at close appositions between the adjoining cells appeared reduced to a narrow gap (Revel and Karnovsky, 1967). Gap junctions are clusters of channels that connect the interiors of adjoining cells and mediate electrical coupling and transfer of small molecules. In most instances of early studies, electrical transmission was thought to take place by way of morphologically distinct junctions of the "zonula occludens" variety (Farquhar and Palade, 1963), where the membranes of the coupled cells come together, creating a narrowed extracellular space. This type of junction was first considered to constitute low resistivity pathways between nerve cells (Robertson, 1963; Bennett et al, 1963; Pappas and Bennett, 1966). Shortly thereafter, however, although features of a strict correlation between electrophysiological and histological data were still missing in a few cases (ref. in Bennett et al, 1967d) the structural correlate for electrotonic coupling was largely concluded to be gap junctions (Robertson, 1963; Payton et al, 1969; Revel and Karnovsky, I967; Asada and Bennett, 1971; Pappas et al, 1971).

The large internal diameter (1.2 nm) of many gap junction channels allows not only flow of electric current, largely carried by K+ ions, but also exchange of small metabolites and intracellular signalling molecules. Gap junctions are characterized by an area of very close

apposition, in the order of 2-4 nm between pre- and post-synaptic membranes. Within this area of apposition, two cells can communicate via cell-to-cell pores that serve as conduits between the cytoplasm of one cell to another. Gap junctions between neurons are the ultrastructural basis for electrical transmission (Bennett, 1969), but may also subserve metabolic coupling. The structural proteins comprising these channels, called connexins (Cx), form a multigene family of members that are distinguished according to their predicted molecular mass in kDa (e.g. Cx32, Cx43) (Beyer et al, 1990; Willecke et al, 2002). The intercellular channels span two plasma membranes and are created by the association of two half channels, called connexons, contributed separately by each of the two participating cells. Each connexon, in turn, is a hexameric assembly of connexin subunits.

Neuronal gap junctions: Connexin36

Cloning of a gene encoding a connexin predominanlty expressed in mammalian neurons lead to the discovery of the first gap junction-forming protein in neurons, namely connexin36 (Cx36) (Condorelli et al, 1998). This connexin has been demonstrated in ultrastructurally-defined neuronal gap junctions and is found abundantly in these junctions (Rash et al, 1996; Bennett, 2000, Rash et al, 2000, 2001, 2005; Fukuda et al, 2006; Kamasawa et al, 2006). Most intercellular channels formed by connexins are voltage-dependent. The conductance of Cx36 channels peaks at a transjunctional potential of ~0 mV. When the transjunctional membrane potential is ~100 mV, the junctional conductance is ~50% of its peak value (Srinivas et al, 1999). So, the conductance of Cx36 is only weakly voltage-sensitive according to this study. In addition, Cx36 channels are unusual in having a low single-channel conductance of ~15 pS (Srinivas et al., 1999; Teubner et al., 2000). Interestingly, in other systems such as retina, horizontal cells and bipolar cells are electrically coupled not only by Cx36, but also by Cx57 and Cx45 (Palacios Prado et al 2010). The discovery of Cx36 allowed implementation of new tools to study electrical synapses in the CNS. In particular, monoclonal antibodies against Cx36 were developed, and knockout mice with deletion of the gene encoding for Cx36 were created (Paul, 2000). These new approaches occurred during the last decade and fostered a revolution in the understanding of electrical synapses. Studies of the role of neuronal gap junctions in the CNS are now taking the field a step further. One example illustrating this was the discovery of a new

connexin, where the group of Klaus Willecke in Germany found that electrical coupling in certain brain regions in Cx36 knockout mice still occurred between interneurones, and may be mediated by a newly described connexin, namely Cx30.2 (Kreuzberg et al, 2008).

Neuronal connectivity via electrical synapses

Studies of gap junctions in mammals using EM lead to the discovery of dendro-dendritic or dendro-somatic 'close appositions' in certain neocortical cells, and the first reports appeared on dendro-dendritic gap junctions in the primate neocortex (Sloper, 1972; Sloper and Powell, 1978). Before this, there was evidence that electrical synapses and their structural correlate (gap junctions) are present in the nervous system of lower vertebrates and invertebrates, but whether or not this form of signalling was used in the mammalian cortex was unknown. In these early studies, the close appositions had the hallmarks of the seven-layered structure of gap junctions. Furthermore, these neocortical gap junctions were found mainly at contacts between cells belonging to a specific class, for example, large basket cells. In his 1972 paper, Sloper concludes: "If this is correct, it follows that direct electrical interaction takes place between the dendrites and somata of certain stellate cells in the primate neocortex. It will be of considerable interest to see whether any physiological evidence of this can be found." It is remarkable that in the same year, Sotelo and Llinas (1972), studying the mammalian cerebellum, reported that "gap junctions are observed only in the molecular layer, between perikarya, dendrites, or perikarya and dendrites of inhibitory interneurons". Thus, anatomical data indicated nearly forty years ago that gap junctions in the neocortex and the cerebellum are specifically formed among GABA-releasing neurons. Later studies in the hippocampus and the neocortex also indicated that some inhibitory neurons might be electrically coupled (Michelson and Wong, 1994). However, the most direct and arguably the only convincing experiments to show the existence of functional electrical synapses require simultaneous recordings from pairs of connected cells. Recently, this evidence has been obtained with dual recordings from inferior olive neurones, neocortical and granular cells as well as in neurones of leech and fish (Devor and Yarom, 2002; Fan et al., 2005; Levavi-Sivan et al., 2005; Mann-Metzer and Yarom, 1999; Nolan et al., 1999; Szabadics et al., 2001) where pairs of coupled neurones have been identified. Studies that show electrical coupling between gabaergic neocortical neurones have made the suggestion that neurons forming

gap junctions are inhibitory, however, this would mean that electrical synapses would be restricted to neurons that make up only 15% of the total number in the neocortex; hence the probability of finding pairs of coupled cells would be very low. Moreover, if electrical synapses are formed exclusively between inhibitory cells of the same class, the probability of finding connected pairs among randomly selected inhibitory neurons would make this even lower. What this is not taking into account is that these inhibitory neurones would form ensembles of large populations of interneurones that would be dynamically modulated. It has also been suggested that electrical synapses could also occur between other neuron phenotypes, such as glutamatergic, noradrenergic or catecolaminergic neurones, however, evidence for this is not yet conclusive. Although gap junctions, electrical coupling and mRNA have been identified in certain groups of inhibitory neurones in the brain (Deans et al, 2001; Tamás et al, 2000), to date there are no anatomical studies confirming Cx36 protein expression on gap junctions between gabaergic neurones in the spinal cord.

Distribution and function of electrical synapses in brain

With technical improvements allowing visualization of individual neurons in brain slice preparations, dual recordings from pairs of specific types of inhibitory neurons became practical. Two methods used by several groups included pair patch clamp recordings from visualized neurons and/or injection of dyes that are permeable to neuronal gap junctions; lucifer yellow and neurobiotin have been used extensively due their polarity and low molecular weight. Previous work showed that in response to near-threshold current injection, a specific type of inhibitory neocortical neuron, the fast-spiking (FS) cell, exhibits a high-frequency discharge of spikes without spike-frequency adaptation (Galarreta and Hestrin, 1999). When two cells are selected in this way, most of the pairs of FS cells have been found to be electrically coupled; injection of current into one cell produces an attenuated response in the non-injected cell (Kamaguchi and Kubota, 1993).

Electrical synapses do not seem to connect heterogeneous populations of neurons. For example, FS cells in the cortex do not seem to establish electrical synapses with other cells, including pyramidal neurons, other types of non-pyramidal cell or glia (Galarreta and Hestrin, 1999; Gibson et al, 1999). These data therefore raise the possibility that electrical synapses are formed exclusively between neurons of a specific class. This is an interesting idea because it may

provide insights into circuit organization of different brain areas, leading to the identification of cells that belong to the same functional class. An example of this occurs in the connectivity of LTS and FS cells in the neocortex indicating that GABAergic neurons of the same class might be connected, whereas glutamate-releasing neocortical cells (pyramidal neurons) are not coupled. In the cerebellum, the projecting neurons are the GABA-releasing Purkinje cells, and the local inhibitory neurons are the basket, stellate and Golgi cells. It was found that electrical synapses are prominent among the local interneurons in the molecular layer, such as stellate and basket cells (Sotelo and Llinas, 1972, Mann Metzer, 1999, Dugue et al, 2009). Electrical coupling between Purkinje cells has not been reported so far. In the striatum, the projecting neurons are medium spiny cells, which account for 95% of the neurons in this structure; and it was found that electrical synapses were specifically formed between local FS interneurons that were positive for parvalbumin and account for less than 3% of neurons (Koos and Tepper, 1999).

In summary, the results of several independent studies indicate that GABA-releasing cells that project their axons locally might be coupled, whereas cells with distally projecting axons are not. It should be noted that these rules are compatible with the data available at present, where Cx36 has been detected in subsets of GABAergic populations in the cortex (Tanas et al, 2000, Ma et al, 2011), but future results might reveal connections across distinct neuron classes. Indeed, it has been reported that electrical coupling occurs both in pairs of excitatory neurones such as inferior olive cerebellar neurones, regular-spiking striatal spiny stellate cells, as well as inhibitory neurones such as striatal output neurones and cortex somatostatin-expressing fusiform cells (Venance et al 2000;Venance et al, 2004). In addition, it has been reported that hippocampal pyramidal cells might also be interconnected by electrical synapses (McVicar and Dudek 1981), and it has been proposed that these contacts could be axo-axonic (Draghun et al, 1998). So far, anatomical examinations in the cortex and the hippocampus have shown gap junctions between excitatory and inhibitory neurons, but the demonstration of the existence of electrical connections between excitatory–inhibitory cell pairs in the CNS remains elusive.

Physiological properties of electrical synapses

In pairs of neurons that are electrically coupled, injection of a current step into the soma of one of the neurons generates a voltage change not only in the injected cell, but also in the non-injected one. In all cases studied so far, electrical coupling between inhibitory interneurons has

been found to be reciprocal, indicating that current flows bi-directionally through electrical synapses. The strength of electrical coupling has been assessed by calculating the coupling coefficient, this is calculated as the ratio between the change of membrane voltage produced in the non-injected cell and that in the injected cell. Similar values for the average coupling coefficient ranging from 2.6-10% have been reported in different studies (Mann-Metzer and Yarom, 1999; Tamas et al, 2000). However, coupling coefficients from individual pairs of electrically coupled cells can vary widely (from 0.3 to 40%). Many factors can influence the measurement of the coupling coefficient. They include the conductance of single gap junction channels, total number of channels that bridge the two cells, distance from the soma to the electrical synapses, input resistance of the cells, and the presence of dendritic or somatic active conductances (Martina et al, 2000). The observation that, in most cases, the coupling coefficient was similar in both directions suggest that the electrotonic distances of the electrical synapses are approximately similar in both cells. No voltage dependency of electrical coupling has been described in two studies of neocortical neurons (Galarreta and Hestrin, 1999; Gibson et al, 1999), but a strong reduction in the coupling coefficient has been reported between cerebellar interneurons when the membrane potential was less than -35 mV (Mann-Metzer and Yarom 1999). This change, however, seems to be explained by a marked decrease in input resistance. The junctional conductance (G_j), or conductance of the electrical synapses between two neurons, has been measured experimentally (Galarreta and Hestrin, 1999) and also estimated assuming a two-neuron model (Gibson et al, 1999; Mann Metzer, 1999; Tanas et al, 2000), where values observed ranged from 235 to 2100 pS.

Electrical synapses can act as low-pass filters, reflecting their electrotonic location and the membrane time constants of both cells (Bennett 2000). The filtering characteristics of interneuron electrical synapses have been studied by injecting subthreshold sine wave currents of different frequencies into one cell. As the frequency of the injected sine wave increases, the efficacy of the electrical connection decrease. So, signalling through electrical connections favours the transmission of slow potential changes. Spikes in non-pyramidal cells are usually faster than in pyramidal cells and are followed by a prominent afterhyperpolarization (AHP) (Connors et al., 2010; Vervaeke et al., 2010). Consequently, the signal transmitted to the postsynaptic cell is also biphasic, with a brief depolarizing component reflecting the spike itself and a slower hyperpolarizing component reflecting the AHP (Connors et al, 2010; Vervaeke et

al, 2010). The average latency between the peak of the presynaptic spike and the peak of the postsynaptic depolarizing response, commonly referred to as a spikelet, has been reported to be 300–500 μs for FS–FS pairs and for cell pairs from the thalamic reticular nucleus (Gibson et al., 1999; Tanas et al, 2000; Ladisman et al, 2000). The minimum value of the hyperpolarizing component at coupled pairs of neurons typically occurs 4–10 ms after the presynaptic spike (Galarreta et al., 2005). The coupling coefficient for the spike has been reported to range from 0.5-2.5% (Gibson et al, 1999; Tanas et al, 2000; Ladisman et al, 2000), a value several times smaller than that observed for step pulses. Given the dependency of electrical transmission on signal frequency, electrical synapses are more efficient in transmitting the AHP than the action potential itself. This might have important functional implications because trains of action potentials result in a net hyperpolarizing effect in the electrically coupled neuron. This is due to the fact that electrical synapses act as low pass filters allowing dynamic passage of presynaptic components to the postsynaptic cell. In this case, is known that when the action potantial gets filtered through electrical synapses it is transformed into two components: a small brief positive spike and a large long lasting hyperpolarizing phase that correspond to the AHP, then depending on the conditions on the postsynaptic cell results in a long hyperpolarizing and inhibitory effect (Galarreta and Hestrin, 2005). The width of action potentials and the shape of the AHP have been shown to differ between different subtypes of gabaergic interneurons. It can therefore be predicted that the electrical transmission of action potentials would differ significantly between different interneurons. Recent studies by Haas et al. (2011) demonstrated that an additional mechanism can result from the activation of electrical synapses in inhibitory thalamic reticular neurones, where plasticity of electrical coupling due to long-term depression (LTD) can occur. This evidence has shown that when synchronized bursts are generated in coupled neurones, this can lead to a decrease of the coupling coefficient and thus modify electrical coupling between coupled neurones, limiting the recruitment of ensembles of neurons, even when neurones are connected through gap junctions.

Electrical synapses: Network oscillations and synchrony

Experiments *in vivo* and *in vitro* have suggested that networks of inhibitory neurons can synchronize neuronal activity (Beierlein et al, 2000). Theoretical models have supported this

proposal, however, synchronization depended on specific constraints when interneurons were interconnected only by gabaergic synapses (Bush and Sejnowski, 1996). The existence of electrical synapses could provide an additional mechanism to facilitate precise synchronous spiking of these cells and contribute to the control of activity in the cortex (Whittington et al., 1995). Moreover, it has been suggested that the time course of the GABA-mediated inhibitory response determines the frequency of the oscillations (Whittington et al, 1995; Jefferys et al, 1996). Spikelets can be followed by a prolonged hyperpolarization that reflects the presynaptic AHP (Galarreta et al, 2005). Oscillatory activity at gamma frequency (30–70 Hz), which reflects the coherent and rhythmic firing of large numbers of cells, is thought to have a role in diverse phenomena including response to sensory input, attention and coordinated motor output in the cortex (Whittington and Traub, 1995; Singer and Gray, 1995). It has been proposed that gap junctions are involved in inducing gamma-frequency rhythmic activity *in vitro* (Tarnas et al, 2000). Furthermore, the speed of electrical signalling at proximal contacts and their dynamic stability indicate that this form of synaptic transmission among inhibitory neurons might mediate the very high frequency discharge (400–900 Hz) observed *in* vivo (Jones et al, 2000) under some conditions.This is in contrast to their ability to act as low pass filters, however in addition to integrate slow signals it is well established that electrical synapses are characterized by fast gating. Further evidence indicates that rhytmic slow oscillations produced in ensemble of coupled neurones could be amplified since the increase of gap junction conductance within the network leads to a decrease on the time required for an action potential to spread across neurones (Cunningham et al, 2012). In addition, axo-axonic gap junctions between excitatory (Draghun et al, 1998) and between inhibitory neurons (Traub et al, 2001) have been proposed to be critical in generating the 200 Hz oscillation observed in hippocampal slices. Recent reports have shown that spike-to-spike transmission between pyramidal cells and GABA interneurons is very precise both in the hippocampus (Fricker and Miles, 2001) and in the neocortex (Galarreta and Hestrin, 2005). These studies have proposed that this property could allow networks of inhibitory interneurons connected by electrical and chemical synapses to be sensitive to the degree of synchrony among their excitatory inputs, in other words, to detect coincidence (Galarreta and Hestrin, 2001). Then, when coincident inputs impact different GABA-releasing cells, synchronous spiking will be promoted by the mutual depolarization mediated by electrical synapses.

Recent studies by Vervaeke (2010) show that inhibitory coupling can also result in inhibition and derecruitment of neurones. This occurs as a result of the to low pass filtering through gap junctions of the afterhyperpolarization component of the action potential, allowing passage of the hyperpolarizing (AHP) component and decreasing the excitability. In addition, this effect is enhanced with out of phase spikes from afferent inputs or coupled cells arrriving to the same network, causing a net hyperpolarization instead of depolarization, with decrease activation of electrically coupled neurones.

Mixed synapses

Mixed synapses in lower vertebrates

The best studied system where mixed chemical-electrical synapses occur at nerve terminals is at club endings on Mauthner cell (M-cell) in goldfish, discovered by Furshpan (1964) and Nakajima (1974). Because of the nature of these neurons and the latencies from their input, electrophysiological recordings have been able to dissect the electrical and the chemical component in the EPSPs. The number of gap junctions per terminal ranges from 100-400, therefore the conductance and the size of the electrical component make electrical coupling more evident. In fish, the Mauthner cell system is used to elude predatory attack by producing a stereotyped escape behavior, which is characterized by a rapid and powerful unilateral bending of the body and tail that involves most of its somatic musculature (for review, see Korn and Faber, 2005). This behavior has a characteristic short latency when triggered by abrupt acoustic stimuli, and it is initiated by the activation of the M-cell. The M-cells are a pair of reticulospinal neurons located in the medulla of teleost fish (Beccari, 1907). These uncommonly large cells are anatomically and physiologically identifiable and have historically constituted a valuable preparation for the study of the cellular correlates of behavior (Faber et al., 1989). Their characteristically large myelinated axons, first noticed by Mauthner (1859), cross the midline and descend the length of the spinal cord, issuing axon collaterals that massively activate cranial and spinal motor systems via reliable (with high safety factor) chemical synapses (Faber et al, 1989). Such an anatomical arrangement allows a single action potential in this cell to initiate an escape response by producing a tail-flip.

Separate intracellular recordings from the pre- and postsynaptic club ending and M-cell elements demonstrated the electrotonic flow of current in both directions across gap junctions (Furshpan, 1964). Furthermore, EM data further suggested that these junctions are, in fact, morphologically mixed, providing for both electrical and chemical transmission (Nakajima, 1974). Since then, electrical coupling has been found in an increasing number of central structures in mammals, although morphologically mixed synapses in mammalian CNS structures have only rarely been found. It is well established that the lateral vestibular nucleus represents one example (Korn et al 1973).

At the Goldfish Mauthner cell, the combined morphological and electrophysiological accessibility of the M-cell, and of its auditory afferents, have allowed the best in-depth study of properties of mixed synapses. For example, recordings in this system proved the hypothesis of dual transmission at single terminals (Lin and Faber, 1988) and demonstrated that electrical transmission is amplified by a subthreshold voltage-dependent sodium current in the presynaptic endings, a mechanism that could be important in cases of weak coupling between dendrites (Curti and Pereda, 2004).

The eight nerve afferents that give rise to the club endings send a single unbranched axon to the M-cell. These endings are segregated to a region 200 to 350 um lateral to the soma, and each terminal contains a number of centrally located gap junctions, which are collections or plaques of intercellular channels, surrounded by a circumferential ring of chemical active zones and clusters of small clear vesicles (Nakajima and Kohno, 1978). A number of studies suggest that these chemical synapses are glutamatergic (Wolszon and Faber, 1988; Sur et al, 1994). Consequently, extracellular stimulation of the eight nerve evokes a compound response in the lateral dendrite (Furshpan, 1964; Faber et al, 1980), with an initial electrotonic or coupling potential followed by a chemically mediated excitatory postsynaptic potential (EPSP). Since the Mauthner cell's membrane time constant is only about 400 to 500 □s (Fukami et al, 1965; Furukawa, 1966; Faber and Korn, 1982), both responses are reasonably fast. Specifically, the waveform of the coupling potential essentially mirrors that of a presynaptic action potential, and the EPSP time course parallels that of the underlying conductance change, which decays with a time constant of 1 to 2 ms (Lin and Faber, 1988). The response to eight-nerve stimulation is typically characterized by an amplitude ratio of 3-4:1, with the coupling potential being as large as 20 mV

when the chemical component is but 5 to 7 mV. That is, electrotonic coupling would seem to be the more effective mode of transmission. Thus, it is a little surprising that the orthodromic spike tends to be triggered by the EPSP, possibly due to the short duration of the coupling potential or membrane non-linearilities (Faber and Korn, 1986).

The presence of a coupling potential evoked in the lateral dendrite by a presynaptic action potential makes it possible to reliably perform simultaneous paired pre-and postsynaptic recordings with a presynaptic electrode located at the presynaptic terminal. In either case, the recording site is less than one space constant from the terminal. Identification of the afferents on the basis of this electrophysiological criterion alone was validated by intraxonal injections of horseradish peroxidase, where the stained fibers always terminated on the M-cell lateral dendrite as club endings (Lin and Faber, 1988). Interestingly, more than 60% of these chemical synapses were silent, such that a presynaptic action potential only produced a coupling potential. However, this feature has been related to the presence of paired-pulse facilitation, also called long-term potentiation after high frequency stimulation (Lin and Faber, 1988).

Mixed synapses in mammalian systems

Electrotonic coupling between neurons in the mammalian brain, suggested by some very early evidence (Nelson, 1966; Ogden, 1966), was clearly demonstrated physiologically for the first time in the case of cells in the mesencephalic nucleus of the Vth nerve of the rat, where about 10% of the neurons were found to be coupled (Baker and Llinas, 1971). Work done by neuroanatomists at the time led them to the discovery of another synaptic structure in mammaliam systems, the mixed synapse. The first report on mixed synapses in the mammalian CNS was by Sotelo and Palay (1970), illustrated in Fig. 8. A subsequent study by Korn et al (1973) demonstrated electrotonic potentials occurring prior to EPSPs and confirming EM ultrastructural data in Deiters giant neurons of the lateral vestibular nucleus (LVN) in rat (Fig. 2). Since then, the search for more examples of mixed synapses in other nuclei in the mammalian CNS has continued. Examples of antidromic interaction between motoneurones and presynaptic terminals were found in cat spinal cord (Decima and Goldberg, 1969; Eccles et al, 1962), similar to those observed in lower vertebrate preparations (Shapovalov 1979). Later studies confirmed the phenomena with different electrophysiological approaches (Curtis and Lodge, 1979), where it was observed that PAD increased in relation to the stimulation of the motor ventral axons.

Ultrastructural evidence of mixed synapses was needed in order to confirm previous electrophysiological findings in the spinal cord, but it was not until the last decade that the use of electron microscopy was improved by implementing freeze-fracture, allowing scans of hundreds of gap junctions at synapses, and increasing the likelihood of observing and quantifying these structures. This approach, developed by Fujimoto (1995), was then used to map the brain and spinal cord. Synaptic structures forming mixed synapses were found in the spinal cord ventral horn, and different patterns of mixed synapses (Fig. 3) were observed on interneurons and motoneurones (Rash et al, 1996). Still, this study did not permit identification of the neurons presenting mixed synapses, nor were the source of the presynaptic terminals forming these synapses identified.

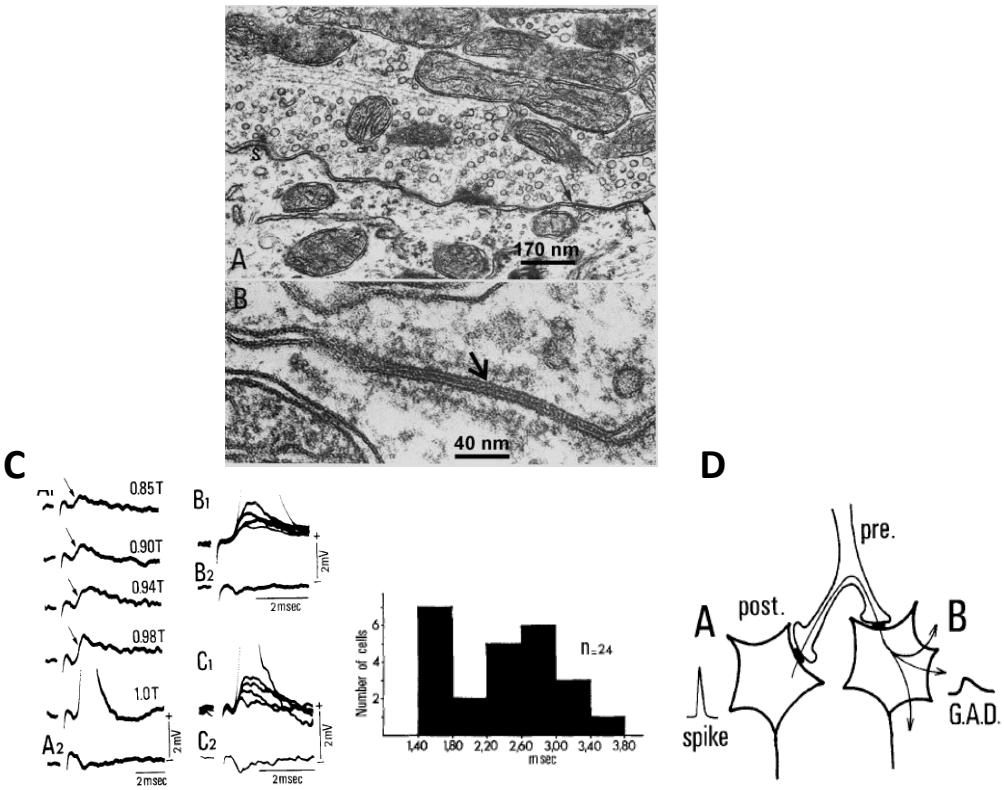

Figure 2. Evidence for the presence of mixed synapses in the lateral vestibular nuclei in adult rat. A: electron micrograph of a large axon terminal synapsing on the perikaryon of a giant cell. Two types of junctional complexes are localized at this synoptic interface constituting a "mixed synapse". At the left an "active" zone (S) with its associated dense projections and vesieles is shown. At the right the opposed plasma membranes converge into a "gap" junction

(arrows). • 59,000. B: high magnification of a "gap" junction between another large axon terminal and the perikaryon of another cell. There is a seven-layered structure of the junction and the layers of semidense cytoplasmic material undercoating the junction on each side. x 230,000 (A-B). Bottom panel (C): top to bottom are successive traces obtained with increasing spinal stimuli. As the stimulus strength is increased from 0.85 to 0.98 T a graded depolarization increases to a peak amplitude of about 1.5 mV; a 1.0 T stimulus evokes an antidromic spike. Histogram of the distribution of the graded antidromic depolarizations (G.A.Ds) delayed onset relative to the foot of the antidromic spike, in 37 neurons. Mean time interval was found to be 55 microseconds. Bottom right panel (D): Schematic model of electrotonic coupling by collaterals of one presynaptic fiber. Two post synaptic Deiter neurons A and B are shown to be coupled via two presynaptic terminals (Korn et al 1973; with permission from the Journal).

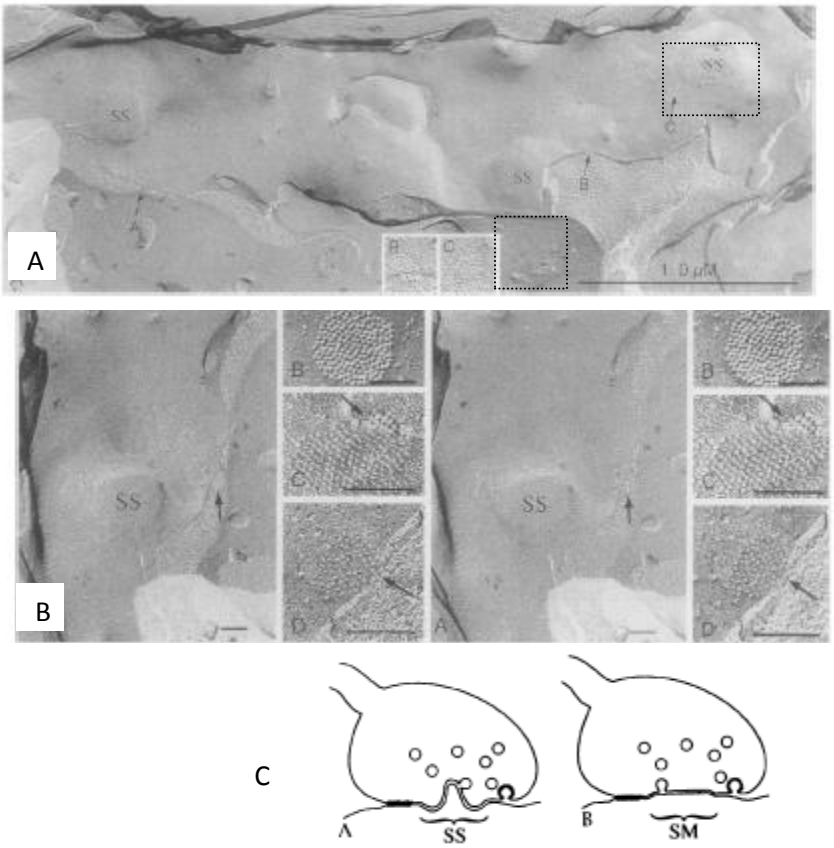

Figure 3. Mixed synapses in adult rat spinal cord. A) Mixed synapse with three active zones designated synaptic sombreros (SS), each with a gap junction (arrows A-C) in the "brim" of the sombrero. Gap junctions are defined by the presence of 7- to 9-nm P-face particles and/or E-face pits in distinctive hexagonal arrays (A) top panels B and C). Bottom panels represent two inset images of two of the gap junctions from (top panels B and C) at higher magnification. Higher magnification stereoscopic image of each inset shows two synaptic sombreros from adult rat spinal cord shown in (B, bottom panels B, C and D) respectively. Note the distinctive raised central "crown" and equally distinctive surrounding brim. Note within the brim there is an irregular gap junction (B-D). C) Drawings of two types of mixed synapses, one with deeply invaginated active zones called synaptic sombreros (A) and one with broader, flatter active zones ("synaptic mesas") (B). Gap junctions are often observed near exocytotic/endocytotic profiles (B) (Rash et al 1996) PNAS copyright.

Electrical synapses in the spinal cord

In the spinal cord, electrical coupling has been found between motoneurones (Gogan et al; 1977; Fulton and Walton, 1986; Walton and Navarrete, 1991; Mentis et al., 2002; Coleman and Sengelaub, 2004; Tresch and Kiehn, 2000) and between parasympathetic preganglionic neurons (Logan et al, 1996). In situ hybridization studies of Cx36 RNA expression in spinal cord showed that Cx36 expression is abundant in motoneurones and dorsal horn neurons during the first postnatal week, and absent in adult stages (Chang et al, 1999). Other studies demonstrated that spinal cord injury causes up regulation of Cx36 protein in the spinal cord (Yates et al, 2009).

Revealing primary afferent terminals in the spinal cord

The second part of the thesis will employ an anatomical method to reveal the sites of termination of primary sensory afferents in the cord. Sensory neurotransmission from primary afferents onto spinal neurons appears to be largely mediated by glutamate. Thus, considerable effort has been focused on the identification of glutamatergic markers in the spinal cord, specifically in relation to sensory afferents. There is extensive physiological evidence of AMPA- and NMDA-mediated

synaptic responses in spinal neurons evoked by dorsal root afferent stimulation (Salt and Hill, 1983; Jessell et al., 1986; Schneider and Perl, 1994; Li et al., 1998) and the presence of AMPA and NMDA receptor subunit immunoreactivities postsynaptic to spinal sensory synapses (Alvarez et al., 1994; Popratiloff et al., 1996, 1998a, b).

Immunohistochemical localization of glutamate, glutaminase, or the expression of reuptake transporters for excitatory amino acids has been used for this purpose (Barbaresi et al, 1985; De Biasi and Rustioni, 1988, 1990; Battaglia and Rustioni, 1988; Broman et al, 1993; Valtschanoff et al, 1994). Unfortunately, interpretation of immunopositive boutons is complicated because of the existence of significant metabolic pools of glutamate and glutaminase that are unrelated to neurotransmission (De Biasi and Rustioni, 1990; Storm-Mathisen et al, 1995). Glutamate reuptake transporters are also not specific markers; they are widely expressed by inhibitory neurons and glia (Masson et al, 1999). Nevertheless, synaptic terminals of spinal sensory afferents are strongly immunoreactive for glutamate, suggesting a glutamatergic function (De Biasi and Rustioni, 1988, 1990; Broman et al., 1993; Valtschanoff et al., 1994). This conclusion is corroborated by extensive pharmacological studies on Ia EPSP´s using glutamatergic blockers through NMDA and AMPA antagonists (Alvarez et al, 1994; Popratiloff et al, 1996, 1998).

Recent discovery of multiple vesicular glutamate transporters (vglut) has provided reliable markers for glutamatergic synapses; their presence is a strong indication that glutamate is accumulated in vesicles from which it can be released. However, the diversity of vglut isoforms raises questions about the significance of synaptic vesicle heterogeneity in glutamatergic synapses. Two major vglut transporters were first identified, vglut-1 and vglut-2. They were found associated with synaptic vesicles in excitatory terminals and selectively accumulate glutamate and confer glutamate release properties to transfected cells or neurons (Bellochio et al, 1998, 2000; Takamori et al, 2000, 2001; Aihara et al, 2000; Bai et al, 2001; Fujiyama et al, 2001; Fremeau et al, 2001; Herzog et al, 2001; Varoqui et al, 1999, 2002). Extensive immunolocalization and in situ hybridization studies have concluded that vglut-1 and vglut-2 are expressed by different neurons, projection systems, and synaptic terminals in the brain (Hisano et al, 2000; Sakata-Haga et al, 2001; Kaneko et al, 2002; Ziegler et al, 2002).

In the second part of this thesis we made use of antibodies for vglut1 in order to identify primary afferent terminals. Although vglut-1 has been consistently found in terminals from primary

afferents (Alvarez et al 2004), a recent study shows that at least 98% of the terminals from corticospinal tract are also positive for vglut-1. Interestingly no other descending tracts such as vestibulospinal or rubrospinal have shown to be positive (Shresta et al, 2012a,b).

Rationale for investigating electrical and mixed synapses in the spinal cord

Overall, this dissertation presents a body of work describing evidence for a role of electrical synapses between neurons that mediate presynaptic inhibition of sensory reflexes, and the first evidence showing morphologically mixed synapses between primary afferents and neurones in mammalian spinal cord. Section 1 characterizes an in vitro model of presynaptic inhibition in juvenile mice. I used this model to study presynaptic inhibition in Cx36 knockout mice, where neuronal gap junctions are largely absent. Section 2 involves an evaluation of connexin (Cx26, Cx32, Cx36, Cx37, Cx40, Cx43, Cx45) expression and association with motoneurons in rodent spinal cord. Section 3 describes anatomical findings in the adult mouse and rat regarding the presence of mixed synapses formed by primary afferents, and section 4 examine the presence of purely electrical synapses in sexually dimorphic spinal cord motor nuclei.

Section 1. Requirement of neuronal connexin36 in pathways mediating presynaptic inhibition of primary afferents in functionally mature mouse spinal cord

1.1. Hypothesis: Gap junctions are involved in gabaergic presynaptic inhibition of the monosynaptic reflex.

Experimental approach: Colonies of C57/B6-129SvEv wild-type and Cx36 ko mice were established at the University of Manitoba through generous provision of wild-type and Cx36 knockout (ko) breeding pairs from Dr. David Paul (Harvard). A total of nineteen wild-type mice and twenty-two Cx36 ko mice at postnatal 8-11 days of age were used for electrophysiological studies. *In vitro* experiments were performed on 7 Wistar rats PD10-15 using procedures similar to those described in the mouse. Extracellular recordings *in vitro* of the ventral and dorsal spinal roots were used to assess presynaptic inhibition of monosynaptic reflexes and DRPs. Sensory evoked presynaptic inhibition was produced by conditioning stimulation of one dorsal root while stimulating an adjacent dorsal root to evoke a ventral root monosynaptic reflex. Five measures of presynaptic inhibition were used and compared to results in the literature using in vivo cat experiments: DRP duration; CDP amplitude and later components; pharmacological $GABA_A$ blockade with bicuculline; time course and pharmacology of sensory evoked presynaptic inhibition of the MSR and primary afferent excitability test (using a modification of Wall technique). See Bautista et al (2012).

1.2. Conclusions: The results in wild-type animals are the first demonstration of the physiology of a presynaptic inhibitory system in mice. The results in wild-type were then compared to those obtained under identical conditions in Cx 36-/- mice. We provide the first demonstration for an involvement of Cx36 in processes that govern presynaptic inhibition of primary afferent terminals. In spinal cord preparations of 9-11 day old mice, the duration of dorsal root potentials (DRPs) evoked by low intensity dorsal root stimulation was reduced by 79% in cords from Cx36 knockout (ko) mice and to a similar degree by gap junction blockers in cords from wild-type mice. Conditioning stimulation of an adjacent dorsal root inhibited monosynaptic ventral root reflexes in wild types, but failed to do so in Cx36 ko cords. The long duration of this inhibition and its antagonism by bicuculline is consistent with a presynaptic inhibition of group Ia afferent terminals on motoneurons. Our results using both physiological and pharmacological approaches

show that this system is very similar to the presynaptic inhibition described in adult cats (Eccles et al, 1963). The results in Cx 36-/- mice provide the first suggestion for an involvement of electrical communication between interneurons in the presynaptic inhibition of the mammalian monosynaptic reflex.

JPn Neuroscience
The Journal of Physiology

Requirement of neuronal connexin36 in pathways mediating presynaptic inhibition of primary afferents in functionally mature mouse spinal cord

Wendy Bautista, James I. Nagy, Yue Dai and David A. McCrea

Spinal Cord Research Centre, University of Manitoba, Winnipeg, Manitoba R3E 0J9, Canada

Key points

- Reflexes evoked by sensory information from muscles and skin play an important role in controlling muscle activity during movement.
- The strength of these reflexes is regulated in part by presynaptic inhibition, a process controlling the release of chemical transmitters from sensory fibres terminating on spinal neurones.
- Our study is the first to show that electrical synapses among spinal neurones in young animals are essential for normal operation of processes that presynaptically regulate synaptic transmission between large diameter sensory fibres and spinal cord neurones.
- Transgenic mice lacking connexin36, a protein that mediates electrical communication via gap junctions between neurones, suffer a severe impairment of presynaptic inhibition and a similar impairment can be produced in normal mice with drugs that disrupt gap junction function.
- The wide distribution of connexin36 in the spinal cord suggests that neuronal gap junctions also play a role in other physiological processes.

Abstract Electrical synapses formed by gap junctions containing connexin36 (Cx36) promote synchronous activity of interneurones in many regions of mammalian brain; however, there is limited information on the role of electrical synapses in spinal neuronal networks. Here we show that Cx36 is widely distributed in the spinal cord and is involved in mechanisms that govern presynaptic inhibition of primary afferent terminals. Electrophysiological recordings were made in spinal cord preparations from 8- to 11-day-old wild-type and Cx36 knockout mice. Several features associated with presynaptic inhibition evoked by conditioning stimulation of low threshold hindlimb afferents were substantially compromised in Cx36 knockout mice. Dorsal root potentials (DRPs) evoked by low intensity stimulation of sensory afferents were reduced in amplitude by 79% and in duration by 67% in Cx36 knockouts. DRPs were similarly affected in wild-types by bath application of gap junction blockers. Consistent with presynaptic inhibition of group Ia muscle spindle afferent terminals on motoneurones described in adult cats, conditioning stimulation of an adjacent dorsal root evoked a long duration inhibition of monosynaptic reflexes recorded from the ventral root in wild-type mice, and this inhibition was antagonized by bicuculline. The same conditioning stimulation failed to inhibit monosynaptic reflexes in Cx36 knockout mice. Immunofluorescence labelling for Cx36 was found throughout the dorsal and ventral horns of the spinal cord of juvenile mice and persisted in mature animals. In deep dorsal horn laminae, where interneurones involved in presynaptic inhibition of large diameter muscle afferents are located, cells were extensively dye-coupled following intracellular neurobiotin injection. Coupled cells displayed Cx36-positive puncta along their processes. Our results indicate that gap junctions formed by Cx36 in spinal cord are required for maintenance of

DOI: 10.1113/jphysiol.2011.225987

presynaptic inhibition, including the regulation of transmission from Ia muscle spindle afferents. In addition to a role in presynaptic inhibition in juvenile animals, the persistence of Cx36 expression among spinal neuronal populations in the adult mouse suggests that the contribution of electrical synapses to integrative processes in fully mature spinal cord may be as diverse as that found in other areas of the CNS.

(Received 9 December 2011; accepted after revision 17 May 2012; first published online 21 May 2012)

Corresponding author D. A. McCrea: Department of Physiology, Faculty of Medicine, University of Manitoba, 745 Bannatyne Avenue, Winnipeg, Manitoba, R3E 0J9, Canada. Email: dave@scrc.umanitoba.ca

Abbreviations CDP, cord dorsum potential; Cx36, connexin36; DRP, dorsal root potential; L, lumbar; MSR, monosynaptic reflex; P, postnatal day; PAD, primary afferent depolarization; T, multiples of the weakest electrical current capable of exciting lowest threshold afferent fibres.

Introduction

It is well established that transmitter release from terminals of primary afferents in the spinal cord is subject to regulation by presynaptic inhibition (Rudomin & Schmidt, 1999). In the case of the monosynaptic reflex (MSR), the prevailing view is that presynaptic inhibition is mediated by GABAergic spinal interneurones that are located in laminae V–VI and that form axo-axonic synapses on the terminals of Ia muscle spindle afferents, as has been well established in cat (Maxwell *et al.* 1990; see Rudomin, 2009) and more recently in rodent (Hughes *et al.* 2005). Activation of these GABAergic neurones by excitatory spinal interneurones receiving large diameter muscle afferent input results in a depolarization of Ia afferent terminals and a presynaptic reduction in the monosynaptic excitation of motoneurones by Ia afferents. Afferent fibre terminal depolarization during presynaptic inhibition can be recorded extracellularly as the dorsal root potential (DRP) or intra-axonally from afferent fibres as primary afferent depolarization (PAD). PAD can also be inferred when current pulses delivered within the spinal cord become more effective in activating afferent fibres, i.e. by the Wall technique (see Willis, 2006). An important feature of presynaptic inhibition of muscle afferents is that the activity of the last order interneurones that mediate this inhibition via contact with intraspinal afferent terminals appears to be highly synchronized even though these interneurones are distributed over large distances in the spinal cord (Lidierth & Wall, 1996; see Rudomin, 2009). Here we sought to determine whether electrical coupling might play a role in the synchronization of spinal interneurones involved in the presynaptic inhibition of large diameter sensory afferents.

The occurrence and functional importance of electrical synaptic transmission between neurones in the mammalian brain has been documented in numerous studies (reviewed in Nagy & Dermietzel, 2000; Bennett & Zukin, 2004; Hormuzdi *et al.* 2004: Meier & Dermietzel, 2006). The ultrastructural correlate of electrical synapses is the gap junction, a structure composed of channel-forming connexin proteins that link the cytoplasmic compartments of coupled cells and allow cell-to-cell passage of ions, metabolites and tracer dyes (see Bennett, 1997). Among the connexin family of proteins that form gap junctions, Cx36 is selectively and most widely expressed in neurones, and has been localized ultrastructurally at inter-neuronal gap junctions (Rash *et al.* 2001*a*, 2007*a*,*b*; see Nagy *et al.* 2004). Electrical synapses mediate communication between diverse types of neurones and often occur between ensembles of GABAergic inhibitory interneurones (see Connors and Long, 2004). It is widely accepted that gap junctions between GABAergic neurones contribute to synchronizing neuronal membrane oscillations and promote synchronous network activity in various brain areas, including the cerebral cortex, hippocampus, reticular thalamic nucleus and cerebellum (reviewed in Connors & Long, 2004; Meier & Dermietzel, 2006). Gap junctions and electrical coupling between neurones have also been described in the mammalian spinal cord (Rash *et al.* 1996; Kiehn & Tresch, 2002; Lemieux *et al.* 2010), including between motoneurones in rat during development (Chang *et al.* 1999), between sexually dimorphic motoneurones (Coleman & Sengelaub, 2002), between Hb9 interneurones (Hinckley & Ziskind-Conhaim, 2006; Wilson *et al.* 2007), between preganglionic sympathetic neurones (Logan *et al.* 1996) and between motoneurones in the adult cat (Gogan *et al.* 1977). Overall, however, the role of electrical synapses formed by gap junctions in spinal cord is poorly understood, as is the involvement of Cx36 in the formation of these synapses.

In the present investigation, we explored the possibility that Cx36-containing gap junctions between spinal interneurones play a role in mechanisms associated with sensory-evoked presynaptic inhibition. *In vitro* experiments were performed in postnatal (P) 8- to 11-day-old wild-type and Cx36 knockout mice. In wild-type mice at these juvenile ages, motor systems are well developed and functionally mature; and unlike younger animals, the animal walks freely, supports its body weight and maintains its torso above the walking

surface (Jiang *et al.* 1999; Hinckley & Ziskind-Condhaim, 2006). Similarly, our casual observations are that the Cx36 knockouts move freely in their cages and can support their body weight during quadrupedal locomotion. However, a detailed characterization of phenotype in juvenile Cx36 knockout mice is not available. Nevertheless, the impact of Cx36 absence on adult mouse motor phenotype includes impairments in the olivary-cerebellar system (Van Der Glessen *et al.* 2008), in coherence of motoneurone firing during harmaline-induced tremor (Placantonakis *et al.* 2004) and in sensory-motor learning (Frisch *et al.* 2005; Zlomuzica *et al.* 2012). The use of juvenile animals allowed us to perform *in vitro* whole cord electrophysiological investigations of functionally mature spinal motor systems. Some results have been presented in abstract form (McCrea *et al.* 2009).

Methods

All experimental procedures were approved by University of Manitoba Central Animal Care Services and conformed to standards of the Canadian Council on Animal Care, with minimization of the number of animals used. All procedures also complied with the policies of *The Journal of Physiology* (Drummond, 2009) and UK regulations on animal experimentation.

Animals

Colonies of wild-type and Cx36 knockout mice, developed from C57/BL6–129SvEv mixed background (Deans *et al.* 2001), were established at the University of Manitoba through generous provision of wild-type and Cx36 knockout breeding pairs from Dr David Paul (Harvard). A total of 19 wild-type and 22 Cx36 knockout mice from ages P8–11 were used for *in vitro* electrophysiological studies. In addition, *in vitro* experiments were performed on seven P10–15 Wistar rats using procedures similar to those described in the mouse. Immunohistochemical studies used an additional nine wild-type and four Cx36 knockout mice at P8–11, and 10 wild-type and two Cx36 knockout adult (P50–55) mice.

Electrophysiological recordings and analysis

Animals were anaesthetized by intraperitoneal administration of ketamine/xylazine (100 mg kg^{-1} diluted in 0.9% saline), decapitated and eviscerated. The remaining tissue was placed in a dissection chamber and superfused continuously with cold oxygenated (95% O_2, 5% CO_2) artificial cerebrospinal fluid (ACSF) containing (in mM) NaCl (128), KCl (4), $CaCl_2$ (1.5), $MgSO_4$ (1), Na_2HPO_4 (0.5), $NaHCO_3$ (21) and D-glucose (30). The spinal cord was exposed by removing surrounding bone using a ventral approach, sparing as much of the cauda equina as possible. Ventral and dorsal roots were cut near the dorsal root ganglia. The spinal cord was transected at T3 and removed from the vertebral column. The isolated spinal cord was kept in cold ACSF for 30 min before transfer to a recording chamber dorsal side up, where it was superfused with oxygenated ACSF. The bath solution was heated gradually to 27°C.

Dorsal root potentials and monosynaptic reflexes were recorded with glass suction electrodes. Extracellular potentials were amplified 2000 times, band pass filtered (−3 db at 0.01 Hz and 300 Hz) and digitized at 2.5 kHz. Single shock stimuli were delivered to dorsal roots through suction electrodes using rectangular, constant current, 0.2 ms duration pulses. Stimulus intensity was expressed in multiples of the threshold current (T) for the afferent volley recorded on the cord dorsum (Fig. 1*Aa*).

Averages of the responses to 8–10 stimulus presentations were created off-line. Single shocks to the L2 dorsal root were delivered once every 10 s to evoke DRPs in the L3 dorsal root. In two experiments the DRP was recorded in L4 following L3 root stimulation. For the conditioning–test paradigm used for inhibition of the MSR, a suction electrode was placed on the L3 ventral root to record the MSR evoked by L3 dorsal root stimulation (the test stimulus, see Fig. 1*Ab*). Conditioning stimulation was delivered to the L2 dorsal root at intervals ranging from 5 to 200 ms preceding the test shock to inhibit the L3 MSR. Stimuli were delivered once every 2 s and presented in an alternating sequence of test stimulus alone followed by combined conditioning and test stimulation. Data analysis was performed using Origin Pro 7 (OriginLab Corp., Northampton, MA, USA) and traces were imported to Corel Draw for assembly of the figures.

PAD was assessed by monitoring changes in the excitability of intraspinal afferent fibre terminals in four wild-type and four Cx36 knockout mice. A monopolar, 15 μm diameter, tungsten electrode was inserted about 300 μm below the dorsal surface of the spinal cord and about half-way between the midline and the dorsal root entry zone (approximately 200–400 μm from the midline, see Fig. 8*A*). This electrode was used to deliver single 0.2 ms duration stimulus pulses for antidromic activation of afferent fibres (the test stimulus). The strength of the test stimulus (typically 5–7 μA) was adjusted to 1.5T for the antidromic volley recorded with a glass suction electrode on the dorsal root in the same spinal cord segment (L3 or L4). A second suction electrode on an adjacent caudal dorsal root was used to deliver (at 1.5T) conditioning stimulation. The condition–test interval was varied from 35 to 200 ms and conditioned and unconditioned test responses were averaged ($n = 18$) and plotted. An increase in the antidromic signal following conditioning stimulation of an adjacent dorsal root (1.5T, conditioning stimulus) was interpreted as an increase in

intraspinal terminal excitability caused by depolarization of afferent terminals, i.e. PAD.

Significant differences were assessed using Student's *t* test. The *P* criterion for significance was 0.05. Means are reported with standard error of the mean (SEM).

Drugs

All drugs were bath applied in the oxygenated recording chamber. Data collection did not begin until at least 30 min after drug application or drug washout. Final concentrations of applied agents were as follows: bicuculline 20 μM (Sigma-Aldrich), carbenoxolone 100 μM, and strychnine 10 μM. Mefloquine at a concentration of 5 μM was first dissolved in DMSO and then diluted in ACSF to yield a 0.1% concentration of DMSO. Controls experiments for mefloquine were done with bath application of 0.1% DMSO.

Neurobiotin injections

Slices from mouse spinal cord were prepared as previously described (Carlin *et al.* 2000; Dai *et al.* 2009). Briefly, 300 μm thick transverse slices from lumbar levels were cut using a vibrating blade microtome and maintained in the ACSF for 1 h. The slices were then transferred to a patch-clamp recording chamber mounted on the stage of an upright Olympus BX50 microscope fitted with differential interference contrast optics and epifluorescence. The chamber was perfused with ACSF at a rate of 2 ml min^{-1}, and oxygenated with 95% O_2, 5% CO_2. Neurones located in lamina IV–VI were visualized using infrared illumination and images were collected using a Hamamatsu camera controller C2400 (Bridgewater, NJ, USA) and Argus image processor. Patch electrodes fabricated from borosilicate glass (5–8 MΩ) were filled with intracellular recording solution containing (in mM): $KMeSO_4$ (150), NaCl (10), Hepes (10), EGTA (0.1), Mg-ATP (3), GTP (0.3), and 3% neurobiotin. Visualized neurones were patched and data acquired using a MultiClamp 700A patch-clamp amplifier (Molecular Devices, Sunnyvale, CA, USA). Whole cell patch recordings were made in current-clamp mode and six depolarizing square pulses (0–60 pA, 3 s duration) were applied for intracellular passage of neurobiotin. Negative pressure was used on the pipette before impalement and making the gigohm seal to prevent leakage extracellularly.

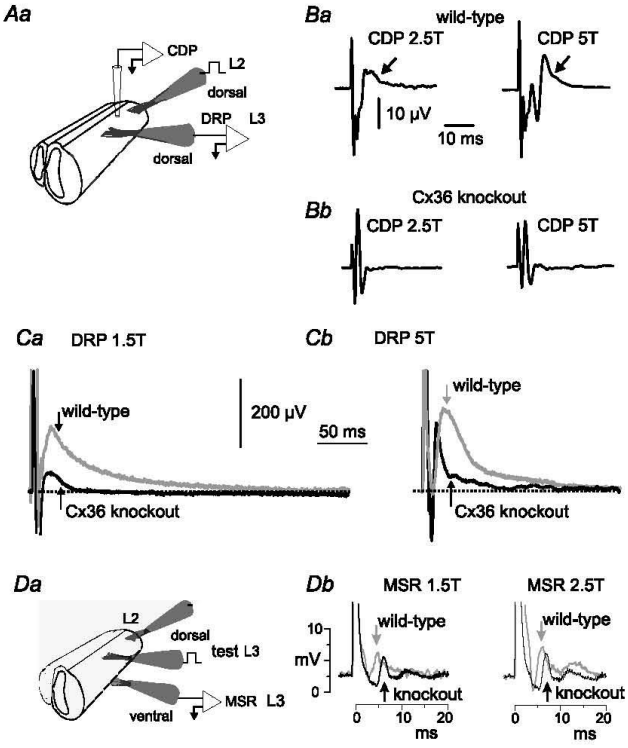

Figure 1. Experimental setup and comparison of CDP, DRP and MSR in P8–11 wild-type and Cx36 knockout mice
Aa, schematic diagram of set-up for evoking the cord dorsum potential (CDP) and dorsal root potential (DRP). *B*, CDP recorded from wild-type (*Ba*) and knockout mice (*Bb*), evoked by stimulation of the L2 dorsal root at 2.5 and 5 times the intensity of threshold for the most excitable afferents (*T*) using a rectangular current pulse 0.2 ms in duration. Arrows indicate the longer latency components seen in wild-type mice, but which are absent in Cx36 knockout mice. *C*, DRP recorded in L3 from a P10 wild-type mouse (grey trace) following single shock stimulation at 1.5*T* (*Ca*) and 5*T* (*Cb*) of the L2 dorsal root overlaid on the DRP from a Cx36 knockout mouse (*Ca* and *Cb*, black trace). The DRP is attenuated and short lasting in mice lacking Cx36. *Da*, schematic diagram of set-up for evoking monosynaptic reflexes (MSRs) in L3 and for stimulation of the L2 dorsal root for evaluating the effects of conditioning stimulation on the monosynaptic reflex. *Db*, reflexes recorded from the L3 ventral root evoked by stimulation of the L3 dorsal root. Grey traces, averaged responses from a wild-type mouse; black traces, from a Cx36 knockout mouse. Arrows indicate the point of MSR amplitude measurement. In this and following figures, stimulus artefacts are truncated for illustration purposes.

The slices were then immersion fixed for 20 min in cold 0.16 M sodium phosphate buffer, pH 7.1, containing 2% freshly depolymerized paraformaldehyde and 0.2% picric acid, and then transferred to 10 ml of 25 mM sodium phosphate buffer, pH 7.1, containing 10% sucrose. Slices were sectioned at a thickness of 15 μm using a cryostat. Sections were blocked by incubation in 10% normal goat serum for 30 min, then incubated for 1.5 h with streptavidin-conjugated AlexaFluor-488 (Jackson Immunoresearch Laboratories Inc.,West Grove, PA, USA) diluted 1:2000 in 50 mM Tris-HCl buffer, pH 7.4, containing 1.5% sodium chloride and 0.3% Triton X-100 (TBSTr) to detect neurobiotin. The sections were then processed for immunohistochemical detection of Cx36, as described below.

Immunohistochemistry

Juvenile and adult mice were deeply anaesthetized by intraperitoneal injection of ketamine/xylazine (100 mg kg^{-1} in 0.9% saline solution) and decapitated. Spinal cords were removed after exposure following laminectomy, immersion fixed for 20 min in 40 ml of cold 0.16 M sodium phosphate buffer, pH 7.1, containing 2% freshly depolymerized paraformaldehyde and 0.2% picric acid, and cryoprotected for at least 24 h in 10 ml of 25 mM sodium phosphate buffer, pH 7.4, containing 10% sucrose. Sections of lumbar regions of the spinal cord were cut at a thickness of 10 μm using a cryostat, collected on gelatinized glass slides and stored at –34°C until use. Sections were thawed, washed for 20 min in TBSTr, and then incubated for 24 h at 4°C with mouse monoclonal antibody against Cx36 (Invitrogen/Zymed Laboratories, Carlsbad, CA, USA) diluted to 2 μg ml^{-1} in TBSTr containing 5% normal donkey serum. Sections were then washed for 1 h in TBSTr and incubated for 1.5 h at room temperature with Cy3-conjugated goat anti-mouse IgG (Jackson ImmunoResearch Laboratories) diluted 1:200 in TBSTr. After secondary antibody incubations, sections were washed in TBSTr for 20 min, followed by two 15 min washes in 50 mM Tris-HCl buffer, pH 7.4, and coverslipped after application of antifade medium. For double immunofluorescence labelling, sections were incubated with rabbit polyclonal anti-peripherin (Chemicon, Temecula, CA, USA) and simultaneously with mouse monoclonal anti-Cx36 for 24 h at 4°C. Sections were then washed in TBSTr for 1 h at room temperature and incubated for 1 h simultaneously with Alexa Fluor 488-conjugated goat anti-rabbit IgG (Molecular Probes, Eugene, OR, USA) diluted 1:1000, in combination with Cy3-conjugated goat anti-mouse IgG (Jackson ImmunoResearch Laboratories) diluted 1:200. Prior to coverslipping, some sections processed for immunolabelling of Cx36 were counterstained with green Nissl fluorescent NeuroTrace (stain N21480; Molecular Probes, Eugene, OR, USA). Fluorescence was examined on a Zeiss Axioskop2 fluorescence microscope with image capture using Axiovision 3.0 software (Carl Zeiss Canada, Toronto, Ontario, Canada), or an Olympus Fluoview IX70 confocal microscope with image capture using Olympus Fluoview software (Markham, Ontario, Canada). Adobe Photoshop and Corel Draw software (Corel Corp., Ottawa, Ontario, Canada) were used for image analyses.

Results

Characteristics of DRP, CDP, MSR inhibition and PAD in wild-type mice

Much of our present knowledge of the organization, mechanism and operation of presynaptic inhibition in the spinal cord originates from observations made over many years in adult cats. The physiology and pharmacology of spinal presynaptic inhibitory systems in juvenile mouse have not been systematically analysed. Therefore, before exploring a potential role of Cx36 in these systems, we first determined whether presynaptic inhibition in the juvenile mouse displays features similar to those described in the adult cat.

The cord dorsum potential (CDP) recorded from the surface of the spinal cord was used as a reference from which to measure latencies, to determine stimulus intensity and to assess activity of dorsally located spinal neurones. Using the recording set-up described in Fig. 1*Aa*, representative CDPs shown in Fig. 1*Ba* from a wild-type mouse were produced by single-shock L2 dorsal root stimulation at 2.5 and 5 times the intensity required for activation of the lowest threshold afferents (*T*). Note the later component (arrow) that follows the large initial and brief deflection produced by the arrival of the afferent volley. The longer latency CDP component reflects population activity in dorsal horn interneurones (Manjarrez *et al.* 2003), which increases with increased stimulus intensity (Fig. 1*Ba*, left and right).

In the cat, depolarization of spinal sensory afferent terminals during presynaptic inhibition produces the DRP – a long lasting, negative going, potential recorded from a dorsal spinal root (Rudomin & Schmidt, 1999; see Rudomin, 2009). Figure 1*Aa* shows the experimental set-up used to evoke DRPs in the *in vitro* preparation. An example of a DRP evoked by single shock stimulation of the L2 dorsal root and recorded in the L3 root in a wild-type P10 mouse is shown in Fig. 1*Ca* and *b* (grey traces). The duration of the DRP evoked by 1.5*T* stimulation was 235 ± 23 ms (SEM) ($n = 19$ preparations) in juvenile wild-type mice, with a time to peak of 25 ± 3 ms. These values are similar to those reported in the adult cat (Eccles *et al.* 1963) but somewhat shorter than values reported in the spinal cord of neonatal rat (Kremer & Lev-Tov, 1998). Increasing stimulus intensity

increased DRP amplitude (Fig. 1*Cb*). Because of the known involvement of GABAergic transmission in presynaptic inhibition and the DRP in the cat (Eccles *et al.* 1963; Rudomin *et al.* 1990) and the hamster (Bagust *et al.* 1985), the effects of bath application of the GABAa antagonist, bicuculline, were examined on the DRP in the juvenile mouse *in vitro* preparation. The traces in Fig. 2*A* (left) show a modest reduction in the amplitude of the 1.5*T* evoked DRP amplitude with bath application of bicuculline. On average (Fig. 2*A*, bar graphs) the peak amplitude of the DRP evoked by 1.5*T* stimulation was decreased by 21% and that of the DRP evoked by 2.5*T* was decreased by 36% ($n = 4$) by 20 μM bicuculline. These results in juvenile mice are in agreement with the actions of $GABA_A$ antagonists on the DRP in neonatal rat and mouse whole cord preparations (Kremer & Lev-Tov, 1998; Wong *et al.* 2001) and those in the cat using picrotoxin (Eccles *et al.* 1963; Rudomin *et al.* 1990) and bicuculline (Curtis *et al.* 1971), but the degree of depression is less than that reported in the hemisected spinal cord of neonatal (P7–14) rats (Shreckengost *et al.* 2010).

Single shock stimulation of the L3 dorsal root was used to evoke a monosynaptic reflex (MSR) recorded in the L3 ventral root (Fig. 1*Da*) using rectangular pulses of 0.2 ms. The grey trace in left panel of Fig. 1*Db* shows the averaged reflex response ($n = 5$) evoked by 1.5*T* stimulation in a wild-type mouse. Increasing the stimulus intensity to 2.5*T* (Fig. 1*Db*, right panel, grey trace) resulted in growth of the early component as well as a later component. Wang *et al.* (2008) using electrical stimulation of the peripheral nerve, determined that the central latency of monosynaptic EPSP onset in motoneurones in P7 mice is about 2.8 ms (4.3 ms total latency minus 1.5 ms afferent conduction time). The central latency of a disynaptic (inhibitory) pathway (Wang *et al.* 2008) is about 6.3 ms. In Fig. 1*Db*, the latency of the earliest reflex response, as measured from the onset of the stimulus artefact, and recorded from the activity of motoneurones in the ventral root, was 3.8 ms in a wild-type mouse and, therefore, clearly a monosynaptic reflex. The mean latency of the MSR in 16 wild-type mouse experiments was 3.67 ± 0.42 ms.

In the cat, presynaptic inhibition of extensor monosynaptic reflexes can be evoked by brief stimulus trains to a flexor nerve (see McCrea *et al.* 1990; Rudomin *et al.* 1990). In the present study, the peak amplitude of the L3 MSR (arrows Fig. 1*Db*) was measured in the absence of stimulation (control amplitude) and in the presence of a single shock to the L2 dorsal root (see Fig. 1*Da*) (conditioned amplitude). Conditioning stimulation of the L2 root at various intervals produced a long lasting inhibition of the L3 monosynaptic reflex. Figure 3*A* (squares) shows the average time course and magnitude of this inhibition in wild-type mice ($n = 6$). Single shock conditioning stimulation to the L2 dorsal root reduced the L3 monosynaptic reflex for more than 200 ms with a maximal inhibition at a conditioning–test interval of 50 ms. Inhibition at these long conditioning–test intervals is considered as more compatible with a presynaptic rather than a postsynaptic inhibition (e.g. Curtis *et al.* 1971). No attempt was made to enhance the inhibition of the MSR by increasing the number of conditioning stimulation shocks. The open circles in Fig. 3*A* are replotted data from Eccles *et al.* (1963) showing MSR inhibition evoked by a brief conditioning stimulus train to a flexor muscle nerve in the cat. Note the qualitative similarities in the time course and degree of MSR inhibition in the cat and juvenile wild-type mouse despite the differences in the species, age and stimulation parameters of the preparations.

Presynaptic inhibition of monosynaptic reflexes in the cat is antagonized by the $GABA_A$ blockers bicuculline (Curtis *et al.* 1971) and picrotoxin (Rudomin *et al.* 1990). Figure 3*B* shows the effects of bicuculline on long latency MSR inhibition in the wild-type juvenile mouse. Instead of inhibition, conditioning stimulation resulted in an

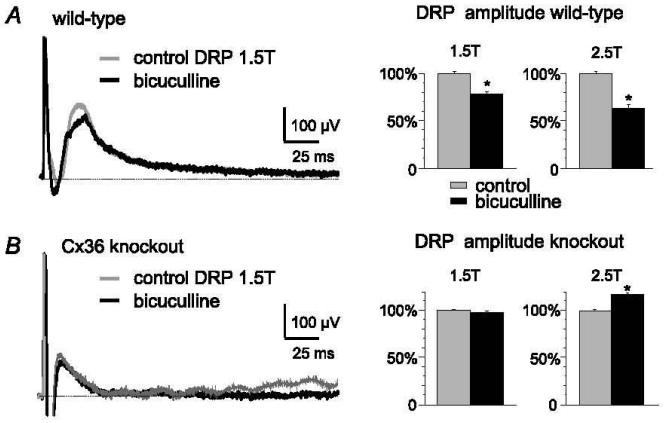

Figure 2. Effects of the $GABA_A$ antagonist bicuculline on DRPs
A and *B*, left, typical effects of bath application of 20 μM bicuculline on DRPs recorded in the fourth lumbar segment and evoked by 1.5*T* stimulation of the L3 dorsal root in wild-type mice (*A*) and Cx36 knockout mice (*B*). Right, bar graphs showing averaged effects of bicuculline on DRP amplitude from four experiments, with L3 dorsal root stimulation at 1.5*T* and 2.5*T* in wild-type mice (*A*) and Cx36 knockout mice (*B*). Results are expressed as means ± SEM; $^*P < 0.05$. The peak amplitudes of DRPs evoked by 1.5*T* and 2.5*T* stimulation were attenuated by bicuculline in wild-types (*A*, bar graphs), whereas the DRPs evoked by 1.5*T* stimulation were unaffected and those evoked by 2.5*T* stimulation were increased in knockouts (*B*).

enhancement of the MSR at longer conditioning–test intervals after bath application of 20 μM bicuculline. Bicuculline had no effect on the amplitude of the unconditioned MSR ($P = 0.81$, $n = 4$; not shown) and no effect on MSR latency (latency of 3.6 ms without bicuculline and 3.7 ms in the presence of bicuculline; $n = 4$). It is well known that conditioning stimulation can activate short-latency, postsynaptic glycinergically mediated inhibition of motoneurones. Bath application of the glycinergic blocker strychnine (10 μM) reduced MSR inhibition at short (5–20 ms) conditioning–test intervals (Curtis *et al.* 1971) but had little effect at longer intervals (not shown). The similarities of the actions of GABA antagonists and the time course of MSR inhibition in the mouse and cat suggest that the long duration inhibition evoked by low intensity dorsal root stimulation shown in Fig. 3*A* is presynaptic in origin. The shorter-latency effects of conditioning stimulation are presumably a mixture of presynaptic inhibition as well as postsynaptic inhibition and excitation (see Bagust *et al.* 1981).

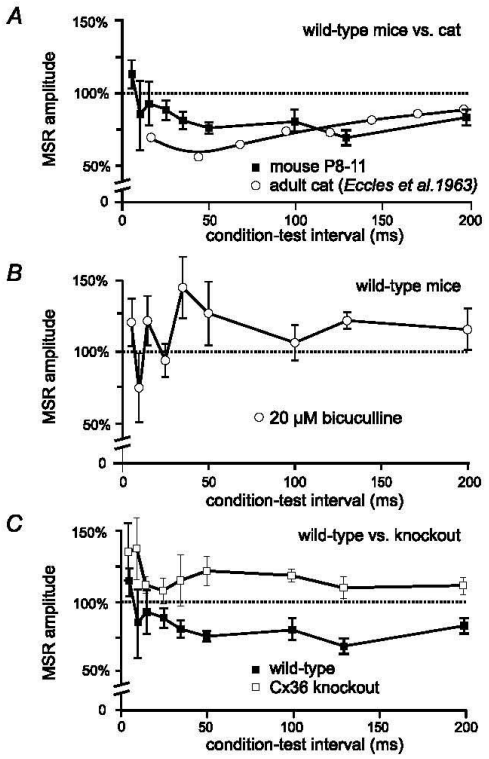

Figure 3. Effects of conditioning stimulation of the MSR in juvenile wild-type and Cx36 knockout mice
Using the paradigm outlined in Fig. 1*Da*, effects of a conditioning stimulus to the L2 dorsal root were examined on the MSR evoked by L3 dorsal root stimulation and recorded in the L3 ventral root. Normalized MSR amplitude is on the ordinate and intervals between the conditioning and test stimuli is on the abscissa. MSR amplitude is normalized to the amplitude of the unconditioned reflex. *A*, mean MSR amplitude (±SEM) following conditioning stimulation from 6 wild-type mice (filled squares). Conditioning stimulation of the L2 dorsal root in wild-types inhibits the L3-evoked MSR for more than 200 ms. Results obtained in adult cat (Eccles *et al.* 1963) are shown for comparison (open circles). *B*, bath administration of bicuculline in wild-type mice ($n = 4$) abolishes long-lasting inhibition of the MSR, showing GABAergic mediation of this inhibition. In the presence of bicuculline, values at conditioning–test intervals greater than 50 ms were significantly different from controls ($P < 0.05$). *C*, conditioning stimulation of the L2 dorsal root failed to inhibit the L3-evoked MSR in Cx36 knockout mice ($n = 7$). Results in wild-types from *A* plotted for comparison.

Figure 3*A* is presynaptic in origin. The shorter-latency effects of conditioning stimulation are presumably a mixture of presynaptic inhibition as well as postsynaptic inhibition and excitation (see Bagust *et al.* 1981).

In the cat (see Rudomin & Schmidt, 1999) and in the rodent (Bagust *et al.* 1981), sensory-evoked presynaptic inhibition causes a primary afferent depolarization that increases the excitability of intraspinal afferent fibre terminals. We examined changes in the excitability of primary afferent terminals in juvenile mice by comparing unconditioned intraspinally evoked antidromic afferent discharges to those conditioned by low intensity (1.5T) stimulation of an adjacent dorsal root. The upper panel in Fig. 4*A* shows the response (black arrow), recorded in the L3 dorsal root, that was evoked by a 6 μA current pulse delivered through an electrode positioned about 300 μm below the surface of the cord in a wild-type mouse. A conditioning stimulus to the L2 dorsal root delivered 35 ms before the intraspinal stimulus (Fig. 4*A*, lower trace, open arrow) resulted in an increase in the intraspinally evoked discharge (compare upper and lower traces in Fig. 4*A*). On average, conditioning stimulation almost doubled the size of the intraspinally evoked antidromic discharge (Fig. 4*C*). The increases in terminal excitability in juvenile wild-type mice are similar to the increases in excitability observed in the cat and previously in the rodent (Bagust *et al.* 1981).

DRPs, MSR inhibition and PAD in Cx36 knockout mice

The results presented in Figs 1–4 show that several characteristics of sensory-evoked presynaptic inhibition recorded in juvenile wild-type mice are similar to those involved in the same process in the adult cat. To examine the potential role of neuronal gap junctions in presynaptic inhibition, we compared results obtained in wild-type mice with those in Cx36 knockout mice.

Figure 1*B* shows representative CDPs in wild-type (*Ba*) and Cx36 knockout mice (*Bb*). Unlike the CDP in wild-type mice, the CDP in knockouts lacked the prolonged later phase and consisted primarily of just the sharp, triphasic, afferent volley. DRPs evoked by L2 dorsal root stimulation at low (Fig. 1*Ca*) and higher (Fig. 1*Cb*) stimulus intensities and recorded in the L3 dorsal root

were also severely attenuated in Cx36 null mice (compare the black and grey traces in Fig. 1*Ca* and *b*). On average, the peak amplitude of DRPs evoked by 1.5T stimulation in Cx36 knockout mice was smaller by 79% ($P < 0.01$; $n = 14$ wild-types and 13 knockouts). Because accurately determining the point at which a DRP returns to baseline is often difficult, comparisons between wild-type and knockout mice were made using the duration of the DRP measured at one-half of its peak amplitude. The half-amplitude duration of the DRP evoked by 1.5T stimulation was 24.0 ± 6.7 ms in wild-type mice ($n = 13$) and fell by 67% ($P < 0.01$) to 8.0 ms ± 0.6 ms in knockout mice ($n = 14$). The duration of the 5T DRP was similarly affected in knockout mice, shortening by 75% (half-amplitude duration 36.6 ± 6.2 ms in wild-type mice; 8.75 ± 1.1 ms in knockout mice, $P < 0.01$). The absence of the later components of the DRP and CDP in knockout mice is consistent with reduced afferent-evoked spinal dorsal horn interneurone activity. In addition to the impairment of the DRP in knockout mice, bicuculline failed to attenuate the DRP evoked with 1.5T stimulation (Fig. 2*A*) while the 2.5T DRP became larger in the presence of the $GABA_A$ blocker in knockout mice (Fig. 2*B*, $n = 10$ in all bar graphs). We currently have no explanation for the bicuculline-induced increase in the amplitude of the higher threshold DRP.

Monosynaptic reflexes evoked by 2.5T dorsal root stimulation were of similar amplitude in wild-type mice and knockout mice (wild-type: 37.8 ± 4.9 μV, $n = 14$; knockout: 36.8 ± 6.9 μV, $n = 11$). The latency of the MSR was, however, longer in knock-out mice. In the example shown in Fig. 1*Db* (left panel, black trace), the latency of the reflex evoked at 1.5T was 4.5 ms; the average latency in 16 experiments was 4.11 ± 0.36 ms (average 3.67 ms in wild-types, see above). Because MSR latency in both wild-type and knockout mice is considerably less than the estimated latency of transmission through spinal disynaptic pathways (6.3 ms; Wang *et al.* 2008; see above), we are confident that the earliest component of the ventral root reflexes reported is monosynaptic. The longer latency responses evoked with increasing stimulus intensity in both wild-type and knock mice (compare left and right panels in Fig. 1*Db*) are likely to reflect transmission through oligosynaptic pathways. No attempt was made to measure or compare longer latency reflexes in wild-type or knockout mice in the present study. While the exact compliment of fibre types activated by electrical dorsal root stimulation in juvenile mice is unknown, it is reasonable to assume that the low intensity stimulation employed here (e.g. 1.5T) recruited lower threshold afferents. Supporting this view is the similarity of the MSR latencies in both wild-type and knockout mice and the latency of monosynaptic EPSPs evoked by mechanical activation of muscle afferents by Wang *et al.* (2008). It thus appears that Ia muscle spindle afferents producing monosynaptic EPSPs and monosynaptic reflexes are among the fibre types activated by low threshold dorsal root stimulation in juvenile wild-type and knockout mice.

The long lasting inhibition of the MSR produced by conditioning stimulation of an adjacent dorsal root in juvenile wild-type mice was absent in Cx36 knockout mice (Fig. 3*C*). Instead, conditioning stimulation increased the amplitude of the MSR in Cx36 knockout mice ($n = 7$) at all conditioning–test intervals examined. Bicuculline had no effect on conditioning of the MSR in Cx36 knockout mice (not shown). There is currently no information available concerning the pathways activated by the conditioning stimulus that contribute to enhancement of the MSR seen at the longer conditioning–test intervals in Cx36 knockout mice (Fig. 3*C*) or following bicuculline administration in wild-types (Fig. 3*B*).

The deficits in Cx36 knockout mice in MSR inhibition, the DRP and the CDP suggest a failure of sensory stimulation to evoke a presynaptic inhibition of sensory

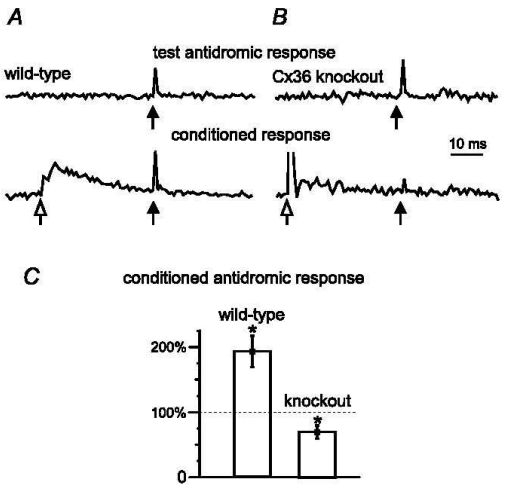

Figure 4. Primary afferent depolarization (PAD) in lumbar spinal cord of P10 wild-type and Cx36 knockout mice
A, antidromic activation of afferent fibres recorded in the L3 dorsal root following intraspinal stimulation (test, black arrow) in the dorsal horn of a wild-type mouse (upper trace). A preceding conditioning stimulus (open arrow) to the L2 dorsal root at 1.5T (lower trace) increased the amplitude of the intraspinally evoked antidromic signal, i.e. PAD. *B*, similar recording from a Cx36 knockout mouse shows the unconditioned antidromic activation of fibres in the dorsal root (upper trace). Conditioning stimulation decreased and often inhibited the antidromic response in knockout mice (lower trace). *C*, comparison of the effects of conditioning stimulation in wild-type *versus* Cx36 knockout mice ($P < 0.05$; $n = 6$). Values of the antidromic response >100% reflect PAD-evoked increased excitability of the afferents produced by the conditioning stimulation. Stars indicate means significantly different ($P < 0.05$) from 100% control.

were also severely attenuated in Cx36 null mice (compare the black and grey traces in Fig. 1*Ca* and *b*). On average, the peak amplitude of DRPs evoked by 1.5T stimulation in Cx36 knockout mice was smaller by 79% ($P < 0.01$; $n = 14$ wild-types and 13 knockouts). Because accurately determining the point at which a DRP returns to baseline is often difficult, comparisons between wild-type and knockout mice were made using the duration of the DRP measured at one-half of its peak amplitude. The half-amplitude duration of the DRP evoked by 1.5T stimulation was 24.0 ± 6.7 ms in wild-type mice ($n = 13$) and fell by 67% ($P < 0.01$) to $8.0 \text{ ms} \pm 0.6$ ms in knockout mice ($n = 14$). The duration of the 5T DRP was similarly affected in knockout mice, shortening by 75% (half-amplitude duration 36.6 ± 6.2 ms in wild-type mice; 8.75 ± 1.1 ms in knockout mice, $P < 0.01$). The absence of the later components of the DRP and CDP in knockout mice is consistent with reduced afferent-evoked spinal dorsal horn interneurone activity. In addition to the impairment of the DRP in knockout mice, bicuculline failed to attenuate the DRP evoked with 1.5T stimulation (Fig. 2*A*) while the 2.5T DRP became larger in the presence of the $GABA_A$ blocker in knockout mice (Fig. 2*B*, $n = 10$ in all bar graphs). We currently have no explanation for the bicuculline-induced increase in the amplitude of the higher threshold DRP.

Monosynaptic reflexes evoked by 2.5T dorsal root stimulation were of similar amplitude in wild-type mice and knockout mice (wild-type: $37.8 \pm 4.9\ \mu$V, $n = 14$; knockout: $36.8 \pm 6.9\ \mu$V, $n = 11$). The latency of the MSR was, however, longer in knock-out mice. In the example shown in Fig. 1*Db* (left panel, black trace), the latency of the reflex evoked at 1.5T was 4.5 ms; the average latency in 16 experiments was 4.11 ± 0.36 ms (average 3.67 ms in wild-types, see above). Because MSR latency in both wild-type and knockout mice is considerably less than the estimated latency of transmission through spinal disynaptic pathways (6.3 ms; Wang *et al.* 2008; see above), we are confident that the earliest component of the ventral root reflexes reported is monosynaptic. The longer latency responses evoked with increasing stimulus intensity in both wild-type and knock mice (compare left and right panels in Fig. 1*Db*) are likely to reflect transmission through oligosynaptic pathways. No attempt was made to measure or compare longer latency reflexes in wild-type or knockout mice in the present study. While the exact compliment of fibre types activated by electrical dorsal root stimulation in juvenile mice is unknown, it is reasonable to assume that the low intensity stimulation employed here (e.g. 1.5T) recruited lower threshold afferents. Supporting this view is the similarity of the MSR latencies in both wild-type and knockout mice and the latency of monosynaptic EPSPs evoked by mechanical activation of muscle afferents by Wang *et al.* (2008). It thus appears that Ia muscle spindle afferents producing monosynaptic EPSPs and monosynaptic reflexes are among the fibre types activated by low threshold dorsal root stimulation in juvenile wild-type and knockout mice.

The long lasting inhibition of the MSR produced by conditioning stimulation of an adjacent dorsal root in juvenile wild-type mice was absent in Cx36 knockout mice (Fig. 3*C*). Instead, conditioning stimulation increased the amplitude of the MSR in Cx36 knockout mice ($n = 7$) at all conditioning–test intervals examined. Bicuculline had no effect on conditioning of the MSR in Cx36 knockout mice (not shown). There is currently no information available concerning the pathways activated by the conditioning stimulus that contribute to enhancement of the MSR seen at the longer conditioning–test intervals in Cx36 knockout mice (Fig. 3*C*) or following bicuculline administration in wild-types (Fig. 3*B*).

The deficits in Cx36 knockout mice in MSR inhibition, the DRP and the CDP suggest a failure of sensory stimulation to evoke a presynaptic inhibition of sensory

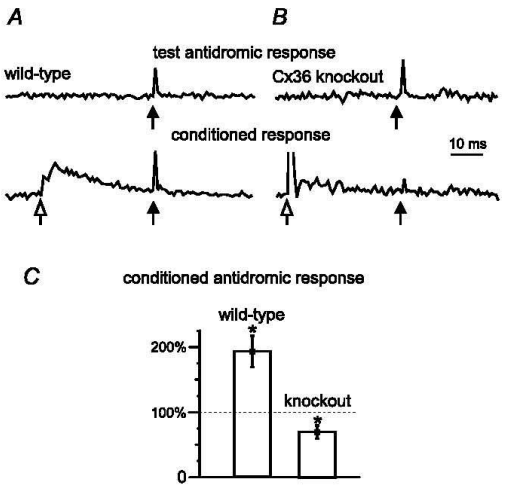

Figure 4. Primary afferent depolarization (PAD) in lumbar spinal cord of P10 wild-type and Cx36 knockout mice
A, antidromic activation of afferent fibres recorded in the L3 dorsal root following intraspinal stimulation (test, black arrow) in the dorsal horn of a wild-type mouse (upper trace). A preceding conditioning stimulus (open arrow) to the L2 dorsal root at 1.5T (lower trace) increased the amplitude of the intraspinally evoked antidromic signal, i.e. PAD. *B*, similar recording from a Cx36 knockout mouse shows the unconditioned antidromic activation of fibres in the dorsal root (upper trace). Conditioning stimulation decreased and often inhibited the antidromic response in knockout mice (lower trace). *C*, comparison of the effects of conditioning stimulation in wild-type *versus* Cx36 knockout mice ($P < 0.05$; $n = 6$). Values of the antidromic response >100% reflect PAD-evoked increased excitability of the afferents produced by the conditioning stimulation. Stars indicate means significantly different ($P < 0.05$) from 100% control.

afferents and hence PAD. Figure 4 compares the ability of conditioning stimulation of a dorsal root to evoke PAD in knockout and wild-type mice. Unlike the PAD produced in wild-types by conditioning stimulation of low threshold sensory afferents (Fig. 4*A*), PAD could not be evoked in Cx36 knockout mice (Fig. 4*B*). On average, the antidromic volley was decreased by conditioning stimulation in knockouts (Fig. 4*C*). Taken together, the results in Figs 1–4 suggest that Cx36, and by implication functional gap junctions, is required to produce presynaptic inhibition of large diameter afferent fibres in the lumbar spinal cord.

Action of gap junction blockers on presynaptic inhibition in wild-types

Given the above results, pharmacological blockade of gap junctions in wild-type mice would be expected to reduce presynaptic inhibition in ways similar to those observed in Cx36 knockouts. Bath application of gap junction blockers antagonized the long-latency MSR inhibition produced by conditioning stimulation and attenuated the long lasting DRP in wild-type rodents. Filled symbols in Fig. 5*A* show long latency inhibition of the MSR evoked by conditioning stimulation in wild-type mice. In the presence of 100 μM carbenoxolone (open symbols), this inhibition was antagonized at all but the shortest conditioning–test intervals. Figure 5*Ba* and *Bb* show the substantial reduction of the DRP produced by carbenoxolone in a P15 rat *in vitro* preparation. Carbenoxolone produced a similar reduction in DRP amplitude in P8–P11 wild-type mice (not shown). Mefloquine, a more selective gap junction blocker (Cruikshank *et al.* 2004), also antagonized long-latency MSR inhibition (not shown) and reversibly attenuated the DRP evoked by 1.5*T* (and 2*T*, not shown) intensity stimulation in the mouse (Fig. 5*Ca* and *b*). The positive-going DRPs in Fig. 5*Ba* and *Ca*, i.e. those going below baseline, presumably reflect a primary afferent hyperpolarization (Mendell, 1972) in the presence of gap-junction blockers. Notwithstanding concerns as to the selectivity of agents used to block gap junction channels (Juszczak & Swiergiel, 2009), the effects of gap junction blockers reported here on processes reflective of the occurrence of presynaptic inhibition parallel results observed in Cx36 knockout mice.

Immunofluorescence localization of Cx36 in spinal cord

The above results indicate that Cx36, presumably at electrical synapses formed by gap junctions between spinal neurones, plays an important role in mediating sensory-evoked presynaptic inhibition of synaptic transmission from large diameter afferents in the spinal cord of juvenile mice. Because Cx36 has not been widely described in spinal cord, we next examined the overall distribution of Cx36 in lumbar 3–5 spinal cord segments in P8–11 and adult mice using immunofluorescence labelling to detect Cx36 protein. Some sections were counterstained for Nissl fluorescence (green) with results shown either as

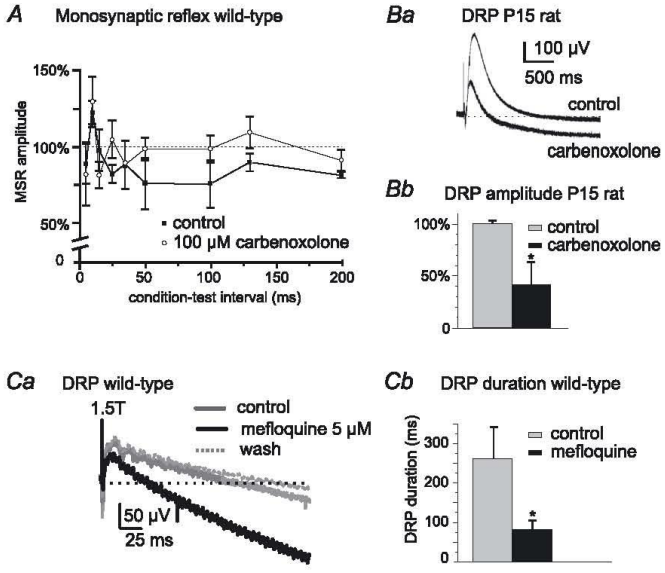

Figure 5. Gap junction blockers reduce presynaptic inhibition of the MSR and DRP amplitude in wild-type mice
A, plot showing prolonged inhibition of the L3 MSR produced by L2 stimulation at conditioning–test intervals >50 ms in P9 wild-type mice (filled symbols) and abolition of this long-lasting MSR inhibition by carbenoxolone (open symbols, $n = 3$). *Ba*, example of the depressive actions of carbenoxolone on a DRP recorded in L4 and evoked by 2*T* stimulation of the third lumbar dorsal root in a P15 rat. *Bb*, summary of effects of carbenoxolone on DRP amplitude in P15 rats ($n = 7$). *Ca*, depressant action of the gap junction blocker mefloquine (5 μM) on a DRP evoked at 1.5*T* in a P9 wild-type mouse (grey trace, control; black trace, mefloquine). DRP amplitude returned to control levels after washout of mefloquine (dotted trace). *Cb*, summary of depressant actions of mefloquine on the DRP duration evoked at 1.5*T* in P9 wild-type mice ($n = 6$). *$P < 0.05$.

Nissl/Cx36 overlays, with Cx36 labelled red, or as separate corresponding images. Because results were similar in lumbar 3–5, only data from the fourth lumbar segment are illustrated.

Immunolabelling for Cx36 consisted exclusively of Cx36-immunopositive puncta, which presumably correspond to the localization of Cx36-containing gap junctions, as observed elsewhere in the CNS (Rash *et al.* 2007*a*,*b*; Kamasawa *et al.* 2006). No specific diffuse labelling for Cx36 was observed intracellularly, precluding attempts to identify Cx36-positive neurons based on their morphology, except in the case of punctate labelling associated with the surface of large motoneurones. Punctate labelling for Cx36 in P11 mice was found in most dorsal and ventral horn laminae (Fig. 6*A*). In lamina I and II (substantia gelatinosa) and the dorsal half of lamina III (Fig. 6*B* and *C*), Cx36-puncta were sparse, more faint and of finer grain compared with those in deeper layers. Intensely fluorescent Cx36-puncta were most evident in laminae IV–VI (Fig. 6*D* and *E*). Qualitatively similar results were obtained in P9 mice, although Cx36-puncta at this age were more densely distributed in most lamina (not shown). In Cx36 knockout mice examined at P9, there was a total absence of immunolabelling for Cx36 (Fig. 6*F*) in a field corresponding to that shown in Fig. 6*E*, indicating specificity of Cx36 detection at punctate sites of labelling. The weak fixation required for visualization of Cx36 immunofluorescence led to some non-specific fluorescence, particularly in cellular nuclei, which was readily distinguishable from specific labelling through comparisons of results from wild-type and Cx36 knockout mice.

Figure 7 shows punctate labelling for Cx36 in the ventral horn of P5 (Fig. 7*A*), P10 (*B*), P11 (*C* and *E*) and adult (>50 days, *D*) wild-type mice. At P5, Cx36-puncta were located between the somata of adjacent motoneurones as seen in those simultaneously immunolabelled for the protein peripherin (Fig. 7*A*), which is highly expressed in these neurones (Duflocq *et al.* 2008; Clarke *et al.* 2010). By P10, Cx36 was additionally seen in proximal dendritic areas (Fig. 7*B*). In mice at P11, lamina IX had the most heterogeneous distribution of labelling, with some areas containing only sparse Cx36-puncta, while others displayed a consistently high density of Cx36-puncta among tightly clustered neurones (Fig. 7*C*). This pattern of immunolabelling for Cx36 in lamina IX persisted in adult mice, where Cx36-puncta remained heterogeneously distributed among motor nuclei, with subsets of motoneurones exhibiting dense accumulations of Cx36-puncta, such as those shown in Fig. 7*D*. A systematic analysis of developmental changes in Cx36 labelling in various regions of the spinal cord was not made in the present study.

Other lumbar spinal cord laminae also displayed labelling for Cx36 in the adult. As seen in Fig. 8*A*, most regions contained a lower density of Cx36-puncta than seen at P11, except ventrolateral areas of the ventral horn (Fig. 8*A*) and medial areas of laminae IV to VI (Fig. 8*B*), where robust punctate labelling persisted. In medial regions of laminae IV to VI and extending into VII, particularly striking were one or two small neurones per section that had numerous Cx36-puncta on their somata and initial dendrites (Fig. 8*C*–*E*). The quality of Nissl fluorescence staining was not sufficient to determine whether these neurones exhibited inter-dendritic appositions where gap junctional coupling could potentially occur.

Association of Cx36-puncta with neurobiotin-coupled neurones

As outlined in the Introduction, the prevailing opinion is that lumbar interneurones located in intermediate laminae are responsible for sensory-evoked presynaptic inhibition of large diameter muscle afferents. The present evidence for the involvement of Cx36 in presynaptic inhibition in mouse spinal cord, together with immunofluorescence labelling for Cx36 in intermediate laminae, raises the possibility that neurones in these laminae are linked by gap junctions. To investigate this possibility, we examined tracer–dye coupling between neurones located in laminae IV to VI in slices of lumbar spinal cord at P11. Neurones were impaled and injected with neurobiotin and the tissue processed with strepavidin-Alexa488. As shown in Fig. 9*A*, injection of a single cell produced intense tracer flourescence in the injected cell and several nearby neurones. The same section immunolabelled for Cx36 (Fig. 9*B*) showed a dense distribution of Cx36-puncta among neurones in this region. Another example of neurobiotin coupling after injection of a neurone is shown in Fig. 9*C*. Higher magnification shows a cluster of coupled neurones in close apposition (Fig. 9*D*). Laser scanning confocal analysis revealed the association of Cx36-puncta with dendrites and/or soma of both neurobiotin-injected (Fig. 9*E*) and neurobiotin-coupled (Fig. 9*F*) neurones. The weak fixation conditions required for detection of Cx36 made further handling and sectioning of the thick slices with injected cells difficult. Consequently, we recovered only four of eight injected cells in cryostat sections; two of these were coupled to other cells, two were not. We succeeded in detecting Cx36-puncta on the two coupled cells.

Discussion

This study is the first to examine the role of Cx36-containing gap junctions in sensory-evoked presynaptic inhibition in the spinal cord. We demonstrate that presynaptic inhibition of large diameter primary

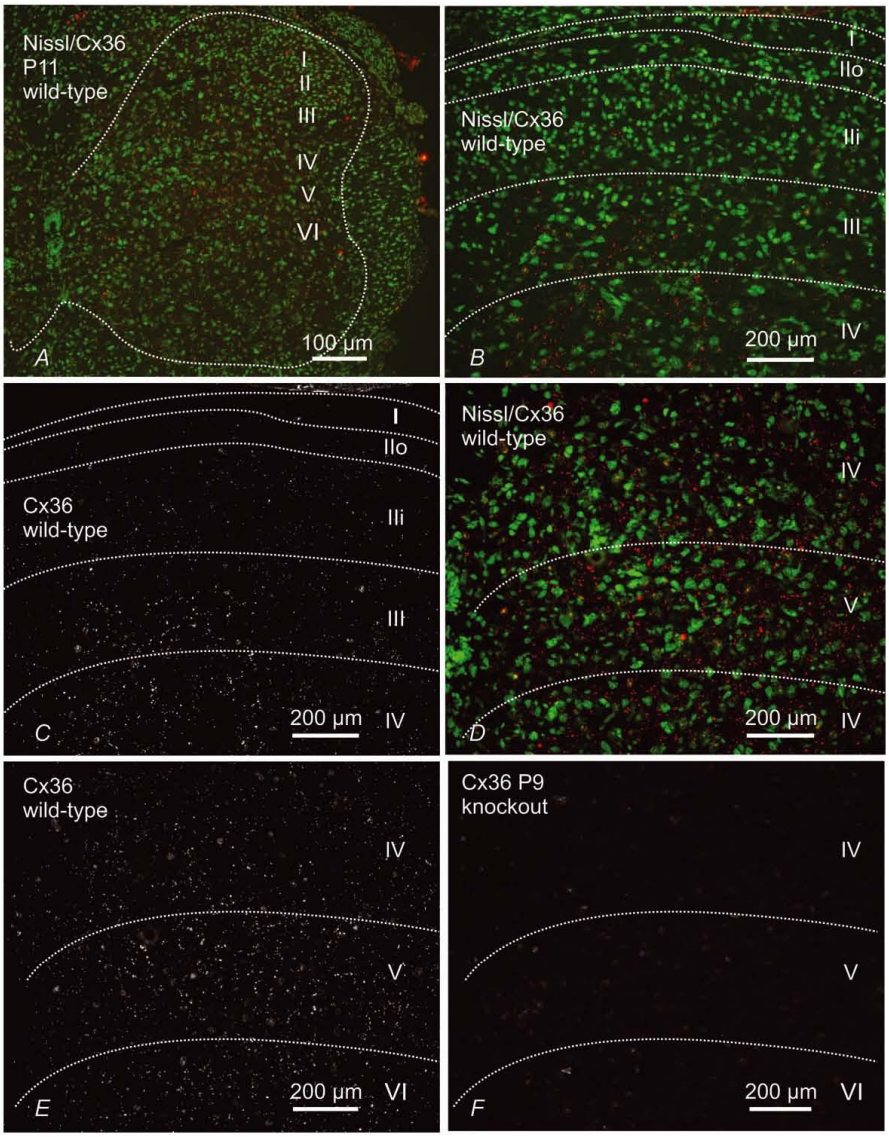

Figure 6. Immunofluorescence labelling for Cx36 in transverse sections of mouse L4 spinal cord in juvenile mice

Panels *A*–*E* are from P11 mice and panel *F* is from a P9 mouse at the fourth lumbar segment. *A*, low magnification, fluorescence Nissl counterstained section (green) showing distribution of Cx36-positive puncta (red) in dorsal and ventral grey matter (outlined by dotted line). *B* and *C*, magnification of superficial dorsal horn laminae (outlined by dotted lines) with (*B*) and without (*C*) Nissl counterstain, showing sparse labelling for Cx36 (red) in lamina I and in outer (IIo) and inner (IIi) lamina II, and moderate labelling in lamina III. *D* and *E*, magnification of deeper dorsal horn laminae (outlined by dotted lines) with (*D*) and without (*E*) Nissl counterstain, showing abundant Cx36-puncta in laminae IV, V and a portion of VI. *F*, section from the dorsal horn of a P9 Cx36 knockout mouse showing absence of labelling for Cx36 in a field similar to that shown in *E*.

afferents is dependent upon the integrity of Cx36-containg neuronal gap junctions between spinal interneurones. Longer duration components of the DRP and CDP, as well as inhibition of the MSR, were absent or substantially attenuated in Cx36 knockout mice. Because spinal motor systems in mice of the ages employed here are considered to be functionally mature (Jiang *et al.* 1999; Hinckley & Ziskind-Conhaim, 2006) and because the Cx36 immunolabelling reported here persists into adulthood, it is likely that electrical contacts between spinal interneurones also contribute to the efficacy of presynaptic inhibition in the adult.

Electrophysiology of presynaptic inhibition in wild-type and Cx36 knockout mice

Several features associated with presynaptic inhibition in wild-type *in vitro* preparations of juvenile mice are similar to those in adult cat. These include the time course of the DRP, the long-lasting inhibition of the MSR, the occurrence of sensory-evoked PAD and the attenuation of the DRP and MSR inhibition by GABA antagonists. Although the DRP is strongly associated with GABAergic mediation of presynaptic inhibition (reviewed by Rudomin & Schmidt, 1999; Rudomin, 2009), its attenuation by GABA antagonists ranges from partial (Rudomin *et al.* 1990; Thompson & Wall, 1996; Kremer & Lev-Tov, 1998; Wong *et al.* 2001; present results – Fig. 2*A*) to complete (Schreckengost *et al.* 2010). GABA antagonists can, however, very effectively attenuate the long-latency inhibition of the MSR evoked by conditioning stimulation (Fig. 3*B*; Eccles *et al.* 1963; Curtis *et al.* 1971). It remains an open question whether non-GABAergic mechanisms also contribute to presynaptic inhibition. Based on the similarities of the present results to those in the cat, it is reasonable to assume that MSR inhibition at the longer conditioning–test intervals in the mouse occurs predominately by a presynaptic mechanism. The inhibition at shorter condition test intervals (<25 ms) is likely to include a postsynaptic inhibitory component involving spinal reflex pathways (Bagust *et al.* 1981; Deshpande & Warnick, 1988; Wang *et al.* 2008).

Later components of the CDP are considered to reflect activity in dorsal horn interneurones and are correlated with activity in presynaptic inhibitory pathways (Rudomin *et al.* 1987; Enriquez *et al.* 1996). Although the shortest latency components of the CDP were qualitatively similar in wild-type and knockout mice, the later components were missing in knockouts. The absence of these components suggests a decrease in dorsal horn interneurone activity in these knockouts and in turn a reduction in the activity of presynaptic inhibitory pathways. Consistent with this suggestion, DRP duration and amplitude were decreased substantially in mice lacking Cx36 compared to wild-types of the same age. Whereas bicuculline attenuated the long lasting DRP in wild-types, the remaining short-duration DRP observed in Cx36 knockout mice was not affected by GABAa antagonists.

Presynaptic inhibition of transmitter release from large diameter primary afferent fibres in the mammalian spinal cord is mediated by GABA release at axo-axonic synapses (Rudomin, 2009), which causes a depolarization of intraspinal afferent fibre terminals, i.e. produces PAD. Consistent with the shortened and attenuated DRP in juvenile Cx36 knockout mice, PAD could not be evoked in lumbar primary afferent terminals of these mice. In wild-types, the ability of the gap junction blockers to

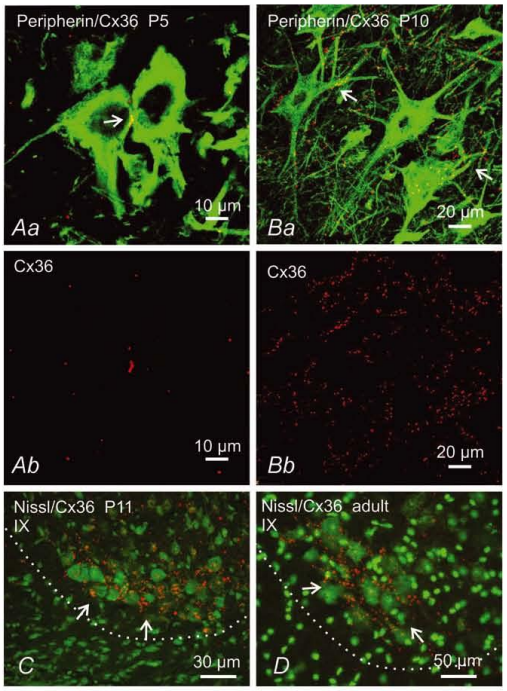

Figure 7. Immunofluorescence labelling of Cx36 in mouse spinal cord ventral horn at different developmental stages
Aa and *Ba*, laser scanning confocal overlay images showing double immunofluorescence labelling for Cx36 (red) and the motoneurone marker peripherin (green) at P5 (*Aa*) and P10 (*Ba*). *Ab* and *Bb* show only the Cx36 labelling (red) from images in *Aa* and *Ba*, respectively. At P5 motoneurones display Cx36-puncta at points of somal contact. At P10, Cx36-puncta are on somata and initial dendrites of motoneurones (*Ba*, arrows). *C*, Nissl counterstained (green) sections showing dense labelling for Cx36 (red) in lamina IX at P11 among a cluster of neurones in the ventrolateral region of lamina IX (arrows), and persistence of these puncta in adult (*D*, arrows). Border between ventrolateral grey and white matter is shown by dotted line.

antagonize the MSR inhibition evoked by conditioning stimulation (Fig. 5*A*) and reduce the DRP (Fig. 5*B* and *C*) provides further support for a critical involvement of neuronal gap junctions in presynaptic inhibition of large diameter sensory afferents.

Cx36 in juvenile and adult mice

There are a number of reports on electrical coupling between neurones in the spinal cord, but there is little anatomical information available on the expression of Cx36 in the cord. Motoneurones in rat express Cx36 mRNA (Chang *et al.* 1999), and diffuse, intracellular labelling for Cx36 protein has been detected in these neurones (Marina *et al.* 2008). Here we demonstrate a much broader distribution of Cx36 in the spinal cord of both developing and adult mouse. Importantly, as elsewhere in the CNS (Li *et al.* 2004; Rash *et al.* 2004, 2007*a*,*b*), we found that specific immunofluorescence labelling for Cx36 in spinal cord (i.e. that which was absent in Cx36 knockout mice) consisted exclusively of Cx36-puncta. Presumably these puncta reflect localization of Cx36 to neuronal gap junctions that have been shown ultrastructurally to contain Cx36 (Rash *et al.* 2001*a*,*b*; Nagy *et al.* 2004).

Although spinal neurones may express other connexins (see Chang *et al.* 1999), the DRP and lasting inhibition of the MSR were severely affected by the absence of Cx36. It thus appears that Cx36 is critically involved in the physiological processes examined here. In other CNS regions and in the spinal cord, developmental decreases in electrical coupling and down-regulation of Cx36 expression are well described (Walton & Navarrete, 1991; Kandler & Katz, 1995; Chang *et al.* 1999; Chang & Balice-Gordon, 2000; Meier & Dermietzel, 2006). The present results show the persistence of moderate to dense levels of Cx36-puncta in both dorsal and ventral horn areas of adult spinal cord. This persistence is perhaps not surprising given the numerous brain structures where functional Cx36-containing electrical synapses are present in the adult (Bennett & Zukin, 2004; Connors & Long, 2004; Hormuzdi *et al.* 2004; Meier & Dermietzel, 2006). Particularly striking in adult cord was the widely distributed immunolabelling for Cx36 in laminae IV–VI, the labelling associated with a small subset of neurones scattered in laminae IV–VII and dense collections of Cx36-puncta among neurones in lamina IX. Our anatomical observations suggest that Cx36-containing gap junctions continue to be of importance in adult pools of spinal neurones and possibly in processes in

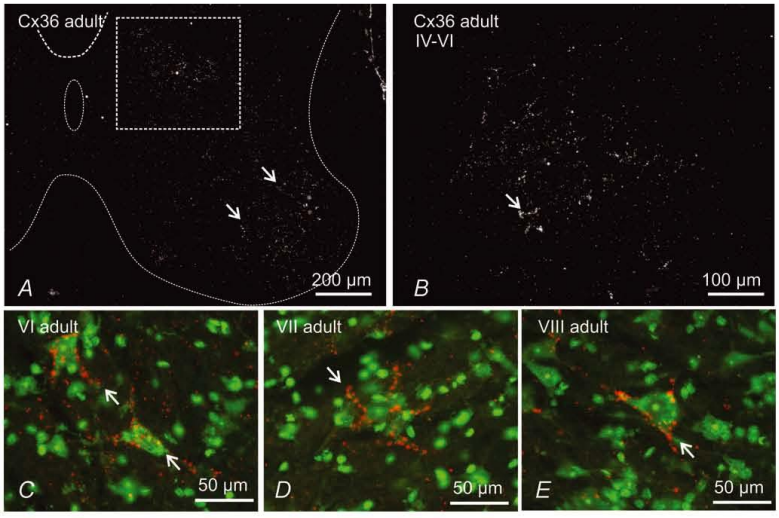

Figure 8. Immunofluorescence labelling of Cx36 in lumbar spinal cord of adult mouse
A, low magnification of deep dorsal horn and the whole of the ventral horn grey matter (outlined by dotted line). Cx36-puncta are distributed throughout, but are most dense in lamina IX (arrows) and within the boxed area straddling the deep dorsal horn and intermediate zone. *B*, magnification of a region corresponding to that of the box in *A*, showing dispersed and clustered Cx36-puncta (arrow). *C–E*, fluorescence Nissl counterstained (green) sections showing examples of Cx36-puncta (red) densely distributed around relatively small neurones (arrows) located in lamina VI (*C*), lamina VII (*D*) and in a mid-region of lamina VIII (*E*).

antagonize the MSR inhibition evoked by conditioning stimulation (Fig. 5*A*) and reduce the DRP (Fig. 5*B* and *C*) provides further support for a critical involvement of neuronal gap junctions in presynaptic inhibition of large diameter sensory afferents.

Cx36 in juvenile and adult mice

There are a number of reports on electrical coupling between neurones in the spinal cord, but there is little anatomical information available on the expression of Cx36 in the cord. Motoneurones in rat express Cx36 mRNA (Chang *et al.* 1999), and diffuse, intracellular labelling for Cx36 protein has been detected in these neurones (Marina *et al.* 2008). Here we demonstrate a much broader distribution of Cx36 in the spinal cord of both developing and adult mouse. Importantly, as elsewhere in the CNS (Li *et al.* 2004; Rash *et al.* 2004, 2007*a*,*b*), we found that specific immunofluorescence labelling for Cx36 in spinal cord (i.e. that which was absent in Cx36 knockout mice) consisted exclusively of Cx36-puncta. Presumably these puncta reflect localization of Cx36 to neuronal gap junctions that have been shown ultrastructurally to contain Cx36 (Rash *et al.* 2001*a*,*b*; Nagy *et al.* 2004).

Although spinal neurones may express other connexins (see Chang *et al.* 1999), the DRP and lasting inhibition of the MSR were severely affected by the absence of Cx36. It thus appears that Cx36 is critically involved in the physiological processes examined here. In other CNS regions and in the spinal cord, developmental decreases in electrical coupling and down-regulation of Cx36 expression are well described (Walton & Navarrete, 1991; Kandler & Katz, 1995; Chang *et al.* 1999; Chang & Balice-Gordon, 2000; Meier & Dermietzel, 2006). The present results show the persistence of moderate to dense levels of Cx36-puncta in both dorsal and ventral horn areas of adult spinal cord. This persistence is perhaps not surprising given the numerous brain structures where functional Cx36-containing electrical synapses are present in the adult (Bennett & Zukin, 2004; Connors & Long, 2004; Hormuzdi *et al.* 2004; Meier & Dermietzel, 2006). Particularly striking in adult cord was the widely distributed immunolabelling for Cx36 in laminae IV–VI, the labelling associated with a small subset of neurones scattered in laminae IV–VII and dense collections of Cx36-puncta among neurones in lamina IX. Our anatomical observations suggest that Cx36-containing gap junctions continue to be of importance in adult pools of spinal neurones and possibly in processes in

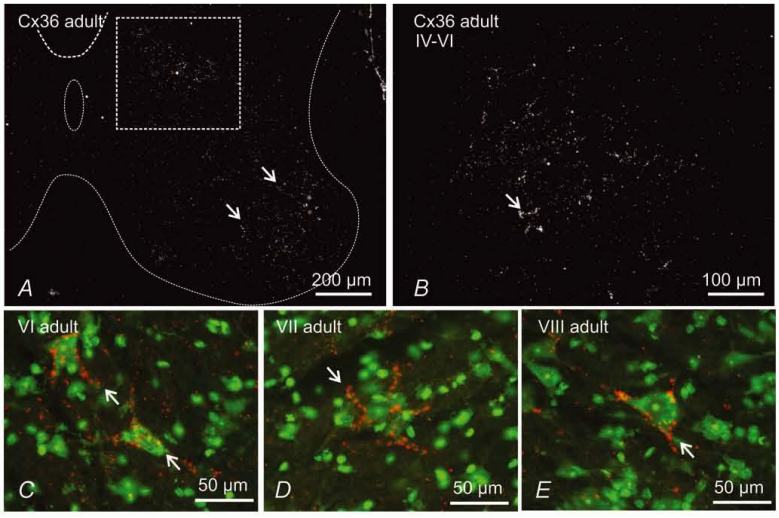

Figure 8. Immunofluorescence labelling of Cx36 in lumbar spinal cord of adult mouse
A, low magnification of deep dorsal horn and the whole of the ventral horn grey matter (outlined by dotted line). Cx36-puncta are distributed throughout, but are most dense in lamina IX (arrows) and within the boxed area straddling the deep dorsal horn and intermediate zone. *B*, magnification of a region corresponding to that of the box in *A*, showing dispersed and clustered Cx36-puncta (arrow). *C–E*, fluorescence Nissl counterstained (green) sections showing examples of Cx36-puncta (red) densely distributed around relatively small neurones (arrows) located in lamina VI (*C*), lamina VII (*D*) and in a mid-region of lamina VIII (*E*).

addition to presynaptic inhibition. In this regard it is noteworthy that there is extensive electrical coupling between motoneurones in very young animals that is largely lost during the second week after birth (Walton & Navarrete, 1991). The re-distribution of Cx36-puncta on motoneurones during development (Fig. 7) presumably reflects changing physiological roles of electrical synapses associated with these cells in the adult, which may be somehow related to the loss of coupling between these neurones during development. The demonstration of Cx36-puncta on motoneurones at P5, an age when these cells are known to be electrically coupled, serves as a positive control for our use of labelling for Cx36 as an indicator of electrical synapse detection. With these considerations, it may be inferred that Cx36-puncta, where present in the adult, reflect functional electrical coupling between spinal neurones such as has been observed between some motoneurones in the adult (Gogan *et al.* 1977).

Because of the present interest in the process of presynaptic inhibition of large diameter primary afferents, dye-coupling between spinal interneurones was investigated only in regions known to contain neurones involved in this process, namely laminae V–VI. These regions contain the GABAergic interneurones that project to the ventral horn and form P boutons on muscle spindle afferents (Hughes *et al.* 2005; discussed below). As shown in Fig. 9, at P11 there is extensive dye-coupling between neurones in these laminae and extensive punctate labelling for Cx36 on dye-coupled neurones. The presence of functional Cx36-containing gap junctions between neurones in these areas is consistent with a role of electrical synapses in presynaptic inhibition. A full appreciation of the identity of dye-coupled neurones in relation to the localization and function of Cx36 in particular neuronal populations will require a more comprehensive analysis.

Role of gap junctions in presynaptic inhibition

Figure 10 shows how Cx36-containing gap junctions might be involved in presynaptic inhibition of group Ia muscle spindle afferents making monosynaptic contacts on motoneurones. For the purposes of the present discussion, the possibility of Cx36-mediated coupling among other spinal cord cell types and afferents is not considered (e.g. Chapman *et al.* 2009). Presynaptic inhibition is believed to involve a three-synapse, two-neurone pathway (Jankowska *et al.* 1981; but see Shreckengost *et al.* 2010) in which glutamatergic sensory afferents activate excitatory first order interneurones. The first order interneurones are thought to be glutamatergic because there is evidence that activation of excitatory glutamatergic interneurones occurs immediately before the onset of presynaptic inhibition (Rudomin, 2009). These neurones then activate a population of GABAergic interneurones that have axo-axonic contacts on primary afferents (see Rudomin, 2009). There is strong electrophysiological and anatomical evidence that deep dorsal horn laminae are the principal locations of GABAergic interneurones mediating presynaptic inhibition of large diameter afferents in the cat and rodent spinal cord (Jankowska *et al.* 1981; Rudomin *et al.* 1987; Maxwell *et al.* 1990; Hughes *et al.* 2005; Betley *et al.* 2009). These interneurones may in part correspond to neurons in the medial laminae IV–VI where we found cells having the capacity for intercellular exchange of neurobiotin, and where neurobiotin-coupled cells were richly endowed with Cx36-puncta (Fig. 9). Based on the foregoing, the

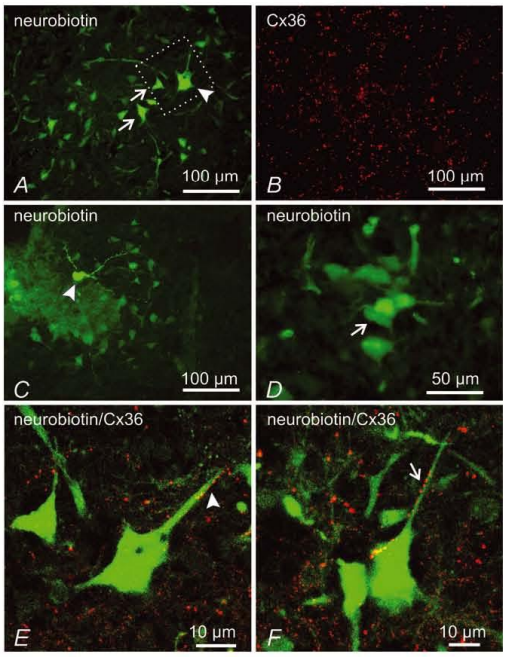

Figure 9. Immunofluorescence labelling of Cx36 (red) associated with neurobiotin-coupled neurones (green) in deep dorsal horn and intermediate zone of mice at P11
A and *B*, low magnification showing a neurobiotin-injected neuron (*A*, arrowhead), giving rise to surrounding neurobiotin-positive neurons (*A*, arrows), and the same field (*B*) showing dense immunolabelling for Cx36 in lamina VI. *C* and *D*, neurobiotin-injected neuron in lamina V (*C*, arrowhead), and higher magnification from an adjacent section showing clusters of neurobiotin-positive neurones (*D*, arrow). *E* and *F*, confocal laser scanning images showing overlays of neurobiotin-positive neurones and immunofluorescence labelling for Cx36, with green/red overlap seen as yellow. The image in *E* is a magnification of the boxed area shown in *A*. Cx36-puncta are seen associated with dendrites and soma of a neurobiotin-injected neurone (*E*, arrowhead) and neurobiotin-coupled neurone (*F*, arrows).

hypothesis presented in Fig. 10 is that GABAergic neurones in deep dorsal horn laminae are gap junctionally coupled and make axo-axonic contacts with large diameter primary afferents and, in particular, Ia spindle afferents. Also depicted in Fig. 10 is the possibility that gap junctions exist between excitatory first order interneurones that activate second order presynaptic inhibitory pathways, but direct evidence for this is presently lacking. However, bearing on this point is that at least some components of the cord dorsum potential are related to activation of excitatory (presumably glutamatergic) interneurones in the dorsal horn (Rudomin, 2009). The depressed CDP observed in the Cx36 knockouts supports equally the possibility that, in the knockout mouse, glutamatergic interneurones lack synchronous robust activity conferred by gap junction coupling.

One of the most emphasised features of inter-neuronal gap junctions is their ability to function as low-pass filters, where longer duration, subthreshold depolarizations, in contrast to spikes, are efficiently transmitted within a network of coupled neurons, allowing synchronization of spike activity of near-threshold neurones (Bennett & Zukin 2004). Equally important, the behaviour of a coupled network will be dependent upon both the nature and duration of the afferent input as well as the intrinsic membrane properties of the coupled neurones (Mann-Metzer & Yarom 1999; Dugué *et al.* 2009; Curti *et al.* 2012). Gap junctions could serve to trigger intrinsic oscillatory currents in coupled neurones, to temporally synchronize action potentials with the onset of afferent input, to prolong activity in the population as the afferent input decays, or to help select a subpopulation of coupled interneurones within a larger population of spinal neurones with similar afferent input. A facilitation of activity within the gap junction coupled networks in Fig. 10 would presumably result in a concerted expression of presynaptic inhibition of primary afferents. This idea is in accord with the suggestion (see Rudomin, 2009) that synchronous activity of subpopulations of interneurones involved in presynaptic inhibition can distribute primary afferent depolarization to selected collaterals of afferents in different spinal locations. It is also in accord with the suggestion that when afferents contact multiple spinal pathways, activity in those displaying synchronous interneuronal activity, e.g. those in presynaptic inhibitory networks, would be promoted over reflex effects mediated through other, unsynchronized, networks (Chavez *et al.* 2012). Accordingly, gap junction coupling may be extensive within subsets of interneurones organized into functionally discrete groups. Based on these considerations, it might be predicted that pharmacological uncoupling of gap junctions in wild-type mice or the loss of Cx36 in transgenic mice would compromise a concerted action of these interneurones on transmission at primary afferents. This proposed mechanism for an essential role of electrical connections between neurones in sensory-evoked presynaptic inhibition is supported by the loss of long-latency inhibition of the MSR in spinal cord preparations from Cx36 knockouts and following bath application of gap junction blockers in cords from wild-type mice. These observations provide strong evidence for the involvement of Cx36-containing gap junctions in the presynaptic control of the synapse between Ia muscle spindle afferents and lumbar motoneurones. The abundance of Cx36-puncta in spinal laminae IV–VI also suggests a role of electrical synapses in the presynaptic control of other segmental reflexes, for example those from tendon organs and spindle secondary afferents. It is noteworthy that gap junctions may also be involved in the presynaptic control of sensory input to dorsal spinocerebellar tract neurones which shares several features of the presynaptic inhibition of Ia terminals on motoneurones. This includes axo-axonic synapses (Walmsley, 1991), sensory-evoked PAD of group I afferent input (Jankowska & Padel, 1984) and GABAergic control of afferent input to dorsal spinocerebellar tract neurones (Hantman & Jessell, 2010).

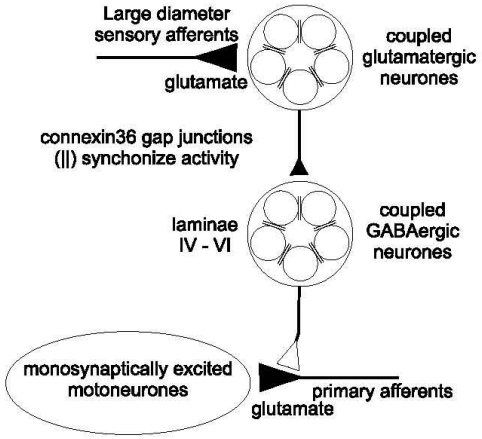

Figure 10. Proposed role of neuronal gap junctions in facilitating presynaptic inhibition
Large diameter sensory afferents contact populations of lumbar spinal interneurones that are excitatory to other interneurones located in intermediate spinal laminae. These second order interneurones release GABA onto the presynaptic terminals of primary afferents causing PAD and a subsequent reduction in glutamate release from sensory afferents. In the circuit depicted here, this presynaptic inhibition results in smaller monosynaptic EPSPs generated in motoneurones by Ia muscle spindle afferents. Gap junctions formed by Cx36 (||) are hypothesized to couple and synchronize activity in interneurone populations responsible for presynaptic inhibition. Ablation of Cx36 or pharmacological inhibition of gap junctions in wild-types results in a severe impairment of the presynaptic regulation of transmission from large diameter sensory afferents.

Interestingly, some previously described laminae V–VI interneurones (Hughes *et al.* 2005) are GAD65 positive and make P-bouton (axo-axonic) contacts with primary afferent terminals in the ventral horn. Since Ia muscle spindle afferents are the only sensory afferents with extensive monosynaptic connections on motoneurones, the present results on MSR inhibition raise the likelihood that at least some of the interneurones described by Hughes *et al.* (2005) are coupled by electrical synapses. Recent reports, however, suggest that at least in very young animals these spinal regions also contain populations of GABAergic interneurones not involved in presynaptic inhibition (Wilson *et al.* 2010). There is also strong physiological evidence that some GABAergic interneurones may be involved in both presynaptic inhibition of afferent transmission and postsynaptic inhibition of motoneurones (Rudomin *et al.* 1990; see Rudomin, 2009). Full identification of GABAergic interneurone populations in these laminae and the organization of gap junctionally coupled networks among them remain to be determined.

Presynaptic inhibition of large diameter muscle and cutaneous afferents in the spinal cord is a regulatory process in which sensory afferent activity results in reduced transmitter release from the same and other afferents and is an integral component of reflex control during locomotion and other movements (Rossignol *et al.* 2006; Rudomin 2009). Studies during locomotion, however, indicate the existence of an additional source of presynaptic inhibition that arises from the operation of central pattern generating circuitry and can occur without sensory stimulation (discussed in Gosgnach *et al.* 2000). It remains an attractive possibility that electrical synapses play a similar role in this centrally evoked presynaptic inhibition as the one described here in sensory-evoked presynaptic inhibition. Dysregulation of presynaptic inhibition is believed to be one of the major factors in human spasticity arising from spinal cord injury, and drugs that augment presynaptic inhibition, such as baclofen, are a mainstay in treatment of spasticity (Simon & Yelnick, 2010). Recently, it has been suggested that injury-induced changes in connexin36 expression in spinal cord contribute to spasticity (Yates *et al.* 2011). The present results directly linking Cx36 to presynaptic inhibition, a process known to malfunction in human spasticity, raise the possibility that this condition arises in part from dysfunction of gap junctionally coupled networks involved in presynaptic inhibition.

References

Allison DW, Wilcox RS, Ellefsen KL, Askew CE, Hansen DM, Wilcox JD, Sandoval SS, Eggett DL, Yanagawa Y & Steffensen SC (2011). Mefloquine effects on ventral tegmental area dopamine and GABA neuron inhibition: a physiologic role for connexin-36 gap junctions. *Synapse* **65**, 805–813.

Bagust J, Green KA & Kerkut GA (1981). Strychnine sensitive inhibition in the dorsal horn of mammalian spinal cord. *Brain Res* **217**, 425–429.

Bagust J, Forsythe D & Kerkut GA (1985). Demonstration of the synaptic origin of primary afferent depolarisation (PAD) in the isolated spinal cord of the hamster. *Brain Res* **341**, 385–389.

Bennett MVL (1997). Gap junctions as electrical synapses. *J Neurocytol* **26**, 349–366.

Bennett MV & Zukin RS (2004). Electrical coupling and neuronal synchronization in the mammalian brain. *Neuron* **41**, 495–511.

Betley JN, Wright CV, Kawaguchi Y, Erdelyi F, Szabo G, Jessell TM & Kaltschmidt JA (2009). Stringent specificity in the construction of a GABAergic presynaptic inhibitory circuit. *Cell* **139**, 161–174.

Carlin KP, Jiang Z & Brownstone RM (2000). Characterization of calcium currents in functionally mature mouse spinal motoneurons. *Eur J Neurosci* **12**, 1624–1634.

Chapman RJ, Cilia La Corte PF, Asghar AUR & King A (2009). Network-based activity induced by 4-aminopyridine in rat dorsal horn in vitro is mediated by both chemical and electrical synapses. *J Physiol* **587**, 2499–2510.

Chang Q & Balice-Gordon RJ (2000). Gap junctional communication among developing and injured motor neurons. *Brain Res Brain Res Rev* **32**, 242–249.

Chang Q, Gonzalez M, Pinter MJ & Balice-Gordon RJ (1999). Gap junctional coupling and patterns of connexin expression among neonatal rat lumbar spinal motor neurons. *J Neurosci* **19**, 10813–10828.

Chávez D, Rodríguez E, Jiménez I & Rudomin P (2012). Changes in correlation between spontaneous activity of dorsal horn neurones lead to differential recruitment of inhibitory pathways in the cat. *J Physiol* **590**, 1563–1584.

Clarke WT, Edwards B, McCullagh KJ, Kemp MW, Moorwood C, Sherman DL, Burgess M & Davies KE(2010). Syncoilin modulates peripherin filament networks and is necessary for large-calibre motor neurons. *J Cell Sci* **123**, 2543–2552.

Coleman AM & Sengelaub DR (2002). Patterns of dye coupling in lumbar motor nuclei of the rat. *J Comp Neurol* **454**, 34–41.

Connors BW & Long MA (2004). Electrical synapses in the mammalian brain. *Annu Rev Neurosci* **27**, 393–418.

Cruikshank SJ, Hopperstad M, Younger M, Connors BW, Spray DC & Srinivas M (2004). Potent block of Cx36 and Cx50 gap junction channels by mefloquine. *Proc Natl Acad Sci U S A* **101**, 12364–12369.

Curtis DR, Duggan AW, Felix D & Johnston GA (1971). Bicuculline, an antagonist of GABA and synaptic inhibition in the spinal cord of the cat. *Brain Res* **32**, 69–96.

Curti S, Hoge G, Nagy JI & Pereda AE (2012). Synergy between electrical coupling and membrane properties promotes strong synchronization of neurons of the mesencephalic trigeminal nucleus. *J Neurosci* **32**, 4341–4359.

Dai Y, Carlin KP, Li X, McMahon DG, Brownstone RM & Jordan LM (2009). Electrophysiological and pharmacological properties of locomotor activity-related neurons in cfos-EGFP mice. *J Neurophysiol* **102**, 3365–3383.

Deans MR, Gibson JR, Sellitto C, Connors BW & Paul DL (2001). Synchronous activity of inhibitory networks in neocortex requires electrical synapses containing connexin36. *Neuron* **16**, 477–485.

Deshpande SB & Warnick JE (1988). Temperature-dependence of reflex transmission in the neonatal rat spinal cord, in vitro: influence on strychnine- and bicuculline-sensitive inhibition. *Neuropharmacology* **27**, 1033–1037.

Drummond GB (2009). Reporting ethical matters in *The Journal of Physiology*: standards and advice. *J Physiol* **587**, 713–719.

Duflocq A, Le Bras B, Bullier E, Couraud F & Davenne M (2008). Nav1.1 is predominantly expressed in nodes of Ranvier and axon initial segments. *Mol Cell Neurosci* **39**, 180–192.

Dugué GP, Brunel N, Hakim V, Schwartz E, Chat M, Lévesque M, Courtemanche R, Léna C & Dieudonné S (2009). Electrical coupling mediates tunable low-frequency oscillations and resonance in the cerebellar Golgi cell network. *Neuron* **61**, 126–139.

Eccles JC, Schmidt R & Willis WD (1963). Pharmacological studies on presynaptic inhibition. *J Physiol* **168**, 500–530.

Enríquez M, Jiménez I & Rudomin P (1996). Segmental and supraspinal control of synaptic effectiveness of functionally identified muscle afferents in the cat. *Exp. Brain Res* **107**, 391–404.

Frisch C, De Souza-Silva MA, Söhl G, Güldenagel M, Willecke K, Huston JP & Dere E (2005). Stimulus complexity dependent memory impairment and changes in motor performance after deletion of the neuronal gap junction protein connexin36 in mice. *Behav Brain Res* **157**, 177–185.

Gogan P, Gueritaud JP, Horcholle-Bossavit G & Tyc-Dumont S (1977). Direct excitatory interactions between spinal motoneurones of the cat. *J Physiol* **272**, 755–767.

Gosgnach S, Quevedo J, Fedirchuk B & McCrea DA (2000). Depression of group Ia monosynaptic EPSPs in cat hindlimb motoneurones during fictive locomotion. *J Physiol* **526**, 639–652.

Hantman AW & Jessell TM (2010). Clarke's column neurons as the focus of a corticospinal corollary circuit. *Nat Neurosci* **13**, 1233–1237.

Hinckley CA & Ziskind-Conhaim L (2006). Electrical coupling between locomotor-related excitatory interneurons in the mammalian spinal cord. *J Neurosci* **26**, 8477–8483.

Hormuzdi SG, Filippov MA, Mitropoulou G, Monyer H & Bruzzone R (2004). Electrical synapses: a dynamic signaling system that shapes the activity of neuronal networks. *Biochim Biophys Acta* **1662**, 113–137.

Hughes DI, Mackie M, Nagy GG, Riddell JS, Maxwell DJ, Szabo G, Erdelyi F, Veress G, Szucs P, Antal M & Todd AJ (2005). P boutons in lamina IX of the rodent spinal cord express high levels of glutamic acid decarboxylase-65 and originate from cells in deep medial dorsal horn. *Proc Natl Acad Sci U S A* **102**, 9038–9043.

Jankowska E, McCrea D, Rudomin P & Sykova E (1981). Observations on neuronal pathways subserving primary afferent depolarization. *J Neurophysiol* **46**, 506–516.

Jankowska E & Padel Y (1984). On the origin of presynaptic depolarization of group I muscle afferents in Clarke's column in the cat. *Brain Res* **295**, 195–201.

Jiang Z, Carlin KP & Brownstone RM (1999). An in vitro functionally mature mouse spinal cord preparation for the study of spinal motor networks. *Brain Res* **816**, 493–499.

Juszczak GR & Swiergiel AH (2009). Properties of gap junction blockers and their behavioural, cognitive and electrophysiological effects: animal and human studies. *Prog Neuropsychopharmacol Biol Psychiatry* **33**, 181–198.

Kamasawa N, Furman CS, Davidson KG, Sampson JA, Magnie AR, Gebhardt BR, Kamasawa M, Yasumura T, Zumbrunnen JR, Pickard GE, Nagy JI & Rash JE (2006). Abundance and ultrastructural diversity of neuronal gap junctions in the OFF and ON sublaminae of the inner plexiform layer of rat and mouse retina. *Neuroscience* **142**, 1093–1117.

Kandler K & Katz LC (1995). Neuronal coupling and uncoupling in the developing nervous system. *Curr Opin Neurobiol* **1**, 98–105.

Kiehn O & Tresch MC (2002). Gap junctions and motor behavior. *Trends Neurosci* **25**, 108–115.

Kremer E & Lev-Tov A (1998). GABA-receptor – independent dorsal root afferents depolarization in the neonatal rat spinal cord. *J Neurophysiol* **79**, 2581–2592.

Li X, Olson C, Lu S, Kamasawa N, Yasumura T, Rash JE & Nagy JI (2004). Neuronal connexin36 association with zonula occludens-1 protein (ZO-1) in mouse brain and interaction with the first PDZ domain of ZO-1. *Eur J Neurosci* **19**, 2132–2146.

Lemieux M, Cabana T & Pflieger JF (2010). Distribution of the neuronal gap junction protein Connexin36 in the spinal cord enlargements of developing and adult opossums, *Monodelphis domestica*. *Brain Behav Evol* **75**, 23–32.

Lidierth M & Wall PD (1996). Synchronous inherent oscillations of potentials within the rat lumbar spinal cord. *Neurosci Lett* **220**, 25–28.

Logan SD, Pickering AE, Gibson IC, Nolan MF & Spanswick D (1996). Electrotonic coupling between rat sympathetic preganglionic neurones *in vitro*. *J Physiol* **495**, 491–502.

Mann-Metzer P & Yarom Y (1999). Electrotonic coupling interacts with intrinsic properties to generate synchronized activity in cerebellar networks of inhibitory interneurons. *J Neurosci* **19**, 3298–3306.

Manjarrez E, Jimenez I & Rudomin P (2003). Intersegmental synchronization of spontaneous activity of dorsal horn neurons in the cat spinal cord. *Exp Brain Res* **148**, 401–413.

Marina N, Becker DL & Gilbey MP (2008). Immunohistochemical detection of connexin36 in sympathetic preganglionic and somatic motoneurons in the adult rat. *Auton Neurosci* **139**, 15–23.

Maxwell DJ, Christie WM, Short AD & Brown AG (1990). Direct observations of synapses between GABA-immunoreactive boutons and muscle afferent terminals in lamina VI of the cat's spinal cord. *Brain Res* **530**, 215–222.

McCrea DA, Shefchyk SJ & Carlen PC (1990). Large reductions in composite EPSP amplitude following conditioning stimulation are not accounted for by increased conductances in motoneurons. *Neurosci Let* **109**, 117–122.

McCrea D, Bautista Guzman W, Nagy J & Fedirchuk B (2009). Presynaptic inhibition in neonatal spinal cord is impaired in connexin36 knockout mice. *2009 Abstract Viewer/Itinerary Planner*, Programme No. 421.14. Society for Neuroscience, Washington, DC.

Mendell L (1972). Properties and distribution of peripherally evoked presynaptic hyperpolarization in cat lumbar spinal cord. *J Physiol* **226**, 769–792.

Meier C & Dermietzel R (2006). Electrical synapses–gap junctions in the brain. *Results Probl Cell Differ* **43**, 99–128.

Nagy J & Dermietzel R (2000). Gap junctions and connexins in the mammalian central nervous system. In *Advances in Molecular and Cell Biol*, vol. 30, ed. Hertzberg, EI, pp 323–396. JAI Press, Greenwich, CT.

Nagy JI, Dudek FE & Rash JE (2004). Update on connexins and gap junctions in neurons and glia in the mammalian nervous system. *Brain Res Brain Res Rev* **47**, 191–215.

Placantonakis DG, Bukovsky AA, Zeng XH, Kiem HP & Welsh JP (2004). Fundamental role of inferior olive connexin 36 in muscle coherence during tremor. *Proc Nat Acad Sci U S A* **101**, 7164–7169.

Rash JE, Dillman RK, Bilhartz BL, Duffy HS, Whalen LR & Yasumura T (1996). Mixed synapses discovered and mapped throughout mammalian spinal cord. *Proc Natl Acad Sci U S A* **93**, 4235–4239.

Rash JE, Olson CO, Davidson KG, Yasumura T, Kamasawa N & Nagy JI (2007*a*). Identification of connexin36 in gap junctions between neurons in rodent locus coeruleus. *Neuroscience* **147**, 938–956.

Rash JE, Olson CO, Pouliot WA, Davidson KG, Yasumura T, Furman CS, Royer S, Kamasawa N, Nagy JI & Dudek FE (2007*b*). Connexin36 vs. connexin32, "miniature" neuronal gap junctions, and limited electrotonic coupling in rodent suprachiasmatic nucleus. *Neuroscience* **149**, 350–371.

Rash JE, Pereda A, Kamasawa N, Furman CS, Yasumura T, Davidson KG, Dudek FE, Olson C, Li X & Nagy JI (2004). High-resolution proteomic mapping in the vertebrate central nervous system, close proximity of connexin35 to NMDA glutamate receptor clusters and co-localization of connexin36 with immunoreactivity for zonula occludens protein-1 (ZO-1). *J Neurocytol* **33**, 131–51.

Rash JE, Yasumura T, Davidson KG, Furman CS, Dudek FE & Nagy JI (2001*a*). Identification of cells expressing Cx43, Cx30, Cx26, Cx32 and Cx36 in gap junctions of rat brain and spinal cord. *Cell Commun Adhes* **8**, 315–320.

Rash JE, Yasumura T, Dudek FE & Nagy JI (2001*b*). Cell-specific expression of connexins and evidence of restricted gap junctional coupling between glial cells and between neurons. *J Neurosci* **21**, 1983–2000.

Rossignol S, Dubuc R & Gossard JP (2006). Dynamic sensorimotor interactions in locomotion. *Physiol Rev* **86**, 89–154.

Rudomin P (2009). In search of lost presynaptic inhibition. *Exp Brain Res* **196**, 139–151.

Rudomin P, Jimenez I, Quevedo J & Solodkin M (1990). Pharmacologic analysis of inhibition produced by last-order intermediate nucleus interneurons mediating nonreciprocal inhibition of motoneurons in cat spinal cord. *J Neurophysiol* **63**, 147–160.

Rudomin P & Schmidt RF (1999). Presynaptic inhibition in the vertebrate spinal cord revisited. *Exp Brain Res* 129, 1–37.

Rudomin P, Solodkin M & Jimenez I (1987). Synaptic potentials of primary afferent fibers and motoneurons evoked by single intermediate nucleus interneurons in the cat spinal cord. *J Neurophysiol* **57**, 1288–1313.

Shreckengost J, Calvo J, Quevedo J & Hochman S (2010). Bicuculline-sensitive primary afferent depolarization remains after greatly restricting synaptic transmission in the mammalian spinal cord. *J Neurosci* **30**, 5283–5288.

Simon O & Yelnik AP (2010). Managing spasticity with drugs. *Eur J Phys Rehabil Med* **46**, 401–410.

Thompson SW & Wall PD (1996). The effect of GABA and 5-HT receptor antagonists on rat dorsal root potentials. *Neurosci Lett* **217**, 153–156.

Van Der Giessen RS, Koekkoek SK, van Dorp S, De Gruijl JR, Cupido A, Khosrovani S, Dortland B, Wellershaus K, Degen J, Deuchars J, Fuchs EC, Monyer H, Willecke K, De Jeu MT, De Zeeuw CI (2008). Role of olivary electrical coupling in cerebellar motor learning. *Neuron* **58**, 599–612.

Walmsley B (1991). Central synaptic transmission: studies at the connection between primary afferent fibres and dorsal spinocerebellar tract (DSCT) neurones in Clarke's column of the spinal cord. *Prog Neurobiol* **36**, 391–423.

Walton KD & Navarrete R (1991). Postnatal changes in motoneurone electrotonic coupling studied in the *in vitro* rat lumbar spinal cord. *J Physiol* **433**, 283–305.

Wang Z, Li L, Goulding M & Frank E (2008). Early postnatal development of reciprocal Ia inhibition in the murine spinal cord. *J Neurophysiol* **100**, 185–196.

Willis WD (2006). John Eccles' studies of spinal cord presynaptic inhibition. *Prog Neurobiol* **78**, 189–214.

Wilson JM, Blagovechtchenski E & Brownstone RM (2010). Genetically defined inhibitory neurons in the mouse spinal cord dorsal horn: a possible source of rhythmic inhibition of motoneurons during fictive locomotion. *J Neurosci* **30**, 1137–1148.

Wilson JM, Cowan AI & Brownstone RM (2007). Heterogeneous electrotonic coupling and synchronization of rhythmic bursting activity in mouse Hb9 Interneurons. *J Neurophysiol* **98**, 2370–2381.

Wong SM, Cheng G, Homanics GE & Kendig JJ (2001). Enflurane actions on spinal cords from mice that lack the beta3 subunit of the $GABA_A$ receptor. *Anesthesiology* **95**, 154–164.

Yates C, Garrison K, Reese NB, Charlesworth A & Garcia-Rill E (2011). Novel mechanism for hyperreflexia and spasticity. *Prog Brain Res* **188**, 167–180.

Zlomuzica A, Viggiano D, Degen J, Binder S, Ruocco LA, Sadile AG, Willecke K, Huston JP & Dere E (2012). Behavioral alterations and changes in Ca/calmodulin kinase II levels in the striatum of connexin36 deficient mice. *Behav Brain Res* **226**, 293–300.

Author contributions

All experiments were performed in the laboratories of the Spinal Cord Research Centre at the University of Manitoba. Most of the data were collected and analysed by W.B. with the assistance of

the other authors. The dye coupling experiments were performed with Y.D. and W.B. D.M., J.N. and W.B. contributed equally to the writing and revision of the manuscript. All authors approved the final version of the manuscript.

Acknowledgements

This work was supported by Canadian Institutes of Health Research grants to D.M. (MOP 37756) and J.I.N. (MOP 106598) and by National Institutes of Health (NS31027, NS44010, NS44295) to J. E. Rash with sub-award to J.I.N. We thank David Paul (Harvard) for providing Cx36 knockout mouse breeding pairs, Dr Fedirchuk for providing electrophysiology facilities, Dr Eugene Zaporozhets for helpful guidance on the dissection techniques, Dr B. D. Lynn for genotyping transgenic mice, and B. McLean and S. McCartney for excellent technical assistance. W.B. was supported by a Manitoba Health Research Council Studentship.

Section 2. Re-evaluation of connexin (Cx26, Cx32, Cx36, Cx37, Cx40, Cx43, Cx45) association with motoneurons in rodent spinal cord, sexually dimorphic motor nuclei and trigeminal motor nucleus.

2.1.Rationale: Despite reports of electrical coupling between motoneurons in immature rodent spinal cord, a comprehensive analysis of the distribution of Cx36 in spinal cord has not been conducted.

2.2. Hypothesis: Electrical coupling of motoneurones occurs only by Cx36 in postnatal mouse spinal cord.

Experimental approach: Immunolabeling with a monoclonal Cx36 antibody was used to map the distribution of Cx36 in adult rodent spinal cord. Cx36 was not detected in Cx36 knockouts. Cx36 localization was examined in the cervical, thoracic, lumbar and sacral spinal cord by immunofluorescence. In order to distinguish which neuronal cell types have Cx36, double staining was carried out using antibodies against markers (peripherin and ChAT) for motoneurons and sympathetic preganglionic neurons. We used goat anti-mouse Cy3, goat anti-rabbit Cy5 and donkey anti-goat FITC as secondaries antibodies. Cx36 immunolabelling was observed in an epifluorescence microscope and some analyses were done using confocal microscopy. We determined whether coupled motoneurons express Cx36 as well as Cx26, Cx32, Cx37, Cx40, Cx43, Cx45**.** Spinal cord sections were processed for immunohistochemistry using antibodies for peripherin to label motoneurons.

Conclusions: Motoneurons were found to be associated with Cx36 and not other connexins, providing evidence that electrical coupling between motoneurons occurs viaCx36 in neonatal rodent spinal cord. There is a widespread distribution of Cx36 labeling in the adult spinal cord at cervical, thoracic, lumbar and sacral segments. As elsewhere in the CNS, immunolabelling for Cx36 in spinal cord was exclusively punctate in appearance, which presumably reflects localization to sites of gap junctions. Cx36 was densely distributed throughout spinal cord gray matter at P10 as we showed in section I. Although Cx36 expression was reduced in adult cord, it persisted in deep laminae of the dorsal horn and some regions of the ventral horn, including areas containing motoneurons. A striking finding was the presence at all spinal levels of densely distributed Cx36-positive puncta on cell bodies and initial dendrites of neurons located near the central canal at the transition between the dorsal and ventral horn.

Associate Editor: John Garthwaite

Section: Synaptic Mechanisms;

Intercellular Communication & Synaptic Plasticity

Re-evaluation of connexin (Cx26, Cx32, Cx36, Cx37, Cx40, Cx43, Cx45) association with motoneurons in rodent spinal cord, sexually dimorphic motor nuclei and trigeminal motor nucleus

W. Bautista and, J. I. Nagy*

Department of Physiology, Faculty of Medicine, University of Manitoba, Winnipeg, Canada

Running title: connexins associated with motoneurons

Keywords: gap junctions, sexually dimorphic motoneurons,

No. of pages:

No. of figures:5

No. of words: Abstract, 273; Introduction,680; Discussion,1422

**Address for correspondence:*

James I. Nagy

Department of Physiology

Faculty of Medicine

University of Manitoba

745 Bannatyne Ave, Winnipeg, Manitoba, Canada R3E 0J9

Email: nagyji@ms.umanitoba.ca

Tel. (204) 789-3767, Fax (204) 789-3934

Abstract

Electrical synapses formed by neuronal gap junctions composed of connexin (Cx36) are now recognized as a common feature in mammalian brain circuitry. These synapses also occur at brain stem and spinal cord levels, but less is known about their depolyment and functions in these regions of the CNS. Gap junction-mediated electrical and dye-coupling between motoneurons has been most studied in hindbrain and spinal cord. Unlike selective expression of Cx36 in many other classes of central neurons, it has been reported based on connexin mRNA and/or protein detection that developing and/or mature motoneurons express a variety of connexins, including Cx26, Cx32, Cx36 and Cx43 in trigeminal motoneurons, Cx36, Cx37, Cx40, Cx43 and Cx45 in spinal motoneurons, and Cx32 in sexually dimorphic motoneurons. We re-examined the localization of these connexins during postnatal development and in adult rat and mouse using immunofluorescence labelling for each connexin in combination with labelling for the motoneuron maker peripherin. We found Cx26 in association only with leptomeninges in the trigeminal motor nucleus, Cx32 only with oligodendrocytes and myelinated fibers among motoneurons in this nucleus and in the spinal cord, and Cx37, Cx40 and Cx45 only with blood vessels in spinal cord, including those among motoneurons. Punctate labelling for Cx36 was seen localized to the somatic and dendritic surfaces of peripherin-positive motoneurons in the trigeminal motor nucleus, spinal cord lamina IX motoneuron throughout the spinal cord and to sexually dimorphic motoneurons in lower lumbar to upper sacral levels. In studies of electrical synapses and electrical transmission related to developing and adult motoneurons, our results serve to focus attention on mediation of this transmission by gap junctions on motoneurons composed of Cx36.

Keywords: Gap junctions, electrical coupling, sexually dimorphic motoneurons,

Introduction

Gap junction channels between cells are composed of connexin proteins that form two apposed hexameric connexons linking across the extracellular space to allow the intercellular movement of ions and small molecules (Evans & Martin, 2002). Among the twenty connexin protein family members, most cells selectively express a particular connexin, although it is not unusual to find some cells concurrently producing two or even three different connexins (Yeh *et al*., 1998). The greatest diversity in the connexin composition of gap junctions is found in the central nervous system (CNS), perhaps not surprisingly given the cellular and morphological heterogeneity of neural tissue. With up to twelve different connexins found in adult brain, considerable efforts aimed to assign these to expression by particular cell types have lead to the general consensus that astrocytes express Cx26, Cx29, Cx30 and oligodendrocytes express Cx32, Cx43, Cx47 (Rash *et al*., 2001; Nagy *et al.,* 2004, 2011; Rash, 2010; Giaume, & Theis, 2010). In addition, a wide variety of neurons express Cx36 (Sohl *et al*., 2005; Meier & Dermietzel, 2006), while Cx45 and Cx57 exhibit more restricted neuronal expression, such as in retina (Hombach *et al*., 2004; Sohl *et al.,* 2005; Ciolofan *et al*., 2007; *Li et al.,* 2008). Reporter gene expression of Cx30.2 has also been found in neurons (Kreuzberg *et al*., 2008), but corresponding expression of Cx30.2 protein has so far not been reported. Connexins in CNS vasculature have not been subject to comprehensive examination, but as in other tissues (Severs *et al.,* 2001), there is evidence in brain for Cx37 and Cx40 expression in endothelial cells, and Cx45 in vascular smooth muscle cells (Yeh *et al.,* 1998; Kruger et al., 2000; Li and Simard, 2001; Nagasawa *et al*., 2006; Haddock *et al.,* 2006).

The identification of cell-specific expression of connexins in brain has been essential for understanding the contribution of gap junctional intercellular communication to myriad of brain functions. In particular, the well establish principle that gap junctions between neurons are the structural basis for electrical synaptic transmission (Bennett, 1997), together with the discovery of Cx36 expression in mammalian neurons (Condorelli *et al*., 1998; Sohl *et al*., 1998) and documentation of its widespread occurrence in neuronal gap junctions (Nagy *et al*., 2004; Sohl et al., 2005; Rash *et al*., 2000,2001a,b,2007a,b), provided the basis for numerous studies, leading to the general acceptance of the physiological importance of electrical synapses composed of Cx36 in mammalian brain (Bennett &, Zukin, 2004; Connors & Long, 2004; Hormuzdi *et al*., 2004).

In spinal cord, the organization of electrical synapses within neural circuitry, the functional roles of these synapses, the distribution of neuronal gap junctions, and the connexins that mediate electrical synaptic transmission are far less understood. As elsewhere in developing CNS, distinct populations of neurons in spinal cord are electrically coupled during development (Hinckley & Ziskind-Conhaim, 2006; Wilson *et al*., 2007), the clearest example of which is coupling between motoneurons during roughly the first postnatal week, with subsequent loss of this coupling (Arasaki *et al*., 1984; Fulton *et al*., 1980; Walton & Navarette, 1991; Bou-Flores & Berger, 2001). In rodents, postnatal motoneurons were found apparently to express five connexins, including Cx36, Cx37, Cx40, Cx43 and Cx45, with persistence of expression of the former three connexins in adult motoneurons (Chang *et al*., 1999; Chang & Balice-Gordon, 2000). It has also been reported that most spinal motoneurons express Cx32 (Micevych & Abelson, 1991), including motoneurons in sexually dimorphic motor nuclei (Matsumoto *et al*., 1991,1992), and that trigeminal motoneurons express Cx26, Cx32, Cx36, and Cx43 (Honma *et al.,* 2004), making the expression of seven connexins in a single cell type highly unusual. We have begun to focus our studies of electrical synapses on detailed examination of those associated with motoneurons, which could represent a daunting task given the plethora of connexins reported to be present in these cells. At the onset, therefore, we conducted a re-evaluation of motoneuron connexin expression. We used immunofluorescence approaches to examine thel localization of Cx36, Cx37, Cx40, Cx43 and Cx45 in relation to spinal motoneurons, and that of Cx26, Cx32, Cx36 and Cx43 in relation to trigeminal motoneurons.

Materials and methods

Animals and antibodies

The present investigations were conducted using brains and spinal cords from fifteen adult C57BL/6 mice, twenty adult Sprague-Dawley rats, and twelve mice and rats at various early postnatal ages. Tissues from some of these animals were taken for use in parallel unrelated studies. Animals were utilized according to approved protocols by the Central Animal Care Committee of University of Manitoba, with minimization of the numbers animals used.

Anti-connexin antibodies were obtained from Life Technologies Corporation (Grand Island, NY, USA) (formerly Invitrogen/Zymed Laboratories), and those used included: two

rabbit polyclonal antibodies (Cat. No. 36-4600 and Cat. No. 51-6300) and one mouse monoclonal antibody (Cat. No. 39-4200) against Cx36; and rabbit polyclonal antibodies against Cx32 (Cat. No. 34-5700), Cx37 (Cat. No. 42-4500), Cx40 (Cat. No. 36-5000 and Cat. No. 37-8900), Cx43 (Cat. No. 35-5000), and Cx45 (Cat. No. 40-7000). Specificity characteristics of the anti-Cx36 for Cx36 detection in various regions of rodent brain have been previously reported (Li *et al*., 2004; Rash et al., 2007a,b; Curti *et al*., 2012). Specificities of the anti-Cx26 and anti-Cx32, with confirmation using Cx26 ko and Cx32 ko mice, and that of anti-Cx43 have also been reported (Rash et al., 2001a; Nagy *et al*., 2003a,2011). Specificity of the anti-Cx37, anti-Cx40 and anti-Cx45 are described in the Results section. Additional antibodies included a chicken polyclonal anti-peripherin that was utilized as a marker of motoneurons (Millipore, Temecula, CA, USA) and used at a dilution of 1:500, and a mouse monoclonal anti-2,'3'-cyclic nucleotide 3'-phosphodiesterase (CNPase) (Sternberger Monoclonals, Baltimore, MD, USA) that was utilized as a marker for oligodendrocytes and used at a dilution of 1:1000. Various secondary antibodies included Cy3-conjugated goat or donkey anti-mouse and anti-rabbit IgG diluted 1:600 (Jackson ImmunoResearch Laboratories, West Grove, PA, USA), Alexa Flour 488-conjugated goat or donkey anti-rabbit and anti-mouse IgG diluted 1:600 (Molecular Probes, Eugene, OR, USA), and AlexaFluor-647 conjugated goat anti-chicken IgG diluted 1:500 (Life Technologies Corporation) and Cy3-conjugated goat anti-chicken, diluted 1:600 (Jackson ImmunoResearch Laboratories). All antibodies were diluted in 50 mM Tris-HCl, pH 7.4, containing 1.5% sodium chloride (TBS), 0.3% Triton X-100 (TBSTr) and 10% normal goat or normal donkey serum.

Tissue preparation

Adult animals were deeply anesthetized with equithesin (3 ml/kg), placed on a bed of ice, and perfused transcardially with cold (4°C) pre-fixative consisting of 50 mM sodium phosphate buffer, pH 7.4, 0.1% sodium nitrite, 0.9% NaCl and 1 unit/ml of heparin, followed by perfusion with fixative solution containing cold 0.16 M sodium phosphate buffer, pH 7.4, 0.2% picric acid and either 1% or 2% formaldehyde prepared from freshly depolymerized paraformaldehyde. Animals were then perfused with a cold solution containing 10% sucrose and 25 mM sodium phosphate buffer, pH 7.4, to wash out excess fixative. Tissues from early postnatal animals were dissected and taken for immersion fixation in 1% or 2% formaldehyde for 30 to 50 min. Tissues

were stored at 4°C for 24-48 h in cryoprotectant containing 25 mM sodium phosphate buffer, pH 7.4, 10% sucrose, 0.04% sodium azide. Sections of spinal cord were cut at a thickness of 10-15 µm using a cryostat and collected on gelatinized glass slides. Slide-mounted sections could be routinely stored at -35 ^{o}C for several months before use. Some detailed considerations regarding fixation conditions required for optimum immunohistochemical detection of Cx36, alone or in combination with other proteins, are described elsewhere (Nagy *et al*., 2012).

Immunofluorescence procedures

Slide mounted sections removed from storage were air dried for 10 min, washed for 20 min in TBSTr, and processed for immunofluorescence staining, as previously described (Li et al., 2008; Bautista et al., 2012; Curti et al., 2012). For single, double or triple immunolabelling, sections were incubated with a single primary antibody, or simultaneously with two or three primary antibodies for 24 h at 4°C. All connexin antibodies were incubated with tissue sections at a concentration of 1-2 µg/ml. The sections were then washed for 1 h in TBSTr and incubated with either a single or appropriate combinations of secondary antibodies for 1.5 h at room temperature. Some sections processed by single or double immunolabelling were counterstained with either green Nissl fluorescent NeuroTrace (stain N21480) or Blue Nissl NeuroTrace (stain N21479) (Molecular Probes, Eugene, OR, USA). All sections were coverslipped with the antifade medium Fluoromount-G (SouthernBiotech, Birmingham, AB, USA). Control procedures involving omission of one of the primary antibodies with inclusion of the secondary antibodies used for double and triple labelling indicated absence of inappropriate cross-reactions between primary and secondary antibodies for all of the combinations used in this study.

Immunofluorescence was examined on a Zeiss Axioskop2 fluorescence microscope and a Zeiss 710 laser scanning confocal microscope, using Axiovision 3.0 software or Zeiss ZEN Black 2010 image capture and analysis software (Carl Zeiss Canada, Toronto, Ontario, Canada). Data from wide field and confocal microscopes were collected either as single scan images or z-stack images with multiple optical scans at z scanning intervals of typically 0.4 to 0.6 µm. Images of immunolabelling obtained with Cy5 fluorochrome were pseudo colored blue. Final

images were assembled using CorelDraw Graphics (Corel Corp., Ottawa, Canada) and Adobe Photoshop CS software (Adobe Systems, San Jose, CA, USA).

Results

Connexins and spinal cord motoneurons

With the reported expression of seven connexin proteins and/or their corresponding mRNAs in motoneurons, we began by re-examining the distribution of immunofluorescence labelling for those connexins in lamina IX of spinal cord, and specifically their purported association with motoneurons. We first show that the antibodies used here against the relevant connexins produce immunolabelling patterns typical of those connexins localized to specific cell types. Anti-Cx37 and anti-Cx40 gave labelling along blood vessels in rat heart, as well as in rat and mouse brain (Fig. 1A-C), indicative of the localization of the connexins detected at gap junctions between endothelial cells (Severs *et al*., 2001). The specificity of Cx37 and Cx40 detection by these antibodies along vasculature has been confirmed using Cx37 knockout and Cx40 knockout mice (A. Simon and JI Nagy, unpublished observations). In addition, the anti-Cx40 gave labelling at intercalated discs and along lateral appositions of atrial cardiac myocytes in heart (Fig. 1D and 1E), where Cx40-containing gap junctions are known to be heavily concentrated (Severs *et al*., 2001). The anti-Cx45 produced punctate labelling along large diameter blood vessels in brain (Fig. 1F), reflective of Cx45 localization at gap junctions between smooth muscle cells along vasculature (Kruger *et al*., 2000; Li & Simard, 2001). Further, we have shown elsewhere that the anti-Cx45 used here labels ultrastructurally-identified interneuronal gap junctions in rodent retina (Li *et al*., 2008). Specificity validation of the other anti-connexin antibodies used is described in Materials and Methods. Confirmation that Cx37 and Cx40 are also localized along blood vessels in spinal cord is presented in Figures 1G and 1H. In the ventral horn of rat lumbar spinal cord, blood vessels labelled with the endothelical cell marker IB4 (Fig. 1G1 and H1) displayed similar labelling for Cx37 (Fig. 1G2) and Cx40 (Fig. 1G2) as seen along vessels in the cerebral cortex.

For studies of spinal cord, animals were examined at early developmental ages when spinal motoneurons were reported to express Cx36, Cx37, Cx40, Cx43, and Cx45, and at an adult stage when these neurons were found to continue expression of protein and/or mRNA for some of

these connexins (Chang et al., 1999; 2000; Chang & Balice-Gordon, 2000), as well as mRNA for Cx32 (Micevych & Abelson, 1991; Matsumoto *et al*., 1991,1992). We previously noted that labelling for Cx36 is present at sites between motoneurons at postnatal day (PD) 5 (Bautista *et al*., 2012). Here, we show that some motor nuclei display particularly robust immunolabelling for Cx36 at this age, as shown by examples with double labelling for Cx36 and the motoneuron marker peripherin (Clarke *et al.,* 2010) in lamina IX of mouse (Fig. 2A,B) and rat (Fig. 2C) lumbar spinal cord. Labelling for Cx36 was exclusively punctate (Cx36-puncta) in appearance, with absence of diffuse or punctate intracellular immunofluorescence. Although scattered sparsely in surrounding regions, Cx36-puncta were most concentrated within motor nuclei, were often localized to peripherin-positive motoneuronal somata or dendrites, and were commonly found at appositions between these neuronal elements (Fig. 2B,C). All clusters of motoneurons encountered displayed scattered Cx36-puncta, but there was considerable heterogeneity in density of Cx36-puncta among motor nuclei, suggesting staggered development of Cx36 expression among these nuclei.

For labelling of the various other connexins examined in fields of spinal cord lamina IX, results are presented with comparison of labelling for Cx36 in the same fields. All sections were triple labelled for Cx36 plus another connexin, with the inclusion of labelling for peripherin to ensure that areas examined contained groups of motoneurons, but labelling for peripherin is not always shown in order to avoid obscuring fine punctate labelling for connexins. In lumbar spinal cord sections labelled for Cx36 and Cx37, areas of lamina IX displaying Cx36-puncta showed immunofluorescence for Cx37 restricted to blood vessels in mouse at PD5 (Fig. 2D) and PD10 (Fig. 2E), and in rat at PD5 (Fig. 2F). [Labelling of all vascular-associated connexins (i.e., Cx37, Cx40 and Cx45) in spinal cord was sparse at these developmental ages, but where possible were included in the fields photographed as positive controls for detection of these connexins with the antibodies used.] Similar results were obtained in comparisons of Cx36 and Cx37 expression in adult spinal cord. A low magnification of the ventral horn labelled for peripherin and counterstained with blue Nissl fluorescence is shown in Figure 2G, with the lower and upper boxed areas in this figure magnified in Figures 2H and 2I, respectively, which show labelling for Cx36, Cx37 and peripherin. As seen at earlier ages, Cx36-puncta are distributed on peripherin-positive motoneurons in lamina IX (Fig. 2H), while labelling for Cx37 is absent on these

motoneurons, but is instead seen localized along blood vessels, as shown by an example of a vessel in lamina VIII (Fig. 2I).

Double immunofluorescence labelling for peripherin and Cx43 in lamina IX of rat lumbar spinal cord at PD5 is shown in Fig. 2J. Labelling for Cx43 is entirely punctate, with negligible diffuse intracellular labelling, which was equal to background fluorescence seen after Cx43 primary antibody omission (not shown). In regions surrounding peripherin-positive motoneurons, Cx43-puncta are sparsely distributed at this age, and is not nearly as dense as seen throughout spinal cord gray matter in adults (Ochalski *et al.*, 1997). Although resolution by immunofluorescence visualization is insufficient to discern whether or not some Cx43-puncta are localized directly on neuronal plasma membranes, these puncta did not display the regularity of association with peripherin-positive motoneuron dendrites and somata at PD5 as that displayed by Cx36-puncta. Adult motoneurons were also devoid of intracellular labelling for Cx43, but very densely distributed Cx43-puncta throughout neuropil precluded cell-type assignment of these puncta (not shown). In any case, Cx43 in adult spinal cord has been previously localized ultrastructurally to gap junctions between astrocytes, and not to those between neurons (Rash *et al.*, 2001a; Ochalski *et al.*, 1997).

Labelling for Cx36 in combination with Cx45 in lamina IX of rat lumbar spinal cord at PD5 is shown in Figure 2K. Areas containing Cx36-puncta (Fig. 2K1) among motoneurons (peripherin labelling not shown) were totally devoid of labelling for Cx45 (Fig. 2K2). Labelling of Cx45 along blood vessels was encountered, but Cx45-puncta on these vessels were particularly sparse and fine at this age (not shown). In lamina IX of adult rat spinal cord, Cx36-puncta are seen decorating the surface of motoneurons (Fig. 2L1), but there is negligible association of labelling for Cx45 with those motoneurons. Instead Cx45-puncta displayed circular or elongated patterns of labelling (Fig. 2L1), as is more evident in the same field shown with labelling of Cx45 alone (Fig. 2L2), reflecting Cx45 localization at blood vessels cut perpendicular or tangential to their long axis.

Results from double labelling of Cx36 with Cx40, and peripherin with Cx40, in lumbar spinal cord are shown in Figure 3, where pairs of images (*e.g.*, A1,A2, etc) show Cx36 and Cx40 labelling or peripherin and Cx40 labelling in the same field. As in the case of Cx37, fields containing Cx36-puncta in lamina IX at PD5 in rat (Fig. 3A1) and mouse (Fig. 3B1), and at

PD10 in mouse (Fig. 3C1), showed an absence of labelling for Cx40 associated with motoneurons (labelling for peripherin not shown), but did display labelling of Cx40 along with blood vessels in the same fields (Fig. 3A2, 3B2, and 3C2). Examples of labelling for peripherin in conjunction with Cx40 in lumbar lamina IX at PD5 are shown in rat (Fig. 3D) and mouse (Fig. 3E), where areas filled with peripherin-positive motoneurons (Fig. 3D1 and 3E1) displayed labelling for Cx40 restricted exclusively to blood vessels in the vicinity of these neurons (Fig. 3D2 and 3E2, respectively). Similar results were obtained in adult cord, where peripherin-positive motoneurons in lamina IX showed an absence of labelling for Cx40 (Fig. 3F1), and Cx40 was localized instead to blood vessels (Fig. 3F2).

Localization of Cx36 and Cx32 among sexually dimorphic motor nuclei

Sexually dimorphic motor nuclei, together with their constituent motoneurons, are defined as such because the morphological appearance and numbers of neurons in these nuclei differ substantially in male and female species (Breedlove, 1986; McKenna & Nadelhaft 1986; Coleman & Sengelaub, 2002). Located at the lumbosacral L6-S1 levels, these nuclei consist of several groups, including a dorsomedial group and a dorsolateral group, on which we fous here. A more comprehensive analysis of Cx36 association with these nuclei is given elsewhere (Bautista et al., 2013).

Comparison of Cx36 with Cx32 localization in spinal cord was examined in sexually dimorphic motor nuclei in which motoneurons were reported to express Cx32 mRNA (Matsumoto *et al*., 1991,1992), and well as in other motor nuclei where in situ hybridization signal for Cx32 mRNA was detected, although we appreciate caveats noted regarding specificity of Cx32 mRNA detection (Micevych & Abelson, 1991). Immunofluorescence labelling for Cx36 and Cx32 among peripherin-positive motoneurons in lamina IX of adult male rats is shown in Figure 4. At lower lumbar spinal levels, containing the locations of sexually dimorphic nuclei (McKenna & Nadelhaft, 1986), labelling for Cx36 was detected in each of these nuclei, as shown by examples of Cx36 localization in the dorsomedial nucleus at its rostral (Fig. 4A) and caudal (Fig. 4B) levels, and in the dorsolateral nucleus at a rostral level (Fig. 4C). At higher magnification, Cx36-puncta were readily seen associated with the somata and dendrites of

peripherin-positive dimorphic motoneurons, as shown in the dorsomedial nucleus (Fig. 4D). In contrast, labelling for Cx32 was sparse in the dimorphic motor nuclei, and was absent on the surface of, or intracellularly within, these motoneurons, but was instead localized to small cells that were delineated by Cx32-puncta decorating their surface (Fig. 4A-D) or was associated with strands of fibers, which resembled patterns of labelling we have previously reported for Cx32 associated with oligodendrocytes and myelinated fibers (Nagy *et al*., 2003a). Examination of other spinal levels containing non-dimorphic motor nuclei in lamina IX showed a similar association of Cx36 with peripherin-positive motoneurons and an absence of Cx32 localization at the surface of these neurons (Fig. 4E). In adult male mice, the sexually dimorphic Onuf's motor nucleus located at the L6 spinal level, and corresponding roughly to the dorsomedial and dorsolateral nuclei in rat, also displayed Cx36-puncta associated with motoneurons (Fig. 4F1), whereas Cx32 was again localized to small cells (Fig. 4F2) that had the size and shape of oligodendrocytes. As in rat, similar results were obtained in non-dimorphic motor nuclei of mouse at other spinal levels, where motoneurons displayed labelling for Cx36 but not Cx32 along their somatic and dendritic surfaces (Fig. 4G). Confirmation of Cx32 localization to oligodendrocytes was obtained by triple labelling for Cx32, peripherin and the oligodendrocyte marker CNPase (Fig. 4H,I), revealing Cx32-puncta distributed on the surface of CNPase-positive cells in lamina IX of lumbar spinal cord. Additional Cx32-puncta not associated with oligodendrocyte somata or with motoneurons were localized along myelinated fibers, as we have previously shown in regions elsewhere in the CNS (Nagy *et al.*, 2003a,b).

Connexins and trigeminal motoneurons

We next examined immunofluorescence localization of Cx26, Cx32, Cx36 and Cx43 in the trigeminal motor nucleus of PD15 and adult mouse, where diffuse labelling for each of these connexins was described to occur in the cytoplasm and/or nucleus of trigeminal motor neurons of developing and adult mice (Honma et al., 2004). In adult mice, labelling of Cx36 is distributed throughout the nucleus, and is remarkably dense to the point of delineating the nucleus from surrounding regions that contained sparse labelling (Fig. 5A). Immunofluorescence consisted exclusively of Cx36-puncta often localized to the surface of peripherin-positive motoneuron somata or along their dendrites (Fig. 5B). Punctate or diffuse intracellular labelling is absent, as

determining by through focus confocal analysis of individual motoneurons. Comparison of labelling for Cx36 and Cx26 among adult trigeminal motoneurons is shown in Figure 5C. In contrast to widely distributed Cx36-puncta (Fig. 5C1), labelling for Cx26 is restricted to a lateral portion of the nucleus largely devoid of motoneuron somata, but containing myelinated fibers belonging to the motor root of the trigeminal nerve (Fig. 5C2). Immunofluorescence for Cx26 is punctate in appearance, and displayed negligible association with trigeminal motoneuronal somata. Diffuse intracellular labelling for Cx26 in these somata is also negligible. Elsewhere in brain, similar parenchymal Cx26-puncta in adult rodent were localized to astrocyte processes labelled for glial fibrillary acidic protein (GFAP) (Nagy et al., 2001, 2011). The trigeminal motor nucleus and the motor root of the trigeminal nerve laying lateral to it were largely devoid of labelling for GFAP under the fixation conditions required to detect Cx26, precluding double labelling for this connexin and the astrocyte marker. At PD15, localization of Cx36 among trigeminal motoneurons was somewhat less dense, and consisted of finer Cx36-puncta (Fig. 5D) than seen in adults mice, suggesting that Cx36-puncta increase in size and density with development, notwithstanding that earlier postnatal ages were not examined. This is in contrast to the reduced labelling for Cx36 previously reported in these motoneurons during development (Honma *et al.*, 2004). Labelling for Cx26 in the trigeminal motor nucleus was absent at PD15, except for Cx26 seen in association with leptomeningeal sheaths of blood vessels, where these meningeal sheath have short projections into the brain (Mercier & Hatton, 2001).

Immunofluorescence labelling for Cx32 in combination with that of either Cx36 and peripherin or with the oligodendrocytes marker CNPase and peripherin in the trigeminal motor nucleus in adult mouse is shown in Figure 5E-G. Labelling of Cx32 is punctate, similar to that of Cx36, but are often assembled in round or oval clusters (Fig. 5E,F), and is absent intracellularly in motoneurons. Again, in contrast to the regular localization of Cx36 to the surface of peripherin-positive motoneurons (Fig. 5E,F), Cx32-puncta usually appeared in areas devoid of labelling for peripherin. Where overlap between these puncta and peripherin occurred in z-stack images, 3-dimentional rotation indicated lack of association of puncta with motoneuron surfaces (not shown). Inclusion of labelling for CNPase revealed the clusters of Cx32-puncta to be associated with CNPase-positive oligodendrocytes and there initial dendritic segments (Fig. 5G). Some CNPase signal (red) is seen above or below (confirmed in single scans) peripherin signal (blue) in these 5 µm z-stack images, but stacks were required to obtain a full compliment of

Cx32-puncta around oligodendrocytes. Similar labelling and localization of Cx32 is seen in mouse trigeminal motor nucleus at PD15 (not shown).

Triple immunofluorescence labelling for Cx36, Cx43 and peripherin in the trigeminal motor nucleus of adult mouse is shown in Figure 5H and I, with similar patterns of labelling observed in this nucleus at PD15 (not shown). Labelling for Cx43 is punctate throughout the brainstem, including the trigeminal motor nucleus, and Cx43-puncta are exceptionally dense compared with that of Cx36-puncta (Fig. 5H). Though Cx43-puncta were observed laying over peripherin-positive motoneuron dendrites in the z-stack image shown in Fig. 5I, through focus analysis indicated absence of intracellular punctate or diffuse Cx43 immunoreactivity. Regardless of whether images were captured as confocal z-stack or as single scans, some Cx43-puncta were invariably found to lie very near peripherin-positive elements, making it impossible by immunofluorescence light microscopy to assign these puncta to plasma membranes of particular cell types. Nevertheless, given the localization of Cx43 to astrocyte gap junctions in most other brain regions, together with the close proximity of some of these junctions to neuronal somatic and dendritic plasma membranes (Yamamoto *et al.*, 1990), which can be <0.5 µm, the close proximity of some Cx43-puncta to trigeminal motoneuron somata and their processes is expected assuming localization of these puncta to astrocyte gap junctions.

Discussion

Extensive gap junctional coupling between neurons throughout the CNS at early postnatal ages is a hallmark of developing neural systems (Meier & Dermietzel, 2006). It has more recently become well established that electrical synapses persists, at higher or lower levels than seen during deveopment, in many CNS areas of adult animals, where they contribute essential feature to integrative processes in neuronal circuitry (Bennett &, Zukin, 2004; Connors & Long, 2004; Hormuzdi *et al*., 2004). Despite earlier acceptance of widespread electrical synapses at early postnatal ages, less is currently known about the functional role of electrical coupling between neurons during development. This is particularly the case in the spinal cord, where detailed studies of neuronal gap junction localization and connexin expression patterns both during development and at maturity have lagged behind those in brain, making it difficult to relate

presence of electrical coupling to incidence and distribution of the morphological substrate of this coupling, namely neuronal gap junctions. Some of the literature available on coupling between motoneurons is especially frought with considerable complexity.

Electrical coupling between early postnatal motoneurons, suggested to be important for generation of synchronous activity among these neurons (Kiehn & Tresch, 2002; Kiehn et al., 2000), was found to be either reduced (Tresch & Kiehn, 2000) or to be unaffected (Tresch & Kiehn, 2002) by gap junction blockers. In a series of long-standing reports, motoneuron coupling was considered in the context of synapse development with target muscles in both intact and peripheral nerve-transected animals (Personius & Balice-Gordon, 2001). In these studies in rodents and cats, postnatal motoneurons were found apparently to express five connexins, including Cx36, Cx37, Cx40, Cx43 and Cx45, with persistence of expression of the former three connexins in adults, despite loss of coupling, and presence of motoneuron plasma membrane labeling for Cx43 (Chang *et al*., 1999; Chang & Balice-Gordon, 2000). Further, motoneuron coupling was reduced in mice with Cx40 knockout, which had an impact on patterns of neuromuscular synapse development (Personius & Balice-Gordon, 2000; Personius *et al*., 2001,2007). Reports generally refer to a loss of motoneuronal gap junctional coupling during maturation. However, gap junctions were observed between some motoneurons in adult rodent spinal cord (van der Want *et al*., 1998), particularly between motoneurons in sexually dimorphic motor nuclei (Matsumoto *et al*., 1988,1989), which is consistent with the persistence of coupling among motoneuronal populations in the dimorphic nuclei of adult animals (Coleman & Sengelaub, 2002), and which was attributed to expression of Cx32 in these dimorphic motoneurons (Matsumoto *et al*., 1991,1992). Inl animals subjected to various treatments, there have been reports of altered motoneuronal coupling without changes (Chang *et al*., 2000) or undetermined changes (Mentis *et al*., 2002; Pastor *et al*., 2003) in connexin expression, or altered Cx36 expression in unidentified cell types without determination of possible changes in coupling (Yates *et al*., 2011). As in spinal cord, complex patterns of connexin expression have also been reported in the trigeminal motor nucleus, where largely diffuse cytoplasmic labelling and even some nuclear labelling for Cx26, Cx32 and Cx43 was described in both developing and adult trigeminal motoneurons (Honma *et al*., 2004).

In a previous report, we described a deficit in presynaptic inhibition in the spinal cord of juvenile mice with Cx36 knockout, correlated this with the presence of Cx36 and neuronal dye-coupling among interneurons that mediate presynaptic inhibition, and noted the persistence of Cx36 expression in various dorsal and ventral horn regions in adult rodent spinal cord, including labelling of Cx36 in association with motoneurons (Bautista *et al*., 2012). The present analyses of various connexins reported to be expressed in developing and adult rodent spinal cord reveals robust and consistent punctate labelling for Cx36 in motor nuclei, often localized to the surface of motoneurons in spinal cord lamina IX and the trigeminal motor nucleus, compared with the absence of similar labelling for the other connexins examined. Localization of Cx37, Cx40 and Cx45 was restricted to blood vessels in this and other spinal cord lamina, and Cx43 showed little evidence of a regular association with motoneurons at early stages of development. Nor did we find Cx37 or Cx45 localized to spinal motoneurons or intracellular diffuse labelling or diffuse plasma membrane labelling of Cx43 protein in these neurons of adult animals, contrasting with earlier descriptions (Chang *et al*., 1999; Chang & Balice-Gordon, 2000). Further, despite reports of widespread Cx32 mRNA expression in spinal motoneurons (Micevych & Abelson, 1991), including sexually dimorphic motoneurons (Matsumoto *et al*., 1991,1992), we found Cx32 protein to be associated only with oligodendrocytes and myelinated fibers in lamina IX, as well as other spinal cord laminae. Similarly, in the trigeminal motor nucleus, we found Cx26 only in association with bundles of white matter and with leptomeninges, and Cx32 only with oligodendrocytes, as occurs elsewhere in brain (Nagy *et al.,* 2003; Lynn *et al.,* 2011), and no evidence of previously described (Honma *et al.,* 2004) diffuse cytoplasmic or nuclear labelling for these connexins or for that of Cx36 or Cx43 in trigeminal motoneurons. It should be noted that, due to limits of resolution afforded by immunofluorescence microscopy, very dense punctate labelling for Cx43 in all areas of the CNS precludes assignment of this labelling to plasma membranes of specific cell types, as was previously done (Chang et al., 1999, 2000; Honma *et al.,* 2004).

Our results stand in marked contrast to previous reports of Cx40, Cx43 and Cx45 protein expression in spinal motoneurons, and Cx26, Cx32 and Cx43 expression in trigeminal motoneurons. Further, our data cast doubt on connexin protein expression from mRNAs for some these connexins and for mRNAs for Cx32 and Cx37 reported to be present in motoneurons (Matsumoto *et al*., 1991,1992; Micevych & Abelson, 1991; Chang *et al.,* 1999, 2000; Chang &

Balice-Gordon, 2000; Honma *et al.*, 2004). It appears that these mRNAs in motoneurons fail to be translated into corresponding protein products. Our results are consistent with ultrastructural localization of Cx32 and Cx43 to gap junctions between glial cells in the spinal cord, and not to those between neurons (Rash *et al*., 1998; 2001a). Previously reported reductions in motoneuron coupling and disruptions in motoneuron synaptic organization in Cx40 knockout mice(Personius et al., 2007) may have arisen from vascular and/or cardiac anomalies in these animals (Simon & McWhorter, 2002). We conclude that Cx36 is the major connexin mediating electrical and dye-coupling between rodent motoneurons at early postnatal ages and in sexually dimorphic motoneurons in adult animals, and suggest that Cx36 be the focus of continued studies of motoneuronal gap junctions in rodent spinal cord. Nevertheless, in absence of data indicating total loss of coupling between motoneurons during early development in Cx36 knockout mice, we cannot exclude the possibility that these neurons may express another as yet unidentified connexin either normally or in a compensatory fashion in the Cx36 knockout, particularly since Cx36-expressing neurons in some systems were reported to display residual coupling after Cx36 ablation (Lee *et al*., 2010; Curti *et al*., 2012).

Cx36 association with adult motoneurons

The abundant Cx36-puncta associated with adult motoneurons in sexually dimorphic motor nuclei almost certainly reflect localization of gap junctions, consistent with demonstrations of dye-coupling between these neurons in adult rats (Coleman & Sengelaub, 2002). However, a relatively high density of Cx36-puncta are also widely distributed on lamina IX motoneurons elsewhere and, indeed, throughout the spinal cord as well as on motoneurons in the trigeminal motor nucleus in adult rodent. Because electrical and dye-coupling between motoneurons is well-established to progressively decrease and disappear during development (Walton & Navarette, 1991; Chang et al, 1999), it may be considered that Cx36-containing gap junctions associated with adult spinal motoneurons in other than sexually dimorphic motor nuclei are unable to support functional coupling, at least at spinal levels that have been studied (coupling of trigeminal motoneurons has not been examined in developing or adult animals). To reconcile lack of coupling between non-dimorphic adult motoneurons with the presence of Cx36-puncta on these neurons, it should be noted that these puncta are associated with axon terminals that

contain vescicular glutamtate transporter1 (vglut1) and that are of primary afferent origin (Bautista *et al.,* 2013a,b), apparently forming morphologically mixed synapses, which have been described in ultrastructural studies of spinal cord (Rash et al., 1996). Such mixed synapses are potentially capable of chemical/electrical transmission, and their presynaptic fibers in other systems appear to be capable of supporting electrical coupling between neurons that receive these synapses, as in rodent vestibular nuclei (see Nagy et al., 2013). Conditions under which a similar mechanism may endow mixed synapses with the ability to support coupling between spinal motoneurons remain to be determined.

Acknowledgements

This work was supported by a grant from the Canadian Institutes of Health Research to J.I.N. (MOP 106598) and to DM (MOP 37756), and by grants from the National Institutes of Health (NS31027, NS44010, NS44295) to JE Rash with sub-award to JIN. We thank B. McLean for excellent technical assistance, and A. Simon (University of Arizona) for collaborations in testing specificity of anti-Cx37 and anti-Cx40 antibodies in Cx37 and Cx40 knockout mice.

Abbreviations

CNS, Central nervous system; CNPase, anti-2,'3'-cyclic nucleotide 3'-phosphodiesterase; Cx36, connexin36; L, lumbar; PBS, phosphate-buffered saline; PD, postnatal day; TBS, 50 mM Tris-HCl, pH 7.4, 1.5% NaCl; TBSTr, TBS containing 0.3% Triton X-100; vglut1, vescicular glutamtate transporter1.

References

Arasaki, K., Kudo, N. & Nakanishi, T. (1984) Firing of spinal motoneurons due to electrical interactions in the rat: an in vitro study. *Exp. Brain Res*., **54**, 437-445.

Bautista, W., Nagy, J.I., Dai, Y. & McCrea, D.A. (2012) Requirement of neuronal connexin36 in pathways mediating presynaptic inhibition of primary afferents in functionally mature mouse spinal cord. *J Physiol*., **590,** 3821-39.

Bautista, W., McCrea, D.A. & Nagy, J.I. (2013) Connexin36 forms purely electrical synapses in sexually dimorphic lumbosacral motor nuclei in spinal cord of developing and adult rat and mouse. Submitted.

Bautista, W., McCrea, D.A. & Nagy, J.I. (2013) Connexin36 identified at primary afferent terminals forming morphologically mixed chemical/electrical synapses in adult rodent spinal cord. Submitted.

Bennett, M.V.L. (1997) Gap junctions as electrical synapses. *J. Neurocytol.,* **26**, 349-366.

Bennett, M.V.L. & Zukin, S.R. (2004) Electrical coupling and neuronal synchronization in the mammalian brain. *Neuron,* **41,** 495-511.

Bou-Flores, C. & Berger, A.J. (2001) Gap junctions and inhibitory synapses modulate inspiratory motoneuron synchronization. *J. Neurophysiol*., **85**, 1543-1551.

Breedlove, S.M. (1986) Cellular analysis of hormone influence on motoneuronal development and function. *J. Neurobiol.,* **17,** 157-176.

Chang, Q. & Balice-Gordon, R.J. (2000) Gap junctional communication among developing and injured motor neurons. *Brain Res. Rev.,* **3,** 242-249.

Chang, Q., Gonzalez, M., Pinter, M.J. & Balice-Gordon, R.J. (1999) Gap junctional coupling and patterns of connexin expression among neonatal rat lumbar spinal neurons. *J. Neurosci.,* **19**, 10813-10828.

Chang, Q., Pereda, A., Pinter, M.J. and Balice-Gordon, R.J. (2000) Nerve injury induces gap junctional coupling among axotomized adult motor neurons. *J. Neurosci.,* **20,** 674-684.

Ciolofan, C., Lynn, B.D., Wellershaus, K., Willecke, K. & Nagy, J.I. (2007) Spatial relationships of connexin36, connexin57 and zonula occludens-1 (ZO-1) in the outer plexiform layer of mouse retina. *Neuroscience,* **148,** 473-488.

Clarke, W.T., Edwards, B., McCullagh, K.J., Kemp, M.W., Moorwood, C., Sherman, D.L., Burgess, M. & Davies, K.E. (2010) Syncoilin modulates peripherin filament networks and is necessary for large-calibre motor neurons. *J. Cell Sci.,* **123**, 2543-52.

Coleman, A.M. & Sengelaub, D.R. (2002) Patterns of dye coupling in lumbar motor nuclei of the rat. *J. Comp. Neurol*., **454**, 34-41.

Condorelli, D.F., Parenti, R., Spinella, F., Salinaro, A.T., Belluardo, N., Cardile, V. & Cicirata, F. (1998) Cloning of a new gap junction gene (Cx36) highly expressed in mammalian brain neurons. *Eur. J. Neurosci.,* **10,** 1202-1208.

Connors, B.W. & Long, M.A. (2004) Electrical synapses in the mammalian brain. Annu. Rev. *Neurosci.,* **27,** 393-418.

Curti, S., Hoge, G., Nagy, J.I. & Pereda, A.E. (2012) Synergy between electrical coupling and membrane properties promotes strong synchronization of neurons of the mesencephalic trigeminal nucleus. *J. Neurosci*., **32**, 4341-4359.

Evans, W.H. & Martin, P.E.M. (2002) Gap junctions: structure and function. *Mol. Membr. Biol.,* **19,** 121-136.

Fulton, B.P., Miledi, R. & Takahashi, T. (1980) Electrical synapses between motoneurons in the spinal cord of the newborn rat. *Proc. R .Soc. London, Ser. B,* **206**, 115-120.

Giaume, C. & Theis, M. (2010) Pharmacological and genetic approaches to study connexin-mediated channels in glial cells of the central nervous system. *Brain Res. Rev*., **63**, 160-176.

Haddock, R.E., Grayson, T.H., Brackenbury, T.D., Meaney, K.R., Neylon, C.B., Sandow, S.L. & Hill, C.E. (2006) Endothelial coordination of cerebral vasomotion via myoendothelial gap junctions containing connexins 37 and 40. *Am. J. Physiol. Heart Circ. Physiol.,* **291,** H2047-H2056.

Hinckley, C.A. & Ziskind-Conhaim, L. (2006) Electrical coupling between locomotor-related excitatory interneurons in the mammalian spinal cord. *J. Neurosci.,* **26**, 8477-8483.

Hombach, S., Janssen-Bienhold, U., Sohl, G., Schubert, T., Bussow, H., Ott, T., Weiler, R. & Willecke, K.. (2004) Functional expression of connexin57 in horizontal cells of the mouse retina. *Eur. J. Neurosci.,* **19,** 2633-2640.

Honma, S., De, S., Li, D., Shuler, C.F. & Turman, Jr. J.E. (2004) Developmental regulation of connexins 26, 32, 36 and 43 in trigeminal neurons. *Synapse,* **52,** 258-271.

Hormuzdi, S.G., Filippov, M.A., Mitropoulon, G., Monyer, H., & Bruzzone, R. (2004) Electrical synapses: a dynamic signaling system that shapes the activity of neuronal networks. *Biochem. Biophys. Acta,* **1662,** 113-137.

Kiehn, O., Kjaerulff, O., Tresch, M.C. & Harris-Warrick, R.M. (2000) Contributions of intrinsic motor neuron properties to the production of rhythmic motor output in the mammalian spinal cord. *Brain Res. Bull.,* **53**, 649-659.

Kiehn, O. & Tresch, M.C. (2002) Gap junctions and motor behavior. *Trends Neurosci*., **25**, 108-115.

Kreuzberg, M.M., Deuchars, J., Weiss, E., Schober, A., Sonntag, S., Wellershaus, K., Draguhn, A. & Willecke, K. (2008) Expression of connexin30.2 in interneurons of the central nervous system in the mouse. *Mol. Cell Neurosci.,* **37,** 119-134.

Kruger, O., Plum, A., Kim, J.-S., Winterhager, E., Maxeiner, S., Hallas, G., Kirchhoff, S., Traub, O., Lamers, W.H. & Willecke, K. (2000) Defective vascular development in connexin45-deficient mice. *Development,* **127,** 4179-4193.

Lee, S.C., Cruikshank, S.J. & Connors, B.W. (2010) Electrical and chemical synapses between relay neurons in developing thalamus. *J. Physiol.*, **588**, 2403-2415.

Li, X., Olson, C., Lu, S., Kamasawa, N., Yasumura, T., Rash, J.E. & Nagy, J.I. (2004) Neuronal connexin36 association with zonula occludens-1 protein (ZO-1) in mouse brain and interaction with the first PDZ domain of ZO-1. *Eur. J. Neurosci.,* **19**, 2132-46.

Li, X., Kamasawa, N., Ciolofan, C., Olson, C.O., Lu, S., Davidson, K.G.V., Yasumura, T., Shigemoto, R., Rash, J.E. & Nagy, J.I. (2008) Connexin45-containing neuronal gap junctions in rodent retina also contain connexin36 in both apposing hemiplaques, forming bi-homotypic gap junctions, with scaffolding contributed by zonula occludens-1. *J. Neurosci.,* **28,** 9769-89.

Li, X. & Simard, J.M. (2001) Connexin45 gap junction channels in rat cerebral vascular smooth muscle cells. *Am. J. Physiol.*, **281,** 1890-1898.

Lynn, B.D., Tress, O., May, D., Willecke, K. & Nagy, J.I. (2011) Ablation of connexin30 in transgenic mice alters expression patterns of connexin26 and connexin32 in glial cells and leptomeninges. *Eur. J. Neurosci.,* **11,** 1783-93.

Matsumoto, A., Arnold, A.P. & Micevych, P.E. (1989) Gap junctions between lateral spinal motoneurons in the rat. *Brain Res.,* **495**, 362-366.

Matsumoto, A., Arnold, A.P., Zampighi, G. & Micevych, P.E. (1988) Androgenic regulation of gap junctions between motoneurons in the rat spinal cord. *J. Neurosci.,* **8**, 4177-4138.

Matsumoto, A., Arai, Y., Urano, A., & Hyodo, S. (1991) Androgen regulates gap junction mRNA expression in androgen-sensitive motoneurons in the rat spinal cord. *Neurosci. Let.*, **131**, 159-162.

McKenna, K.E., & Nadelhaft, I. (1986) The organization of the pudendal nerve in the male and female rat. *J. Comp. Neurol.*, **248,** 532-549.

Matsumoto, A., Arai, Y., Urano, A. & Hyodo, S. (1992) Effect of androgen on the expresssion of gap junction and beta-actin mRNAs in adult rat motoneurons. *Neurosci. Res.*, **14,** 133-144.

Meier, C. & Dermietzel, R. (2006) Electrical synapses--gap junctions in the brain. *Results Probl. Cell Differ.*, **43**, 99-128.

Mercier, F. & Hatton, G.I. (2004) Connexin26 and basic fibroblast growth factor are expressed primarily in the subpial and subependymal layers in adult brain parenchyma: roles in stem cell proliferation and morphological plasticity? *J. Comp. Neurol.*, **431,** 88-104.

Mentis, G.Z., Diaz, E., Moran, L.B. & Navarrete, R. (2002) Increased incidence of gap junctional coupling between spinal motoneurons following transient blockade of NMDA receptors in neonatal rats. *J Physiol*., **544**, 757-764.

Micevych, P. E. & Abelson, L. (1991) Distribution of mRNAs coding for liver and heart gap junction proteins in the rat central nervous system. *J. Comp. Neurol.*, **305**, 96-118.

Nagasawa, K., Chiba, H., Fujita, H., Kojima, T., Saito, T., Endo, T. & Sawada, N. (2006) Possible involvement of gap junctions in the barrier function of tight junctions of brain and lung endothelial cells. *J. Cell Physiol.,* **208,** 123-132.

Nagy, J.I., Ionescu, A.V., Lynn, B.D. & Rash, J.E. (2003) Coupling of astrocyte connexins Cx26, Cx30, Cx43 to oligodendrocyte Cx29, Cx32, Cx47: Implications from normal and connexin32 knockout mice, *Glia,* **44**, 205-218.

Nagy, J.I., Dudek, F.E. & Rash, J.E. (2004) Update on connexins and gap junctions in neurons and glia in in the mammalian central nervous system. *Brain Res. Rev*., **47**, 191-215.

Nagy, J.I., Lynn, B.D., Tress, O., Willecke, K. & Rash, J.E. (2011) Connexin26 expression in brain parenchymal cells demonstrated by targeted connexin ablation in transgenic mice. *Eur. J. Neurosci.,* **34,** 263-271.

Nagy, J.I. (2012) Evidence for connexin36 localization at hippocampal mossy fiber terminals suggesting mixed chemical/electrical transmission by granule cells. *Brain Res*., **1487,** 107-122.

Nagy, J.I., Bautista, W., Blakley, B. & Rash, J.E. (2012) Morphologically mixed chemical-electrical synapses formed by primary afferents in rodent vestibular nuclei as revealed by immunofluorescence detection of connexin36 and vesicular glutamate transporter-1. *Neuroscience*, Submitted.

Ochalski, P.A.Y., Frankenstein, U.N., Hertzberg, E.L. & Nagy, J.I. (1997) Connexin43 in rat spinal cord: Localization in astrocytes and identification of heterotypic astro-oligodendrocytic gap junctions. *Neuroscience,* **76**, 931-945.

Pastor, A.M., Mentis, G.Z., de la Cruz, R.R., Diaz, E. & Navarrete, R. (2003) Increased electrotonic coupling in spinal motoneurons after transient botulinum neurotoxin paralysis in the neonatal rat. *J. Neurophysiol.,* **89,** 793-805.

Personius, K.E. & Balice-Gordon, R.J. (2000) Activity-dependent editing of neuromuscular synaptic connections. *Brain Res. Bull.,* **53**, 513-522.

Personius, K.E. & Balice-Gordon, R.J. (2001) Loss of correlated motor neuron activity during synaptic competition at developing neuromuscular synapses. *Neuron,* **31**, 395-408.

Personius, K.E, Chang, Q., Bittman, K., Panzer, J. & Balice-Gordon, R.J. (2001) Gap junctional communication among motor and other neurons shapes patterns of neural activity and synaptic connectivity during development. *Cell Commun. Adhes.,* **8,** 329-333.

Personius, K.E., Chang, Q., Mentis, G.Z., O'Donovan, M.J. & Balice-Gordon, R.J. (2007) Reduced gap junctional coupling leads to uncorrelated motor neuron firing and precocious neuromuscular synapse elimination. *Proc. Natl. Acad. Sci.,* **104**, 11808-11813.

Rash, J.E., Dillman, R.K., Bilhartz, B.L., Duffy, H.S., Whalen, L.R. & Yasumura, T. (1996) Mixed synapses discovered and mapped throughout mammalian spinal cord. *Proc. Natl. Acad. Sci.,* **93**, 4235-4239.

Rash, J.E., Staines, W.A., Yasumura, T., Pate, D., Hudson, C.S., Stelmack, G.L. & Nagy, J. (2000) Immunogold evidence that neuronal gap junctions in adult rat brain and spinal cord contain

connexin36 (Cx36) but not Cx32 or Cx43. *Proc. Natl. Acad. Sci.,* **97,** 7573-7578.

Rash, J. E., Yasumura, T., Davidson, K., Furman, C.S., Dudek, F.E. & Nagy, J.I. (2001a) Identification of cells expressing Cx43, Cx30, Cx26, Cx32 and Cx36 in gap junctions of rat brain and spinal cord. *Cell Commun. Adhes.*, **8**, 315-320.

Rash, J.E., Yasumura, T., Dudek, F.E. & Nagy, J.I. (2001b) Cell-specific expression of connexins and evidence for restricted gap junctional coupling between glial cells and between neurons. *J. Neurosci*., **21**, 1983-2000.

Rash, J.E., Olson, C.O., Davidson, K.G.V., Yasumura, T., Kamasawa, N. & Nagy, J.I. (2007a) Identification of connexin36 in gap junctions between neurons in rodent locus coeruleus. *Neuroscience*, **147**, 938-956.

Rash, J.E., Olson, C.O., Pouliot, W.A., Davidson, K.G.V., Yasumura, T., Furman, C.S., Royer, S., Kamasawa, N., Nagy, J.I. & Dudek, F.E. (2007b) Connexin36 vs connexin32, "miniature" neuronal gap junctions, and limited electrotonic coupling in rodent suprachiasmatic nucleus. *Neuroscience*, **149**, 350-371.

Rash, J.E. (2010) Molecular disruptions of the panglial syncytium block potassium siphoning and axonal saltatory conduction: pertinence to neuromyelitis optica and other demyelinating diseases of the central nervous system. *Neuroscience*, **168**, 982-1008.

Severs, N.J., Rothery, S., Dupont, E., Coppen, S.R., Yeh, H.I., Ko, Y.S., Matsushita, T., Kaba, R. & Halliday, D. (2001) Immunocytochemical analysis of connexin expression in the healthy and diseased cardiovascular system. *Microsc. Res. Tech.,* **52,** 301-322.

Simon, A.M. & McWhorter A.R. (2002) Vascular abnormalities in mice lacking the endothelial gap junction proteins connexin37 and connexin40. *Dev. Biol.*, **251**, 206-220.

Söhl, G., Degen, J., Teubner, B. & Willecke, K. (1998) The murine gap junction gene connexin36 is highly expressed in mouse retina and regulated during brain development. *FEBS Lett.*, **428,** 27-31.

Sohl, G., Maxeiner, S. & Willecke, K. (2005) Expresssion and functions of neuronal gap junctions. *Nat. Rev. Neurosci.,* **6,** 191-200.

Tresch, M.C. & Kiehn, O. (2000) Motor coordination without action potentials in the mammalian spinal cord. *Nature*, **3**, 593-599.

Tresch, M.C. & Kiehn, O. (2002) Synchronization of motor neurons during locomotion in the neonatal rat: predictors and mechanisms. *J Neurosci*., **22**, 9997-10008.

van der Want, J.J.L., Gramsbergen, A., Ijema-Paassen, J., de Weerd, H. & Liem, R.S.B. (1998) Dendro-dendritic connections between motoneurons in the rat spinal cord: an electron microscopic investigation. *Brain Res*., **779**, 342-345.

Vis, J.C., Nicholson, L.F., Faull, R.L., Evans, W.H., Severs, N.J. & Green, C.R. (1998) Connexin expression in Huntington's diseased human brain. *Cell Biol. Int.*, **22,** 837-847.

Walton, K.D. & Navarette, R. (1991) Postnatal changes in motoneurone electronic coupling studied in the *in vitro* rat lumbar spinal cord. *J. Physiol.*, **433**, 283-305.

Wilson, J.M., Cowan, A.I. & Brownstone, R.M. (2007) Heterogeneous electrotonic coupling and synchronization of rhythmic bursting activity in mouse Hb9 Interneurons. *J. Neurophysiol.*, **98,** 2370-2381.

Yamamoto, T., Ochalski, A., Hertzberg, E.L. & Nagy, J.I. (1990) On the organization of astrocytic gap junctions in rat brain as demonstrated by LM and EM immunohistochemistry of connexin43 expression. *J. Comp. Neurol.*, **302,** 853-883.

Yates, C., Garrison, K., Reese, N.B., Charlesworth, A. & Garcia-Rill, E. (2011) Novel mechanism for hyperreflexia and spasticity. *Prog. Brain Res.*, **188,** 167-180.

Yeh, H.-I, Rothery, S., Dupont, E., Coppen, S.R. & Severs, N.J. (1998) Individual gap junction plaques contain multiple connexins in arterial endothelium. *Circ. Res.*, **83,** 1248-1263.

Figure legends

Fig. 1. Confirmation of immunofluorescence labelling with anti-connexin antibodies in various tissues of adult rat and mouse. (A-C) Immunolabelling for Cx37 in rat heart (A), and Cx40 in rat (B) and mouse (C) cerebral cortex, showing detection of linear arrangements of these connexins along blood vessels (arrows), in accordance with patterns of their organization and localization at gap junctions between endothelial cells. (D,E) Labelling for Cx40 at low (D) and higher (E) magnification in atrium of mouse heart, where Cx40 is concentrated in gap junctions between lateral membranes of cardiomyocytes (D, arrows) and in gap junctions at intercalated discs (E, arrows). (F) Labelling of Cx45 along a blood vessel in mouse cerebral cortex (arrow), reflecting association of Cx45-puncta with vascular smooth muscle cells. (G,H) Images showing blood vessels in the spinal cord ventral horn labelled for the vessel marker IB4 (G1,H1, arrows) and images of the same vessels labelled for either Cx37 (G2, arrow) or Cx40 (H2, arrow), respectively, confirming vascular localization of the two connexins in spinal cord.

Fig. 2. Comparison of immunofluorescence labelling for Cx36, Cx37, Cx43 and Cx45 among lumbar spinal motoneurons in lamina IX of neonatal and adult mouse and rat. In all figures, color code for secondary antibody fluorochrome and target protein is as indicated. (A-C) Images showing Cx36-puncta among peripherin-positive motoneurons (A, arrows) in mouse spinal cord at PD5, and higher magnification showing association of Cx36-puncta with motoneuron somata and dendrites in mouse (B, arrows) and rat (C, arrows) spinal cord at PD5. (D-F) Double immunofluorescence for Cx36 and Cx37 among motoneurons (peripherin labelling excluded), showing widely distributed Cx36-puncta in mouse at PD5 (D) and PD10 (E), and in rat at PD5 (F), with labelling for Cx37 restricted to blood vessels (arrows). (G) Adult rat spinal cord ventral horn labelled for peripherin and counterstained with blue fluorescence Nissl. (H,I) Magnifications of boxed areas in G (H, lower box; I, upper box) triple labelled for Cx36, Cx37 and peripherin, showing Cx36-puncta among two peripherin-positive motoneuronal groups (H, large arrows), absence of labelling for Cx37 among these groups, and labelling of Cx37 restricted to small blood vessels (H, small arrows) and a single large vessel in lamina VIII (I, arrow). (J) Double labelling of Cx43 with peripherin in lamina IX of rat at PD5, showing very little association of sparsely distributed Cx43-puncta with the surface of peripherin-positive

motoneurons. (K) Double labelling of Cx36 with Cx45 in lamina IX of rat at PD5, showing Cx36-puncta among motoneurons (K1) and only a low level of background fluorescence in the same field labelled for Cx45 (K2). (L) Triple labelling for Cx36, Cx45 and peripherin in lamina IX of adult rat, showing Cx36-puncta on the surface of peripherin-positive motoneurons (L1, arrows), minimal Cx45 localization to these neurons, and association of Cx45 with what appear to be blood vessels (L1, arrowheads), also shown in the same field with labelling of Cx45 alone (L2).

Fig. 3. Immunofluorescence labelling for Cx36, Cx40 and peripherin in lamina IX of lumbar spinal cord in rat and mouse. Double labelling is shown in the same fields in pairs of images: A1,A2; B1,B2, etc, through to F1,F2. (A-C) Fields displaying punctate labelling for Cx36 (A1, B1 and C1) in lamina IX show labelling for Cx40 only along blood vessels in rat at PD5 (A2, arrow), and in mouse at PD5 (B2, arrow) and at PD10 (C2, arrow). The image in (A) shows a portion of ventral white matter (delineated by dotted lines) in order to allow inclusion of an underlying blood vessel as a positive control for labelling of Cx40. (D,E) Labelling of peripherin (D1,E1) and Cx40 (D2,E2) in lamina IX, showing absence of labelling for Cx40 specifically within or among peripherin-positive motoneurons, and association of Cx40 with blood vessels (arrows) in rat (D) and mouse (E) at PD5. (F) Labelling of peripherin (F1) and Cx40 (F2) in lamina IX of adult rat, showing absence of labelling for Cx40 in association with peripherin-positive motoneurons, and association of Cx40 with a blood vessel (F2, arrow).

Fig. 4. Immunofluorescence labelling for Cx36, Cx32, and peripherin in sexually dimorphic and non-dimorphic lumbar motor nuclei in adult male rat and mouse spinal cord. (A-C) Images from rat showing dorsal (A) and ventral (B) divisions of the dimorphic dorsomedial nucleus, and the dorsolateral nucleus (C). Cx36-puncta are seen among clusters of peripherin-positive motoneurons (arrows), and labelling for Cx32 is seen largely in surrounding regions (arrowheads). Boxed area (B, magnified in inset, without labelling for peripherin) shows Cx32 localized to myelinated fibers passing between motoneuron dendrites. (D,E) Higher magnifications showing Cx36-puncta localized to the surface of peripherin-positive motoneurons

in the dorsomedial dimorphic nucleus (D, arrows) and in a non-dimorphic motor nucleus at L4 (E, arrows), with little Cx32 (arrowheads) association at motoneurons. Cx36-puncta follow apposition of two neuronal somata (D, left arrow). (F) Images of sexually dimorphic Onuf's nucleus in mouse, showing Cx36-puncta associated with peripherin-positive Onuf motoneurons (F1, arrows) and, in the same field, labelling for Cx32 localized to small cells among these motoneurons (F2, arrowheads). (G) Image of non-dimorphic motor nucleus from L4 of mouse, showing a similar pattern of Cx36-puncta associated with motoneurons (G1, arrows), and labelling for Cx32 at small cells (G2, arrowheads). (H,I) Triple labelling for Cx32, CNPase and peripherin in the dorsomedial dimorphic nucleus at low magnification (H), with boxed area in H magnified in (I), showing Cx32 localized to CNPase-positive oligodendrocytes (arrowsheads) and not to peripherin-positive motoneurons.

Fig. 5. Immunofluorescence labelling of Cx36, Cx26, Cx32, Cx43, peripherin and CNPase in the trigeminal motor nucleus (Mo5) of adult and PD15 mouse. (A) Low magnification showing a high density of labelling for Cx36 among peripherin-positive motoneurons in the Mo5 (large arrows) and sparse labelling in surrounding regions. (B) Magnification showing punctate appearance of labelling for Cx36, association of Cx36-puncta with motoneuron somata and dendrites (arrows), and absence of intracellular labelling for Cx36. (C) Triple immunofluorescence showing overlay of labelling for Cx36 with peripherin and, in the same field, overlay of labelling for Cx26 and peripherin. Cx36-puncta are seen throughout the field, including those associated with medially located motoneurons (C1, arrows), while Cx26-puncta are seen restricted to the lateral edge of the Mo5, in a region largely devoid of peripherin-positive motoneuron somata, but containing bundles of myelinated fibers in the motor root of the trigeminal nerve (C2, arrowheads). (D) Triple labelling in Mo5 at PD15, showing Cx36-puncta decorating motoneuron somata and dendrites (arrows), absence Cx26 labelling in or around these somata, and Cx26-puncta associated with leptomeninges along a blood vessel (arrowhead). (E,F) Low (E) and higher (F) magnification showing labelling of Cx36 and Cx32 among peripherin-positive Mo5 motoneurons. Cx36-puncta are seen on the surface of peripherin-positive motoneurons, (arrows), while Cx32-puncta are largely in regions devoid of peripherin labelling (arrowheads). (G) Triple labelling, showing CNPase localized to oligodendrocyte

somata (G1, arrows) and myelinated fibers, and localization of Cx32-puncta to CNPase-positive oligodendrocyte somata (G2, arrows), as shown in overlay (G3, arrows). (H,I) Low (H) and higher (I) magnification showing overlay of triple labelling for Cx36 and Cx43 among peripherin-positive Mo5 motoneurons. Dense Cx43-puncta are seen in the vicinity of motoneurons (arrowhead), and display a random distribution compared with lining of Cx36-puncta on the surface of motoneurons (H,I, arrows). Motoneurons lack intracellular labelling for Cx43.

Figure 1

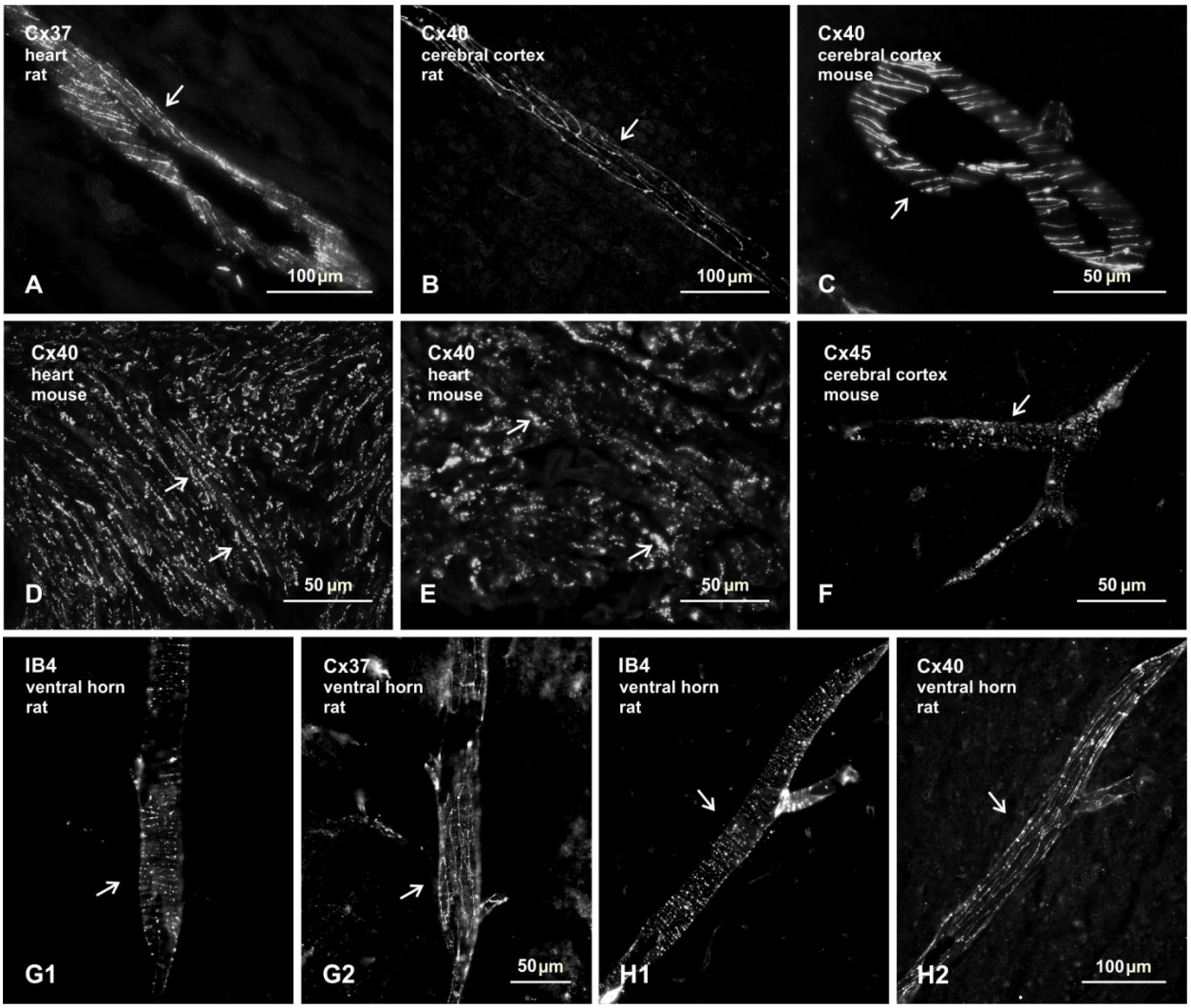
Cx37
heart
rat
A
100 µm
Cx40
cerebral cortex
rat
B
100 µm
Cx40
cerebral cortex
mouse
C
50 µm
Cx40
heart
mouse
D
50 µm
Cx40
heart
mouse
E
50 µm
Cx45
cerebral cortex
mouse
F
50 µm
IB4
ventral horn
rat
G1
Cx37
ventral horn
rat
G2
50 µm
IB4
ventral horn
rat
H1
Cx40
ventral horn
rat
H2
100 µm

Figure 2

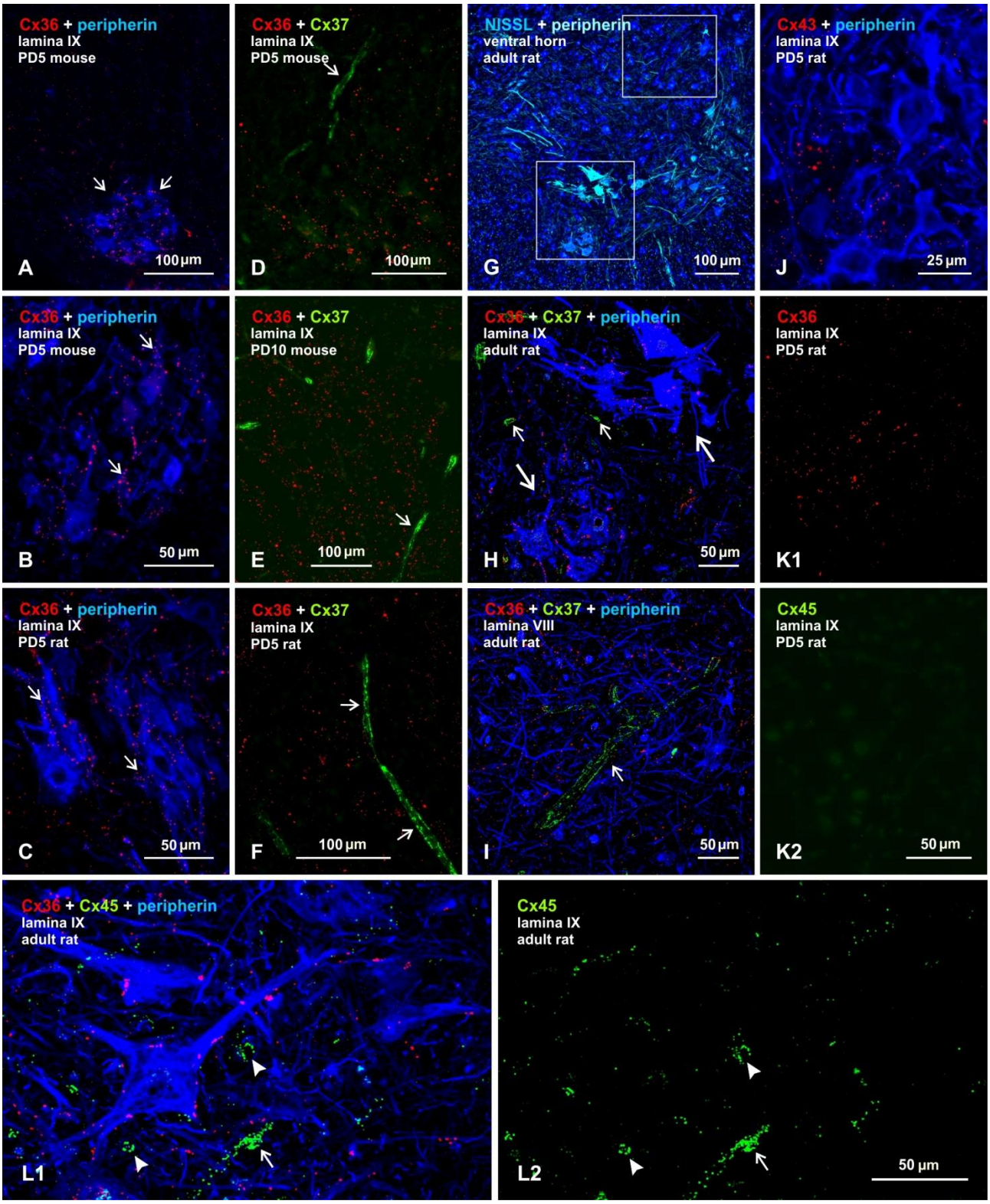
Cx36 + peripherin
lamina IX
PD5 mouse
A
100 µm
Cx36 + Cx37
lamina IX
PD5 mouse
D
100 µm
NISSL + peripherin
ventral horn
adult rat
G
100 µm
Cx43 + peripherin
lamina IX
PD5 rat
J
25 µm
Cx36 + peripherin
lamina IX
PD5 mouse
B
50 µm
Cx36 + Cx37
lamina IX
PD10 mouse
E
100 µm
Cx36 + Cx37 + peripherin
lamina IX
adult rat
H
50 µm
Cx36
lamina IX
PD5 rat
K1
Cx36 + peripherin
lamina IX
PD5 rat
C
50 µm
Cx36 + Cx37
lamina IX
PD5 rat
F
100 µm
Cx36 + Cx37 + peripherin
lamina VIII
adult rat
I
50 µm
Cx45
lamina IX
PD5 rat
K2
50 µm
Cx36 + Cx45 + peripherin
lamina IX
adult rat
L1
Cx45
lamina IX
adult rat
L2
50 µm

Figure 3

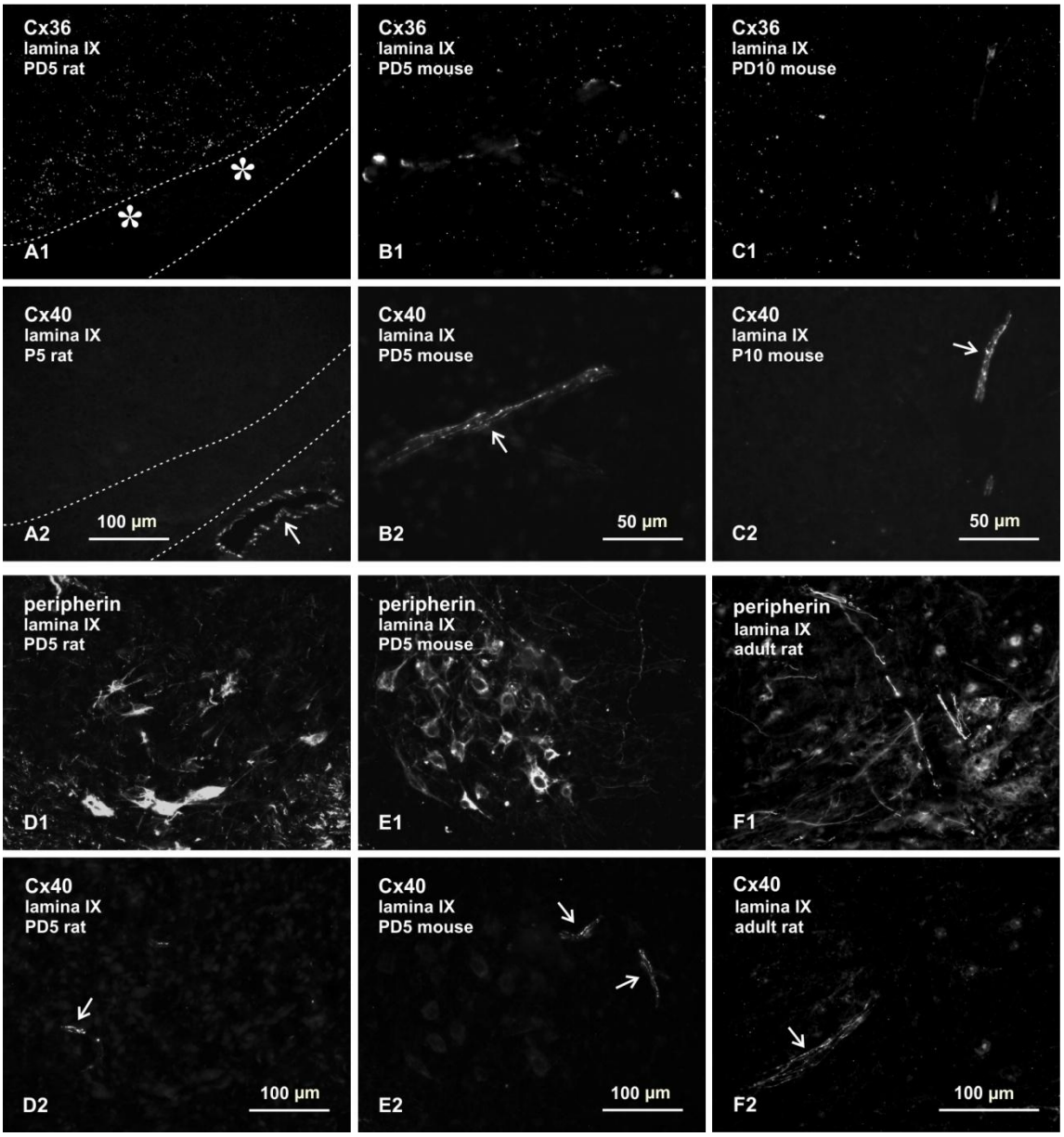
Cx36
lamina IX
PD5 rat
A1
Cx36
lamina IX
PD5 mouse
B1
Cx36
lamina IX
PD10 mouse
C1
Cx40
lamina IX
P5 rat
A2
100 µm
Cx40
lamina IX
PD5 mouse
B2
50 µm
Cx40
lamina IX
P10 mouse
C2
50 µm
peripherin
lamina IX
PD5 rat
D1
peripherin
lamina IX
PD5 mouse
E1
peripherin
lamina IX
adult rat
F1
Cx40
lamina IX
PD5 rat
D2
100 µm
Cx40
lamina IX
PD5 mouse
E2
100 µm
Cx40
lamina IX
adult rat
F2
100 µm

Figure 4

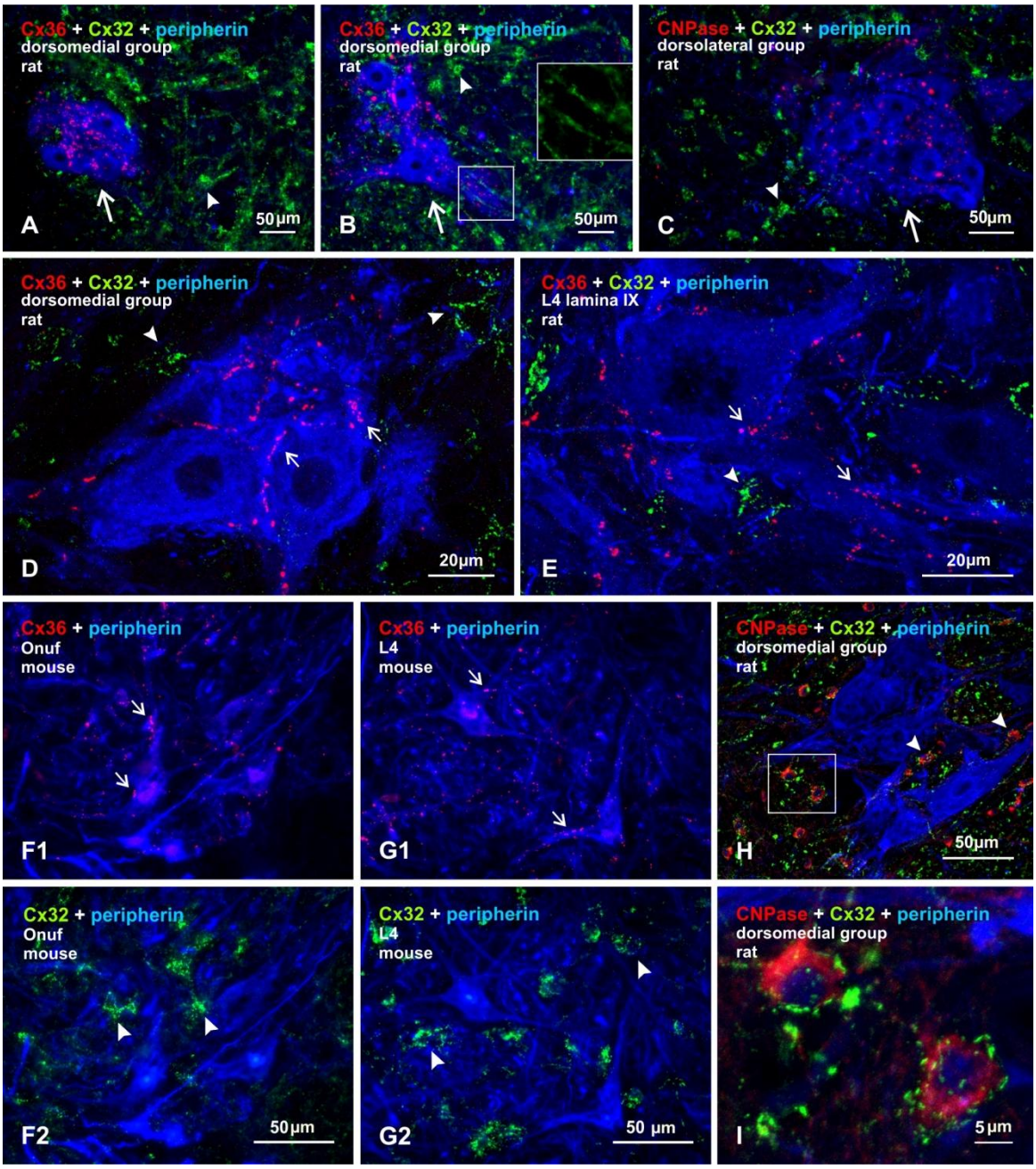
Cx36 + Cx32 + peripherin
dorsomedial group
rat
A
50µm
Cx36 + Cx32 + peripherin
dorsomedial group
rat
B
50µm
CNPase + Cx32 + peripherin
dorsolateral group
rat
C
50µm
Cx36 + Cx32 + peripherin
dorsomedial group
rat
D
20µm
Cx36 + Cx32 + peripherin
L4 lamina IX
rat
E
20µm
Cx36 + peripherin
Onuf
mouse
F1
Cx36 + peripherin
L4
mouse
G1
CNPase + Cx32 + peripherin
dorsomedial group
rat
H
50µm
Cx32 + peripherin
Onuf
mouse
F2
50µm
Cx32 + peripherin
L4
mouse
G2
50 µm
CNPase + Cx32 + peripherin
dorsomedial group
rat
I
5µm

Figure 5

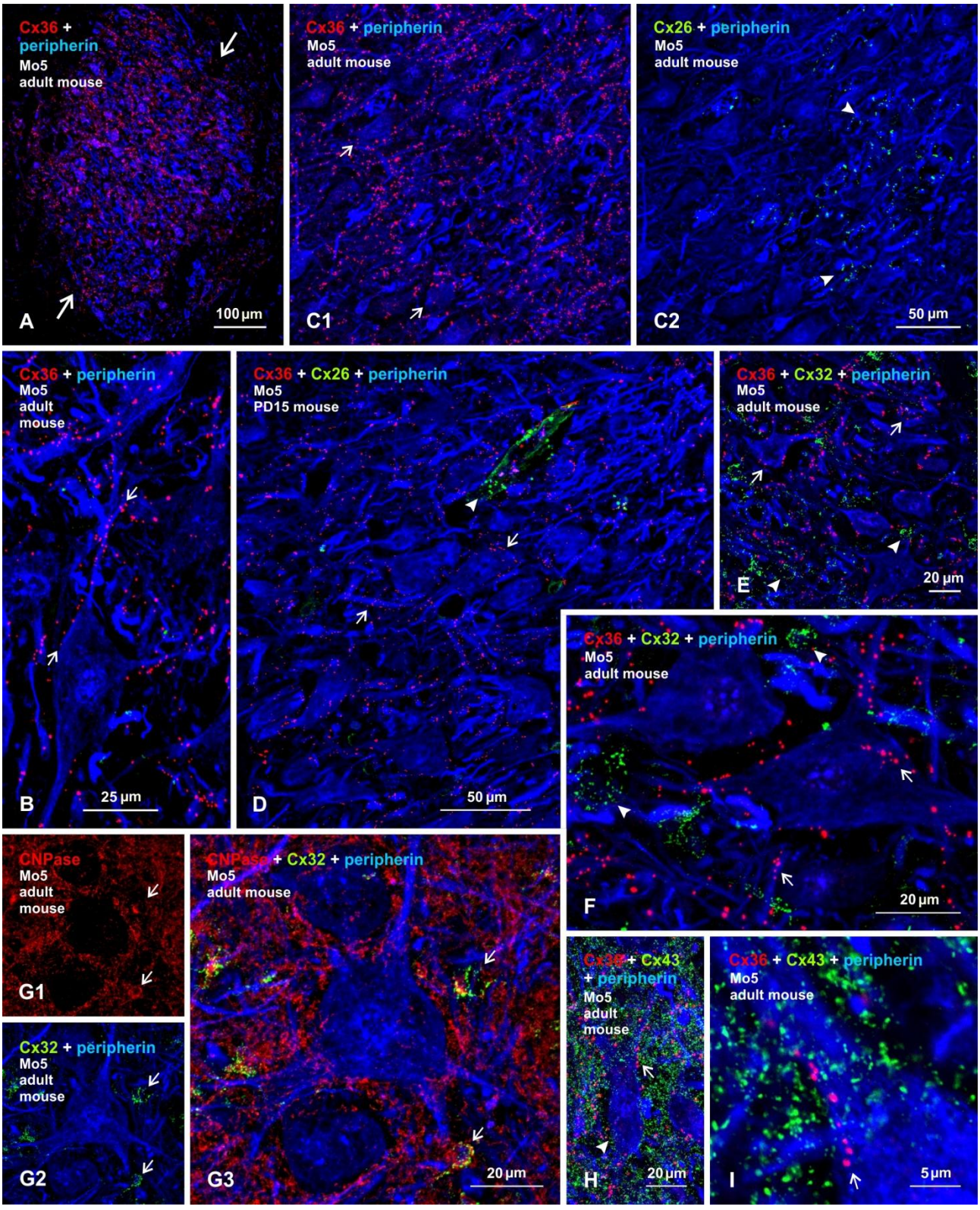
Cx36 + peripherin
Mo5
adult mouse
A
100 µm
Cx36 + peripherin
Mo5
adult mouse
C1
Cx26 + peripherin
Mo5
adult mouse
C2
50 µm
Cx36 + peripherin
Mo5
adult mouse
B
25 µm
Cx36 + Cx26 + peripherin
Mo5
PD15 mouse
D
50 µm
Cx36 + Cx32 + peripherin
Mo5
adult mouse
E
20 µm
Cx36 + Cx32 + peripherin
Mo5
adult mouse
F
20 µm
CNPase
Mo5
adult
mouse
G1
CNPase + Cx32 + peripherin
Mo5
adult mouse
G3
20 µm
Cx32 + peripherin
Mo5
adult
mouse
G2
Cx36 + Cx43
+ peripherin
Mo5
adult
mouse
H
20 µm
Cx36 + Cx43 + peripherin
Mo5
adult mouse
I
5 µm

Section 3. Connexin36 identified at primary afferent terminals forming morphologically mixed chemical/electrical synapses in adult rodent spinal cord.

3.1. Hypothesis: Primary afferent terminals form mixed chemical and electrical synapses in adult spinal cord.

Experimental Approach: Male and female Sprague–Dawley rats and C57 mice were used. Spinal cord sections were processed for imunohistochemistryusing antibodies against Cx36, the nerve terminal marker Vglut1 and peripherin as motoneurone marker. Observations were made on animals of P5, 10, 15, 20, 25 and 30 postnatal days.

Adult Sprague Dawley rats were unilaterally deafferented at the level of L2 and L5 and then spinal cord sections were processed for immunolabeling of Vglut1, Cx36 and peripherin. Confocal microscopy confirmed co-localization of markers and counts were made of the number of Cx36 puncta associated with Vglut1-positive terminals. We also examined the effect of de-afferentation in the distribution of mixed and electrical synapses in the spinal cord.

3.2. Conclusions:

Since Vglut-1 in the spinal cord is considered to be localized mainly in the terminals of myelinated primary afferents, our results suggest that Cx36 is contained in gap junctions formed by these terminals, raising the possibility that neurotransmission from a subpopulation of primary afferents occurs via mixed chemical/electrical synapses not only in intermediate lamina but also and most importantly on motoneurones. Extensive confocal analyses at different ages allowed us to observe that these mixed synapses start to appear by postnatal day 15 in intermediate laminae and at P25 in the motoneurones, however, levels similar to the adult are not seen until P30. These observations indicate that a percentage of Cx36-positive puncta in adult spinal cord is co-localized with the nerve terminal marker Vglut-1, and raises the possibility that neurotransmission from a subpopulation of primary afferents occurs via mixed chemical/electrical synapses on rodent spinal neurons and motoneurones.

Section Editor: Cellular Neuroscience ─ Constantino Sotelo

Connexin36 identified at primary afferent terminals forming morphologically mixed chemical/electrical synapses in adult rodent spinal cord

W. Bautista, D. A. McCrea, J. I. Nagy*

Department of Physiology, Faculty of Medicine, University of Manitoba, Winnipeg, Canada

Running title: Cx36 at mixed synapses in spinal cord

No. of pages: 40

No. of figures: 10

No. of supplementary figures: 2

No. of words: Abstract, 279 ; Introduction 693, Discussion, 2036

Address for correspondence:

James I. Nagy

Department of Physiology

Faculty of Medicine

University of Manitoba

745 Bannatyne Ave, Winnipeg, Manitoba, Canada R3E 0J9

Email: nagyji@ms.umanitoba.ca

Tel. (204) 789-3767, Fax (204) 789-3934

Abbreviations

CeVe, central cervical nucleus; CNS, Central nervous system; C, cervical; Cx36, connexin36; GAD65, glutamic acid decarboxylase65; L, lumbar; Mo5, trigeminal motor nucleus; PBS, phosphate-buffered saline; PD, postnatal day; TBS, 50 mM Tris-HCl, pH 7.4, 1.5% NaCl; TBSTr, TBS containing 0.3% Triton X-100; T, thoracic; vglut1, vesicular glutamate transporter-1; vglut2, vesicular glutamate transporter-2.

Abstract - Mixed chemical/electrical neurotransmission at axon terminals, with the electrical component of transmission mediated by gap junctions is commonly observed in the CNS of lower vertebrates. In mammalian CNS, evidence for the presence of morphologically mixed synapses has been obtained in only a few locations. Here, we used immunofluorescence approaches to examine the localization of the neuronally expressed gap junction forming protein connexin36 (Cx36) in relation to the axon terminal marker vesicular glutamate transporter1 (vglut1) in spinal cord and trigeminal motor nucleus (Mo5) of developing and adult rat and mouse. In adult rodents, immunolabelling for Cx36 appeared exclusively as Cx36-puncta, and was widely distributed at all rostro-caudal levels of the spinal cord, in most spinal cord laminae and in the Mo5. A high proportion of these Cx36-puncta was co-localized with vglut1, forming morphologically mixed synapses on motoneurons, as well as in intermediate spinal cord lamina, particularly in regions of medial lamina VII along the entire length of the spinal cord, where vglut1-containing terminals associated with Cx36 converged on clusters of neurons adjacent to the central canal. Unilateral transection of lumbar dorsal roots caused large reductions in immunolabelling of both vglut1 and Cx36 in intermediate lamina and lamina IX. Further, vglut1-terminals displaying Cx36-puncta in the spinal cord were contacted by terminals labelled for glutamic acid decarboxylase65, which is known to be contained in presynaptic terminals on large diameter primary afferents. Developmentally, mixed synapses begin to emerge in the spinal cord only after the second to third postnatal week and thereafter increase to adult levels. Our findings indicate that axon terminals of primary afferent origin form morphologically mixed synapses containing Cx36 in broadly distributed areas of adult rodent spinal cord and Mo5.

Keywords: gap junctions, vesicular glutamate transporter1, motoneurons, interneurons

Introduction

A surge of reports over the past decade on electrical synapses formed by gap junctions between neurons in mammalian brain was fueled in part by the discovery of the first gap junction forming protein expressed in neurons, namely, connexin (Cx36) (Condorelli et al., 1998; Söhl et al., 1998). Subsequent findings of widespread neuronal expression of Cx36, (Condorelli et al., 2000), demonstrations of Cx36 in ultrastructurally-identified neuronal gap junctions in adult rodent brain (Nagy et al., 2004; Rash et al., 2000,2001a,b,2007a,b), and indications of the physiological relevance of these junctions, partly deduced from functional deficits in Cx36 knockout (ko) mice, all contributed to the general acceptance of the prevalence of electrical transmission in most major regions of mammalian CNS (Bennett and Zukin, 2004; Connors and Long, 2004; Hormuzdi et al., 2004; Söhl et al., 2005; Meier and Dermietzel, 2006). Specifically, electrical coupling is considered to generate synchrony of subthreshold membrane oscillations and to promote synchronous recruitment of rhythmic firing (Bennett and Zukin, 2004; Connors and Long, 2004), which is emerging as a key feature of information processing in neuronal networks (Singer, 1999; Whittington and Traub, 2003; Senkowski et al., 2008). Nearly all electrical synapses so far studied in mammalian brain occur between dendrites and/or somata of specific classes of neurons. However, gap junctions can also be found at axon terminals, as in many systems of lower vertebrates (Bennett and Goodenough, 1978; Bennett, 1997;), creating "mixed synapses" that provide for dual chemical and electrical neurotransmission. Mixed synapses in rodent CNS have been described in only a few CNS areas, including the lateral vestibular nucleus (LVN) (Sotelo and Palay, 1970; Korn et al., 1973; Nagy et al., 2013), hippocampus (Vivar et al., 2012; Hamzei-Sichani et al., 2012; Nagy, 2012) and spinal cord (Rash et al., 1996).

Electrical synapses and neuronal gap junctions in mammalian spinal cord have to date received far less attention than those in brain. In developing and juvenile rodent spinal cord, gap junctional coupling between distinct subsets of interneurons has been described (Hinckley and Ziskind-Conhaim, 2006; Wilson et al., 2007; Bautista et al., 2012), but better characterized is coupling between motoneurons during the first postnatal week, with progressive loss of coupling during the second week of life (Arasaki et al., 1984; Fulton et al., 1980; Walton and Navarette, 1991; Bou-Flores and Berger, 2001). Electrical coupling between developing motoneurons

parallels the extensive coupling that occurs between developing neurons in other CNS areas and, as in other areas, was suggested to support synchronous neuronal activity prior to the maturation of chemical synaptic connectivity (Kiehn et al., 2000; Kiehn and Tresch, 2002; Tresch and Kiehn, 2000,2002). Although the loss of coupling between motoneurons with age is also typical of other developing CNS systems, neuronal gap junctions and/or functional neuronal coupling persist among specific neuronal populations in spinal cord of adult animals (Matsumoto et al., 1988,1989; van der Want et al., 1998; Logan et al., 1996; Coleman and Sengelaub, 2002; Bautista et al., 2012), just as occurs in brain. The connexins expressed in spinal and trigeminal motoneurons, and suggested to form gap junctions mediating motoneuronal coupling, include Cx26, Cx32, Cx36, Cx37, Cx40, Cx43 and Cx45 (Chang et al., 1999; Chang and Balice-Gordon, 2000; Chang et al., 2000; Personius and Balice-Gordon, 2000, 2001; Personius et al., 2001,2007; Micevych and Abelson, 1991; Matsumoto et al., 1991,1992). We recently examined the localization of these connexins among trigeminal and spinal cord motoneurons in postnatal and adult rodent, and reported evidence indicating the association of only Cx36 with these neurons (Bautista et al., 2013a,b), suggesting that Cx36 is the major connexin mediating electrical and dye-coupling between motoneurons at early postnatal ages.

Of additional note was our detection of abundant labelling of Cx36 in most spinal cord laminae, including far greater immunolabelling for Cx36 among adult motoneurons in lamina IX than would be predicted from the loss of coupling between these neurons at maturity. Here, we provide a more comprehensive analysis of the immunofluorescence localization of Cx36 in ventral horn and deep dorsal horn laminae as well as the trigmeninal motor nucleus of mouse and rat spinal cord, with a focus on Cx36 association with axon terminals containing the vesicular glutamate transporter1 (vglut1).

EXPERIMENTAL PROCEDURES

Animals and antibodies

Animals used included twenty-two adult adult male Sprague-Dawley rats, and eighteen adult wild-type mice and four Cx36 knockout mice from colonies of C57BL/6-129SvEv mice (Deans et al., 2001) that were established at the University of Manitoba through generous provision of

breeding pairs of these mice from Dr. David Paul (Harvard). In addition, four male rats and four male wild-type mice were used at each of various development ages, including postnatal day (PD) 5, 10, 15, 20, 25 and 30. Tissues from some of these animals were taken for use in parallel unrelated studies. Animals were utilized according to approved protocols by the Central Animal Care Committee of University of Manitoba, with minimization of the numbers animals used.

Three different antibodies against Cx36 were obtained from Life Technologies Corporation (Grand Island, NY, USA) (formerly Invitrogen/Zymed Laboratories), and included two rabbit polyclonal antibodies (Cat. No. 36-4600 and Cat. No. 51-6300) and one mouse monoclonal antibody (Cat. No. 39-4200), each used in incubations of tissue sections at a concentration of 1-2 µg/ml. The monoclonal anti-Cx36 was used for most of the studies involving double or triple immunolabelling with two or three different primary antibodies. Specificity characteristics of Cx36 detection by the anti-Cx36 antibodies in various regions of rodent brain have been previously reported (Li et al., 2004; Rash et al., 2007a,b; Curti et al., 2012). Additional antibodies included: guinea pig polyclonal antibodies against vesicular glutamate transporter-1 (vglut1) and vesicular glutamate transporter-2 (vglut2) obtained from Millipore (Temecula, CA, USA), and used at a dilution of 1:1000; a chicken polyclonal anti-peripherin obtained from Millipore, and used at a dilution of 1:500; an anti-glutamic acid decarboxylase65 (GAD65) obtained from BD Biosciences (Birmingham, UK) and used at a dilution of 1:100. Various secondary antibodies included Cy3-conjugated goat or donkey anti-mouse and anti-rabbit IgG (Jackson ImmunoResearch Laboratories, West Grove, PA, USA), Alexa Flour 488-conjugated goat or donkey anti-rabbit and anti-mouse IgG (Molecular Probes, Eugene, OR, USA), and AlexaFluor-647 conjugated goat anti-chicken IgG (Life Technologies Corporation) and Cy3-conjugated goat anti-chicken (Jackson ImmunoResearch Laboratories). All secondary antibodies were used at a dilution of 1:600, and were diluted in 50 mM Tris-HCl, pH 7.4, containing 1.5% sodium chloride (TBS), 0.3% Triton X-100 (TBSTr) and 10% normal goat or normal donkey serum.

Dorsal rhizotomy

Primary afferent input to the lumbar spinal cord of rats was unilaterally disrupted by dorsal rhizotomy. Animals (n = 4) weighing from 250-280 grams were anesthetized with isofluorane delivered via a nose cone, and monitored for anesthesia (heart rate, respiratory rate) using an infrared oximeter placed in a forepaw. Temperature was maintained at 37^{o}C with a heating blanket and monitored through a rectal thermometer. After shaving the hind lumbar dorsal skin area and sanitizing with betadine, the lumbar segments L1 to L5 were exposed and a laminectomy was performed, with care to prevent inadvertent injury to the spinal cord. The dura was then opened to allow access to the right L1 to L4 dorsal roots, which were then transected approximately 3 mm proximal to the dorsal root ganglia. Lidocaine (2%) was applied locally to the dorsal roots before section to prevent an afferent barrage to the spinal cord. After rhizotomy, the exposed roots were extensively rinsed with sterile saline solution to remove surplus lidocaine, the exposed spinal cord was covered with sterile gel foam, the muscle layers were closed using 4-0 silk sutures, and the skin wound was closed with stainless steel skin clips. During recovery over the first two days post-surgery, animals were treated every 12 hr with buprenorphine as an analgesic. Rats were taken for experiments after a survival period of seven days.

Tissue preparation

Adult animals and those at PD15 to PD30 were deeply anesthetized with equithesin (3 ml/kg), placed on a bed of ice, and perfused transcardially with cold (4°C) pre-fixative consisting of 50 mM sodium phosphate buffer, pH 7.4, 0.1% sodium nitrite, 0.9% NaCl and 1 unit/ml of heparin, followed by perfusion with fixative solution containing cold 0.16 M sodium phosphate buffer, pH 7.4, 0.2% picric acid and either 1% or 2% formaldehyde prepared from freshly depolymerized paraformaldehyde. Animals were then perfused with a cold solution containing 10% sucrose and 25 mM sodium phosphate buffer, pH 7.4, to wash out excess fixative. Spinal cords from animals at PD5 and PD10, and some at PD15, were removed from euthanized animals and taken for immersion fixation in fixative containing 1-2% formaldehyde prepared as above. No major differences in immunolabelling quality were observed in tissues from PD15 animals fixed by perfusion *vs.* immersion.

Animals taken for dorsal rhizotomy as described above were perfused with fixative containing either 1% or 4% formaldehyde. Use of the two different fixatives was necessary because weak tissue fixation was required for optimum detection of Cx36 (*e.g.*, 1-2% formaldehyde) and stronger fixative was required for optimum detection of vglut1 (*e.g.*, 2-4% formaldehyde). As a control procedure to insure that double labelling for vglut1 and Cx36 with weaker fixations, chosen as a compromise for detection of these proteins, reflected a representative proportion of vglut1-terminals on the control *vs.* rhizotomy side, vlgut1 was examined in some animals prepared with the stronger fixative. Some detailed consideration regarding fixation conditions required for optimum immunohistochemical detection of Cx36 and vglut1, alone or in combination, are described elsewhere (Nagy *et al*., 2012).

After fixation, spinal cords were stored at 4°C for 24-48 h in cryoprotectant containing 25 mM sodium phosphate buffer, pH 7.4, 10% sucrose, 0.04% sodium azide. Transverse or horizontal sections of spinal cord were cut at a thickness of 10-15 μm using a cryostat and collected on gelatinized glass slides. Slide-mounted sections could be routinely stored at -35 ^{o}C for several months before use.

Immunofluorescence procedures

Slide mounted sections removed from storage were air dried for 10 min, washed for 20 min in TBSTr, and processed for immunofluorescence staining, as previously described (Bautista et al., 2012; Curti et al., 2012). For single, double, or triple immunolabelling, sections were incubated with a single primary antibody, or simultaneously with two or three primary antibodies for 24 h at 4°C. The sections were then washed for 1 h in TBSTr and incubated with a single or appropriate combinations of secondary antibodies for 1.5 h at room temperature. Some sections processed by single or double immunolabelling were counterstained with Blue Nissl NeuroTrace (stain N21479) (Molecular Probes, Eugene, OR, USA). All sections were coverslipped with the antifade medium Fluoromount-G (SouthernBiotech, Birmingham, AB, USA). Control procedures involving omission of one of the primary antibodies with inclusion of the secondary antibodies used for double and triple labelling indicated absence of inappropriate cross-reactions between primary and secondary antibodies for all of the combinations used in this study.

Immunofluorescence was examined on a Zeiss Axioskop2 fluorescence microscope and a Zeiss 710 laser scanning confocal microscope, using Axiovision 3.0 software or Zeiss ZEN image capture and analysis software (Carl Zeiss Canada, Toronto, Ontario, Canada). Data from wide field and confocal microscopes were collected either as single scan images or z-stack images with multiple optical scans capturing a thickness of 2 to 14 μm of tissue at z scanning intervals of 0.4 to 0.6 μm. Images of immunolabelling obtained with Cy5 fluorochrome were pseudo colored blue. Final images were assembled using CorelDraw Graphics (Corel Corp., Ottawa, Canada) and Adobe Photoshop CS software (Adobe Systems, San Jose, CA, USA). Movie files included as supplementary data were constructed using Zeiss ZEN software.

Quantitative analyses

Sections of spinal cords from adult rats and mice from these animals at various postnatal ages (PD 5, 10, 15, 20, 25, 30) were double-labelled for Cx36 and vglut1 and taken for quantitative analysis of the proportion of Cx36-immunopositive puncta associated with vglut1-positive nerve terminals in selected regions of spinal cord. In each of four animals at each age, confocal immunofluorescence images ranging from 17 to 19 fields of spinal cord in the regions of interest were collected at sufficient magnification, using a x60 objective lens, to resolve and visualize individual Cx36-puncta. Single confocal scans rather than z-stack image were used to avoid false-positive overlap of Cx36-puncta with vglut1-positive terminals, which may be encountered in stacked images. Puncta with and without vglut1 association were then counted manually, and averaged over the total fields examined per animal. The data from each animal was then normalized by calculating the percentage of total Cx36-puncta associated with vglut1-positive terminals, and an average percentage was then obtained from the number of animals examined and expressed as mean + s.e.m.

Lumbar spinal cord sections from animals receiving dorsal rhizotomy were triple-labelled for Cx36, vglut1 and peripherin, and taken for quantitative analysis of Cx36-puncta and vglut1-positive terminals remaining among peripherin-positive motoneurons in lamina IX and lamina VII on the rhizotomy *vs.* intact contralateral side. Similar procedures for analysis were used as described above, except that one or two images of labelling were acquired on the control intact

side, and images of corresponding areas were obtained on the rhizotomy side. Counts of Cx36-puncta and vglut1-positive terminals was conducted using Zeiss ZEN software (Zeiss Canada), with appropriate thresholding for signal-to-noise and for size of objects to be counted. In a few images, the reliability of automated counting was compared to manual counting, and the two methods were found to yeild similar results.

RESULTS

Cx36 in adult spinal cord

Immunofluorescence labelling of Cx36 in gray matter of mouse and rat spinal cord is heterogeneously distributed in areas of both dorsal and ventral horn. As in all other areas of the CNS we have examined, immunolabelling is exclusively punctate (Cx36-puncta) in appearance, with absence of diffuse or punctate intracellular immunofluorescence (Fig. 1), indicating either inaccessibility of anti-Cx36 antibody to cytoplasmic Cx36, or rapid trafficking of Cx36 leaving insufficient cytoplasmic levels to be detectable by immunofluorescence. Absence of Cx36 immunoreactivity throughout the interior of cells precludes immediate identification of cell-type Cx36 expression, but Cx36-puncta are often localized to the surface of neuronal somata and dendrites, which allows cell identification in the case of morphologically distinctive cells such as motoneurons, or when labelling for Cx36 is combined with, for example, labelling of a neuron specific marker.

In the overview of labelling for Cx36 in deep dorsal horn and ventral horn laminae in adult mouse spinal cord shown in Figure 1A, with blue Nissl counterstaining, Cx36-puncta are less visible at the low magnification presented, but become evident with application of the zoom function in the electronic version of the image. Although Cx36-puncta are scattered throughout these laminae, they are most concentrated in four spinal cord regions, three of which are indicated by the boxed areas in Figure 1A, with the corresponding boxed areas magnified in Figures 1B-D. These regions include: i) The medial portion of lamina VII, specifically encompassing an area just lateral to the central canal (Fig. 1A,B); ii) The intermediate and ventral horn lamina VII and VIII (Fig. 1A,C), where Cx36-puncta are associated with many small and a few large neurons; and iii) The ventral horn lamina IX, where Cx36-puncta are often

localized to motoneurons at all spinal levels, as shown at a lumbar level (Fig. 1A,D) and at a thoracic level (Fig. 1E). A fourth region containing a relatively high density of Cx36-puncta, as we noted in an earlier report (Bautista et al., 2012), encompasses medial regions of deep dorsal horn lamina and will be the subject of a separate report. Immunolabelling for Cx36 in all these regions of adult mouse is absent in Cx36 knockout mice, shown by comparison of a field in lamina IX from a wild-type mouse (Fig. 1D) with a corresponding field in lamina IX from a Cx36 knockout mouse, where motoneurons are labelled for peripherin (Fig. 1F1) and where the same field shows an absence of labelling for Cx36 (Fig. 1F2), indicating specificity of anti-Cx36 antibody. As there is some variation in the literature on the designation of boundaries between spinal cord lamina, we use the mouse and rat spinal cord atlas of Watson et al. (2009) for lamina and spinal nuclear locations.

The persistence of Cx36-puncta in adult spinal cord, particularly those associated with motoneurons, and the presence of ultrastructurally-identified gap junctions associated with some populations of motoneurons in adult rodent spinal cord (Matsumoto et al., 1988,1989; van der Want et al., 1998; Rash et al., 1996), appears to be at odds with the developmental loss of electrical coupling and dye-coupling that was reported between motoneurons at early postnatal ages (Fulton et al., 1980; Walton and Navarette, 1991; Chang et al., 1999). To reconcile this disparity, we considered subcellular locations at which Cx36-containing neuronal gap junctions occur, which includes gap junctions at axon terminals, forming mixed synapses, presumably capable of dual chemical-electrical transmission, as described in the vestibular nuclear complex of rodents (Korn et al., 1973; Nagy et al., 2013) and as found in lower vertebrates (Bennett, 1997; Bennett & Goodenough, 1978). Such mixed synapses have also been reported to occur widely in ventral horn of rodent spinal cord (Rash et al., 1996). Thus, we examined localization of Cx36 in relation to a marker of excitatory axon terminals, specifically vesicular glutamate transporter-1 (vglut1).

Cx36 at vglut1-containing axon terminals in lamina IX

Triple immunofluorescence labelling of Cx36, vglut1, and the motoneuron marker peripherin (Clarke et al., 2010) in lamina IX of adult rat spinal cord is shown at the L4 level (Fig. 2). The

set of four images in Figures 2A1-4 show the same field, with different combinations of image overlay. In overlay of labels for vglut1 (green) and peripherin (blue), most vglut1-positive terminals are seen contacting peripherin-positive motoneuronal somata or dendrites (Fig. 6A1). Many of these terminals are relatively large, with the largest reaching approximately 4 μm in diameter, and likely representing terminations of low threshold, large diameter primary afferents, including group Ia and II afferents from muscle spindle organs and Golgi tendon organs that are known to form monosynaptic, excitatory glutamatergic contacts with motoneurons (Fleshman et al., 1981; Jankowska and Edgley, 1993). In overlay of labels for Cx36 (red) and peripherin (blue), many though not all Cx36-puncta are localized to the surface of peripherin-positive motoneuron somata and along their proximal dendrites (Fig. 2A2). Overlay of green and red labels reveals that many Cx36-puncta are localized to vglut1-positive terminals (Fig. 2A3), as further shown by overlay of all three labels (Fig. 2A4). Higher confocal magnification of Cx36/vglut1 association is shown in Figure 2B, where many vglut1-positive terminals (Fig. 2B1) and Cx36-puncta in the same field (Fig. 2B2) are seen to overlap along large, peripherin-positive dendrites (Fig. 2B3, overlay). Individual terminals often display several Cx36-puncta (Fig. 7B3, inset), as do extended axonal segments appearing to form en passant terminals (Fig. 2C), which are characteristic of primary afferents ending on motoneurons (Brown and Fyffe, 1978).

These results suggest that vglut1-terminals in lamina IX may form morphologically mixed chemical/electrical synapses. However, as evident in Figures 2A and B, not all vglut1-terminals display labelling for Cx36, suggesting mixed synapse formation by specific classes of afferent terminals. Conversely, some Cx36-puncta lack overlap with vglut1-terminals, and these may represent purely electrical synapses between as yet unidentified neuronal elements. Similar results were obtained in motoneuronal pools at cervical, thoracic, sacral and other lumbar levels in both rat and mouse, except among sexually dimorphic motor nuclei where abundant Cx36-puncta localized to motoneurons lack association with vglut1 (Bautista et al., 2013). One other exception was encountered at a lower cervical level (C8). At this level, ventrolaterally located motor nuclei, which correspond to the location containing motoneurons innervating tricepts and pectoral muscles (Watson *et al.,* 2009), were conspicuous in that they nearly totally lacked vglut1-terminals (Fig. S1A, B1) and contained only a sparse scattering of Cx36-puncta (Fig. S1C, B2), compared with adjacent dorsally located motor nuclei, which contained an abundance of both Cx36-puncta and vglut1-terminals that displayed co-localization as observed at other

spinal levels (Fig. S1B1). The reason for the anomalous characteristics of these motoneurons with respect their absence of vglut1-containing primary afferent input remains to be determined.

Cx36 at vglut1-terminals in intermediate lamina VI, VII and VIII

A moderate density of immunolabelling for vglut1 and Cx36 in lamina VI, VII and VIII is seen widely but unevenly distributed among small, medium-sized, and large neurons. Cx36-puncta and vglut1-terminals tend to be concentrated in arrays sweeping horizontally or vertically across lamina VI (Fig. 3A) and VII (Fig. 3B), or are seen heavily decorating the somata and initial dendrites of a few, relatively large neurons per section in lamina VII (Fig. 7C) and lamina VIII (not shown). Immunolabelling of Cx36 appeared as isolated puncta, or more often as an assembly of 5 to 10 closely-clustered puncta (Fig. 37A1, B1 and C2). These clusters were invariably co-localized with vglut1-terminals, as seen in overlay images (Fig. 3A2, B2 and C3). As in lamina IX, not all vglut1-terminals displayed Cx36-puncta, but nearly all such terminals surrounding infrequently encountered neurons in lamina VII (Fig. 3C; neurons not counterstained, but marked by asterisk), were decorated with these puncta. Immunolabelled terminal boutons, having a somewhat flattened shape against their postsynaptic elements, could be viewed *en* face (Fig. 3C1, D1), in which case Cx36-puncta were seen distributed largely within the confines of the terminal (Fig. 3C3, 2D3), giving the impression that these puncta were contained within the terminal interior. Alternatively, vglut1-positive terminals could be viewed on edge, such as those contacting a large dendrite in Figure 3D (dendrite marked by asterisks). In these views, Cx36-puncta were seen aligned along bouton surfaces that were in contact with the dendrite (Fig. 3D2, 3D3), as might be expected given the plasma membrane localization of Cx36-containing gap junctions, and presumptive gap junction formation at points of apposition between the terminals and the dendrite.

Lack of co-localization of Cx36-puncta with vglut2-containing terminals

We tested whether another class of glutamatergic terminals containing the vesicular glutamate transporter-2 (vglut2) shared a similar co-localization relationship with Cx36. Nerve terminals

containing vglut2 are distributed throughout spinal cord gray matter, far out number terminals containing vglut1 (Fig. 3E), but only very rarely contain both vglut1 and vglut2. Terminals containing vglut2 are considered to arise largely from other than primary afferent neurons (Persson et al., 2006). Double labelling revealed a total lack of Cx36 co-localization with terminals containing vglut2 in all spinal cord areas examined, as shown by example in lamina IX (Fig. 3F1, 3F2).

Cx36 at vglut1-terminals in medial regions of lamina VII

Particularly striking is the organization of fibers and terminals immunopositive for vglut1 and their relationship with labelling for Cx36 in medial portions of lamina VII immediately adjacent to the central canal at cervical, thoracic, lumbar and sacral levels. In adult rat, dense collections of fibers labelled for vglut1 along their length course in a ventro-medial direction, producing a confluence of terminals in a region adjacent, as well as dorsolateral, to the central canal (Fig. 4A). This region contains a mix of small and medium-sized neurons, with diameters ranging from 25 to 50 μm. Some of these neurons are heavily laden with Cx36-puncta distributed mostly on their somata and initial dendrites (Fig. 4B1). Most of these neurons are targets of dense innervation by vglut1-positive afferents (Fig. 4B2). In transverse sections, these neurons were erratically encountered, making it difficult to appreciate their relative numbers and distribution in a single section. Examination of horizontal sections, however, reveals a clear pattern to their organization. A photomontage illustrating immunolabelled for Cx36 in a 2 mm length of spinal cord at a T9 level in the horizontal plane of the central canal is shown in Fig. 4C. Although the section is not counterstained, locations of neurons displaying Cx36-puncta are readily discernible by densely distributed puncta around their somata. Only in this view did it became evident that these neurons occur in clusters of usually 2 to 4 cells and occasionally up to 6 cells, that the clusters are distributed intermittently along the length of the spinal cord, and that these clusters often appeared to be in register between the left and right side of the cord. At higher magnification with blue fluorescence Nissl counterstaining, neurons decorated with Cx36-puncta are seen intermingled with neurons of similar size lacking these puncta (Fig. 4D). Confocal analysis showed that the labelling was exclusively punctate, and through focus analysis indicated that Cx36 immunofluorescence was localized to the neuronal surface (Fig. 4E). Double

immunolabelling for Cx36 and vglut1, with fluorescence Nissl counterstaining, further revealed that vglut1-terminals are concentrated in intermittent patches among the clusters of Cx36-positive and negative neurons, and that these terminals target both neurons displaying or lacking Cx36-puncta (Fig. 4F1-F4, showing the same field). The patches of vglut1-terminals, together with their clusters of neurons decorated with Cx36-puncta, were roughly round or oval, and sometimes appeared to merge with adjacent patches. On average, there were about 8-9 patches per segment at cervical, thoracic and lumbar levels, and the diameters of the vglut1-patches were not significantly different at these various levels (190 + 7.9 μm, 235 + 13 μm, 223 + 18 μm, respectively). However, the distances from the center of one patch to the center of an adjacent patch were less at cervical (206 + 12 μm) and lumbar (266 + 24 μm) than at thoracic (338 + 9 μm) levels, indicating that they were more closely spaced at the two former levels.

Immunolabelling for vglut1 and Cx36 among neurons in medial lamina VII was compared with labelling for vglut2 in this region. From a global view in transverse sections, shown at a lower lumbar level, patches of dense vglut1 labelling are seen to occupy regions displaying a near total void in labelling for vglut2 (Fig. 5A1; and overlay with labelling for vglut1 in 5A2), which was especially remarkable considering that nearly the entire remainder of the spinal cord gray matter contains a dense distribution of vglut2. Similarly, horizontal sections reveal a nearly exact correspondence between patches of dense vglut1-containing terminals in regions adjacent to the central canal (Fig. 15B1) and patches devoid of vglut2 labelling in these regions (Fig. 5B2 and overlay in 5B3). At a higher lumbar level, two distinct medially located regions are seen to be devoid of labelling for vglut2; a ventral region adjacent to the central canal, containing clusters of neurons decorated with Cx36-puncta (Fig. 5C, shown magnified in 5D), and a dorsal region corresponding to the dorsal nucleus of Clarke (Fig. 5E), which was previously found to contain low levels of vglut2 and high levels of vglut1 (Shrestha et al., 2012). Although not examined in detail here, the nucleus of Clarke was delineated by dense labeling for vglut1 (Fig. 5F1) and was also enriched in Cx36-puncta that were randomly distributed (Fig. 5F2), rather than concentrated on individual neuronal somata, and these Cx36-puncta were extensively co-localized with vglut1-terminals (Fig. 5G,H).

It is of note that previous studies have described a moderate concentration of vglut1-terminals in the medial region of lamina VII (Alvarez et al., 2004; Persson et al., 2006), which at

lower thoracic levels was reported to consist of a continuous column of vglut1-labelling and was considered to represent Clark's Column (Alvarez et al., 2004). Our results at this spinal level distinguish Clark's Column located dorsally from the region in medial lamina VII that contained the intermittent patches of vglut1-labelling and clusters of neurons labelled with Cx36-puncta. Likewise, at cervical levels, vglut1-terminals are concentrated in two medially located regions; one immediately adjacent to ventral portions of the dorsal column, and the other corresponding to the central cervical nucleus (CeCv) located adjacent to the central canal (Fig. 5I). The CeCv contained clusters of neurons decorated with Cx36-puncta (Fig. 5J1), and these puncta displayed co-localization with vglut1-terminals (Fig. 5J2). Thus, the CeCv appears to represent a rostral extension of the patches of vglut1-terminals that contain neurons bearing Cx36-puncta at more caudal spinal levels.

Confocal examination of labelling for Cx36 in patches of vglut1-terminals in medial lamina VII of rat spinal cord is presented in Fig. 6, where a single patch is shown in a transverse section at an upper lumbar level (Fig. 6A). Triple labelling shows patches to be rich in peripherin-positive primary afferent fibers (Fig. 6B,C), consistent with the primary afferent origin of vglut1-containing terminals in the patches (see below). Among terminals and fibers labelled for vglut1 and peripherin, neurons are seen outlined by Cx36-puncta overlapping or located near vglut1-terminals along their initial dendritic segments (Fig. 6B,C). Examination of mouse spinal cord showed a similar association of Cx36-puncta with vglut1-terminals surrounding neurons in medial areas of lamina VII (Fig. 6D). The image in Figure 6E is a magnification of the boxed area in Figure 6A, showing a z-stack of a single neuron (somata indicated by asterisk), where many vglut1-terminals and their associated Cx36-puncta are seen en face covering several initial dendrites and the somata surface. Rotation of a 3D version of this image provides appreciation of Cx36-puncta localized at vglut1-terminals at all angles of rotation (Supplementary movie Fig. S2), indicating that this association does not arise as an artifact of z-stack imaging, where labels for Cx36 and vglut1 separated in the z-axis could result in false-positive overlap. As in lamina IX, vglut1-terminals viewed en face are seen to display multiple Cx36-puncta on their surface (Fig. 6F). Confocal examination of double labelling for vglut2 and Cx36 in medial regions of lamina VII showed a negligible overlap of Cx36-puncta with vglut2-terminals (Fig. 6G).

Cx36 at vglut1-terminals in the trigeminal motor nucleus

We next examined one other location where Cx3-puncta are densely distributed among motoneurons, namely the trigeminal motor nucleus (Mo5) in rat and mouse. Motoneurons in Mo5 are tighly packed (7A1) and receive a greater density of vglut1-containing terminals compared with their spinal counterparts (Fig. 7A2). In both rat and mouse, labelling for Cx36 is remarkably dense throughout the Mo5 (Fig. 7A3, 7B2), effectively delineating the nucleus, particularly because there is very little detectable Cx36 in immediately surrounding regions. Nearly all labelling for vglut1 (Fig. 7C1) and Cx36 (7C2) appears to be associated with peripherin-positive motoneurons, and nearly all Cx36 appears to be associated with vglut1-terminals (Fig. 7C3). As in spinal cord, labelling for Cx36 has a punctate appearance in Mo5, and Cx36-puncta are seen localized to individual vglut1-positive terminals (7D-F). However, vglut1-terminals in Mo5 are somewhat smaller and displayed fewer Cx36-puncta (Fig. E2, inset) than those in lamina IX of spinal cord, although this was not examined quantitatively. The Cx36-puncta are seen in association with vglut1-terminals contacting motoneuronal somata (Fig. 7D), but many more are seen along initial dendritic segments (Fig. 7E), as well as more distal portions of dendrites (Fig. 7F).

The source of vglut1-containing axon terminal in the Mo5 has, to our knowledge, not been determined, but the trigeminal sensory ganglion and/or mesencephalic nucleus of the trigeminal nerve are likely candidates based on the primary afferent origin of similar terminals at spinal levels. The Mo5 appears to be unique among cranial motor nuclei in displaying such a rich content of Cx36; the facial motor nucleus is nearly devoid of labelling for Cx36, the hypoglossal nucleus has sparse Cx36-puncta associated with only a few small neurons, and the remaining nuclei contain only a scattering of these puncta (not shown).

Primary afferent origin of terminals associated with Cx36-puncta

We next examined the source of vglut1-terminals at which Cx36-puncta were localized in the lumbar spinal cord. There is evidence that vglut1 in spinal cord gray matter is contained largely,

though not exclusively, in terminals of primary afferent origin (Oliveira et al., 2003; Alvarez et al., 2004; Wu et al., 2004; Persson et al., 2006). The association of Cx36 with nerve terminals containing vglut1 suggests that some of these afferents form mixed synapses. This possibility would require transport of Cx36 from dorsal root ganglion neurons to the presynaptic terminal membrane for gap junction formation by docking of connexons in hemiplaques contributed by the pre- and postsynaptic elements. Because we have found Cx36 so far only in intact gap junctions (*i.e.*, never in a gap junctional hemiplaque without an apposing hemiplaque) (Rash *et al*., 2000, 2001a,2007a,b), it can be predicted that elimination of terminals bearing Cx36 will result in the loss of gap junctions at these terminals (*i.e*., loss of both pre and postsynaptic hemiplaques). To test this and to confirm primary afferent localization of Cx36 in spinal cord regions examined above, we performed unilateral dorsal rhizotomies, involving transection of dorsal roots at the L1 to L4 spinal segments in adult rats. Typical labelling for vglut1 is obtained among peripherin-positive motoneurons in lamina IX on the control unoperated side, as shown at an L3 spinal level (Fig. 8A1), and a large loss of labelling is seen in lamina IX in corresponding fields on the side of the rhizotomy (Fig. 8B1). The same fields show comparisons of Cx36 labelling density on the control *vs*. rhizotomy side at the L3 level, with labelling for Cx36 alone (Fig. 8A2 *vs.* 8B2), and after overlay with labelling for vglut1 and peripherin (Fig. 8A3 and 8B3). There was a large reduction in the density of Cx36-puncta, and some of those remaining on the rhizotomy side displayed the typical co-localization with vglut1 (Fig. 8B3) seen on the unoperated control side (8A3). After perfusion of animals with fixative containing 4% formaldehyde, depletion of vglut1 on the rhizotomy side was similar to that seen with the weaker fixative (Fig. 8C *vs.* 8D), indicating that less than optimal fixation for vglut1 did not qualitatively confound the results.

Results from quantitative analyses (Fig. 8E,F) showed that vglut1-terminals in lamina IX at deafferented lumbar levels was reduced by 80 ± 1.2% (n = 4), and Cx36-puncta were reduced by 65 ± 3% (n = 4). Because primary afferents ascend and descend several segments upon entering the spinal cord, giving off numerous collaterals at each segment, and because only four dorsal roots were transected, it is likely that the L1-4 regions examined receive input from above and below the level the rhizotomy, and that depletions of vglut1 and Cx36 may have been greater with more extensive dorsal rhizotomy. The extent of vglut1 and Cx36 depletions in other lamina of spinal cord were not examined quantitatively, but it appeared from visual inspection that loss

of vglut1 in dorsal horn lamina were not as great, whereas loss of vglut1-terminals and Cx36-puncta in intermediate lamina and other areas of the ventral horn was similar to or greater than that seen in lamina IX. In particular, dorsal rhizotomy at the L1-L4 levels caused a massive depletion of the patches of vglut1 labelling adjacent to the central canal, as shown by comparison of the control intact side *vs*. the contralateral deafferented side in a Nissl counterstained section (Fig. 8G). This depletion was accompanied by an equally extensive loss of Cx36-puncta, as shown by images of labelling for Cx36 alone on the intact side [(Fig. 8H, magnified from field in left box of (G)] *vs*. rhizotomy side [(Fig. 8I, magnified from field in right box of (G)].

In view of the above results, indicating association of Cx36-puncta with primary afferent terminals, we explored the localization of labelling for vglut1 and Cx36 in relation to that of terminals labelled for glutamic acid decarboxylase65 (GAD65). It is known that GAD65 is contained largely in terminals of gamma-aminobutyric acid (GABAergic) neurons that form presynaptic inhibitory contacts on terminals of large diameter primary afferents ending on various classes of spinal cord neurons, including motoneurons (Hughes et al., 2005). Specifically, we determined whether those terminals bearing Cx36-puncta in lamina IX and medial lamina VII are among afferent terminals contacted by presynaptic GAD65-containing P boutons (Hughes et al., 2005). In lamina IX, GAD65-positive terminals were frequently seen closely apposed to vglut1-terminals displaying co-localization with Cx36-puncta (Fig. 9A-C). In these images, vglut1 is pseudo-colored blue rather than green, to avoid obscuring fluorochrome labels for Cx36 and GAD65. As shown at successively higher magnifications, these relationships were found at vglut1-terminals forming what appeared to be en passant type contacts with motoneurons (Fig. 9A), at series of clustered terminals (Fig. 9B), and at individual isolated terminals (Fig. 9C). Similar results were obtained in medial lamina VII, where terminals labelled for GAD65 were invariably seen in apposition to vglut1-terminals that overlap with Cx36-puncta. These associations of the three labels were seen on neuronal somata (Fig. 9D) and were especially prominent at large initial dendrites encircled by vglut1-terminals (Fig. 9E). As shown by high magnification at vglut1-terminals viewed on edge and in apposition to neuronal somata, Cx36-puncta appeared at sites on these terminals closest to the somata, whereas GAD65-positive terminals were more distally located on these terminals (Fig. 9F). Also seen are cases of close proximity of Cx36-puncta to GAD65-positive P boutons (Fig. 9G). Although requiring

ultrastructural confirmation, this result suggests that primary afferent terminals subject to presynaptic inhibition are among those afferents that form (morphologically) mixed synapses.

Developmental profile of mixed synapses in the spinal cord

The possibility of an electrical component to transmission by primary afferents in rodent spinal cord would be most amenable to investigation using *in vitro* preparations from early postnatal or juvenile animals, where neural tissues remain viable for extended periods of electrophysiological recording. We therefore determined the developmental profile of Cx36 association with vglut1-terminals in rodent spinal cord. At each age examined, fields in lamina IX and VII containing numerous Cx36-puncta and vglut1-labelled terminals were photographed at medium confocal magnification and taken for counts of total Cx36-puncta. The data are presented as the average of total Cx36-puncta counted in the two spinal cord areas from four animals (Fig. 10A1 and 10B1), the average number of Cx36-puncta co-localized with vglut1 in these animals (Fig. 10A2 and 10B2), and the average percentage of Cx36-puncta/vglut1-terminal co-localization (Fig. 10A3 and 10B3). Surprisingly, in both lamina IX and VII, Cx36-puncta were rarely co-localized with labelling for vglut1 prior to the end of the second postnatal week, and minimally even up to the end of the third postnatal week. Co-localization thereafter increased, reaching values of 50% in lamina IX and 42% in lamina VII of adults rats. Mice were examined in less detail, but also showed a paucity of Cx36/vlgut-1 co-localization during early development and reached 28% co-localization in lamina IX at PD30 and 38% in adults.

We emphasize that there are several reasons for considering these values of Cx36/vglut1 co-localization to be, in all probability, substantial underestimates, which impacts functional considerations regarding the remaining fraction of Cx36-puncta that presumably form pure electrical synapses in the spinal cord regions examined. First, the localization of Cx36-puncta around the periphery rather than within terminals makes more likely the possibility of instances where these puncta could be visualized in the focal plane viewed, but their associated vglut1-terminal may be out of the plane of focus or even in an adjacent section, giving false-negative co-localization. Second, synaptic vesicles in primary afferent terminals, such as those on motoneurons, are not always crowded against the presynaptic plasma membranes. Thus, Cx36-

puncta localized to these membranes may be close to, but separated from, intra-terminal labelling for vglut1. Indeed, Cx36-puncta were often seen very near vglut1-positive terminals, but were not counted as co-localized with these terminals. And third, the differences in fixation conditions for optimal detection of Cx36 *vs.* vglut1, requiring a compromise in fixation to allow double labelling for these proteins, likely resulted in some reduction of labelling for vglut1. We estimate that the above three factors together may have created an underestimate of Cx36-puncta association with vglut1-terminals by as much as 25-35%, as judged from the large number of puncta that were very near vglut1-terminals but not counted, and from a few instances in adult animals, where such co-localization in areas of spinal cord ventral horn appeared to reach 80-90%. Nevertheless, since these considerations apply to each of the ages examined, the relative Cx36/vglut1 co-localization values observed at the ages examined are nervertheless reflective of a late developmental pattern of morphologically mixed synapses.

DISCUSSION

Our results show widespread expression of Cx36 protein among motoneurons in spinal cord lamina IX and in the trigeminal motor nucleus, as well as among neurons in intermediate laminae of spinal cord in both adult rat and mouse. In these areas, Cx36 was extensively localized either at vglut1-containing axon terminals or in very close proximity (*i.e.,*<1 μm) to these terminals. It was previously shown that a substantial proportion of vglut1-containing terminals distributed in various regions of the spinal cord are endings of primary afferent fibers (Alvarez *et al*., 2004). In agreement with these earlier observations, we found a large loss of these terminals in dorsal and ventral horn areas following dorsal rhizotomy. Taken together with our observations of Cx36/vglut1 co-localization, the results suggest association of Cx36 with primary afferent terminals, which is supported by our finding that dorsal rhizotomy caused correspondingly large reductions in labelling for Cx36, not only in lamina IX, but also in other spinal cord laminae. It thus appears that primary afferent terminals in adult rat and mouse form morphologically "mixed synapses" that are potentially capable of dual chemical/electrical transmission. Although the proportion of vglut1-terminals displaying Cx36-puncta was not examined quantitatively, it was clear that Cx36 is associated with only a subpopulation of these vglut1-containing afferents in most of the spinal lamina examined. The sensory input conveyed by these afferents and whether

mixed synapses are restricted to a specific functional class of sensory afferents is currently unknown, but from their presence on for example motoneurons, these must include Ia muscle spindle and tendon afferents that are known to end on motoneurones and intermediate zone interneurones (Scheibel and Scheibel; 1968; Mendell and Henneman, 1971; Hongo et al., 1978; Brown and Fyffe, 1978; Munson et al., 1982). Because these afferents are known to be subject to presynaptic inhibition mediated by P boutons (Hugues et al 2005), our finding of these boutons in association with vglut1-containing afferents forming morphologically mixed synapses further supports the spindle and tendon origin of at least some of these afferents.

While the vast majority of spinal motor nuclei displayed Cx36/vglut1 co-localization on motoneurons, we report elsewhere (Bautista et al., 2013b) that a separate class of rodent motoneurons found in sexually dimorphic motor nuclei at lower lumbosacral levels exhibit dense Cx36-puncta at their somatic and dendritic appositions, but that these puncta lack co-localization with vglut1, and indeed that the dimorphic nuclei themselves were largely devoid of vglut1-containing terminals. Thus, we distinguish two classes of motor nuclei: one where Cx36 is affiliated with vglut1-containing nerve terminals, forming morphologically mixed synapses, and another where Cx36 occurs entirely in the absence of vglut1, forming gap junctions may be "purely electrical synapses". Also found was a rare third class at a lower cervical level (C8), where motor nuclei were nearly devoid of both vglut1 and Cx36. Based on the spinal cord atlas of Watson et al. (2009), these motor nuclei contain motoneurons innervating tricepts and pectoral muscles. Among motor nuclei and in intermediate spinal laminae harbouring mixed synapses in adult rat and mouse, Cx36-puncta were also seen lacking association with vglut1. The extent to which these reflect purely electrical synapses between either motoneurons or other types of neurons, or represent false-negative Cx36/vglut1 co-localization remains uncertain due to technical limitations, as discussed in Results, and will require resolution by ultrastructural immunolabelling for Cx36. Notwithstanding our emphasis on the likely underestimate of the proportion of Cx36-puncta that co-localize with vglut1 in adult rat and mouse spinal cord, we do not exclude the possibility that some motoneurons, in addition to those in the dimorphic nuclei, remain coupled in adults. Indeed, gap junctions have been found between dendrites of soleus muscle motoneurons in adults rats (van der Want et al., 1998).

Development of mixed synapses in ventral horn laminae

The widespread presence of Cx36-puncta observed in spinal cord at early postnatal ages is consistent with reports of electrical- and dye-coupling between developing spinal neurons, particularly motoneurons (see Introduction). In contrast, mixed synapses in each of the spinal cord gray matter regions examined had a surprisingly late developmental appearance and were first observed, in for example lamina IX, at a time (*i.e.* PD8-13) when motoneurons cease to exhibit their earlier patterns of direct intercellular electrical coupling (Walton & Navarrete, 1991). Equally remarkable was the continued increase in the incidence of these synapses even after the third postnatal week to adulthood. Our results thus indicate that motoneurons transition from an early state of coupling with each other to a later state of mixed synapse formation with their resident afferent terminals. The functional relevance of these mixed synapses and the physiological processes for which they would presumably be required at such a late onset (*e.g.*, past PD20-25), but less so earlier at a juvenile stage in what are functionally mature animals, remain to be determined, perhaps in relation to developmental events that have an equally protracted period, such as myelination and motor unit pruning, etc, which continue during the first few postnatal weeks (Navarrete and Vrbova, 1993).

Mixed synapses in spinal cord and their structural/functional correlate

Functional mixed synapses with a chemical and electrical components formed by primary afferents on motoneurons have been described in lower vertebrates (Shapovalov *et al*., 1980), and morphologically mixed synapses have been demonstrated ultrastructurally in rodent spinal cord (Rash *et al.*, 1996). By thin-section electron microscopy (EM), terminals forming these synapses in rat spinal cord were large (3 μm in diameter) and were more often encountered than purely electrical synapses at increasing developmental age (Motorina, 1989,1991). By freeze-fracture EM, gap junctions at mixed synapses in rat spinal cord: i) were found throughout the rostro-caudal spinal cord axis; ii) detected in lamina III-IX at various spinal levels; iii) were located on interneurons as well as motoneurons; iv) were distributed often on neuronal somata and initial dendrites; v) occurred in clusters at axon terminals, with up to six gap junctions per cluster; and vi) were estimated to be present at a frequency of about 300 per spinal neuron (Rash

et al., 1996; 1997,1998). These series of findings are remarkably harmonious with our results on the overall distribution and cellular localization of Cx36-puncta in adult rodent spinal cord. In particular, the relatively large number of mixed synapses estimated to contact spinal neurons is easily envisioned when considering what the projected density of Cx36-puncta associated with terminals would be on motoneurons such as those shown in Figure 6, if these neurons were subject to full 3D reconstruction.

Given their relatively high density in rodent spinal cord, it may be surprising that mixed synapses have not been more frequently encountered in nearly a half century of ultrastructural studies of spinal cord synaptology. Similarly, the electrophysiology of synaptic transmission by primary afferents on motoneurons has arguably been the most extensively studied in mammalian CNS, but evidence for an electrical component at these synapses has rarely been reported. There are several possible reasons for this. First, it is generally recognized that neuronal gap junctions in the CNS are difficult to find, even when intentionally searched for, and could be overlooked at EM magnifications typically used for studies of synaptic connectivity. This is especially the case with technical limitations imposed by thin-section EM identification of the typically small gap junctions that occur between neurons, though some of these limitations are mitigated by freeze-fracture EM (Rash *et al*., 1998). Second, tissue preparation has not always been optimal for gap junction detection, especially in early EM work, where less than optimal conditions sometimes precluded distinguishing between gap junctions, tight junctions and desmosomes in mammalian CNS (Rash *et al*., 1998). And third, many of the early classic EM studies of spinal cord synaptology were conducted using cat, and there is evidence suggestive of gap junctions between cat motoneurons, for coupling between these motoneurons, and for possible mixed synaptic transmission onto these neurons (Nelson, 1966; Decima & Goldberg, 1970; Matthews et al., 1971; Werman & Carlen, 1976; Gogan et al., 1977; Engberg & Marshall, 1979; Curtis *et al.*, 1979). While we have succeeded in detecting Cx36 by immunofluorescence in some areas of cat brain (Nagy et al., 2013), we do not yet have sufficient confidence in labelling of this connexin in adult cat spinal cord, thus precluding correlation of Cx36 expression with reports of electrical coupling in feline preparations.

Electrical coupling between motoneurons has rarely been examined in adult rodents, or in young adolecent rodents when mixed synapses become abundant. Yet, this is now of relevance

because, besides mediation of coupling by purely electrical synapses, mixed synapses represent another potential means of establishing electrical communication between neurons. In the lateral vestibular nucleus of adult rat, for example, it has been deduced that electrical coupling occurs between neurons that themselves appear not to be linked by gap junctions; rather, coupling was proposed to be mediated by way of mixed synapses formed by presynaptic fibers, where collaterals of individual fibers forming mixed synapses with separate neurons provide a pathway for electrical coupling of those neurons (Korn et al., 1973). Neuronal coupling mediated by presynaptic fibers has been extensively documented in lower vertebrates (see Bennett & Goodenough, 1978). In the spinal cord, primary afferent fibers are known to form up to 50 collaterals that innervate scores of motoneurons (Brown & Fyffe, 1978, 1981). Assuming that fibers with such collateral terminations include those at which we find mixed synapses, these fibers potentially could mediate coupling between motoneurons in adult rodents.

Mixed synapses in medial intermediate lamina

Clusters of Cx36-laden neurons located in medial lamina VII near the central canal displayed a complex organization, with characteristic features distinguishing these clusters from surrounding regions, including: i) the regularity and high density of vglut1-containing primary afferent ("PA") convergence on these clusters ; ii) their intermittent rostro-caudal occurrence in separated domains at all spinal levels; iii) the presence of neurons receiving mixed synapses from Cx36-containing ("Cx") primary afferents intermingled with those lacking these synapses; and iv) their paucity of innervation by vglut2-containing terminals. Based on these features and for ease of reference, we term these clusters, together with their contingent of vglut1-containing primary afferents, as medial lamina VII PACx (M-VII PACx) domains. A coalescence of primary afferents and/or their collaterals with intermittent fields of arborizations generating a modular pattern has been described in this area of the spinal cord (Scheibel & Scheibel, 1969; Szentagathai 1966; Smith, 1983). Studies of terminal degeneration following dorsal rhizotomy have also identified plexuses of primary afferent terminations that were located lateral and ventrolateral to the central canal and that had an intermittent distribution (Imai & Kusama, 1969), corresponding to the distances between the PACx domains measured here. Further, at lower thoracic and lumbar levels, distinct sets of primary afferent fibers entering Clark's column

were distinguished from those with deeper trajectories terminating in the medial area of lamina VII (Rethelyi 1968), corresponding to the area of the M-VII PACx domains identified here.

Importantly, the PACx domains are distinct from the nearby intermediomedial nucleus, which is known to contain ChAT-positive neurons (Stepien et al 2010), whereas our results show these domains to contain only a few neuronal somata immunopositive of ChAT (not shown), and these ChaT-positive somata did not correspond to those heavily laden with Cx36-puncta and vglut1-terminals. Similarly, the PACx domains are distinct from Clarke's nucleus at lower thoracic and upper lumbar levels. However, at cervical levels, the PACx domains appear to correspond to the central cervical nucleus (CeVe), which also occupies medial regions of lamina VII.

Neurons in the M-VII PACx domains displayed size heterogeneity at thoracic *vs.* lumbar levels, being somewhat smaller and more medially located in thoracic segments. Their dendrites almost certainly extend beyond the domains containing their somata, which are delineated by diminished vglut2-containing terminals. Consequently, while the extent of excitatory input to their dendrites from vglut2-terminals is uncertain, it is likely that excitatory vglut1-containing afferents concentrated on their somata and initial dendrites exert a powerful influence on their activity. The sensory information conveyed by these afferents is unclear, but likely does not include group Ia fibers that lack terminations in medial areas of lamina VII (Brown & Fyffe, 1978; Ishizuka *et al*., 1979). It remains to be determined whether this influence is further augmented by a functional electrical component at the morphologically mixed primary afferent synapses that some of these neurons receive.

Acknowledgements - This work was supported by a grant from the Canadian Institutes of Health Research to J.I.N. (MOP 106598) and to DM (MOP 37756), and by grants from the National Institutes of Health (NS31027, NS44010, NS44295) to JE Rash with sub-award to JIN. We thank B. McLean for excellent technical assistance, Dr. D. Paul (Harvard University) for providing breeding pairs of Cx36 knockout and wild-type mice.

REFERENCES

Alvarez FJ, Villalba RM, Zerda R, Schneider SP (2004) Vesicular glutamate transporters in the spinal cord, with special reference to sensory primary afferent synapses. J Comp Neurol 472:257-280.

Arasaki K Kudo N, Nakanishi T (1984) Firing of spinal motoneurons due to electrical interactions in the rat: an in vitro study. Exp Brain Res 54:437-445.

Barber RP, Phelps PE, Houser CR, Crawford GD, Salvaterra PM, Vaughn JE (1984) The morphology and distribution of neurons containing choline acetyltransferase in the adult rat spinal cord: an immunocytochemical study. J Comp Neurol 229:329-346.

Bautista W, Nagy JI, Dai Y, McCrea DA (2012) Requirement of neuronal connexin36 in pathways mediating presynaptic inhibition of primary afferents in functionally mature mouse spinal cord. J Physiol 590:3821-39.

Bautista W, Nagy JI (2013) Re-evaluation of connexin (Cx26, Cx32, Cx36, Cx37, Cx40, Cx43, Cx45) association with motoneurons in rodent spinal cord, sexually dimorphic motor nuclei and trigeminal motor nucleus. Submitted.

Bautista W, McCrea DA, Nagy JI (2013) Connexin36 forms purely electrical synapses in sexually dimorphic lumbosacral motor nuclei in spinal cord of developing and adult rat and mouse. Submitted.

Bennett MVL, Goodenough DA (1978) Gap junctions, electrotonic coupling, and intercellular communication. Neurosci Res Prog Bull 16:373-485.

Bennett MVL (1997) Gap junctions as electrical synapses. J Neurocytol 26:349-366.

Bennett MVL, Zukin SR (2004) Electrical coupling and neuronal synchronization in the mammalian brain. Neuron 41:495-511.

Bou-Flores C, Berger AJ (2001) Gap junctions and inhibitory synapses modulate inspiratory motoneuron synchronization. J Neurophysiol 85:1543-1551.

Brown AG, Fyffe RE (1978) The morphology of group Ia afferent fibre collaterals in the spinal cord of the cat. J Physiol 274:111-127.

Brown AG, Fyffe RE (1981) Direct observations on the contacts made between Ia afferent fibres and alpha-motoneurones in the cat's lumbosacral spinal cord. J Physiol 313:121-140.

Chang Q, Balice-Gordon RJ (2000) Gap junctional communication among developing and injured motor neurons. Brain Res Rev 3:242-249.

Chang Q, Gonzalez M, Pinter MJ, Balice-Gordon RJ (1999) Gap junctional coupling and patterns of connexin expression among neonatal rat lumbar spinal neurons. J Neurosci 19:10813-10828.

Chang Q, Pereda A, Pinter MJ, Balice-Gordon RJ (2000) Nerve injury induces gap junctional coupling among axotomized adult motor neurons. J Neurosci 20:674-684.

Clarke, W.T., Edwards, B., McCullagh, K.J., Kemp, M.W., Moorwood, C., Sherman, D.L., Burgess, M. & Davies, K.E. (2010) Syncoilin modulates peripherin filament networks and is necessary for large-calibre motor neurons. J. Cell Sci., 123, 2543-52.

Coleman AM, Sengelaub DR (2002) Patterns of dye coupling in lumbar motor nuclei of the rat. J Comp Neurol 454:34-41.

Condorelli DF, Parenti R, Spinella F, Salinaro AT, Belluardo N, Cardile V, Cicirata F (1998) Cloning of a new gap junction gene (Cx36) highly expressed in mammalian brain neurons. Eur J Neurosci 10:1202-1208.

Condorelli DF, Belluardo N, Trovato-Salinaro A, Mudo G (2000) Expression of Cx36 in mammalian neurons. Brain Res Rev 32: 72-85.

Connors BW, Long MA (2004) Electrical synapses in the mammalian brain. Annu Rev Neurosci 27:393-418.

Curti S, Hoge G, Nagy JI, Pereda AE (2012) Synergy between electrical coupling and membrane properties promotes strong synchronization of neurons of the mesencephalic trigeminal nucleus. J Neurosci 32:4341-4359.

Curtis DR, Lodge D, Headley PM (1979) Electrical interaction between motoneurons and afferent terminals in cat spinal cord. J Neurophysiol 3:635-41.

Deans MR, Gibson JR, Sellitto C, Connors BW, Paul DL (2001) Synchronous activity of inhibitory networks in neocortex requires electrical synapses containing connexin36. Neuron 31:477-485.

Decima EE, Goldberg LJ. (1969) Time course of excitability changes of primary afferent terminals as determined by motoneuron-presynaptic interaction. Brain Res 1:288-90.

Engberg I, Marshall KC (1979) Reversal potential for Ia excitatory post synaptic potentials in spinal cord motoneurons of cats. Neusocience 4:1583-1591.

Fleshman JW, Munson JB, Sypert GW (1981) Homonymous projection of individual group Ia-fibers to physiologically characterized medial gastrocnemius motoneurons in the cat. J Neurophysiol 6:1339-48.

Fulton BP, Miledi R, Takahashi T (1980) Electrical synapses between motoneurons in the spinal cord of the newborn rat. Proc R.Soc London Ser B 206:115-120.

Gogan P, Gueritaud JP, Horcholle-Bossavit G, Tyc-Dumont S (1977) Direct excitatory interactions between spinal motoneurones of the cat. J Physiol 272:755-767.

Hamzei-Sichani F, Davidson KGV, Yasumura T, Janssen WGM, Wearne SL, Hof PR, Traub RD, Gutierrez R, Ottersen OP, Rash JE (2012) Mixed electrical-chemical synapses in adult rat hippocampus are primarily glutamatergic and coupled by connexin-36. Front Neuroanat 6:1-26.

Hinckley CA, Ziskind-Conhaim L (2006) Electrical coupling between locomotor-related excitatory interneurons in the mammalian spinal cord. J Neurosci 26:8477-8483.

Hormuzdi SG, Filippov MA, Mitropoulon G, Monyer H, Bruzzone R (2004) Electrical synapses: a dynamic signaling system that shapes the activity of neuronal networks. Biochem Biophys Acta 1662:113-137.

Hughes DI, Mackie M, Nagy GG, Riddell JS, Maxwell DJ, Szabo G, Erdelyi F, Veress G, Szucs P, Antal M, Todd AJ (2005) P boutons in lamina IX of the rodent spinal cord express high levels of glutamic acid decarboxylase-65 and originate from cells in deep medial dorsal horn. Proc Natl Acad Sci 102:9038-9043.

Imai Y, Kusama T (1969) Distribution of the dorsal root fibers in the cat:. An experimental study with the Nauta Methods. Brain Res 13:338-359.

Ishizuka N, Mannen H, Hongo T, Sasaki S (1979) Trajectory of group Ia afferent fibers stained with horseradish peroxidase in the lumbosacral spinal cord of the cat: Three dimensional reconstruction from serial sections. J Comp Neurol 186:189-212.

Jankowska E, Edgley S (1993) Interactions between pathways controlling posture and gait at the level of spinal interneurones in the cat. Prog Brain Res 97:161-71.

Kiehn O, Kjaerulff O, Tresch MC, Harris-Warrick RM (2000) Contributions of intrinsic motor neuron properties to the production of rhythmic motor output in the mammalian spinal cord. Brain Res Bull 53:649-659.

Kiehn O, Tresch MC (2002) Gap junctions and motor behavior. Trends Neurosci 25:108-115.

Korn H, Sotelo C, Crepel F (1973) Electrotonic coupling between neurons in the lateral vestibular nucleus. Exp Brain Res 16:255-275.

Li X, Olson C, Lu S, Kamasawa N, Yasumura T, Rash JE, Nagy JI (2004) Neuronal connexin36 association with zonula occludens-1 protein (ZO-1) in mouse brain and interaction with the first PDZ domain of ZO-1. Eur J Neurosci 19:2132-46.

Logan SD, Pickering AE, Gibson IC, Nolan MF, Spanswick D (1996) Electrotonic coupling between rat sympathetic preganglionic neurones in vitro. J Physiol 495:491-502.

Matsumoto A, Arnold AP, Micevych PE (1989) Gap junctions between lateral spinal motoneurons in the rat. Brain Res 495:362-366.

Matsumoto A, Arnold AP, Zampighi G, Micevych PE (1988) Androgenic regulation of gap junctions between motoneurons in the rat spinal cord. J Neurosci 8:4177-4138.

Matsumoto A, Arai Y, Urano A, Hyodo S (1991) Androgen regulates gap junction mRNA expression in androgen-sensitive motoneurons in the rat spinal cord. Neurosci Lett 131:159-162.

Matsumoto A, Arai Y, Urano A, Hyodo S (1992) Effect of androgen on the expresssion of gap junction and beta-actin mRNAs in adult rat motoneurons. Neurosci Res 14:133-144.

Matthews MA, Willis WD, Williams V (1971) Dendrite bundles in lamina IX of cat spinal cord: a possible source for electrical interaction between motoneurons? Anat Rec 171:313-328.

Meier C, Dermietzel R (2006) Electrical synapses--gap junctions in the brain. Results Probl Cell Differ 43:99-128.

Mendell LM, Henneman E (1971) Terminals of single Ia fibers: location, density, and distribution within a pool of 300 homonymous motoneurons. J Neurophysiol 1:171-87.

Micevych PE, Abelson L (1991) Distribution of mRNAs coding for liver and heart gap junction proteins in the rat central nervous system. J Comp Neurol 305:96-118.

Motorina MV (1989) Electrotonic synapses in the spinal cord of Mammals. Neurosci Behav Physiol 19:72-78.

Motorina MV (1991) Structural organization of the synaptic connections of the spinal cord motor neurons of mammals. Struc Behav Physiol 25:273-289.

Nagy JI, Dudek FE, Rash JE (2004) Update on connexins and gap junctions in neurons and glia in in the mammalian central nervous system. Brain Res Rev 47:191-215.

Nagy JI (2012) Evidence for connexin36 localization at hippocampal mossy fiber terminals suggesting mixed chemical/electrical transmission by granule cells. Brain Res 1487:107-122.

Nagy JI, Bautista W, Blakley B, Rash JE (2013) Morphologically mixed chemical-electrical synapses in rodent vestibular nuclei as revealed by immunofluorescence detection of connexin36 and vesicular glutamate transporter-1. Neuroscience Submitted.

Nelson PG (1966) Interaction between spinal motorneurons of the cat. J Neurophysiol 29:275-287.

Oliveira ALR, Hydling F, Olsson E, Shi T, Edwards RH, Fujiyama F, Kaneko T, Hokfelt T, Cullheim T, Meister B (2003) Cellular localization of three vesicular glutamate transporter mRNAs and proteins in rat spinal cord and dorsal root ganglia. Synapse 50:117-129.

Personius KE, Balice-Gordon RJ (2000) Activity-dependent editing of neuromuscular synaptic connections. Brain Res Bull 53:513-522.

Personius KE, Balice-Gordon RJ (2001) Loss of correlated motor neuron activity during synaptic competition at developing neuromuscular synapses. Neuron 31:395-408.

Personius KE, Chang Q, Bittman K, Panzer J, Balice-Gordon RJ (2001) Gap junctional communication among motor and other neurons shapes patterns of neural activity and synaptic connectivity during development. Cell Commun Adhes 8:329-333.

Personius KE, Chang Q, Mentis GZ, O'Donovan MJ, Balice-Gordon RJ (2007) Reduced gap junctional coupling leads to uncorrelated motor neuron firing and precocious neuromuscular synapse elimination. Proc Natl Acad Sci 104:11808-11813.

Persson S, Boulland J-L, Aspling M, Larsson M, Fremeau RT Jr, Edwards RH, Storm-Mathisen J, Chaudhry FA, Broman J (2006) Distribution of vesicular glutamate transporters 1 and 2 in the rat spinal cord, with a note on the spinocervical tract. J Comp Neurol 497:683-701.

Rash JE, Dillman RK, Bilhartz BL, Duffy HS, Whalen LR, Yasumura T (1996) Mixed synapses discovered and mapped throughout mammalian spinal cord. Proc Natl Acad Sci 93:4235-4239.

Rash JE, Duffy HS, Dudek FE, Bilhartz BL, Whalen LR, Yasumura T (1997) Grid-mapped freeze-fracture analysis of gap junctions in gray and white matter of adult rat central nervous system, with evidence for a "panglial syncytium" that is not coupled to neurons. J Comp Neurol 388:265-292.

Rash JE, Yasumura T, Dudek FE (1998) Ultrastructure, histological, distribution, and freeze-fracture immunocytochemistry of gap junctions in rat brain and spinal cord. Cell Biol Int 22:731-749.

Rethelyi M (1968) The Golgi architecture of Clark's column. Acta Morphologica Acad Sci Hung 16:311-330.

Scheibel ME, Scheibel AB (1969) Terminal patterns in cat spinal cord. III. Primary afferent collaterals. Brain Res 13:417-443.

Rash JE, Staines WA, Yasumura T, Pate D, Hudson CS, Stelmack GL, Nagy J (2000) Immunogold evidence that neuronal gap junctions in adult rat brain and spinal cord contain connexin36 (Cx36) but not Cx32 or Cx43. Proc Natl Acad Sci 97:7573-7578.

Rash JE, Yasumura T, Dudek FE, Nagy JI (2001a) Cell-specific expression of connexins, and evidence for restricted gap junctional coupling between glial cells and between neurons. J Neurosci 21:1983-2000.

Rash JE, Yasumura T, Davidson K, Furman CS, Dudek FE, Nagy JI (2001b) Identification of cells expressing Cx43, Cx30, Cx26, Cx32 and Cx36 in gap junctions of rat brain and spinal cord. Cell Commun Adhes 8:315-320.

Rash JE, Olson CO, Davidson KGV, Yasumura T, Kamasawa N, Nagy JI (2007a) Identification of connexin36 in gap junctions between neurons in rodent locus coeruleus. Neuroscience 147:938-956.

Rash JE, Olson CO, Pouliot WA, Davidson KGV, Yasumura T, Furman CS, Royer S, Kamasawa N, Nagy JI, Dudek FE (2007b) Connexin36 vs connexin32, “miniature” neuronal gap junctions, and limited electrotonic coupling in rodent suprachiasmatic nucleus. Neuroscience 149:350-371.

Senkowski D, Schneider, TR, Foxe JJ, Engel K (2008) Crossmodal binding through neural coherence: implications for multisensory processing. Trends Neurosci 31:401-409.

Shapovalov AI (1980) Interneuronal synapses with electrical dual and chemical mode of transmission in vertebrates. Neuroscience 5:1113-1124.

Shrestha SS, Bannatyne BA, Jankowska E, Hammar I, Nilsson E, Maxwell DJ (2012) Excitatory inputs to four types of spinocerebellar tract neurons in the cat and rat thoraco-lumbar spinal cord. J Physiol 590:1737-1755.

Singer W (1999) Neuronal synchrony: a versatile code for the definition of relations? Neuron 24:49-65.

Smith CL (1983) The development and postnatal organization of primary afferent projections to the rat thoracic spinal cord. J Comp Neurol 220:29-43.

Söhl G, Degen J, Teubner B, Willecke K (1998) The murine gap junction gene connexin36 is highly expressed in mouse retina and regulated during brain development. FEBS Lett 428:27-31.

Söhl G, Maxeiner S, Willecke K (2005) Expression and functions of neuronal gap junctions. Nat Rev Neurosci 6:191-200.

Sotelo C, Palay SL (1970) The fine structure of the lateral vestibular nucleus in the rat. II. Synaptic organization. Brain Res 18:93-115.

Stepien AE, Tripodi M, Arber S (2010) Monosynaptic rabies virus reveals premotor network organization and synaptic specificity of cholinergic partition cells. Neuron 68:456-472.

Szentagothai J (1966) Pathways and subcortical relay mechanisms of visceral afferents. Acta Neuroveg 28:103-120.

Tresch MC, Kiehn O (2000) Motor coordination without action potentials in the mammalian spinal cord. Nature 3:593-599.

Tresch MC, Kiehn O (2002) Synchronization of motor neurons during locomotion in the neonatal rat: predictors and mechanisms. J Neurosci 22:9997-10008.

van der Want JJL, Gramsbergen A, Ijema-Paassen J, de Weerd H, Liem RSB (1998) Dendro-dendritic connections between motoneurons in the rat spinal cord: an electron microscopic investigation. Brain Res 779:342-345.

Vivar C, Traub RD, Gutierrez R (2012) Mixed electrical–chemical transmission between hippocampal mossy fibers and pyramidal cells. Eur J Neurosci 35:76–82.

Walton KD, Navarette R (1991) Postnatal changes in motoneurone electronic coupling studied in the in vitro rat lumbar spinal cord. J Physiol 433:283-305.

Watson C, Paxinos G, Kayalioglu G (2009) The spinal cord; A Christopher and Dana Reeve Foundation Text and Atlas. Academic Press, Amsterdam.

Werman R, Carlen PL (1976) Unusual behavior of the Ia EPSP in cat spinal motoneurons. Brain Res 112:395-401.

Whittington MA, Traub RD (2003) Interneuron diversity series: inhibitory interneurons and network oscillations in vitro. Trends Neurosci 26:676-682.

Wilson JM, Cowan AI, Brownstone RM (2007) Heterogeneous electrotonic coupling and synchronization of rhythmic bursting activity in mouse Hb9 Interneurons. J Neurophysiol 98:2370-2381.

Wu S-X, Koshimizu Y, Feng Y-P, Okamoto K, Fujiyama F, Hioki H, Li Y-Q, Kaneko T, Mizuno N (2004) Vesicular glutamate transporter immunoreactivity in the central and peripheral endings of muscle-spindle afferents. Brain Res 1011:247-251.

FIGURE LEGENDS

Fig. 1. Overview of widely distributed immunofluorescence labelling of Cx36 in transverse sections of adult mouse spinal cord, counterstained by blue fluorescence Nissl or labelled for peripherin. (A) Low magnification at an L5 level, with border between gray and white matter outlined by coarse dotted line, and the central canal outlined by fine dotted line. Boxed areas indicate regions examined in greater detail in subsequent Figures. (B-D) Higher magnifications of the boxed areas in (A), showing dense collections of Cx36-puncta in medial regions of lamina VII near the central canal (B, arrows), a moderate distribution of Cx36-puncta in intermediate lamina VII and VIII (C, arrows), and Cx36-puncta localized to somata and dendrites of motoneurons in lamina IX (D, arrows). (E) Lamina IX at a thoracic level, showing Cx36-puncta (arrows) distributed among motoneurons. (F) Lamina IX at L5 level from spinal cord of a Cx36 knockout mouse, showing peripherin-positive motoneurons (F1) and, in the same field, an absence of labelling for Cx36 (F2).

Fig. 2. Triple immunofluorescence labelling for Cx36, vglut1 and peripherin in lamina IX at the L4 level in adult rat spinal cord. (A1-A4) Images showing the same field, with overlay of labelling for peripherin and vglut1 (A1), peripherin and Cx36 (A2), Cx36 and vglut1 (A3), and for all three proteins (A4). Red/green overlay appears as yellow, and red/green/blue overlay appears as white. Peripherin-positive motoneurons receiving a moderate innervation by vglut1-containing terminals (A1, arrows) display Cx36-puncta localized on their somata or dendrites (A2, arrows). Most though not all of these Cx36-puncta are co-localized with vglut1-positive terminals (A3 and A4, arrows). (B1-B3) Higher magnification confocal triple immunofluorescence showing immunolabels (arrows) for vglut1 (B1) and Cx36 (B2) associated with initial dendrites of peripherin-positive motoneurons. A proportion of Cx36-puncta are seen co-localized with vglut1-positive terminals, as seen in overlay (B3, arrows), but not all of these terminals harbor Cx36-puncta. (C) Individual vglut1-positive boutons or fibers appearing to form en passant terminal contacts display several Cx36-puncta; also shown in inset in (B3).

Fig. 3. Confocal double immunofluorescence labelling of Cx36 with vglut1 or vglut2 in adult rat lumbar spinal cord. (A,B) Images show the same field in lamina VI (A1,A2) and in lamina VII (B1,B2), with labelling for Cx36 alone (A1,B1) and after overlay with labelling for vglut1 (A2,B2). Arrays of Cx36-puncta are seen streaming across mid regions of these lamina (A1,B1, arrows). Labelling for vglut1 follows similar trajectories as the Cx36-puncta, and nearly all Cx36-puncta are either co-localized with, or lie close to, vglut1-terminals (A2,B2, arrows). (C1-C3) Images show the same field of a single medium sized neuron in lamina VII (not counterstained, but marked with asterisk). The neuron is contacted by vglut1-terminals (C1, arrows) displaying clusters of Cx36-puncta (C2 and C3, arrows). (D1-D3) Images of the same field in lamina VII, showing label for vglut1 (D1) and Cx36 (D2) on a large initial dendrite (not counterstained, but marked with asterisks). Terminals labelled for vglut1 are viewed on edge flattened against the dendrite (D3, arrowheads) or *en* face (D3, arrow). In edge views, Cx36-puncta are localized to the side of the terminal contacting the dendrite, and straddle sites of terminal/dendrite apposition.. (E,F) Double immunofluorescence labelling of Cx36 (red) and vglut2 (yellow) in lamina IX at low (E) and higher confocal magnification (F), showing clusters of Cx36-puncta (F1) that in the same field lack association with vglut2-positive terminals (F2).

Fig. 4. Immunofluorescence localization of Cx36 in relation to vglut1-terminals in medial lamina VII at a thoracic level in adult rat spinal cord. (A) Low magnification transverse section, showing vglut1-positive fibers and terminals (outlined by boxed area) lateral to the central canal (cc, arrow). (B) Magnification of a similar area as the boxed region in (A), showing a single neuron decorated with Cx36-puncta (B1, arrow) and, in the same field, a confluence of vglut1-positive terminals (arrowheads) terminating on that neuron (B2, arrow). (C) Photomontage of a field 2 mm in length, showing immunolabelling for Cx36 in a horizontal section taken at a dorso-ventral plane indicated by the dotted line in (A), with the central canal lying at midline (dashed line). Cx36-puncta are sufficiently concentrated on neurons to reveal intermittent clusters of Cx36 laden cells (arrows) flanking the central canal. (D,E) Higher magnifications of one of these clusters in a section counterstained with blue fluorescence Nissl, showing Cx36-puncta on some neurons (D, arrows) intermingled with those lacking Cx36-puncta (D, arrowheads). A confocal image shows the punctate appearance of labelling associated with and delineating two neurons

(E, arrows). (F1-F4) Horizontal section showing the same field double-labelled and blue Nissl counterstained, revealing that clusters of these neurons (F1, arrows), with their associated Cx36-puncta (F2, arrows), are all targeted by vglut1-terminals (F3, arrows), producing patches of labelling for vglut1 that demarcate locations of the clusters (F4, arrows).

Fig. 5. Comparison of immunofluorescence labelling for vglut1 and vglut2 in relation to Cx36-puncta on neurons in medial lamina VII in adult rat spinal cord. (A1-A2) The same field of a double-labelled transverse section at L6, showing immunofluorescence for vglut2 (yellow) nearly throughout spinal cord gray matter, except in a restricted region of medial lamina VII devoid of vglut2-terminals (A1, arrows), which corresponds to an area rich in vglut1-terminals (A2, arrows). (B1-B3) Horizontal thoracic section at the level of the central canal (cc), showing more broadly the correspondence between patches of dense vglut1-terminals (B1, arrows) and voids in labelling for vglut2 (B, arrows), as seen in overlay (B3, arrows). (C-E) Transverse sections at mid lumbar levels, showing two voids in labelling for vglut2 in medial lamina VII: one adjacent to the central canal (C, boxed area), containing neurons densely decorated with Cx36-puncta (D, arrows; magnification of box in C); and the other corresponding to the nucleus of Clarke (E, arrows). (F-H) Images showing nucleus of Clarke outlined by dense labelling for vglut1 (F1) and containing a moderate distribution of scattered Cx36-puncta (F2) that display co-localization with vglut1, as shown by examples in two regions of Clark's nucleus (G,H). (I) Image of adult rat spinal cord at C8, showing dense labelling for vglut1 in the central cervical nucleus (CeCv) (boxed area). (J) Higher magnification of CeCv showing neurons decorated with Cx36-puncta (J1, arrow) display co-localization with vglut1-terminals (J2, arrow), similar to those seen in medial lamina VII at other spinal levels.

Fig. 6. Confocal immunofluorescence of vglut1 and Cx36 in medial lamina VII of adult rat and mouse lumbar spinal cord. (A) Image from rat cord, showing a vglut1-positive patch of terminals outlining a neuron decorated with Cx36-puncta (boxed area). (B-D) Higher magnification immunofluorescence images from medial lamina VII of mouse cord, showing a dense meshwork of peripherin-positive primary afferent fibers (blue) within a vglut1-positive patch, and

individual neurons (marked by asterisks) with Cx36-puncta concentrated along their initial dendritic segments (B, arrows), where many are associated with vglut1-terminals (C, arrows), or with Cx36-puncta associated with vglut1-terminals distributed around the entire neuronal somata (D). (E) Higher magnification of the neuron (marked by asterisk) in the boxed area in (A), showing Cx36-puncta co-distributed with vglut1-terminals contacting the neuronal somata and several initial dendrites (arrows). The inset shows the same field as in (E), with labelling for Cx36 alone delineating the entire neuronal somata. (F) Magnification showing multiple Cx36-puncta localized to most vglut1-terminals (arrows). (G) Double immunofluorescence of Cx36 and vglut2 in a field similar to that in (A), showing lack of Cx36-puncta co-localization with vglut2-positive terminals.

Fig. 7. Triple immunofluorescence labelling of Cx36, vglut1 and peripherin in the trigeminal motor nucleus (Mo5) of adult rat and mouse brainstem. (A,B) Low magnification images of the same field of the Mo5 in rat (A1-A3) and in mouse (B1,B2), showing peripherin-positive motoneurons (A1, arrow), dense labelling for vglut1 (A2,B1, arrows) and Cx36 (A3,B2, arrows) throughout the nucleus, and sparse labelling for these proteins outside the nucleus. (C) Higher magnification showing the distribution of labelling for Cx36 (C1) and vglut1 (C2) among peripherin-positive motoneurons and, in the same field, co-localization of labelling for Cx36 with vglut1-terminals (C3, arrows). (D,E) Higher magnification confocal images, where the fields in D1 and D2 are the same and those in E1 and E2 are the same. Images show punctate labelling of Cx36, distribution of Cx36-puncta around a motoneuronal soma (D1, arrow), association of Cx36-puncta with initial dendrite segments (E1, arrows) as well as more distally along dendrites (F1, arrow), and overlap of the vast majority of Cx36-puncta with vglut1-terminals (D2,E2,F2, arrows). Inset in E2 shows multiple Cx36-puncta localized to individual vglut1-terminals.

Fig. 8. Association of Cx36 with vglut1-containing axon terminals of primary afferent origin in lamina IX and VII of adult rat. (A,B) Triple immunofluorescence labelling for vglut1, peripherin and Cx36 in lamina IX after unilateral dorsal rhizotomy at the L1-L4 levels. Images at L3 on the

intact side (A1-A3, same field) and rhizotomy side (B1-B3, same field) show vglut1/peripherin overlay (A1,B1), Cx36 alone (A2,B2) and overlay of labelling for all three proteins (A3,B3). The intact side shows normal labelling of vglut1 (A1) and Cx36 (A2). The rhizotomy side shows reduced labelling of vglut1 (B1) and Cx36 (B2). Overlay shows vglut1/Cx36 co-localization at some of the remaining vglut1-terminals on the rhizotomy side (B3). (C,D) Labelling for vglut1 and peripherin under optimum fixation conditions for vglut1 (4% formaldehyde), showing vglut1 on the intact side (C) and extensive loss of vglut1-terminals on the rhizotomy side (D). (E,F) Quantitation of vglut1-terminals and Cx36-puncta in fields of lamina IX on the intact and rhizotomy side. Values are presented as the means (+ s.e.m.) from multiple fields in four animals, with percentage reductions as indicated. (G) Low magnification blue fluorescence Nissl counterstained transverse section showing areas adjacent to the central canal after unilateral dorsal rhizotomy. Dense labelling for vglut1 is seen on the intact side (boxed region at left), and depletion of labelling is seen on the rhizotomy side (boxed region at right). (H,I) Immunolabelling for Cx36 in the boxed areas shown in (G), with the left box magnified in (H) showing clusters of Cx36-puncta on the intact side, and the right box magnified in (I) showing only a few puncta remaining on the rhizotomy side.

Fig. 9. Confocal triple immunofluorescence labelling for Cx36 (red), vglut1 (blue) and GAD65 (green), showing localization of GAD65-positive P boutons on vglut1-terminals displaying Cx36-puncta in lamina IX and VII of adult rat. Terminals labelled for vglut1 are pseudo colored blue to avoid obscuring GAD65 P boutons and Cx36-puncta. GAD65-positive P boutons are seen associated with what appear to be en passant type vglut1-terminals (A) or clusters of these terminals (B), with often multiple P boutons and Cx36-puncta associated with individual vglut1-terminals (C). (D-G) Images from lamina VII showing a single neuron (D, outlined by dotted line), and two tangentially cut dendrites (E, asterisks). In each image, Cx36-puncta are seen co-localized with large vglut1-terminals that contact neuronal somata and dendrites, and that are themselves contacted by GAD65-positive P boutons. (F,G) Boxed areas in (D) and (E) (magnified in F and G, respectively), showing Cx36-puncta (F, arrow) localized along portions of vglut1-terminals nearest the neuronal soma (F, dotted line), and GAD65-positive P boutons

(F, arrowheads) at more distal portions of the vglut1-terminals. Cx36-puncta are occasionally in close proximity to GAD65-positive P boutons (G, arrow).

Fig. 10. Developmental profile of Cx36 association with vglut1-terminals in lamina IX and VII in rat lumbar spinal cord. (A,B) Histograms show the average of total Cx36-puncta counted in fields of lamina IX and VII from four animals are each age indicated (A1,B1), the total Cx36-puncta co-localized with vglut1-terminals averaged from the four animals (A2,B2), and the average percentage of Cx36/vglut1 co-localization (A3,B3). The values at different ages in (A1,B1) reflect differences in the number of fields/per animal taken for counts and/or heterogeneities in numbers of Cx36-puncta in fields chosen for counts, rather than absolute differences in density of Cx36-puncta at the ages examined. In lamina XI, the average percentage of Cx36-puncta/vglut1 co-localization was 0.4% at PD10, 2.7% at PD15, 5.7% at PD20, 25% at PD25, 36% at PD30 and 49% in adult. In lamina VII, the values were 0.3% at PD10, 0.9% at PD15, 4% at PD20, 33% at PD25, 34% at PD30 and 41% in adult. Values are means + s.e.m. (n = 4).

Supplementary Information

Supplementary Figure legends

Supplementary Fig. 1. Triple immunofluorescence labelling of Cx36, vglut1 and peripherin at a lower cervical level (C8) in adult rat spinal cord. (A) Low magnification showing the distribution of vglut1-terminals in spinal cord gray matter (outlined by dotted line), and the heterogeneous density of these terminals among groups of motor nuclei in lamina IX (arrows, high levels; arrowheads, low levels). (B1) Higher magnification of boxed area in (A), showing a moderate density of vglut1-terminals among a dorsally located group of motoneurons (arrows), and few vglut1-terminals in a ventrally located motoneuron group (arrowheads). Cx36-puncta in the

upper group of motoneurons show extensive co-localization with vglut1-terminals (shown in inset). (B2) The same field as in (B1), with labelling of Cx36 alone, showing a high density of Cx36-puncta in the upper motoneuronal group (arrows) and sparse Cx36-puncta in the lower group (arrowheads). (C) Magnification of the boxed area in (B2), showing only a few Cx36-puncta (arrows) associated with peripherin-positive motoneurons in the lower group and their lack of co-localization with vglut1.

Supplementary Fig. 2. Movie file of the image in Fig. 6E (z-stack of 9 μm), showing maintained association of Cx36-puncta (red) with vglut-1-positive nerve terminals (green) at all angles of rotation shown. Immunolabelled terminals are located on the initial dendrites and somata of a non-counterstained neurons (marked by asterisks) located in the medial area of lamina VII near the central canal.

Figure 1

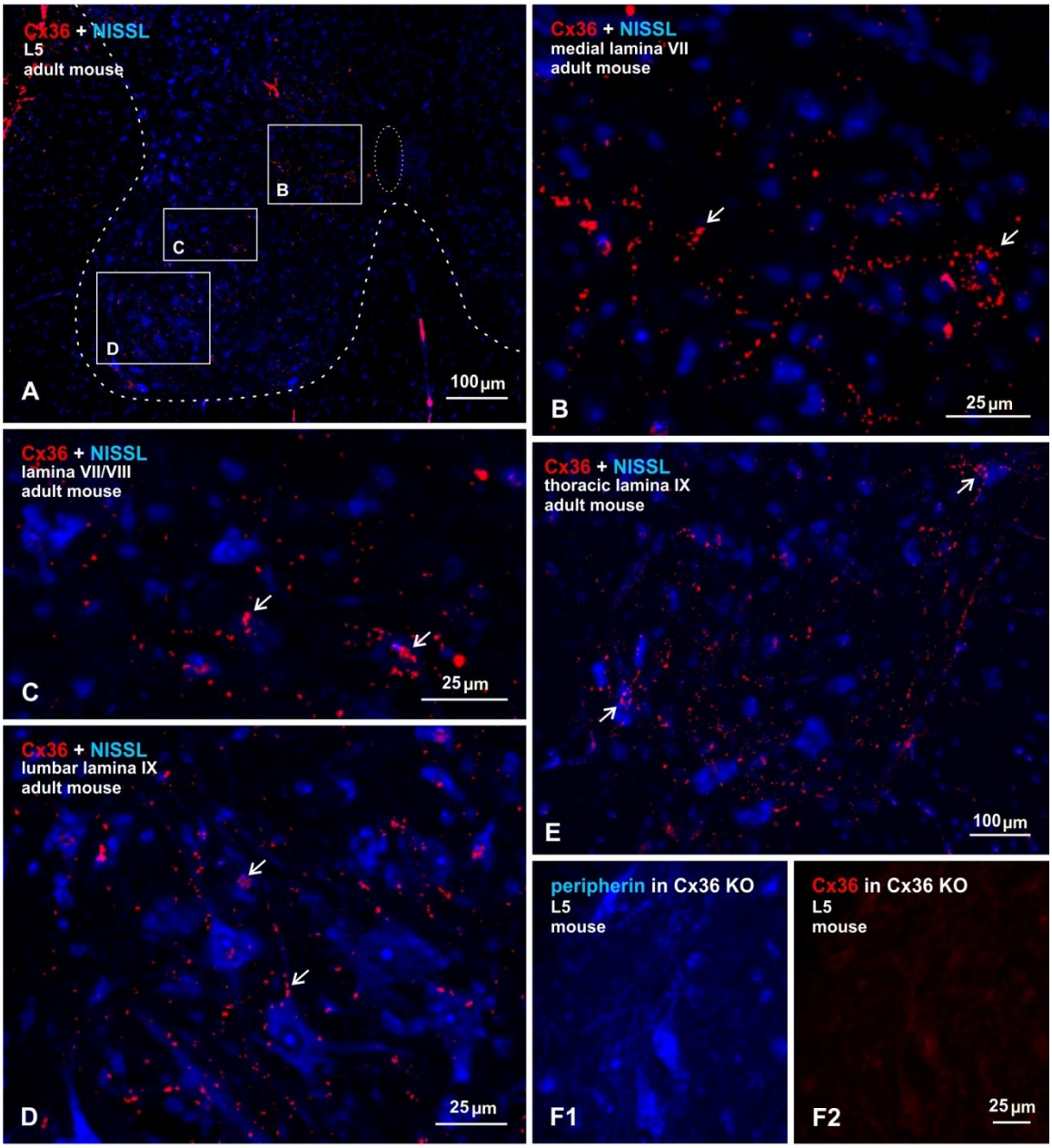
Cx36 + NISSL
L5
adult mouse
B
C
D
A
100 µm
Cx36 + NISSL
medial lamina VII
adult mouse
B
25 µm
Cx36 + NISSL
lamina VII/VIII
adult mouse
C
25 µm
Cx36 + NISSL
thoracic lamina IX
adult mouse
E
100 µm
Cx36 + NISSL
lumbar lamina IX
adult mouse
D
25 µm
peripherin in Cx36 KO
L5
mouse
F1
Cx36 in Cx36 KO
L5
mouse
F2
25 µm

Figure 2

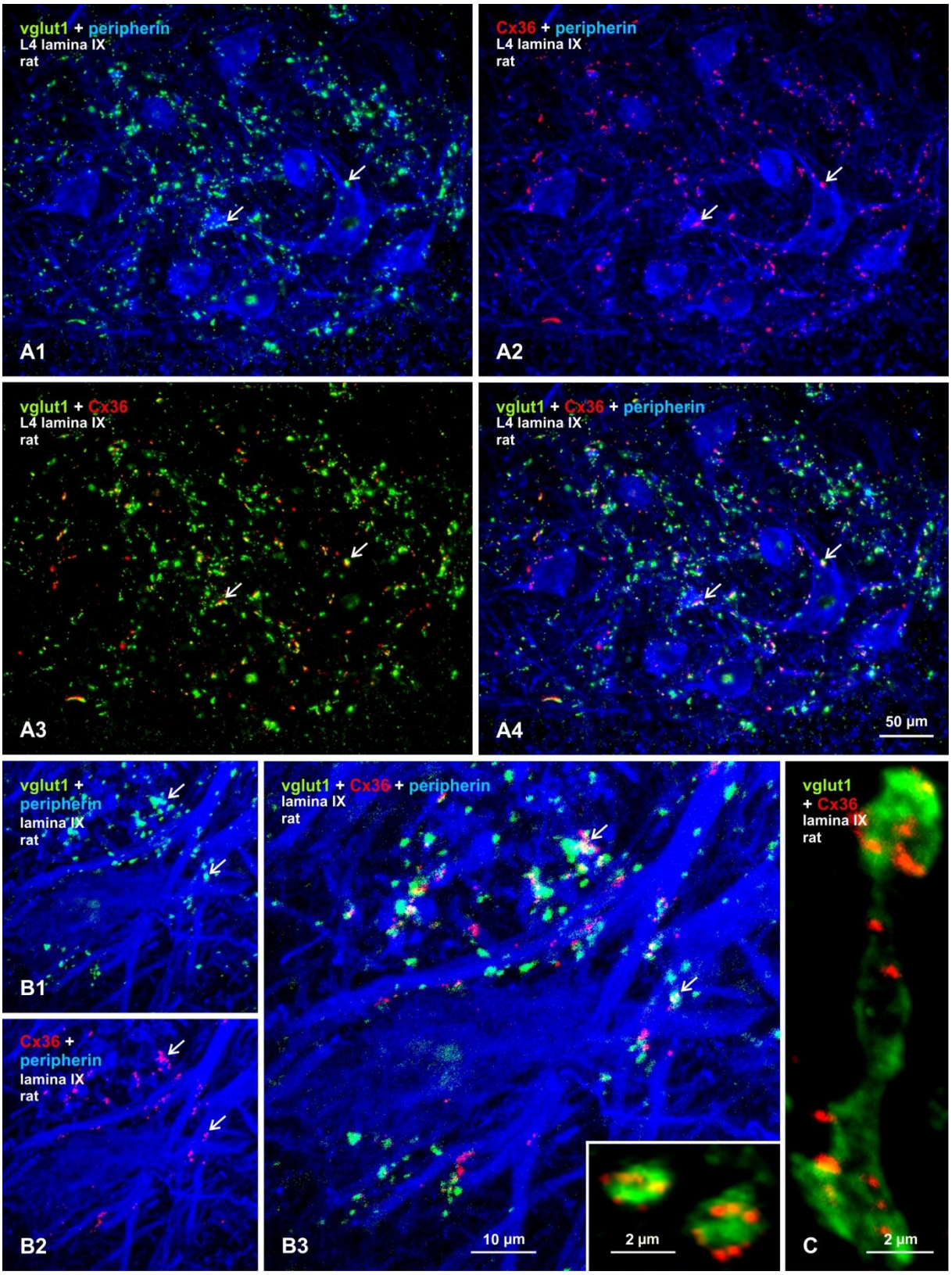
vglut1 + peripherin
L4 lamina IX
rat
A1
Cx36 + peripherin
L4 lamina IX
rat
A2
vglut1 + Cx36
L4 lamina IX
rat
A3
vglut1 + Cx36 + peripherin
L4 lamina IX
rat
A4
50 µm
vglut1 +
peripherin
lamina IX
rat
B1
Cx36 +
peripherin
lamina IX
rat
B2
vglut1 + Cx36 + peripherin
lamina IX
rat
B3
10 µm
2 µm
vglut1
+ Cx36
lamina IX
rat
C
2 µm

Figure 3

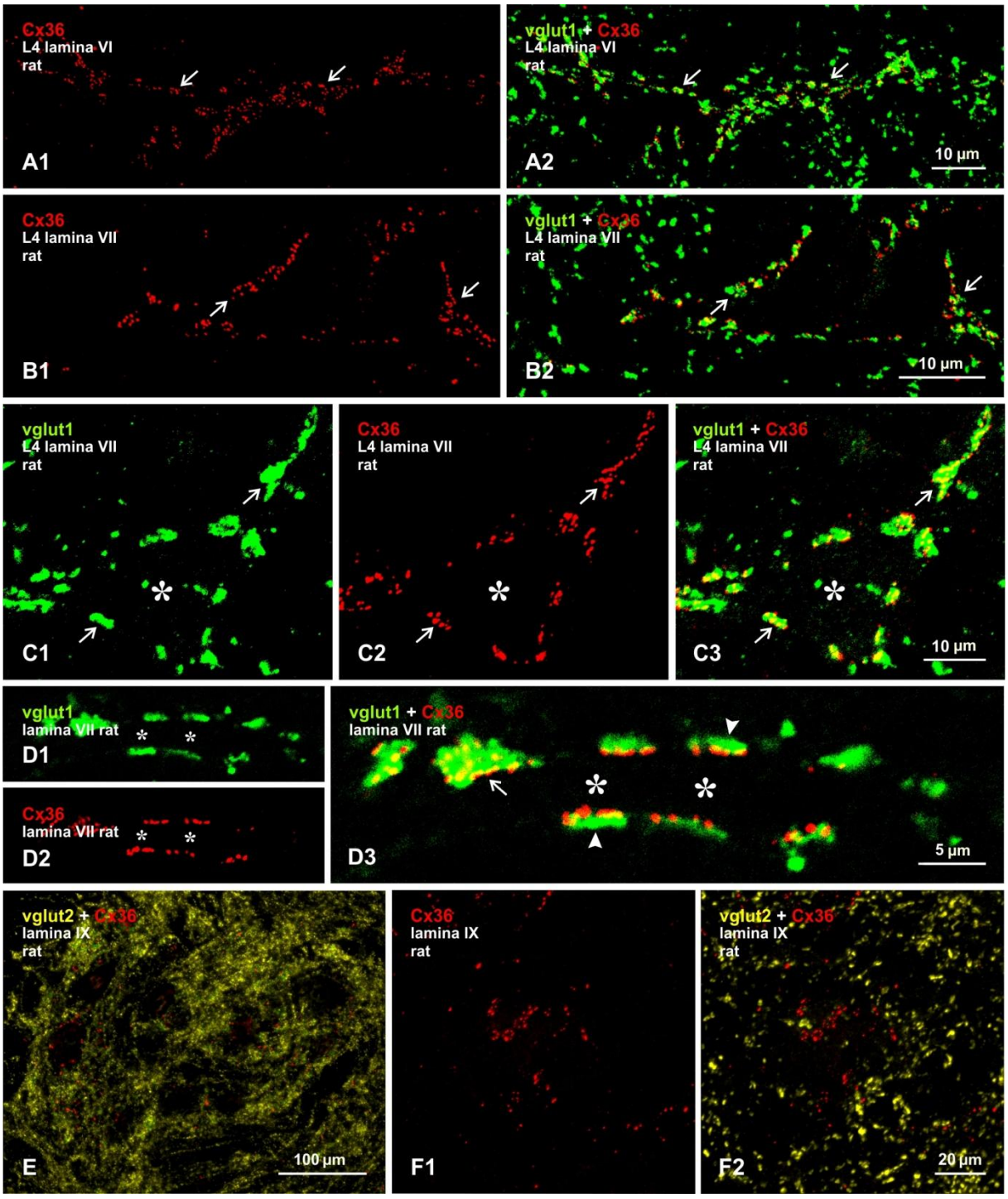
Cx36
L4 lamina VI
rat
A1
vglut1 + Cx36
L4 lamina VI
rat
A2
10 µm
Cx36
L4 lamina VII
rat
B1
vglut1 + Cx36
L4 lamina VII
rat
B2
10 µm
vglut1
L4 lamina VII
rat
C1
Cx36
L4 lamina VII
rat
C2
vglut1 + Cx36
L4 lamina VII
rat
C3
10 µm
vglut1
lamina VII rat
D1
Cx36
lamina VII rat
D2
vglut1 + Cx36
lamina VII rat
D3
5 µm
vglut2 + Cx36
lamina IX
rat
E
100 µm
Cx36
lamina IX
rat
F1
vglut2 + Cx36
lamina IX
rat
F2
20 µm

Figure 4

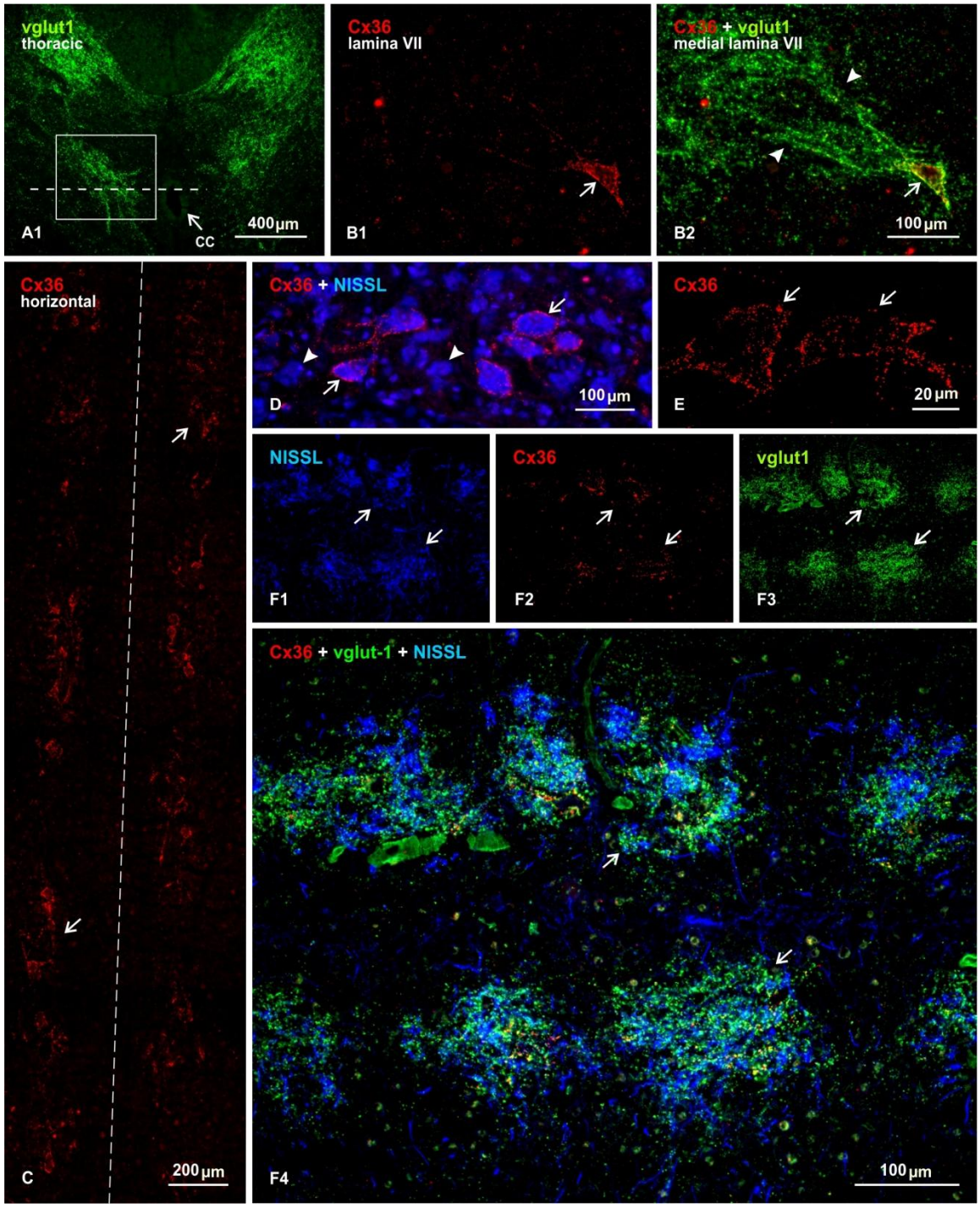
vglut1
thoracic
A1
CC
400 µm
Cx36
lamina VII
B1
Cx36 + vglut1
medial lamina VII
B2
100 µm
Cx36
horizontal
C
200 µm
Cx36 + NISSL
D
100 µm
Cx36
E
20 µm
NISSL
F1
Cx36
F2
vglut1
F3
Cx36 + vglut-1 + NISSL
F4
100 µm

Figure 5

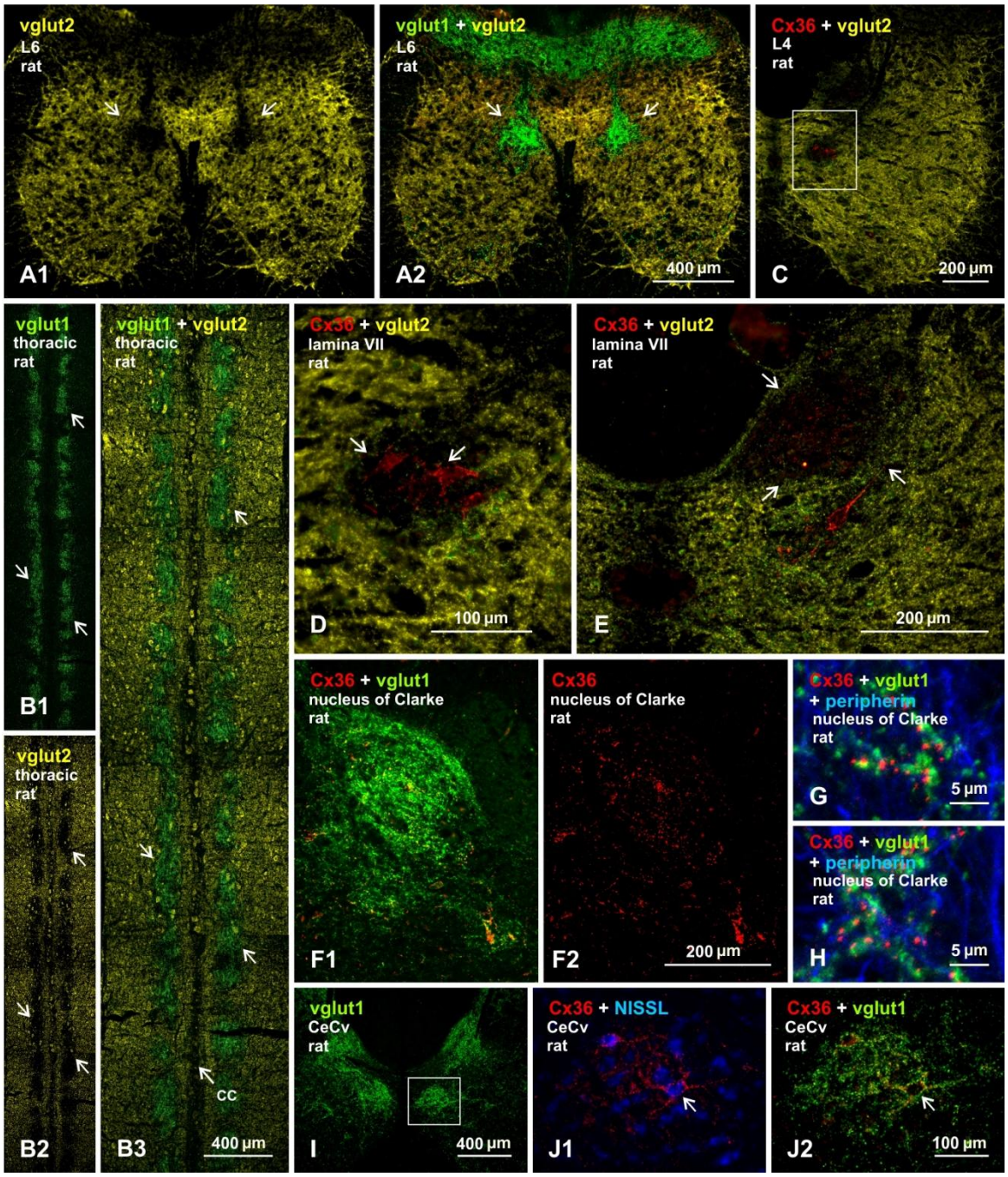
vglut2
L6
rat
A1
vglut1 + vglut2
L6
rat
A2
400 µm
Cx36 + vglut2
L4
rat
C
200 µm
vglut1
thoracic
rat
B1
vglut1 + vglut2
thoracic
rat
vglut2
thoracic
rat
B2
cc
B3
400 µm
Cx36 + vglut2
lamina VII
rat
D
100 µm
Cx36 + vglut2
lamina VII
rat
E
200 µm
Cx36 + vglut1
nucleus of Clarke
rat
F1
Cx36
nucleus of Clarke
rat
200 µm
F2
Cx36 + vglut1
+ peripherin
nucleus of Clarke
rat
G
5 µm
Cx36 + vglut1
+ peripherin
nucleus of Clarke
rat
H
5 µm
vglut1
CeCv
rat
400 µm
I
Cx36 + NISSL
CeCv
rat
J1
Cx36 + vglut1
CeCv
rat
100 µm
J2

Figure 6

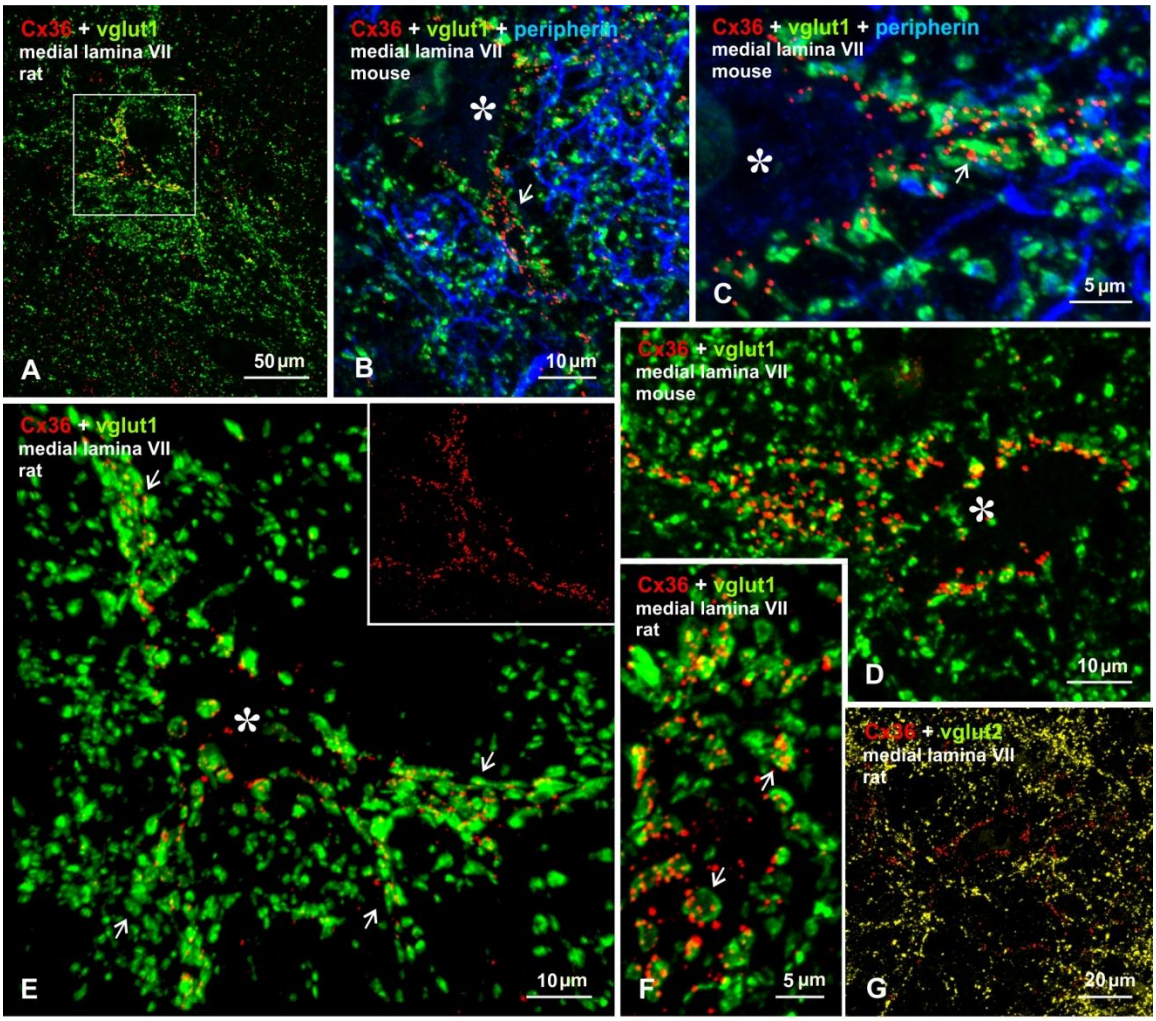
Cx36 + vglut1
medial lamina VII
rat
50 µm
A
Cx36 + vglut1 + peripherin
medial lamina VII
mouse
10 µm
B
Cx36 + vglut1 + peripherin
medial lamina VII
mouse
5 µm
C
Cx36 + vglut1
medial lamina VII
mouse
10 µm
D
Cx36 + vglut1
medial lamina VII
rat
10 µm
E
Cx36 + vglut1
medial lamina VII
rat
5 µm
F
Cx36 + vglut2
medial lamina VII
rat
20 µm
G

Figure 7

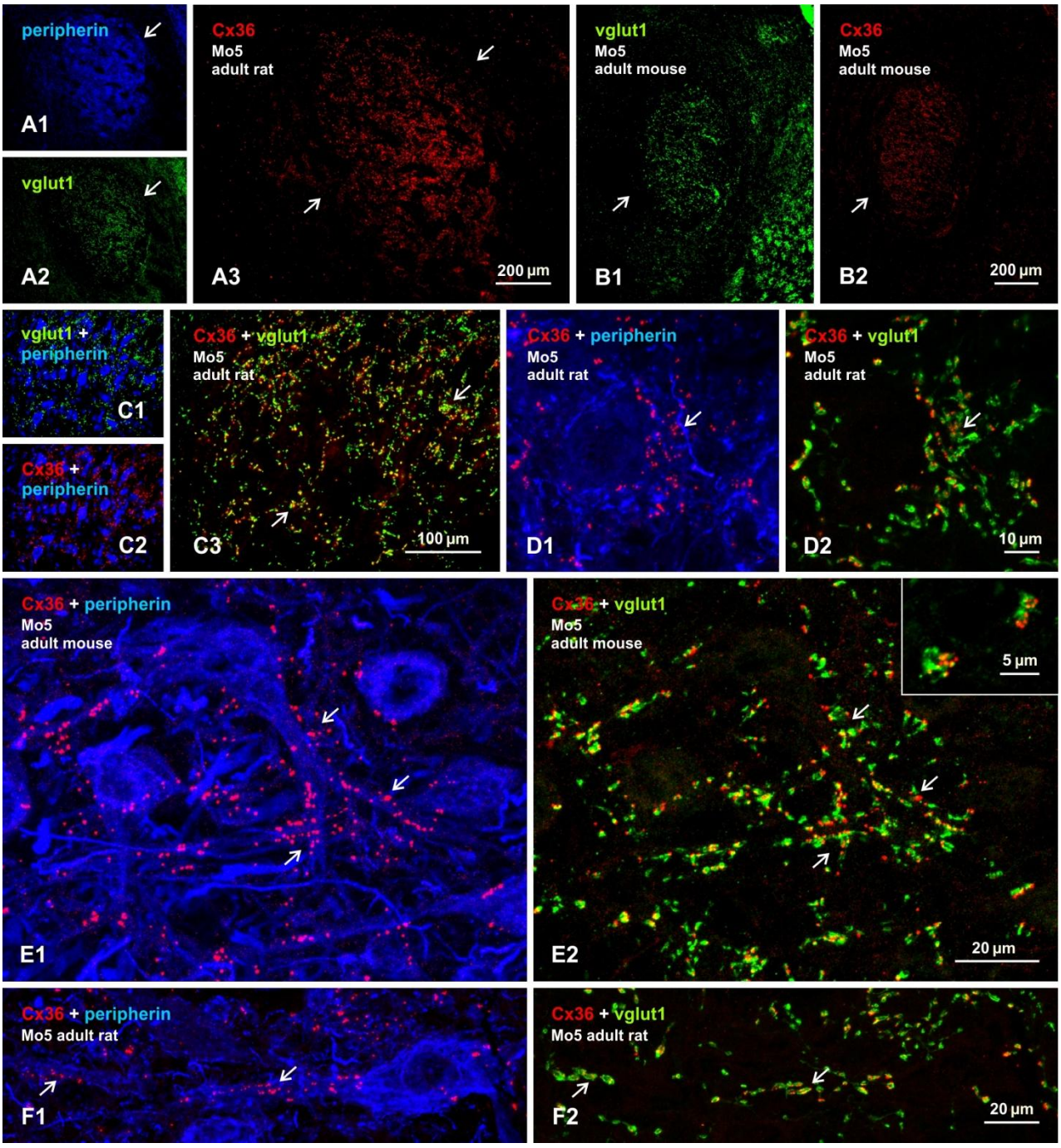
peripherin
A1
vglut1
A2
Cx36
Mo5
adult rat
A3
200 µm
vglut1
Mo5
adult mouse
B1
Cx36
Mo5
adult mouse
B2
200 µm
vglut1 +
peripherin
C1
Cx36 +
peripherin
C2
Cx36 + vglut1
Mo5
adult rat
C3
100 µm
Cx36 + peripherin
Mo5
adult rat
D1
Cx36 + vglut1
Mo5
adult rat
D2
10 µm
Cx36 + peripherin
Mo5
adult mouse
E1
Cx36 + vglut1
Mo5
adult mouse
5 µm
E2
20 µm
Cx36 + peripherin
Mo5 adult rat
F1
Cx36 + vglut1
Mo5 adult rat
F2
20 µm

Figure 8

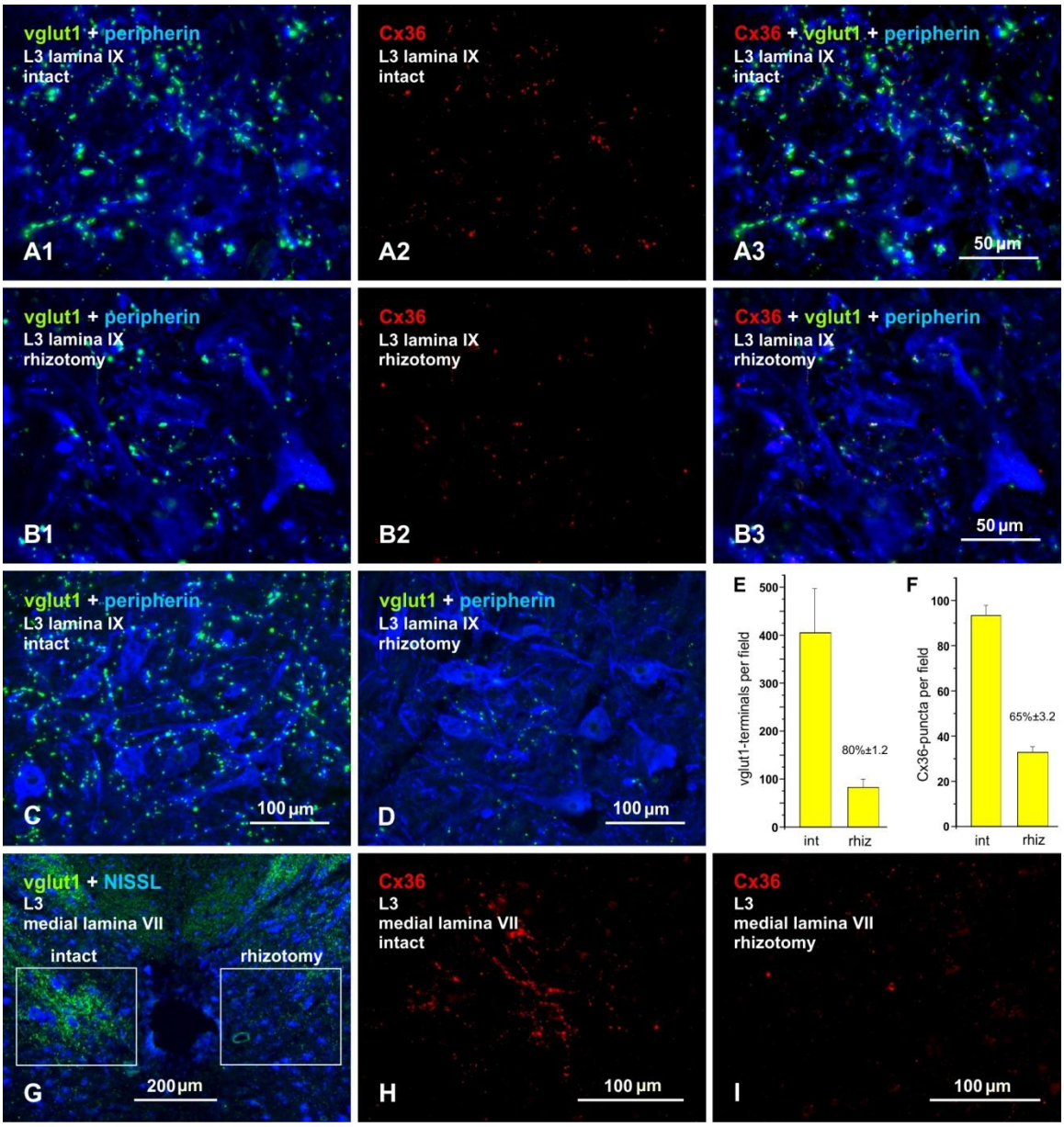
vglut1 + peripherin
L3 lamina IX
intact
A1
Cx36
L3 lamina IX
intact
A2
Cx36 + vglut1 + peripherin
L3 lamina IX
intact
50 µm
A3
vglut1 + peripherin
L3 lamina IX
rhizotomy
B1
Cx36
L3 lamina IX
rhizotomy
B2
Cx36 + vglut1 + peripherin
L3 lamina IX
rhizotomy
50 µm
B3
vglut1 + peripherin
L3 lamina IX
intact
100 µm
C
vglut1 + peripherin
L3 lamina IX
rhizotomy
100 µm
D
E
vglut1-terminals per field
500
400
300
200
100
0
80%±1.2
int
rhiz
F
Cx36-puncta per field
100
80
60
40
20
0
65%±3.2
int
rhiz
vglut1 + NISSL
L3
medial lamina VII
intact
rhizotomy
200 µm
G
Cx36
L3
medial lamina VII
intact
100 µm
H
Cx36
L3
medial lamina VII
rhizotomy
100 µm
I

Figure 9

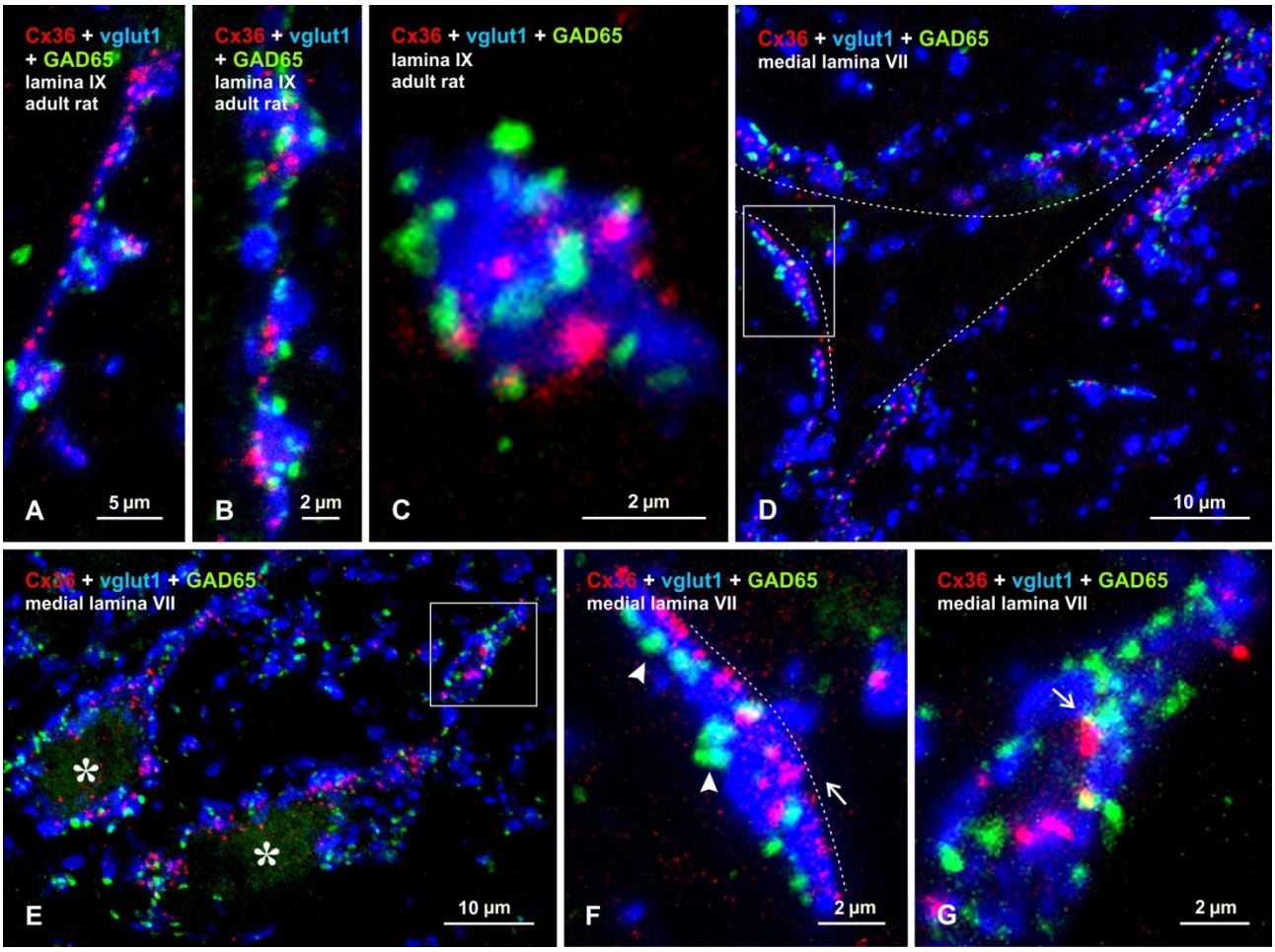
Cx36 + vglut1 + GAD65
lamina IX
adult rat
A
5 µm
Cx36 + vglut1 + GAD65
lamina IX
adult rat
B
2 µm
Cx36 + vglut1 + GAD65
lamina IX
adult rat
C
2 µm
Cx36 + vglut1 + GAD65
medial lamina VII
D
10 µm
Cx36 + vglut1 + GAD65
medial lamina VII
E
10 µm
Cx36 + vglut1 + GAD65
medial lamina VII
F
2 µm
Cx36 + vglut1 + GAD65
medial lamina VII
G
2 µm

Figure 10

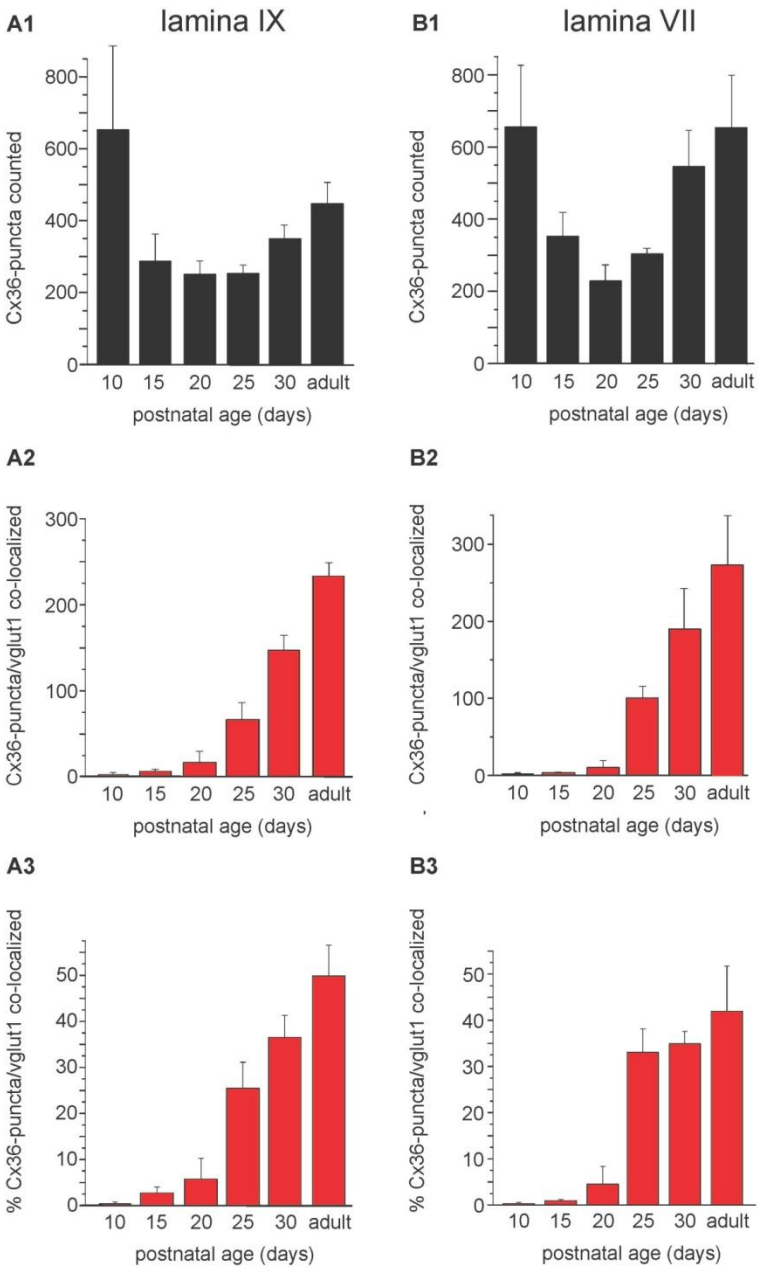
A1
lamina IX
Cx36-puncta counted
postnatal age (days)
B1
lamina VII
Cx36-puncta counted
postnatal age (days)
A2
Cx36-puncta/vglut1 co-localized
postnatal age (days)
B2
Cx36-puncta/vglut1 co-localized
postnatal age (days)
A3
% Cx36-puncta/vglut1 co-localized
postnatal age (days)
B3
% Cx36-puncta/vglut1 co-localized
postnatal age (days)

Fig S1

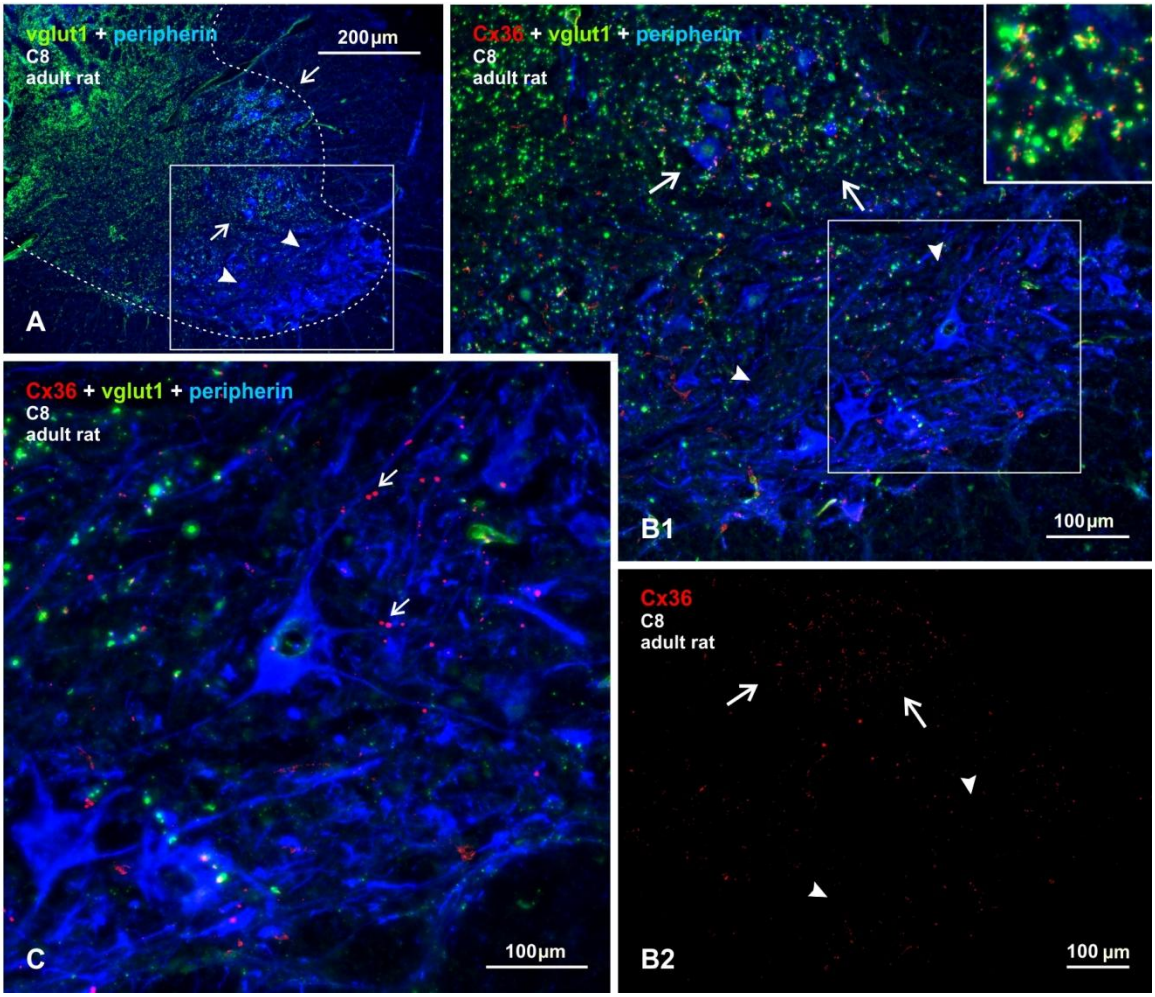
vglut1 + peripherin
C8
adult rat
200 µm
A
Cx36 + vglut1 + peripherin
C8
adult rat
B1
100 µm
Cx36 + vglut1 + peripherin
C8
adult rat
C
100µm
Cx36
C8
adult rat
B2
100 µm

Section 4. Connexin36 in gap junctions forming electrical synapses between sexually dimorphic motor nuclei in spinal cord of rat and mouse.

4.1. Hypothesis: Sexual dimorphic motoneurones express Cx36 containing gap junctions in the adult rodent.

Experimental Approach: Male and female Sprague–Dawley rats and C57 mice were used. Spinal cord sections were processed for imunohistochemistry using antibodies against Cx36, the nerve terminal marker Vglut1 and peripherin as motoneurone marker. Observations were made on animals of P9, 15, 50 postnatal days. Cx36 BAC EGFP mice were used to examine Cx36 GFP expression in motoneurones. Spinal cord sections were processed for immunolabeling of Vglut1, Cx36 and peripherin. Confocal microscopy confirmed Cx36 detection on motoneurones and counts were made of the number of motoneurones with Cx36 puncta.

4.2. Conclusions: Our results demonstrate for the first time that Cx36 is contained in gap junctions forming electrical synapses between adult sacral sexual dimorphic motoneurones, and sphincter motoneurones. Our results strongly suggest that neuronal gap junctions play a critical role in maintaining tonic activation of sphincter motoneurones during bladder continence and urination as well as for defecation. The same finding could extend to motoneurones innervating pelvic floor muscles involve in ejaculation reflex in the male. Extensive confocal analyses at different ages allowed us to observe that Cx36 have a different pattern of distribution according to the ages being widely dispersed at postnatal day 9 and more restricted to the soma-somatic appositions after postnatal day 15 and the adult. Cx36 protein expression found in mouse motoneurones was confirmed by detecting the GFP positive motoneurones in Cx36 EGFP mice, indicating that motoneurones contain Cx36 gene. Vglut-1 expression in these motoneurones was scarce and therefore did not present any co-localization. Overall our results show the evidence that Cx36 expression remains in the adulthood, and that different motor pools, depending on the function of the muscle innervated, require maintenance of electrical synapses in order to generate a motor output.

Associate Editor: John Garthwaite

Section: Synaptic Mechanisms;

Intercellular Communication & Synaptic Plasticity

Connexin36 in gap junctions forming electrical synapses between sexually dimorphic motor nuclei in spinal cord of rat and mouse

W. Bautista, D. A. McCrea, J. I. Nagy*

Department of Physiology, Faculty of Medicine, University of Manitoba, Winnipeg, Canada

Running title: Cx36 in dimorphic motor nuclei

Keywords: gap junctions, motoneurons EGFP-Cx36 reporter, immunofluorescence

No. of pages:

No. of figures:

No. of supplementary figures:

No. of words: Abstract, ; Introduction, ; Discussion,

**Address for correspondence:*

James I. Nagy

Department of Physiology

Faculty of Medicine

University of Manitoba

745 Bannatyne Ave, Winnipeg, Manitoba, Canada R3E 0J9

Email: nagyji@ms.umanitoba.ca

Tel. (204) 789-3767, Fax (204) 789-3934

Abstract

Pools of motoneurons in the lower lumbar spinal cord innervate sexually dimorphic perineal musculature and are themselves sexually dimorphic, displaying striking differences in numbers and size in male *vs.* female rodents. In two of these pools, the dorsomedial nucleus (DMN) and the dorsolateral nucleus (DLN), dimorphic motoneurons are intermixed with non-dimorphic neurons innervating anal and external urethral sphincter (EUS) muscles. In addition to their distinguishing features vis-a-vis gender, motoneurons in these nuclei were reported to be linked by gap junctions in an androgen-sensitive fashion in adult male rats. Here, we examined immunofluorescence labelling for the gap junction-forming protein connexin36 (Cx36) in developing and adult male and female rodents. In male rat and mouse, dense punctate labelling for Cx36 was detected at appositions between motoneurons in the DMN and DLN, while labelling was sparse in the dimorphic retrodorsolateral and ventral nuclei. In female rats, labelling of Cx36 in the DLN was similar to that seen in males, and was also present but at a reduced level in the DMN. During development, Cx36-puncta were sparsely present at postnatal day (PD) 9, increased dramatically by PD15, and beyond that appeared to undergo some cellular redistribution before reaching patterns seen in adults. In EGFP-Cx36 transgenic mice, subpopulations of motoneurons in the DMN and DLN were intensely labelled for EGFP reporter in males, and a vastly reduced number were observed in females. The results reveal a high density of Cx36-containing gap junctions in the sexually dimorphic DMN and DLN of males rodents, and the presence of these junctions in the same nuclei of females, suggesting coupling of not only dimorphic but also non-dimorphic motoneurons in these nuclei.

Introduction

Clusters of intercellular channels spanning the extracellular space create gap junctions at close plasma membrane apposition between neurons, and provide the basis for electrical transmission or electrical coupling (Bennett, 1997) as well as for the cell-to-cell passage of small molecules, which can be visualized as dye-coupling after intracellular injection of tracers. The channels are formed by particular members of the family of mammalian gap junction-forming connexin proteins (Evans and Martin, 2002) that are selectively expressed in neurons, and include connexin45 (Cx45) and connexin57 (Cx57), which are highly expressed in retina (Hombach et al., 2004; Kamasawa et al., 2006; Ciolofan et al., 2007), and connexin36 (Cx36), which is widely expressed in subpopulations of neurons in most major brain regions (Condorelli et al., 2000; Sohl et al., 2005; Meier & Dermietzel, 2006). Although long known to be of critical physiological relevance in the CNS neural circuitry of lower vertebrates (Bennett and Goodenough, 1978), the prevalence and functional importance of electrical coupling between neurons in mammalian brain has gained general acceptance only in the last decade or so. A key feature endowed by electrical transmission among ensembles of coupled neurons is synchronization of their subthreshold membrane oscillations, which promotes recruitment of synchronous activity when threshold for firing is reached (Bennett &, Zukin, 2004; Connors & Long, 2004; Hormuzdi *et al*., 2004). Such synchronous activity is emerging as a hallmark of information processing in neuronal networks (Singer, 1999; Deans et al., 2001; LeBeau et al., 2003; Whittington and Traub, 2003; Senkowski et al., 2008).

The discovery of Cx36 expression in neurons (Condorelli et al., 1998; Söhl et al., 1998), demonstrations of its occurrence in ultrastructurally-identified neuronal gap junctions in adult rodent brain (Nagy et al., 2004), and reports of functional deficits in Cx36 knockout (ko) mice (Söhl et al., 2004) were among some factors contributing to current understanding of electrical synapses in mammalian CNS. It is likely, however, that many more Cx36-expressing neurons remain to be identified, which will be aided by the development of transgenic mice expressing reporter proteins driven by the Cx36 promoter (Degen et al., 2004; Wellershaus et al., 2008; Helbig et al., 2010) and by immunohistochemical localization of Cx36. We have found that Cx36 protein is rarely detectable intracellularly in neurons *in vivo*, but rather is visualized exclusively as punctate labelling (Cx36-puncta) localized to neuronal plasma membranes.

Because these Cx36-puncta are reflective of the localization of neuronal gap junctions, as indicated by correlative immunofluorescence and ultrastructural analysis of immunolabelling for Cx36 (Rash et al., 2000,2001a,b,2007a,b; Kamasawa et al., 2006; Li et al., 2008), immunolocalization of Cx36 reveals sites of electrical synapses between neurons. Among the CNS areas in which we have examined Cx36 immunolocalization, few display the striking density and patterns of Cx36-puncta that we now report in sexually dimorphic motor nuclei of the spinal cord.

These nuclei are termed sexually dimorphic because the development and maintenance of their constituent motoneurons in males is dependent on adequate levels of circulating androgens, and these neurons in females are far fewer and smaller in size (Breedlove and Arnold, 1980; Jordan et al., 1982; Sengelaub & Arnold, 1986; Breedlove, 1986; Sengelaub and Forger, 2008). An additional feature of these motoneurons is their linkage by gap junctions, as reported in adult male rats (Matsumoto et al., 1988,1989; Coleman and Sengelaub, 2002), which is in contrast to other motoneuronal populations that are electrically coupled early during postnatal development, but loose this coupling by the end of the second postnatal week (Arasaki et al., 1984; Fulton et al., 1980; Walton & Navarette, 1991; Bou-Flores & Berger, 2001). While coupling between the dimorphic motoneurons was suggested to be mediated by gap junctions composed of Cx32 (Matsumoto et al., 1991,1992), we found no evidence for Cx32 expression in these motoneurons, which instead expressed Cx36, as reported in preliminary form elsewhere (Bautista et al., 2013). Here, we provide a more comprehensive immunofluorescence analysis of Cx36 association with these neurons.

Materials and methods

Animals and antibodies

A total of thirty-eight mice and rats were used in the present study, consisting of the following animals of specified age, sex, transgenic and treatment groups: Normal male Sprague-Dawley rats at adult age (n = 12), postnatal day (PD) nine (n = 3) and PD fifteen (n = 3); normal adult male C57BL/6-129SvEv wild-type mice (n = 6) and transgenic Cx36 knockout mice (n = 2); normal adult female Sprague-Dawley rats (n = 3); adult male castrated (n = 3) and sham (n = 3)

operated rats; transgenic adult male (n = 3) and female (n = 3) mice in which Cx36 expression is normal and bacterial artificial chromosome provides EGFP expression driven by the Cx36 promoter, designated EGFP-Cx36 mice. The C57BL/6-129SvEv wild-type and Cx36 ko mice (Deans *et al*., 2001) were established at the University of Manitoba through generous provision of breeding pairs of these mice from Dr. David Paul (Harvard). The EGFP-Cx36 mice were taken from a colony of these mice established at the University of Manitoba starting with breeding pairs obtained from UC Davis Mutant Mouse Regional Resource Center (Davis, CA, USA; see also http://www.gensat.org/index.html). Tissues from some of these animals were taken for use in parallel unrelated studies. Animals were utilized according to approved protocols by the Central Animal Care Committee of University of Manitoba, with minimization of the numbers animals used.

Immunofluorescence labelling in this study was conducted with a total of five primary antibodies, used in various combinations. Anti-Cx36 antibodies were obtained from Life Technologies Corporation (Grand Island, NY, USA) (formerly Invitrogen/Zymed Laboratories), and those used included two rabbit polyclonal antibodies (Cat. No. 36-4600 and Cat. No. 51-6300) and one mouse monoclonal antibody (Cat. No. 39-4200). These anti-Cx36 antibodies were incubated with tissue sections at a concentration of 1-2 µg/ml. Anti-peripherin developed in chicken was obtained from Millipore (Temecula, CA, USA) and used at a dilution of 1:500 to detect peripherin protein as a marker of motoneurons (Clarke et al., 2010). A monoclonal anti-EGFP developed in rabbit was obtained from Life Technologies Corporation and used at a concentration of 1-2 µg/ml to immunolabel EGFP in sections from EGFP-Cx36 mice. A polyclonal antibody against vesicular glutamate transporter-1 (vglut1) was obtained from Millipore and used at a dilution of 1:1000 to label vglut1-containing axon terminals in the spinal. An polyclonal goat anti-choline acetyltransferase (ChAT) antibody was obtained from Millipore and used at a dilution of 1:300 to immunolabel cholinergic motoneurons in the spinal cord.

Various secondary antibodies used included Cy3-conjugated goat or donkey anti-mouse and anti-rabbit IgG diluted 1:600 (Jackson ImmunoResearch Laboratories, West Grove, PA, USA), AlexaFlour 488-conjugated goat or donkey anti-rabbit, anti-mouse and anti-guinea pig IgG used at a dilution of 1:600 (Molecular Probes, Eugene, OR, USA), AlexaFluor-647

conjugated goat anti-chicken IgG used at a dilution of 1:500 (Life Technologies Corporation), Cy3-conjugated goat anti-chicken used at a dilution of 1:600 (Jackson ImmunoResearch Laboratories). All primary and secondary antibodies were diluted in 50 mM Tris-HCl, pH 7.4, containing 1.5% sodium chloride (TBS), 0.3% Triton X-100 (TBSTr) and 10% normal goat or normal donkey serum.

Tissue preparation

All animals were euthanized with an overdose of equithesin (3 ml/kg), placed on a bed of ice, and perfused transcardially with cold (4°C) pre-fixative consisting of 50 mM sodium phosphate buffer, pH 7.4, 0.1% sodium nitrite, 0.9% NaCl and 1 unit/ml of heparin. The prefixative was administered at a volume of 20 ml per 100 g body weight, and was adjusted accordingly for animals in this study weighing 25 g to 300 g. For experiments involving immunohistochemical detection of Cx36, pre-fixative perfusion was followed immediately by perfusion with fixative solution containing cold 0.16 M sodium phosphate buffer, pH 7.4, 0.2% picric acid and either 1% or 2% formaldehyde prepared freshly from depolymerized paraformaldehyde. Volumes of fixative given ranged from 100-200 ml per 200 g body weight, again adjusted for the body weight of animals used. Typically, greater volumes were used at 1% fixative and lower volumes at 2% fixative. For experiments involving immunohistochemical detection of EGFP, the pre-fixative perfusion was followed by perfusion with fixative solution containing cold 0.16 M sodium phosphate buffer, pH 7.4, 0.2% picric acid and 4% formaldehyde. As our standard immunohistochemical protocol often excludes a step involving postfixation of extracted tissues, after both 1-2% or 4% fixative perfusions, animals were perfused with a cold solution containing 10% sucrose and 25 mM sodium phosphate buffer, pH 7.4, to wash out fixative thereby reducing extent of tissue fixation. Spinal cords were removed and stored at 4°C for 24-48 h in cryoprotectant containing 25 mM sodium phosphate buffer, pH 7.4, 10% sucrose, 0.04% sodium azide. Sections of spinal cord were cut at a thickness of 10-15 μm using a cryostat and collected on gelatinized glass slides. Slide-mounted sections could be routinely stored at -35 ^{o}C for several months before use.

Immunofluorescence procedures

Slide mounted sections were removed from storage, air dried for 10 min, washed for 20 min in TBSTr, and processed for immunofluorescence staining, as previously described (Li et al., 2008; Bautista et al., 2012; Curti et al., 2012). With the weak 1-2% formaldehyde fixations employed, sections mounted on gelatinized slides occasionally have poor adherence to slides and tend to float off during processing. In such instances, this was prevented by fixation of rehydrated slide-mounted sections in 1% formaldehyde for 15, 30 or 60 seconds. For double or triple immunolabelling, sections were incubated simultaneously with two or three primary antibodies for 24 h at 4°C. The sections were then washed for 1 h in TBSTr and incubated with appropriate combinations of secondary antibodies for 1.5 h at room temperature. Some sections processed for double immunolabelling were counterstained with either green Nissl fluorescent NeuroTrace (stain N21480) or Blue Nissl NeuroTrace (stain N21479) (Molecular Probes, Eugene, OR, USA). All sections were coverslipped with the antifade medium Fluoromount-G (SouthernBiotech, Birmingham, AB, USA), and were either viewed immediately or were stored at -20 ^{o}C until taken for examination. Control procedures involving omission of one of the primary antibodies with inclusion of the secondary antibodies used for double and triple labelling indicated absence of inappropriate cross-reactions between primary and secondary antibodies for all of the combinations used in this study.

Immunofluorescence was examined on a Zeiss Axioskop2 fluorescence microscope and a Zeiss 710 laser scanning confocal microscope, using Axiovision 3.0 software or Zeiss ZEN Black 2010 image capture and analysis software (Carl Zeiss Canada, Toronto, Ontario, Canada). Data from wide field and confocal microscopes were collected either as single scan images or z-stack images with multiple optical scans capturing a thickness of 4 to 12 μm of tissue at z scanning intervals of 0.4 to 0.6 μm. Images of immunolabelling obtained with Cy5 fluorochrome were pseudo colored blue. Final images were assembled using CorelDraw Graphics (Corel Corp., Ottawa, Canada) and Adobe Photoshop CS software (Adobe Systems, San Jose, CA, USA). Movie files of 3D rendered images were created using Zeiss ZEN Black 2010 software (Carl Zeiss Canada).

Results

Sexually dimorphic motor nuclei and nomenclature

Sexually dimorphic motor nuclei at lower lumbar levels were identified in part according to the spinal cord atlas of Watson et al. (2009) as well as from description of motoneurons in these nuclei retrogradely labelled from the pudendal nerve and their target muscles (Schroder, 1980; McKenna and Nadelhaft, 1986). These nuclei in rodents are distributed at L5-L6 levels in the spinal cord ventral horn, and their constituent motoneurons collectively innervate groups of striated muscles located in the pelvic floor. The dimorphic motor nuclei and the muscles they innervate include: i) The dorsolateral nucleus (DLN), which occupies a position in the ventrolateral corner of the ventral horn, and innervates the ischiocavernosus muscle as well as striated muscle forming the external urethral sphincter around the neck of the urinary bladder; and ii) The dorsomedial nucleus (DMN) (a.k.a., spinal nucleus of the bulbocavernosus), which is located near midline beneath the central canal at the apex and flanking the dorsolateral portions of the ventral funiculus, and innervates the bulbospongiosus (a.k.a., bulbocavernosus) muscle, as well as striated muscle forming the external anal sphincter; iii) A less prominent ventral nucleus (VN), which is located midway between the DLN and DMN at the ventral margin of the ventral horn, innervates the pelvic diaphragm or pelvic floor muscle (Thor and De Groat, 2010), and is only weakly dimorphic (Mckenna and Nadelhaft, 1986); And iv) A larger retrodorsolateral nucleus (RDLN), which is located in the lateral part of the ventral horn and dorsal to the DLN, and innervates plantar foot muscles (Nicolopoulos-Stournaras and Iles, 1983; Zuloaga et al., 2007).

Four points regarding nomenclature are of note; First, the DMN is also often referred to as the spinal nucleus of the bulbocavernosus (SNB) (Breedlove, 1986), but we use the term DMN here to be consistent with reference to spinal cord location of the other nuclei examined. Second, motoneurons in the DMN are often said to innervate the bulbocavernosus and levator ani muscles (Sengelaub and Forger, 2008), but a convincing case has been made for considering the levator ani as part of the bulbospongiosus muscle complex (McKenna and Nadelhaft, 1986), which is consequently the nomenclature we use here. Third, on historical grounds and to avoid confusion, we use the term external urethral sphincter to refer to striated muscles associated with the urethra, but recognize that the more anatomically accurate term urethral rhabdosphincter is

becoming convention (Thor and Groat, 2010). And fourth, although RDLN motoneurons are sometimes referred to as being sexually non-dimorphic (McKenna and Nadelhaft, 1986; Coleman and Sengelaub, 2002), RDL motoneurons innervating the intrinsic foot muscle flexor digitorum brevis have been reported to exhibit male/female differences, albeit small, that are used to define sexual dimorphism (Leslie et al., 1991), and are therefore referred to here as dimorphic.

Cx36 in sexually dimorphic motor nuclei of male rat and mouse

An overview of the locations of the dimorphic nuclei at L5-L6 in adult rat, with labelling for peripherin and Cx36, is presented bilaterally at low magnification in Figure 1, where peripherin is shown pseudo colored sky blue for better visualization of the nuclear groups (Fig. 1), or deep blue allowing better visualization of Cx36-puncta (red) against peripherin-positive motoneurons (Fig. 1B-E). Immunolabelling for vglut1 in combination with Cx36 and peripherin is also shown (Fig. 1C-E) to provide a comparison of Cx36/vglut1 relationships in the dimorphic nuclei *vs.* Cx36 association with vglut1-containing primary afferent terminals that we have observed at most other spinal levels (Bautista et al., 2013), where vglut1 is localized largely in terminals of primary afferent origin (Alvarez et al., 2004). Indeed, sexually dimorphic motoneurons were reported to contain a paucity of primary afferent innervation (Jankowska et al., 1978; Taylor et al., 1982; McKenna and Nadelhaft, 1986; Thor and de Groat, 2010), and scarce vglut1-containing terminals among tightly clustered motoneuronal somata in the dimorphic nuclei (discussed below) proved to be another convenient means of locating these nuclei.

As seen in transverse sections, the somata of motoneurons in the dimorphic motor nuclei were either packed tightly together forming compact globular clusters, as in the DMN and DLN (Fig. 1A-E), or were dispersed such as those in the V group (Fig. 1A,B). The RDL displayed a mixture of both dispersed (Fig. 1A) and clustered (Fig. 1D) motoneurons along its rostrocaudal dimensions, with the former located caudally and the latter located rostrally. Compared with scattered Cx36-puncta observed in areas of intermediate lamina of spinal cord (Fig. 1B), immunofluorescence labelling for Cx36 was consistently more intense in some of the dimorphic nuclear groups, and immunolabelling was organized in patterns distinctly different than observed

at other spinal locations. In general, labelling of Cx36 was robust in the DMN and DLN (Fig. 1B-E), moderate in the V nucleus (Fig. 1B), and ranged from sparse in regions of the RDLN containing dispersed motoneurons (Fig. 1A,C) to moderate in those regions containing motoneurons that were more clustered (Fig. 1D).

Immunolabelling of Cx36 in the DMN and DLN was also examined in horizontal sections or rat (Fig. 2A,B) and mouse (Fig. 2C,D), where a greater expanse of these nuclei can be visualized in their rostro-caudally oriented columns. As previously described (Schroder, 1980; Ueyama et al., 1987), motoneurons in the DMN tended to be organized in intermittent clusters straddling the apex of the ventral funiculus (Fig. 2A), with the bulbospongiosus and anal sphincter motoneurons completed intermingled within these clusters (Rose and Collins, 1985; McKenna and Nadelhaft, 1986). The horizontal view more clearly revealed the remarkable density of Cx36-puncta associated with individual motoneuronal somata and their proximal dendrites within these clusters. Also more evident is the extent to which dendrites from these clusters cross the midline and form bundles of intermingled dendrites emerging from opposite sides (Rose and Collins, 1985). These bundles were typically laden with Cx36-puncta (Fig. 2A), consistent with the possibility of electrical coupling between motoneurons with contralaterally projecting dendrites, as previously suggested (Coleman and Sengelaub, 2002; see however Foster and Sengelaub, 2004). In the DLN, motoneurons are more tightly packed in both rostrocaudal and mediolateral dimensions of the nucleus (Fig. 2B1). However, in rat, medially located motoneurons innervating ischiocavernosus muscles were previously reported to be somewhat segregated from more laterally located motoneurons innervating urethral sphincter muscles (Mckenna and Nadelhaft, 1986). Punctate immunolabelling for Cx36 was distributed throughout the DLN, and appeared to consist of both small and relatively larger Cx36-puncta (Fig. 2B2). There were no discernible differences in density or size of Cx36-puncta associated with motoneurons in the medial *vs.* lateral half of this nucleus (Fig. 2B2). Similar results were obtained in horizontal sections through the DMN (Fig. 2C) and DLN (Fig. 2D) of mouse spinal cord. In both rat and mouse, it appeared visual inspection that the vast majority, if not all, motoneurons in these two nuclei were invested with Cx36-puncta on their somata and/or initial dendrites, suggesting that in each nuclei, both sexually dimorphic and non-dimorphic (i.e., bulbospongiosus and anal sphincter in the DMN; ischiocavernosus and urethral sphincter in the DLN) are gap junctionally coupled. This was supported by quantitative estimates where, in

images such as those in Figure 2, we counted the number of peripherin-positive motoneurons that displayed or lacked Cx36-puncta on their somata, or initial dendrites where these could be followed back to somata. In three rats, counts of a total of 566 motoneurons in DMN and 1027 in DLN revealed that 98% and 98%, respectively, of these neurons has associated with them at least a few, but often many, Cx36-puncta. In three mice, counts of 98 motoneurons in the DMN and 206 neurons in the DLN showed that 94% and 96%, respectively, of these neurons were invested with a few to many Cx36-puncta.

Specificity characteristics for Cx36 detection in various regions of rodent brain have been previously reported (Li et al., 2004; Rash et al., 2007a,b; Curti et al., 2012). As found in developing mouse spinal cord (Bautista et al., 2012), comparison of a field in the DLN from a wild-type adult mouse with a corresponding field in the DLN from a Cx36 knockout mouse, shows Cx36-puncta among peripherin-positive motoneurons in wild-type (Fig. 2E) and an absence of labelling for Cx36 in the knockout (Fig. 2F), indicating specificity of the anti-Cx36 antibody.

Laser scanning confocal analysis of immunofluorescence labelling for Cx36 associated with peripherin-positive motoneurons in the DMN, DLN and RDLN is shown in Fig. 3. In the DMN, the intermingled anal sphincter and bulbospongiosus motoneurons are difficult to distinguish from each other. However, as previously described (McKenna and Nadelhaft 1986), bulbospongiosus motoneurons have dendrite bundles extending medial and ventral (Fig. 3A), whereas anal sphincter motoneurons have dendrites directed dorsally traversing regions just lateral and dorsal to the central canal (Fig. 3B), as well as extending contralaterally via the commissural ventral gray matter. Labelling for Cx36 among closely packed pairs or triples of these large neurons at caudal levels of the DMN was seen in regions of apposition between their somata, as well as linearly arranged along their initial dendrites (Fig. 3A-C). At rostral levels, where slightly more ventrally located DMN motoneurons are of smaller size and are clustered in greater numbers, labelling of Cx36 was similarly distributed among peripherin-labelled neuronal somata (Fig. 3D,E), but the initial dendrites of these neurons were less distinctive and displayed fewer Cx36-puncta (not shown). In the DLN, Cx36 labelling among clustered neurons was heterogeneous, consisting of a few large patches of labelling and a greater density of smaller Cx36-puncta than seen in DMN (Fig. 3F). Throughout all these nuclei, immunolabelling for

Cx36 had an exclusively punctate appearance, with no evidence of either punctate or diffuse intracellular labelling, as determined by confocal through focus examination of individual neurons. Further, Cx36 labelling appeared to be localized exclusively to the surface (i.e., presumably plasma membrane) of motoneuronal somata and dendrites, as deduced from displays of thick (12 μm) z-stack images in 3D and rotation of these images at all angles (Supplementary Fig. 1). Similar analysis indicated that Cx36-puncta were often localized at appositions between motoneurons, which included soma-somatic (Fig. 3G), dendro-somatic (Fig. 3H) and dendro-dendritic (Fig. 3I) appositions. At lower magnification, individual Cx36-puncta appeared to be heterogeneous in size, ranging from 0.5 to 3 μm in diameter. Larger patches of Cx36 labelling were also encountered, ranging from 5 μm in diameter to as much as 5 μm x 17 μm in diameter and length, respectively. As shown at higher magnification, the larger patches in fact consisted of clusters of Cx36-puncta (Fig. 3J, and inset), which were best viewed when captured *en face* on the surface of neurons or dendrites. These clusters were often irregular in shape and contained up to dozens of Cx36-puncta.

Vglut1-containing terminals in sexually dimorphic motor nuclei

In contrast to nearly all other motor nuclei that contained an abundance of vglut1-terminals, with a substantial proportion of Cx36-puncta associated with those terminals (Bautista et al., 2013), Cx36-puncta in the sexually dimorphic motor nuclei were only rarely associated with these terminals. Indeed, motoneuron somata and their initial dendrites in the DMN and DLN either totally lacked or contained only a paucity of vglut1-terminals (Fig. 1C,D,E, and 3A-C) in comparison to adjacent motor nuclei (unidentified), where these terminals were see distributed at moderate density among peripherin-positive motoneurons (Fig. 1E). However, regions of the RDLN containing both dispersed and clustered motoneurons (Fig. 1C,3F) as well as the V group of dimorphic nuclei displaying moderate to low levels of Cx36-puncta also contained a scattering of there terminals, where Cx36-puncta either lacked or showed co-localization with these terminals (Fig. 3K). More generally, it also appeared that vglut1-terminals were more sparsely distributed in the intermediate laminae and in ventral horn at spinal levels containing the sexually dimorphic nuclei than in these regions at other spinal levels (Fig. 1C).

Cx36 in sexually dimorphic nuclei at PD9 and PD15

Electrophysiological analyses of spinal cord systems in vitro is often conducted using preparations from early postnatal or juvenile animals, where viability of the systems under investigation are better preserved in reduced preparations. To provide the basis for future such studies involving electrical coupling in sexually dimorphic motor nuclei, we examined the appearance of Cx36 in these nuclei at two developmental ages, PD9 and PD15, of male rats. As is typical in spinal cord at younger ages *vs.* adults, labelling for Cx36 in the form of Cx36-puncta was more widely distributed throughout gray matter at PD9, including ventral horn areas outside of motor nuclei (Fig. 4A). Labelling in RDLN was similar to that in surrounding regions, while labelling in DLN was somewhat more dense, and contained coarse as well as very fine Cx36-puncta (Fig. 4B). Cx36-puncta were also present in the DMN, where they were prominent on motoneuronal somata (Fig. 4C) and dendrites (Fig. 4D). In general, motoneurons in the DLN and DMN had much smaller somata and less developed dendritic arborizations than seen at at PD9 than at PD15 or in adults, as previously reported (Goldstein et al., 1990; Goldstein and Sengelaub, 1993). The density of Cx36-puncta among these neurons was also far less and did not occur in tight clusters as seen at later ages. At PD15, motoneurons in each of the dimorphic nuclei were well developed, and displayed robust labelling for peripherin in their somata and widely distributed dendrites (Fig. 4D-O). Labelling for Cx36 was still seen in regions surrounding motor nuclei (Fig. 4E,F,K), but Cx36-puncta were more concentrated within DMN, DLN and RDLN than in surrounding areas. Although not examined quantitatively, several features of this labelling at PD15 differed qualitatively from patterns seen in adult rats. First, Cx36-puncta appeared to be present in greater abundance along peripherin-positive dendrites within, and extending from, the DMN, DLN and RDLN (Fig. 4E-K). The puncta often occurred along bundles of intertwined dendrites (Fig. 4H,I,J,K), including at intersections between dendrites (Fig. 4M,N), and likely represent mature rather than nascent gap junctions. Second, although Cx36-puncta were also heavily concentrated among neuronal somata in the dimorphic nuclei, these more often appear as individual puncta (Fig. 4F,G,I,J), rather than assemblies of puncta in clusters as seen in adults. Clusters of puncta were, nevertheless, encountered but far less frequently than in mature animals (Fig. 4L,M). And third, very fine Cx36-puncta barely

visible at low magnification (Fig. 4G) were often seen distributed along the surface of motoneuron somata and dendrites (Fig. 4M,O). These fine puncta had diameters that were about 5-10 fold smaller than their larger counterparts, and they were not seen on motoneurons in adult animals. These results suggest that considerable remodeling of Cx36-containing gap junctions in sexually dimorphic nuclei takes place between the end of the second postnatal week and adulthood.

Cx36 in sexually dimorphic nuclei of female rat

Motoneurons in sexually dimorphic motor nuclei in female rats are present in about one-third the number, are smaller and have less extensive dendritic arborizations compared with their male counterparts (Breedlove, 1986; Sengelaub and Arnold, 1986). In males, dimorphic motoneurons in DMN and DLN innervating the dimorphic bulbospongiosus and ischiocavernosus muscles, respectively, are intermingled with non-dimorphic motoneurons innervating the anal sphincter and urethral sphincter muscles, respectively. In females, motoneurons innervating the two sphincters represent the vast majority of neurons in the DMN and DLN (McKenna and Nadelhaft, 1986). Thus, females provide the unique opportunity to determine whether non-dimorphic motoneurons in these nuclei express Cx36. As shown in Figure 5, both the dimorphic DMN and DLN, as well as the non-dimorphic RDLN, contained Cx36-puncta. Labelling of Cx36 was particularly striking in the DLN, which appeared smaller than its male counterpart, but displayed a density of Cx36-puncta similar to that seen in males (Fig. 5A-C). Patterns of dispersed Cx36-puncta and patches of these puncta in regions of RDLN containing loosely arrayed motoneurons (Fig. 5D,E), as well as those at rostral levels containing more clustered motoneurons (Fig. 5F), were also similar to that seen in males. In contrast, labelling in the DMN was considerably less in females, which was not simply a consequence of the smaller and reduced number of motoneurons in this nucleus of females *vs.* males. Although not examined quantitatively, Cx36-puncta along initial dendritic shafts and clusters of Cx36-puncta on the somata of DM motoneurons were clearly fewer (Fig. 5G-I) than seen in males, and those clusters that were present tended to be smaller (Fig. 5H,I).

Distribution of dimorphic motoneurons in EGFP-Cx36 mice

Mice exhibit similar sexually dimorphic patterns of their lower lumbar motoneurons as observed in rats (Wee and Clemens, 1987; Forger et al., 1997; Zuloaga et al., 2007). As previously noted (Forger et al., 1997; Zuloaga et al., 2007), however, motoneurons in DMN of mice appear more dispersed and, in addition to their location at the apex of the ventral funiculus, tend to occupy areas more ventrally and laterally near the border between white and gray matter. Thus, whereas DMN and DLN are largely segregated in rat, some dimorphic motoneurons in mouse are found to be distributed between these two nuclei in mouse.

To further characterize these neurons, we examined immunolabelling for EGFP in relation that of peripherin in the dimorphic nuclei of transgenic EGFP-Cx36 mice, in which EGFP expression on a bacterial artificial chromosome (BAC) is driven by the Cx36 promoter. Although expression of Cx36 in these mice is left intact, it was not possible to double label for EGFP and Cx36 due to the incompatibility of the strong fixation required for adequately labelling EGFP (*i.e.,* 4% formaldehyde), and the loss of labelling for Cx36 with this fixation. The EGFP-Cx36 BAC mice have not been widely used as yet for studies of neurons expressing Cx36. Nevertheless, as expected based on pilot examination of these mice during their production (Nagy, unpublished observations), together with the above results showing abundant Cx36-puncta associated with dimorphic motoneurons, EGFP fluorescence (not shown) as well as immunolabelling for EGFP was detected in many though not all spinal sexually dimorphic motoneurons. Small and medium size neuronal somata labelled for EGFP were also seen sparsely distributed in other areas of the ventral horn and moderately in the dorsal horn.

A comparison of labelling for peripherin and, in the same field, labelling for EGFP is shown in Figure 6A1 and 6A2, respectively. As in rat, labelling for peripherin clearly delineated the locations motoneurons in the DMN, DLN and RDLN (Fig. 6A1). Labelling for EGFP was prominent in the DMN and DLN (Fig. 6A2), where both neuronal somata and their dendritic extensions were intensely labelled (Fig. 6B-D), but in the RDLN, EGFP-positive neurons ranged from very sparse to undetectable (Fig. 6A2). Detail comparisons of labelling in matching fields of the DMN (Fig. 6E1, E2), the DLN and RDLN (Fig. 6F1,F2) and RDLN (Fig. 6G1,G2) revealed that both the DMN and DLN contained peripherin-positive neurons that were EGFP-negative, although the proportion of those that were negative was not determined quantitatively.

The RDLN contained only a few ventrally located peripherin-positive neurons that were labelled for EGFP (Fig. 6G). Peripherin-positive motoneurons lacking EGFP were often well intermingled with, and in close somal apposition to, other motoneurons labelled for peripherin, as shown at higher magnification in the DLN (Fig. 6H,I). The lack of labelling for EGFP in some did not appear to be a peculiarity of peripherin detection in other than motoneurons in the dimorphic nuclei because some ChAT-positive neurons in these nuclei were similarly devoid of EGFP (not shown). In female EGFP-Cx36 mice, neurons positive for EGFP were also found in both the DMN and DLN (Fig. 6J,K,), as well as midway between these nuclei in a ventromedial region corresponding to the area of VN (Fig. 6M). However, only a few neurons per section were encountered, and these were much smaller than observed in males and their dendrites were only weakly labelled for EGFP (Fig. 6L,M).

Discussion

The appearance of motoneurons in the sexually dimorphic motor nuclei as visualized here by their labelling for peripherin was comparable to that derived from the use of other anatomical methods (McKenna and Nadelhaft, 1986). Early ultrastructural studies of motoneurons in the lumbosacral spinal cord of cat described close appositions of their dendrites, which were considered in the context of possibly contributing to electrical interactions between these neurons (Mathews et al. 1971; Takahashi and Yamamoto, 1979). Following the discovery of gap junctions between sexually dimorphic motoneurons in adult rat (Matsumoto *et al*., 1988,1989), there have been only a few subsequent studies focused on this topic. Consistent with these early reports describing the localization of gap junctions at dimorphic motoneuronal somata and their initial dendrites, we found the greatest densities of Cx36-puncta at these neuronal compartments, where labelling often seen at soma-somatic, dendro-somatic and dendro-dendritic appositions almost certainly reflect localization of gap junctions. Outside of the dimorphic nuclei in regions containing extensive dendritic arborizations of dimorphic motoneurons, Cx36-puncta were far more sparsely distributed, suggesting that gap junctions may link distal dendrites of the motoneurons, but at vastly lower levels. Our results raise several points for consideration.

Connexin expression in motoneurons

There has been some confusion and uncertainty regarding connexins expressed by motoneurons. Like neurons elsewhere in the developing CNS, motoneurons in an assortment of motor nuclei in rodent spinal cord are known to be electrically coupled and dye-coupled via gap junctions at early postnatal ages (Arasaki et al., 1984; Fulton et al., 1980; Walton & Navarette, 1991; Bou-Flores & Berger, 2001). The connexins that have been considered to mediate this coupling include Cx36, Cx37, Cx40, Cx43 and Cx45 (Chang et al., 1999; Chang and Balice-Gordon, 2000). Multipe connexins were also reported to be expressed in trigeminal motoneurons, including Cx26, Cx32, Cx36 and Cx43 (Honma et al., 2004). Similarly, expression of Cx32 mRNA was reported in sexually dimorphic motoneurons of adult rats (Matsumoto et al., 1991,1992). However, we have found widespread association of only Cx36 with motoneurons, and Cx32 protein in dimorphic nuclei (*i.e.*, DMN, DLN) was found to be assocociated only with oligodendrocytes and along myelinated fibers (Bautista et al., 2013a), consistent with the ultrastructural localization of Cx32 to gap junctions formed by oligodendrocytes and not to those between neurons in spinal cord (Rash et al., 1998; 2001b). In contrast, the robust and consistent labelling for Cx36 observed in these two sexually dimorphic nuclei, often localized to the surface of motoneurons, was among the most stricking seen anywhere in the CNS. The results provide compeling evidence that previously described gap junctions linking these motoneurons (Matsumoto *et al*., 1988,1989) are composed of Cx36, and suggest Cx36-mediation of electrical coupling between these neurons. In analogy with recent findings surrounding the biophysical properties of electrical coupling between neurons in the mesencephalic trigeminal nucleus (Curti et al., 29120), the high density of Cx36-containing gap junctions linking dimorphic motoneurons might be predicted to maintain strong coupling coeficients between these cells even if only a small proportions of these channels were in an open state a any given moment.

Coupling between developing *vs.* adult motoneurons

The notion that gap junction-mediated coupling between neurons uniformly diminishes during development and is lost in many areas of adult CNS is no longer tenable. Dispite the reported loss of motoneuronal coupling during development (Walton & Navarette, 1991), evidence for

electrical coupling and of motoneuronal gap junctions has been described in several motoneuronal systems in adult animals (Gogan et al., 1974, 1977; Lewis, 1994; van der Want et al., 1998). Dendritic bundling and close somal appositions of sexually dimorphic motoneurons are especially prominent (Schroder, 1980; McKenna and Nadelhaft, 1986; Bellinger and Anderson, 1987), and it was suggested that these might be sites of direct electrical interactions (Rose and Collins, 1985). As predicted, gap junctions are especially prominent between sexually dimorphic motoneurons in the DMN and DLN in *adult* male rats (Matsumoto et al., 1988,1989), and such junctions have even been described between these neurons in their equivalent Onuf's nucleus in adult human spinal cord (Feirabend et al., 1997). Moreover, our results based on Cx36 localization indicate that these junctions increase from PD9 to PD15 and are further deployed at motoneuronal somatic appositions beyond this developmental period. In keeping with these findings, motoneurons in the DMN, DLN and RDLN of adult animals were reported to exhibit dye-coupling following injection of Neurobiotin into single motoneurons (Coleman and Sengelaub, 2002). However, these motoneurons were also found to be coupled to interneurons in these nuclei, which is unsusual as neuronal coupling in other systems typically occurs in a homologous fashsion (*i.e.*, coulping between same cell types). It should be noted that although dye-coupling in these studies was eliminated by the relatively non-specific gap junction blocker oleamide, those studies were conducted using formadehyde-fixed sections, under which the preservation of a normal physiological state of gap junctions is uncertain. Interneurons would not have been identified by the peripherin marker used in the present study, precluding possible identification of Cx36-puncta at appositions between these neurons and motoneurons. In any case, the association of dye-coupling, ultrastructurally-identified gap junctions and Cx36 with sexually dimorphic adult motoneurons are all consistent with a brief report (the only one we are aware of) describing electrical coupling between these neurons in adult rat (Collins and Erichsen, 1988).

Cx36 at purely electrical vs. mixed synapses

It has previously been reported that motoneurons in the sexually dimorphic DMN and DLN, unlike those at most other spinal levels, receive very little monosynaptic primary afferent input (Jankowska et al., 1978; McKenna and Nadelhaft, 1986; Thor and de Groat, 2010). Because

vglut1 is contained largely in axon terminals of primary afferent origin (Alvarez et al., 2004), our findings of a near total absence of vglut1-containing terminals on motoneuronal somata and dendrites within the DMN and DLN confirm these earlier reports. In gray matter regions surrounding these nuclei, labelling for vglut1 was far less dense than seen at other spinal levels, suggesting a paucity of vglut1-terminals also on the extensive dendritic arborizations that the dimorphic neurons have in these regions (Goldstein et al., 1990; Goldstein and Sengelaub, 1993). The dearth of vglut1-containing terminals on sexually dimorphic motoneurons, unlike motoneurons in other spinal cord motor nuclei, where these terminals are abundant and largely of primary afferent origin, indicates lack of a monosynaptic primary afferent influence on, or reflex control of, these motoneurons, the functional significance of which is poorly understood.

We originally examined primary afferent vglut1-containing terminals in the context of their relationship to labelling for Cx36 in the sexually dimorphic *vs.* other spinal motor nuclei. We recently reported (Bautista et al., 2013b) that abundant Cx36-puncta persist on the vast majority of motoneurons along the spinal axis in *adult* rat and mouse, but these puncta rarely appeared at appositions between motoneurons. Rather, they were localized to a considerable extent at vglut1-positive primary afferent axon terminals on these neurons, forming what we deduced to be Cx36-containing gap junctions between axon terminals and postsynaptic neurons. Such structures, termed morphologically "mixed synapses" with potential for dual chemical/electrical transmission (Bennett and Goodenough, 1978), were much earlier reported to be widespread in rodent spinal cord (Rash et al., 1996), and have been described in other areas of the mammalian CNS, including the lateral vestibular nucleus (Korn et al., 1973) and hippocampus (Vivar et al., 2012; Hamzei-Sichani et al., 2012; Nagy, 2012). Gap junctions at mixed synapses are presumably incapable or less effective in the mediation of coupling between their postsynaptic cells (see however, Nagy et al., 2013), possibly explaining the absence of coupling between most motoneurons despite persitance of Cx36-puncta on these neurons in adult rodents. The dimorphic motor nuclei, in contrast, embody an exception where all Cx36-puncta occurring on motoneuronal somata and their initial dendrites lack association with vglut1-terminals, and where these puncta therefore may be considered to represent "purely electrical synapses".

EGFP expression in dimorphic nuclei of EGFP-Cx36 mice

In male mice, both the DMN and DLN displayed EGFP-positive motoneurons in EGFP-Cx36 mice, consistent with detection of Cx36 protein in these nuclei. The absence of EGFP in some peripherin-positive motoneurons in each of these nuclei suggests the presence of both gap junctionally coupled and non-coupled motoneurons. However, our analyses in mouse revealed that, at minimum, a few Cx36-puncta were associated with nearly all peripherin-positive motoneuronal somata in the DMN and DLN. This, together with the near total absence of EGFP in the RDLN, where Cx36-puncta though sparse were clearly seen on motoneurons, raises an additional and/or alternative possibility, namely false-negative EGFP expression in Cx36-expressing cells, which may occur with incomplete rather than intact BAC transgene integration (van Keuren et al., 2009). Further, we note that there was an absence of EGFP expression in motor nuclei lying in the vicinity of the sexually dimorphic groups (not shown), which is also in contrast to the dense distribution of Cx36-puncta associated with vglut1-terminals at mixed synapses on motoneurons in these nuclei (Bautista et al., 2013). Absence of EGFP in those motoneurons receiving mixed synapses may again reflect false-negative EGFP expression or, alternatively, the existence of heterotypic gap junctions at these mixed synapses, such that primary afferent terminals contain Cx36, whereas motoneurons express another as yet unidentified connexin. Analysis of dye-coupling in the EGFP-Cx36 mice as well as ultrastructural studies in combination with immunolabelling for Cx36 will be required to distinguish between these various possibilities.

Dimorphic and non-dimorphic motoneurons in the DMN and DLN

Despite reports of gap junctions, dye-coupling and electrical coupling in sexually dimorphic nuclei discussed above, little is known about the organization of this coupling among motoneuronal populations contained in these nuclei. In males, sexually dimorphic motoneurons in the DMN and DLN are intermixed with anal sphincter and external urethral sphincter (EUS) motoneurons, respectively, which are not considered to be sexually dimorphic because their number and size do not vary between males vs. females (McKenna and Nadelhaft, 1986). It remains unresolved whether both dimorphic and non-dimorphic motoneurons in these nuclei are

coupled and, if both, whether the former are additionally coupled to the latter. Several of our observations suggest coupling of both dimorphic and non-dimorphic pools of motoneurons in both the DMN and DLN. First, the association of Cx36-puncta with nearly all peripherin-positive motoneurons in the DMN and DLN suggests that the vast majority of these neurons are gap junction communication competent. Second, the DMN contains many more motoneurons in male than in female rats (Jordan et al., 1982). In female rats lacking ischiocavernosus and bulbospongiosus muscles, it has been noted that motoneurons in the DMN projecting to the anal sphincter and those in DLN projecting to the EUS appear to account for all of the motoneurons in these nuclei (McKenna and Nadelhaft, 1986). The presence of Cx36-puncta at a high density in the DLN and an albeit lower density in DMN of female rats suggests coupling between EUS motoneurons and between anal sphincter motoneurons. This is further supported by the presence of EGFP-positive motoneurons in both DMN and DLN of female EGFP-Cx36 mice. And third, bulbospongiosus and anal sphincter motoneurons are highly intermingled in the DMN, while ischiocavernosus and EUS motoneurons are somewhat segregated in the DLN of rat, with the former lying medially and the latter occupying a lateral position in the nucleus (Rose and Collins, 1985; McKenna and Nadelhaft, 1986). Our finding that medially and laterally located motoneurons in DLN were equally decorated with Cx36-puncta suggests a similar capacity of coupling among the two motoneuronal pools. However, we cannot shed light on whether the sexually dimorphic motoneurons are coupled to the sphincter motoneurons. Such heteronymous coupling is likely based on observations of gap junctions between DM motoneurons with and without projections to bulbospongiosus (Matsumoto et al., 1988). Definitive studies to resolve this will require examination of dye-coupling or electrical coupling between anatomically or electrophysiologically identified EUS and simultaneously identified ischiocavernosus motoneurons in the DLN and similar examination of coupling between anal sphincter and ischiocavernosus motoneurons in the DMN.

Functional considerations

A fundamental role of electrical synapses in the mammalian brain is their promotion of synchronous activity in networks of coupled neurons. This is achieved by synchronizing subthreshold membrane oscillations so that the network may reach threshold for firing in unison

following an excitatory input. Direct electrical interactions between developing spinal motoneurons was also considered to be important in driving synchronous activity of these neurons (Kiehn and Tresch, 2002). In adult rodent spinal cord, the presence of neuronal gap junctions and the synchronous neuronal activity they presumably confer among sexually dimorphic motoneurons may give rise to coupled network activity of these neurons and their target muscles. As previously discussed (Coleman & Sengelaub, 2002), this coupling could be required for production of synchronous activity of motoneurons to maintain concerted action of the constellation of perineal muscles that support the physiology and behaviour of copulation. Though Cx36 knockout mice are able to reproduce, parameters of their copulatory behavior in the absence of electrical coupling has not been examined.

In male rodents, it is generally accepted that the ischiocavernosus and bulbospongiosus muscles contribute to various parameters of sexual behavior (Hart and Melese-D'Hospital, 1983; Elmore and Sachs, 1988; Holmes et al., 1991; Schmidt and Schmidt 1993). Patterns of activity of these and related muscles was remarkably revealed in sexual reflexes elicited in anesthetized rats after acute spinal transection (McKenna et al., 1991), which was considered to remove tonic descending inhibition of these reflexes (Marson and McKenna, 1990). The urethrogenital reflex, as it was termed, reproduced some features of copulation in the intact male, including penile erection, pelvic muscle activation and ejaculation. For plausible reasons given, this reflex could be evoked only by sensory stimulation of the urethra (McKenna et al., 1991). Recordings from the ischiocavernosus and bulbospongiosus muscles, as well as from the pudendal nerve innervating these two muscles and the anal and urethral sphincters, indicated that all the perineal muscle contractions were synchronous during reflex activation (McKenna et al., 1991), reflecting requirment of the dimporphic muscles in erectile and ejaculatory functions and, as suggested (McKenna and Nadelhaft, 1989), maintenance of tonic activity in the sphincter muscles for closure of the anal and urethral sphincters during sexual activity. We speculate that removal of tonic descending inhibition of sexual reflexes unmasks the considerable extent to which motoneurons in DMN and DLN appear to be electrically coupled, which is manifest by the observed synchronous activity of their target muscles following elicitation of the urethrogenital reflex. Further, the more complex sequelae of perineal muscle activity seen in normal male rats during sexual activity (Holmes et al., 1991; Schmidt and Schmidt 1993) suggests that moment-

to-moment patterns of coupling between motoneuronal pools in these nuclei may be subject to strict regulation.

Acknowledgements

This work was supported by a grant from the Canadian Institutes of Health Research to J.I.N. (MOP 106598) and to DM (MOP 37756), and by grants from the National Institutes of Health (NS31027, NS44010, NS44295) to JE Rash with sub-award to JIN. We thank B. McLean for excellent technical assistance, Dr. B.D. Lynn for help with genotyping EGFP-Cx36 transgenic mice, Dr. D. Paul (Harvard University) for providing breeding pairs of Cx36 knockout and wild-type mice, and A. Simon (University of Arizona) for collaborations in testing specificity of anti-Cx37 and anti-Cx40 antibodies in Cx37 and Cx40 knockout mice.

Abbreviations

CNS, central nervous system; ChAT, choline acetyltransferase; Cx36, connexin36; DLN, dorsolateral nucleus; DMN, dorsomedial nucleus; EGFP, enhanced green fluorescent protein; L, lumbar; PBS, phosphate-buffered saline; RDLN, retrodorsolateral nucleus; TBS, 50 mM Tris-HCl, pH 7.4, 1.5% NaCl; TBSTr, TBS containing 0.3% Triton X-100; T, thoracic; vglut1, vesicular glutamate transporter-1.

References

Alvarez FJ, Villalba RM, Zerda R & Schneider SP (2004) Vesicular glutamate transporters in the spinal cord, with special reference to sensory primary afferent synapses. J Comp Neurol 472, 257-280.

Arasaki K, Kudo N & Nakanishi T (1984) Firing of spinal motoneurons due to electrical interactions in the rat: an in vitro study. Exp Brain Res 54, 437-445.

Bautista W, Nagy JI Dai Y, & McCrea DA (2012) Requirement of neuronal connexin36 in pathways mediating presynaptic inhibition of primary afferents in functionally mature mouse spinal cord. J Physiol 590, 3821-39.

Bautista W, Rash JE & Nagy JI (2013a) Re-evaluation of connexin (Cx26, Cx32, Cx36, Cx37, Cx40, Cx43, Cx45) association with motoneurons in rodent spinal cord, sexually dimorphic motor nuclei and trigeminal motor nucleus. Submitted.

Bautista W, McCrea DA & Nagy JI (2013b) Connexin36 identified at primary afferent terminals forming mixed chemical/electrical synapses in adult rodent spinal cord. Submitted.

Bellinger DL & Anderson WJ (1987) Postnatal development of cell columns and their associated dendritic bundles in the lumbosacral spinal cord of the rat. I. The ventrolateral cell column. Dev Brain Res 35:55-67.

Bennett MVL & Goodenough DA (1978) Gap junctions, electrotonic coupling, and intercellular communication. Neurosci Res Prog Bull 16, 373-485.

Bennett MVL (1997) Gap junctions as electrical synapses. J Neurocytol 26, 349-366.

Bennett MVL & Zukin SR (2004) Electrical coupling and neuronal synchronization in the mammalian brain. Neuron 41, 495-511.

Bou-Flores C & Berger AJ (2001) Gap junctions and inhibitory synapses modulate inspiratory motoneuron synchronization. J Neurophysiol 85, 1543-1551.

Breedlove SM and Arnold AP (1980) Hormone accumulation in a sexually dimorphic motor nucleus in the rat spinal cord. Science 210:564-566.

Breedlove SM (1986) Cellular analysis of hormone influence on motoneuronal development and function. J Neurobiol 17, 157-176.

Chang Q & Balice-Gordon RJ (2000) Gap junctional communication among developing and injured motor neurons. Brain Res Rev 3, 242-249.

Chang Q, Gonzalez M, Pinter MJ & Balice-Gordon RJ (1999) Gap junctional coupling and patterns of connexin expression among neonatal rat lumbar spinal neurons. J Neurosci 19, 10813-10828.

Ciolofan C, Lynn BD, Wellershaus K, Willecke K & Nagy JI (2007) Spatial relationships of connexin36, connexin57 and zonula occludens-1 (ZO-1) in the outer plexiform layer of mouse retina. Neuroscience 148:473-488.

Clarke WT, Edwards B, McCullagh KJ, Kemp MW, Moorwood C, Sherman DL, Burgess M & Davies KE (2010) Syncoilin modulates peripherin filament networks and is necessary for large-calibre motor neurons. J Cell Sci 123, 2543-52.

Coleman AM & Sengelaub DR (2002) Patterns of dye coupling in lumbar motor nuclei of the rat. J Comp Neurol 454, 34-41.

Collins III WF & Erichsen JT (1988) Direct excitatory interactions between rat penile motoneurons. Abstr Soc Neurosci 14:181.

Condorelli DF, Parenti R, Spinella F, Salinaro AT, Belluardo N, Cardile V & Cicirata F (1998) Cloning of a new gap junction gene (Cx36) highly expressed in mammalian brain neurons. Eur J Neurosci 10, 1202-1208.

Condorelli DF, Belluardo N, Trovato-Salinaro A & Mudo G (2000) Expression of Cx36 in mammalian neurons. Brain Res Rev 32, 72-85.

Connors BW & Long MA (2004) Electrical synapses in the mammalian brain. Annu Rev Neurosci 27, 393-418.

Curti S, Hoge G, Nagy JI, Pereda AE (2012) Synergy between electrical coupling and membrane properties promotes strong synchronization of neurons of the mesencephalic trigeminal nucleus. J Neurosci 32, 4341-4359.

Deans MR, Gibson JR, Sellitto C, Connors BW & Paul DL (2001) Synchronous activity of inhibitory networks in neocortex requires electrical synapses containing connexin36. Neuron 31:477-485.

Degen J, Meier C, van der Giessen RS, Sohl G, Petrasch-Parwez E, Urschel S, Dermietzel R, Schilling K, de Zeeuw CI & Willecke K (2004) Expression pattern of lacZ reporter gene representing connexin36 in transgenic mice. J Comp Neurol 473:511-525.

Elmore LA and Sachs BD (1988) Role of the bulbospongiosus muscles in sexual behavior and fertility in the house mouse. Physiol Behav 44, 125-129.

Evans WH & Martin PEM (2002) Gap junctions: structure and function. Mol Membr Biol 19, 121-136.

Feirabend HKP, Hoitsma E, Choufoer H & Ploeger S (1997) Light and electron microscopic study of Onuf's nucleus in man: Qualitative and quantitative aspects. Eur J Morphol 35, 371.

Forger NG, Howell ML, Bengston L, MacKenzie L, DeChiara TM & Yancopoulos GD (1997) Sexual dimorphism in the spinal cord is absent in mice lacking the ciliary neurotrophic factor receptor. J Neurosci 17:9605-9612.

Foster AM and Sengelaub DR (2004) Bilateral organization of unilaterally generated activity in lumbar spinal motoneurons of the rat. Brain Res 1009, 98-109.

Fulton BP, Miledi R & Takahashi T (1980) Electrical synapses between motoneurons in the spinal cord of the newborn rat. Proc R Soc London Ser B 206, 115-120.

Gogan P, Gueritaud JP, Horcholle-Bossavit G & Tyc-Dumont S (1974) Electrotonic coupling between motoneurons in the abducens nucleus of the cat. Exp Brain Res 21:139-154.

Gogan P, Gueritaud JP, Horcholle-Bossavit G & Tyc-Dumont S (1977) Direct excitatory interactions between spinal motoneurones of the cat. J Physiol 272, 755-767.

Goldstein LA, Kurz EM & Sengelaub DR (1990) Androgen regulation of dendritic growth and retraction in the development of a sexually dimorphic spinal nucleus. J Neurosci 10:935-948.

Goldstein LA & Sengelaub DR (1993) Motoneuron morphology in the dorsolateral nucleus of the rat spinal cord: Normal development and androgen regulation. J Comp Neurol 338:588-600.

Haas JS, Zavala B, Landisman CE. (2011) Activity-dependent long-term depression of electrical synapses. Science; 334(6054):389-93.

Hamzei-Sichani F, Davidson KGV, Yasumura T, Janssen WGM, Wearne SL, Hof PR, Traub RD, Gutierrez R, Ottersen OP & Rash JE (2012) Mixed electrical-chemical synapses in adult rat hippocampus are primarily glutamatergic and coupled by connexin36. Front Neuroanat 6:1-26.

Hart BL and Melese-D'Hospital PY (1983) Penile mechanisms and the role of the striated penile muscles in penile reflexes. Physiol Behav 31, 807-813.

Helbig I, Sammler E, Eliava M, Bolshakov AP, Rozov A, Bruzzone R, Monyer H & Hormuzdi SG (2010) In vivo evidence for the involvement of the carboxy terminal domain in assembling connexin36 at the electrical synapse. Mol Cell Neurosci 45:47-58.

Hombach S, Janssen-Bienhold U, Söhl G, Schubert T, Bussow H, Ott T, Weiler R, Willecke K (2004) Functional expression of connexin57 in horizontal cells of the mouse retina. Eur J Neurosci 19:2633-2640.

Honma S, De S, Li D, Shuler CF & Turman Jr JE (2004) Developmental regulation of connexins 26, 32, 36 and 43 in trigeminal neurons. Synapse 52, 258-271.

Hormuzdi SG, Filippov MA, Mitropoulon G, Monyer H & Bruzzone R (2004) Electrical synapses: a dynamic signaling system that shapes the activity of neuronal networks. Biochem Biophys Acta 1662, 113-137.

Jankowska E, Padel Y and Zarzecki P (1978) Crossed disynaptic inhibition of sacral motoneurons. J Physiol 285, 425-444.

Jordan CL, Breedlove SM and Arnold AP (1982) Sexual dimorphism and the influence of neonatal androgen in the dorsolateral motor nucleus of the rat lumbar spinal cord. Brain Res 249:309-314.

Kamasawa N, Furman CS, Davidson KGV, Sampson JA, Magnie A R, Gebhardt B, Kamasawa M, Morita M, Yasumura T, Pieper M, Zumbrunnen JR, Pickard G E, Nagy JI & Rash JE (2006)

Abundance and ultrastructural diversity of neuronal gap junctions in the OFF and ON sublaminae of the inner plexiform layer of rat and mouse retina. Neuroscience 142:1093-1117.

Kiehn O and Tresch MC (2002) Gap junctions and motor behavior. Trends Neurosci 25, 108-115.

Korn H, Sotelo C & Crepel F (1973) Electrotonic coupling between neurons in the lateral vestibular nucleus. Exp Brain Res 16, 255-275.

LeBeau FEN, Traub RD, Monyer H, Whittington MA & Buhl EH (2003) The role of electrical signaling via gap junctions in the generation of fast network oscillations. Brain Res Bull 62:3-13.

Leslie ML, Forger NG & Breedlove SM (1991) Sexual dimorphism and androgen effects on spinal motoneurons innervating the rat flexor digitorum brevis. Brain Res 561:269-273.

Lewis DI (1994) Dye-coupling between vagal motoneurones within the compact region of the adult rat nucleus ambiguus, in-vitro. J Aut Nerv Syst 47, 53-58.

Li X, Olson C, Lu S, Kamasawa N, Yasumura T, Rash JE & Nagy JI (2004) Neuronal connexin36 association with zonula occludens-1 protein (ZO-1) in mouse brain and interaction with the first PDZ domain of ZO-1. Eur J Neurosci 19, 2132-46.

Li X, Kamasawa N, Ciolofan C, Olson CO, Lu S, Davidson KGV, Yasumura T, Shigemoto R, Rash JE & Nagy JI (2008) Connexin45-containing neuronal gap junctions in rodent retina also

contain connexin36 in both apposing hemiplaques, forming bi-homotypic gap junctions, with scaffolding contributed by zonula occludens-1. J Neurosci 28, 9769-89.

Marson L and McKenna KE (1990) The identification of a brainstem site controlling spinal sexual reflexes in male rats. Brain Res 515, 303-308.

Matthews MA, Willis WD and Williams V (1971) Dendrite bundles in lamina IX of cat spinal cord: a possible source for electrical interaction between motoneurons? Anat Rec 171, 313-328.

Matsumoto A, Arai Y, Urano A, & Hyodo S (1991) Androgen regulates gap junction mRNA expression in androgen-sensitive motoneurons in the rat spinal cord. Neurosci Lett 131, 159-162.

Matsumoto A, Arai Y, Urano A & Hyodo S (1992) Effect of androgen on the expresssion of gap junction and beta-actin mRNAs in adult rat motoneurons. Neurosci Res 14, 133-144.

Matsumoto A, Arnold AP & Micevych PE (1989) Gap junctions between lateral spinal motoneurons in the rat. Brain Res 495, 362-366.

Matsumoto A, Arnold AP, Zampighi G & Micevych PE (1988) Androgenic regulation of gap junctions between motoneurons in the rat spinal cord. J Neurosci 8, 4177-4138.

McKenna KE, & Nadelhaft I (1986) The organization of the pudendal nerve in the male and female rat. J Comp Neurol 248, 532-549.

McKenna KE and Nadelhaft I (1989) The pudendo-pudendal reflex in male and female rats. J Aut Ner Syst 27, 67-77.

McKenna KE, Chung SK and McVary KT (1991) A model for the study of sexual function in anesthetized male and female rats. Am J Physiol 261, 1276-85.

Meier C & Dermietzel R (2006) Electrical synapses--gap junctions in the brain. Results Probl Cell Differ 43, 99-128.

Nagy JI, Dudek FE & Rash JE (2004) Update on connexins and gap junctions in neurons and glia in in the mammalian central nervous system. Brain Res Rev 47, 191-215.

Nagy JI (2012) Evidence for connexin36 localization at hippocampal mossy fiber terminals suggesting mixed chemical/electrical transmission by granule cells. Brain Res 1487:107-122.

Nagy JI, Bautista W & Blakley B (2013) Morphologically mixed chemical-electrical synapses in developing and adult rodent vestibular nuclei as revealed by immunofluorescence detection of connexin36 and vesicular glutamate transporter-1. Neuroscience Submitted.

Nicolopoulos-Stournaras S & Iles JF (1983) Motor neuron columns in the lumbar spinal cord of the rat. J Comp Neurol 217:75-85.

Rash JE, Dillman RK, Bilhartz BL, Duffy HS, Whalen LR & Yasumura T (1996) Mixed synapses discovered and mapped throughout mammalian spinal cord. Proc Natl Acad Sci 93, 4235-4239.

Rash JE, Yasumura T & Dudek FE (1998) Ultrastructure, histological, distribution, and freeze-fracture immunocytochemistry of gap junctions in rat brain and spinal cord. Cell Biol Int 22, 731-749.

Rash JE, Staines WA, Yasumura T, Pate D, Hudson CS, Stelmack GL & Nagy J (2000) Immunogold evidence that neuronal gap junctions in adult rat brain and spinal cord contain connexin36 (Cx36) but not Cx32 or Cx43. Proc Natl Acad Sci 97, 7573-7578.

Rash JE, Yasumura T, Dudek FE & Nagy JI (2001a) Cell-specific expression of connexins, and evidence for restricted gap junctional coupling between glial cells and between neurons. J Neurosci 21, 1983-2000.

Rash JE, Yasumura T, Davidson K, Furman CS, Dudek FE & Nagy JI (2001b) Identification of cells expressing Cx43, Cx30, Cx26, Cx32 and Cx36 in gap junctions of rat brain and spinal cord. Cell Commun Adhes 8, 315-320.

Rash JE, Pereda A, Kamasawa N, Furman CS, Yasumura T, Davidson KGV, Dudek FE, Olson C & Nagy JI (2004) High-resolution proteomic mapping in the vertebrate central nervous system: Close proximity of connexin35 to NMDA glutamate receptor clusters and co-localization of connexin36 with immunoreactivity for zonula occludens protein-1 (ZO-1). J Neurocytol 33:131-152.

Rash JE, Olson CO, Davidson KGV, Yasumura T, Kamasawa N & Nagy JI (2007a) Identification of connexin36 in gap junctions between neurons in rodent locus coeruleus. Neuroscience 147, 938-956.

Rash JE, Olson CO, Pouliot WA, Davidson KGV, Yasumura T, Furman CS, Royer S, Kamasawa N, Nagy JI & Dudek FE (2007b) Connexin36 vs connexin32, "miniature" neuronal gap junctions, and limited electrotonic coupling in rodent suprachiasmatic nucleus. Neuroscience 149, :350-371.

Schroder HD (1980) Organization of the motoneurons innervating the pelvic muscles of the male rat. J Comp Neurol 192, 567-587.

Sengelaub DR & Arnold AP (1986) Development and loss of early projections in a sexually dimorphic rat spinal nucleus. J Neurosci 6, 1613-1620.

Sengelaub DR & Forger NG (1986) The spinal nucleus of the bulbocavernosus: Firsts in androgen-dependent neural sex differences. Horm Behav 53:596-612.

Senkowski D, Schneider TR, Foxe JJ & Engel K (2008) Crossmodal binding through neural coherence: implications for multisensory processing. Trends Neurosci 31, 401-409.

Söhl G, Degen J, Teubner B & Willecke K (1998) The murine gap junction gene connexin36 is highly expressed in mouse retina and regulated during brain development. FEBS Lett 428, 27-31.

Söhl G, Odermatt B, Maxeiner S, Degen J, Willecke K (2004) New insights into the expression and function of neural connexins with transgenic mouse mutants. Brain Res Rev 47:245-259.

Söhl G, Maxeiner S & Willecke K (2005) Expression and functions of neuronal gap junctions. Nat Rev Neurosci 6, 191-200.

Singer W (1999) Neuronal synchrony: a versatile code for the definition of relations? Neuron 24, 49-65.

Takahashi, K. & Yamamoto, T (1979) Ultrastructure of the cell group X of Onuf in the cat sacral spinal cord. Z. Mikrosk. Anat. Forcsh., 93, 244-256.

Van Keuren ML, Gavrillina GB, Filipiak WE, Zeidler MG & Saunders TL (2009) Generating transgenic mice from bacterial artificial chromosomes: transgenesis efficiency, integration and expression outcomes. Transgenic Res 18, 769-785.

van der Want, JJL, Gramsbergen A, Ijema-Paassen J, de Weerd H & Liem RSB (1998) Dendro-dendritic connections between motoneurons in the rat spinal cord: an electron microscopic investigation. Brain Res 779, 342-345.

Vivar C, Traub RD, Gutierrez R (2012) Mixed electrical–chemical transmission between hippocampal mossy fibers and pyramidal cells. Eur J Neurosci 35:76–82.

Walton KD & Navarette R (1991) Postnatal changes in motoneurone electronic coupling studied in the in vitro rat lumbar spinal cord. J Physiol 433, 283-305.

Watson C, Paxinos G & Kayalioglu G (2009) The spinal cord; A Christopher and Dana Reeve Foundation Text and Atlas. Academic Press, Amsterdam.

Wee BEF & Clemens LG (1987) Characteristics of the spinal nucleus of the bulbocavernosus are influenced by genotype in the house mouse. Brain Res 424:305-310.

Wellershaus K, Degen J, Deuchars J, Theis M, Charollais A, Caille D, Gauthier B, Janssen-Bienhold U, Sonntag S, Herrera P, Meda P & Willecke K (2008) A new conditional mouse mutant reveals specific expression and functions of connexin36 in neurons and pancreatic beta-cells. Exp Cell Res 314:997-1012.

Whittington MA & Traub RD (2003) Interneuron diversity series: inhibitory interneurons and network oscillations in vitro. Trends Neurosci 26, 676-682.

Zuloaga DG, Morris JA, Monks DA, Breedlove SM & Jordan CL (2007) Androgen-sensitivity of somata and dendrites of spinal nucleus of the bulbocavernosus (SNB) motoneurons in male C57BL6J mice. Horm Behav 51:207-212.

Figure legends

Fig. 1. Overview of sexually dimorphic motor nuclei in relation to immunofluorescence labelling for Cx36 and vglut1 in transverse spinal cord sections of adult male rat. Motoneurons are labelled for peripherin, pseudo colored sky blue to better visualize motor nuclei (A), or deep blue to better visualize Cx36 and vglut1 (B-E). (A) Bilateral view at a lower lumbar level showing locations of, and labelling for Cx36 in, the DMN, DLN, RDLN and VN. (B-E) Images showing relative densities of labelling for Cx36 and/or vglut1, with dense labelling in the DMN and DLN (B-D) and moderate in the VN (B). Sparse labelling is seen in the RDLN, as shown at a caudal level (C) and a more rostral level (D), with labelling for Cx36 shown alone (D1) and after overlay with labelling for peripherin (D2). Labelling for vglut1 is largely absent in the DMN and DLN (C,D2), and is of moderate density in the RDLN (C,D2). (E) Comparison of the absence of vglut1-terminals in DLN (arrow) *vs.* their presence in an adjacent unidentified motor nucleus (arrowhead).

Fig. 2. Immunofluorescence labelling of Cx36 in association with peripherin-positive motoneurons in horizontal sections through the DMN and DLN of adult rat and mouse. (A) The DMN in rat, showing intermittent clusters of motoneurons (arrowheads), with some of these neurons having contralaterally projecting dendrites. Midline is shown by dotted line. Cx36-puncta are seen densely concentrated along appositions between motoneuronal somata in the clusters (small arrows) and along bundles of intermingled dendrites spanning the midline (large arrows). (B1,B2) The same field of the DLN in rat, showing overlay of labelling for peripherin and Cx36, where Cx6-puncta are seen associated with nearly all motoneurons (B1), and labelling for Cx36 alone, where a similar density of Cx36-puncta is seen in the medial (lower half of field) and lateral (upper half of field) portions of the nucleus (B2) containing ischiocavernosus and urethral sphincter motoneurons, respectively. (C,D) The DMN (C) and DLN (D), showing in each nucleus a similarly large proportion of motoneurons invested with Cx36-puncta as seen in rat. (E,F) Images of the DLN from a wild-type mouse showing the same field labelled for peripherin and Cx36 (E1,E2), and from a Cx36 knockout mouse showing the same field with absence of Cx36 among peripherin-positive motoneurons (F1,F2).

Fig. 3. Confocal triple immunofluorescence demonstrating patterns of Cx36-puncta and vglut1-terminals associated with motoneurons in DMN, DL, and RDLN in transverse sections of adult male rat spinal cord. (A,B) Images at a caudal level of the DMN, showing closely apposed peripherin-positive motoneurons, with Cx36-puncta lining dendrites directed either horizontally across the midline (A, arrow) or directed dorsally and laterally (B, arrows) in the vicinity of the central canal (cc). (C-F) Magnifications of clusters of motoneuron somata in the caudal DMN (C), rostral DMN (D,E) and DLN (F), showing punctate appearance of labelling for Cx36 and absence of diffuse intracellular labelling for Cx36. Also evident are both large heterogeneously sized patches of Cx36 immunofluorescence (C,D, arrowheads), dispersed Cx36-puncta (F, double arrows), Cx36-puncta localized around the periphery of motoneurons (single arrows). (G-I) Images of the DMN, showing Cx36-puncta localized at soma-somatic (G, arrow; also shown in inset), dendro-somatic (H, arrow; boxed area magnified in inset), and dendro-dendritic (I, arrow; and inset) appositions between peripherin-positive motoneurons. (J) Magnification of a peripherin-positive motoneuron in the DMN, showing large patches of labelling for Cx36 (arrows), consisting of clusters of individual Cx36-puncta (one cluster shown in inset). (K) Magnification of the RDLN, showing sparse distribution of vgut1-terminals among motoneurons, and Cx36-puncta with (boxed area, shown separately as green and red labels in inset) and without (arrow) co-localization at vglut1-terminals. All other images (A-J) show only occasional association of vglut1-terminals with the somata or initial dendrites of peripherin-positive motoneurons.

Fig. 4. Immunofluorescence labelling of Cx36 associated with peripherin-positive motoneurons in the DMN, DLN and RDLN in transverse sections of male rat spinal cord at PD9 (A-D) and PD15 (E-N). (A-D) At PD9, Cx36-puncta are seen throughout the ventral horn, with moderate levels in the RDLN (A, arrowhead) and slightly higher concentrations in the DLN (A, arrow), which contains both coarse (B, arrowhead) and fine puncta (B, arrows). Low levels of Cx36-puncta are seen in the DMN in association with neuronal somata (C, arrow) and dendrites (D, arrow). (E-G) Low magnifications of labelling for Cx36 in the DMN and DLN at PD15. Clusters of motoneurons located dorsally (E, arrow) and ventrally (E, arrowhead) at a rostral level of the

DMN display intermingling of their dendrites (E, boxed area), and a similar cluster at a more caudal level displays numerous laterally directed dendrites (F, boxed area). Cx36-puncta are densely distributed in the DMN (E,F) and DLN (G), and moderately in regions surrounding the DMN (E,F). (H,I) Magnifications of the boxed areas in E and F, respectively, showing Cx36-puncta among intermingled dendrites emerging from clusters of motoneurons (H, arrows), and puncta among laterally directed dendrites (I, arrows). (J,K) Images of DMN motoneurons with dorsally directed dendrites (J, arrowheads) and with a thick bundle of dendrites traversing ventrolaterally (K, arrowhead), showing Cx36-puncta along proximal as well as more distal dendritic segments (arrows). (L-N) Images of the RDLN, showing Cx36-puncta dispersed (L,M, single arrows) and in patches (L,M, single arrowheads) on motoneuron somata and dendrites, and Cx36-puncta at points of dendritic intersections (M, double arrow and boxed area in M, magnified in N). Also evident are very fine puncta on dendrites and neuronal somata (L, double arrowhead). (O) Image showing very fine Cx36-puncta (arrows) on neuronal somata in the DLN, shown with labelling for Cx36 alone (magnified from the box area in G).

Fig. 5. Immunofluorescence labelling of Cx36 associated with peripherin-positive motoneurons in the DMN, DLN and RDLN in transverse sections of adult female rat spinal cord. (A) Low magnification showing presence of Cx36-puncta within each of the nuclei (DMN, shown bilaterally). (B,C) Higher magnifications of the DLN, showing densely concentrated Cx36-puncta (B, arrow), absence of labelling for vglut1 (B), and association of Cx36-puncta with motoneuronal somata and dendrites (C, arrows). (D,E) Images of dispersed motoneurons in the RDLN at a caudal level, showing moderate levels of Cx36-puncta and vglut1-positive terminals within the nucleus (D), and higher magnification showing presence of patches of Cx36-puncta associated with peripherin-positive somata and dendrites (E, arrowheads), where they largely lack co-localization with vglut1-terminals. (F) The RDLN at a more rostral level, showing a diminutive cluster of small motoneurons decorated with moderate levels of Cx36-puncta (arrows). (G) Magnification of the DMN from (A), showing a few motoneurons with small somata, thin and short dendrites, and a sparse distribution of Cx36-puncta. (H,I) Magnification of the DMN and RDLN, showing sparse Cx36-puncta, and patches of Cx36-puncta at apposition between peripherin-positive dendrites

Fig. 6. Immunofluorescence labelling of EGFP and peripherin in motoneurons of the DMN, DLN and RDLN in spinal cord of adult male (A-G) and female (J-M) mice (EGFP-Cx36 mice) in which EGFP expression on a bacterial artificial chromosome is driven by the Cx36 promoter. (A) Low magnification showing the distribution of labelling for EGFP (A1) and, in the same field, the distribution of peripherin (A2) in the DMN, DLN and RDLN. (B-D) Images of EGFP-positive motoneurons in the DMN, showing dendritic arborizations directed ventrally (B, arrow) and laterally (C, arrow), and clustering of motoneurons and dendrites in the DLN group (D, arrow). (E-G) Pairs of images (E1,E2), (F1,F2) and (G1,G2) showing the same field in each pair labelled for either peripherin (E1,F1,G1) or EGFP (E2,F2,G2). In each pair, many peripherin-positive motoneurons in the DMN and DLN are also EGFP-positive, but most though not all (G, arrow) of those in RDLN and a few of those in the DMN and DLN are negative for EGFP (arrowheads). (H,I) Higher magnifications of similar pairs of images as in (E-G), showing examples of peripherin-positive motoneurons either labelled (arrows) or unlabelled (arrowheads) for EGFP. (J-M) Images from spinal cord of EGFP-Cx36 female mice, showing only a few EGFP-positive motoneurons per section in the DMN (J, arrows), DLN (K, arrow), and DMN/DLN (M), and the smaller size of these neurons (L,M, arrrows) than seen in males (labelling for peripherin not shown).

Supplementary Figure legends

Fig. S1 movie. Z-stack image of the DMN from Fig. 3J, with 3D rendering and rotation, demonstrating localization of Cx36-puncta and clusters of puncta at the surface of peripherin-positive motoneurons, and at appositions between these motoneurons.

Figure 1

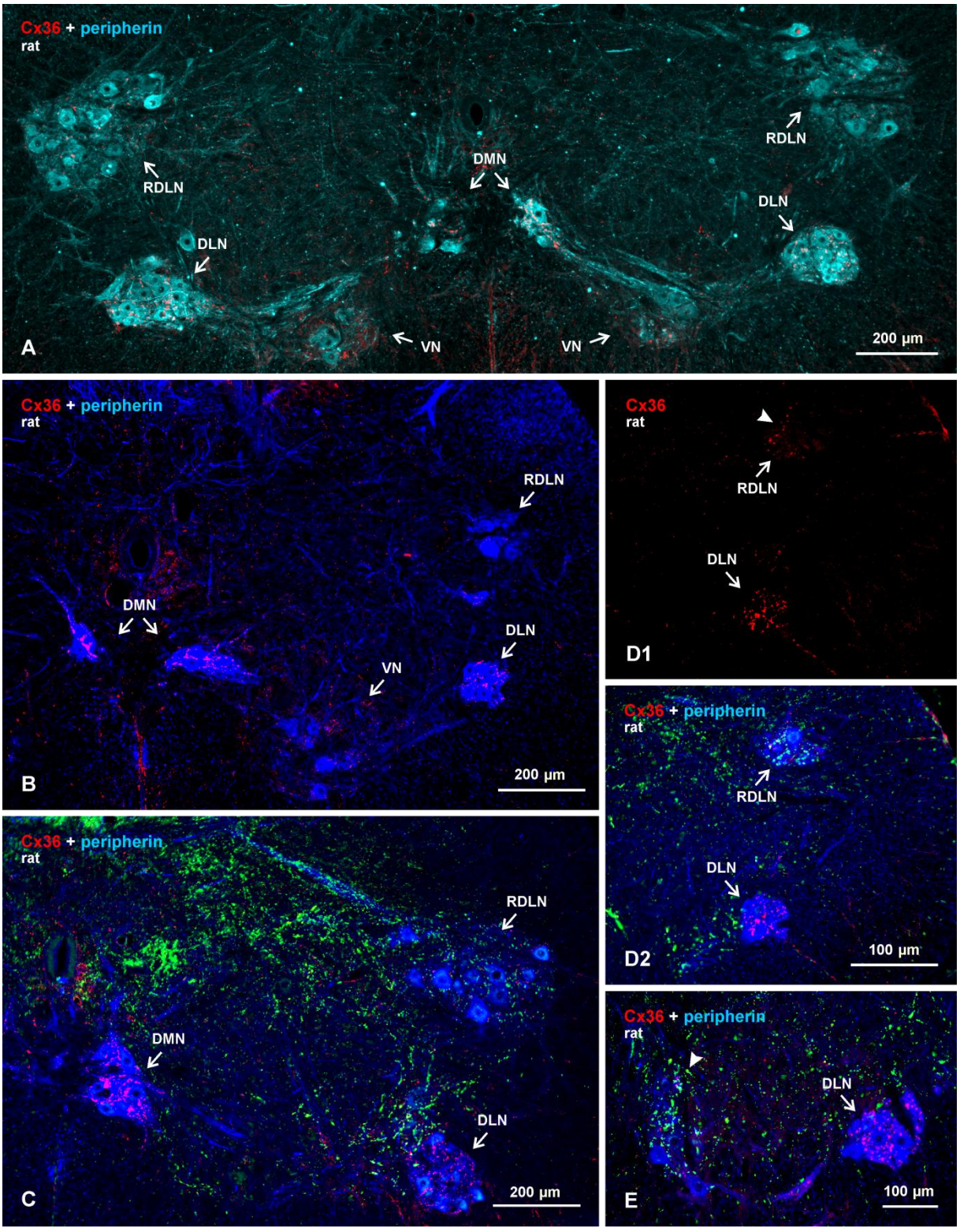
Cx36 + peripherin
rat
RDLN
DMN
RDLN
DLN
DLN
A
VN
VN
200 µm
Cx36 + peripherin
rat
RDLN
DMN
DLN
VN
B
200 µm
Cx36
rat
RDLN
DLN
D1
Cx36 + peripherin
rat
RDLN
DLN
D2
100 µm
Cx36 + peripherin
rat
RDLN
DMN
DLN
C
200 µm
Cx36 + peripherin
rat
DLN
E
100 µm

Figure 2

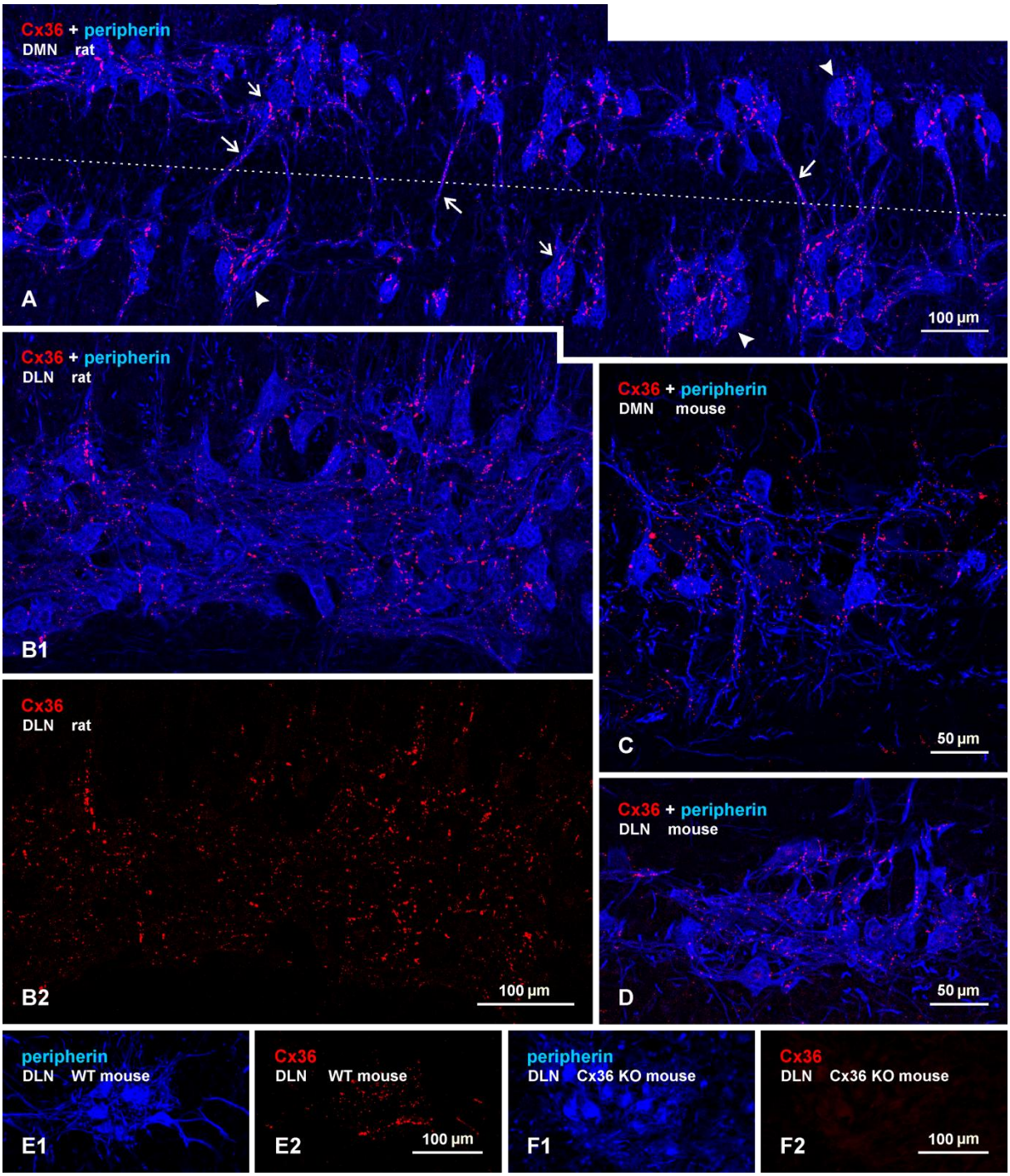
Cx36 + peripherin
DMN rat
A
100 µm
Cx36 + peripherin
DLN rat
B1
Cx36 + peripherin
DMN mouse
C
50 µm
Cx36
DLN rat
B2
100 µm
Cx36 + peripherin
DLN mouse
D
50 µm
peripherin
DLN WT mouse
E1
Cx36
DLN WT mouse
E2
100 µm
peripherin
DLN Cx36 KO mouse
F1
Cx36
DLN Cx36 KO mouse
F2
100 µm

Figure 3

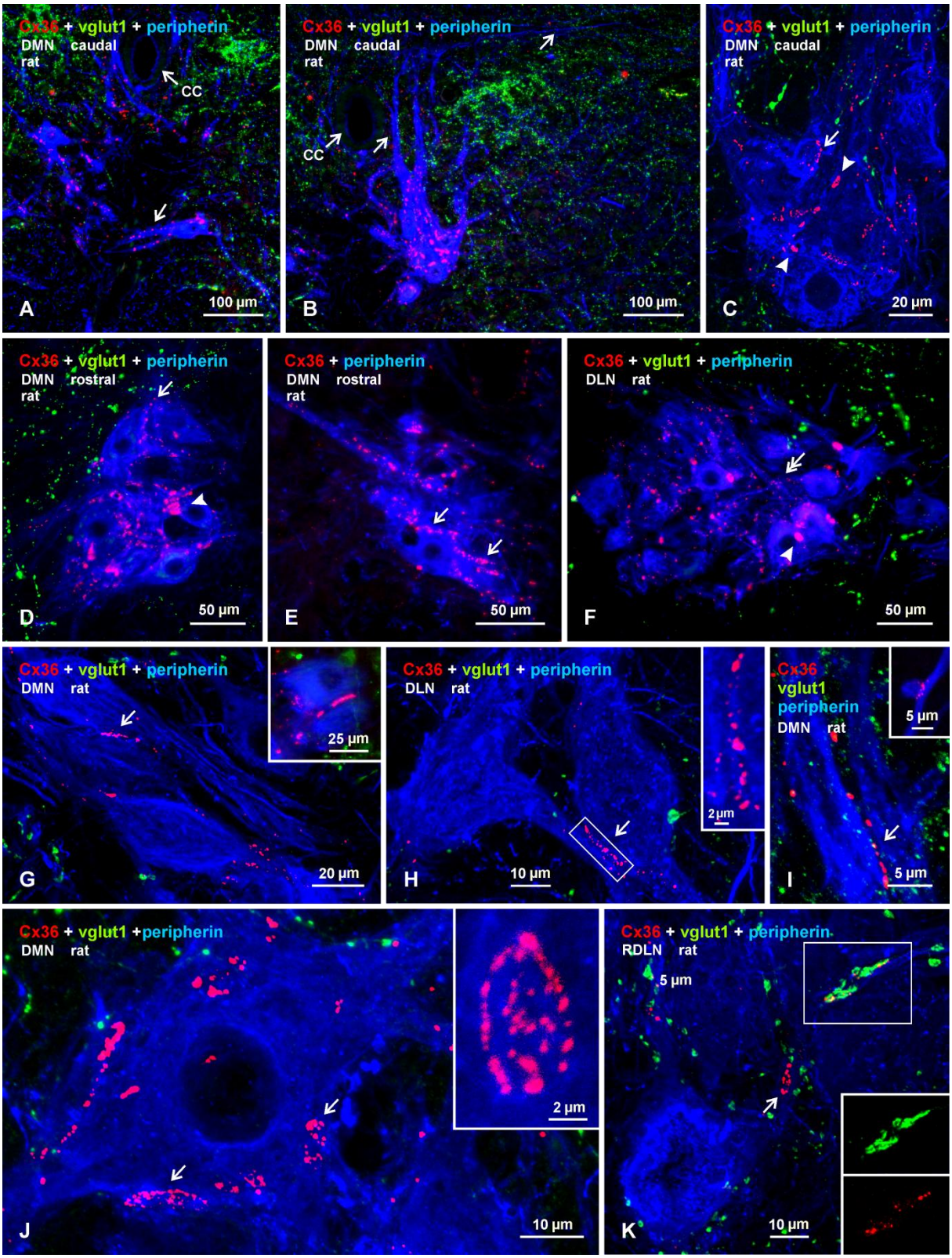
Cx36 + vglut1 + peripherin
DMN caudal
rat
CC
100 µm
A
Cx36 + vglut1 + peripherin
DMN caudal
rat
CC
100 µm
B
Cx36 + vglut1 + peripherin
DMN caudal
rat
20 µm
C
Cx36 + vglut1 + peripherin
DMN rostral
rat
50 µm
D
Cx36 + peripherin
DMN rostral
rat
50 µm
E
Cx36 + vglut1 + peripherin
DLN rat
50 µm
F
Cx36 + vglut1 + peripherin
DMN rat
25 µm
20 µm
G
Cx36 + vglut1 + peripherin
DLN rat
2 µm
10 µm
H
Cx36
vglut1
peripherin
DMN rat
5 µm
5 µm
I
Cx36 + vglut1 +peripherin
DMN rat
2 µm
10 µm
J
Cx36 + vglut1 + peripherin
RDLN rat
5 µm
10 µm
K

Figure 4

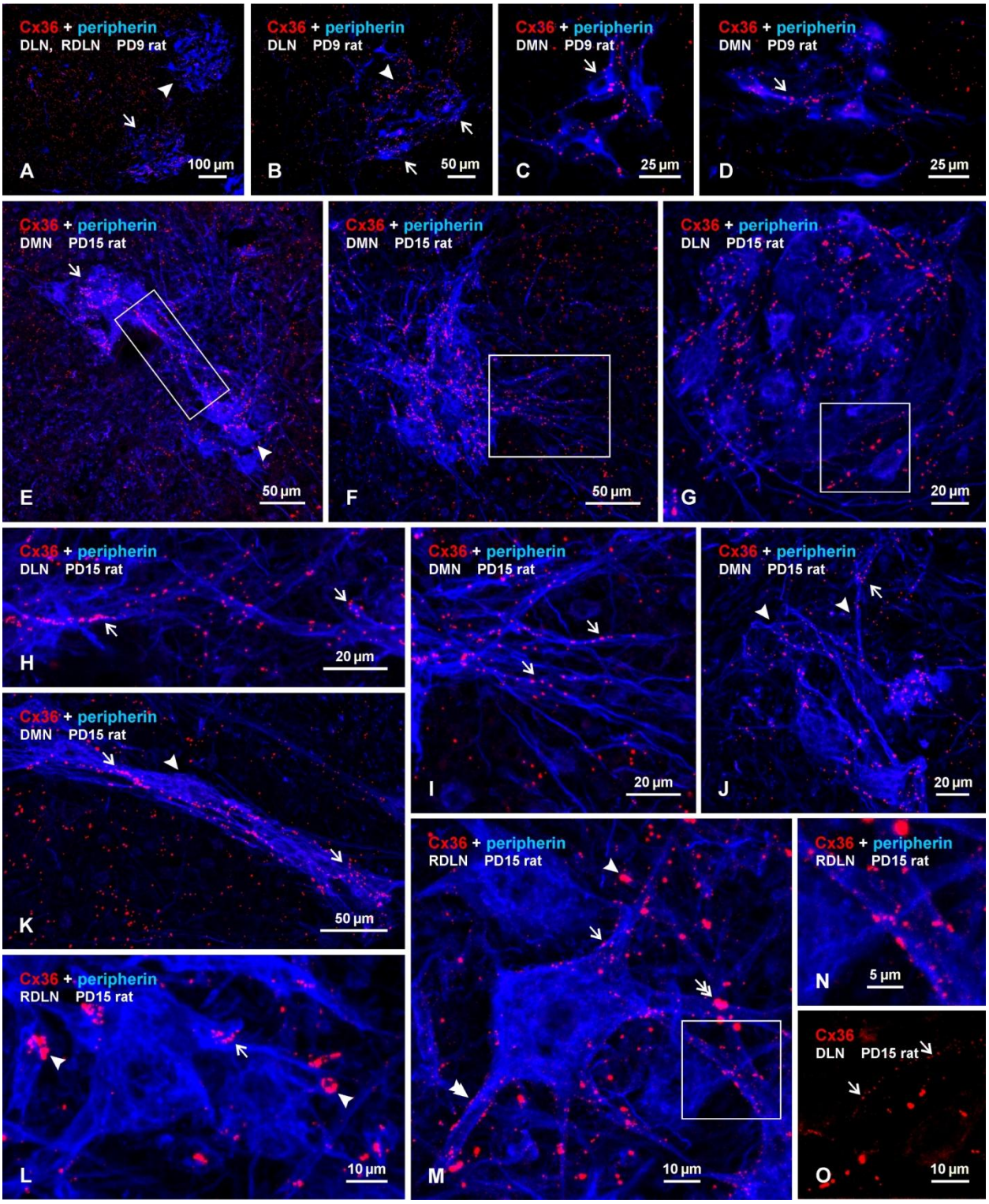
Cx36 + peripherin
DLN, RDLN PD9 rat
A
100 µm
Cx36 + peripherin
DLN PD9 rat
B
50 µm
Cx36 + peripherin
DMN PD9 rat
C
25 µm
Cx36 + peripherin
DMN PD9 rat
D
25 µm
Cx36 + peripherin
DMN PD15 rat
E
50 µm
Cx36 + peripherin
DMN PD15 rat
F
50 µm
Cx36 + peripherin
DLN PD15 rat
G
20 µm
Cx36 + peripherin
DLN PD15 rat
H
20 µm
Cx36 + peripherin
DMN PD15 rat
I
20 µm
Cx36 + peripherin
DMN PD15 rat
J
20 µm
Cx36 + peripherin
DMN PD15 rat
K
50 µm
Cx36 + peripherin
RDLN PD15 rat
L
10 µm
Cx36 + peripherin
RDLN PD15 rat
M
10 µm
Cx36 + peripherin
RDLN PD15 rat
N
5 µm
Cx36
DLN PD15 rat
O
10 µm

Figure 5

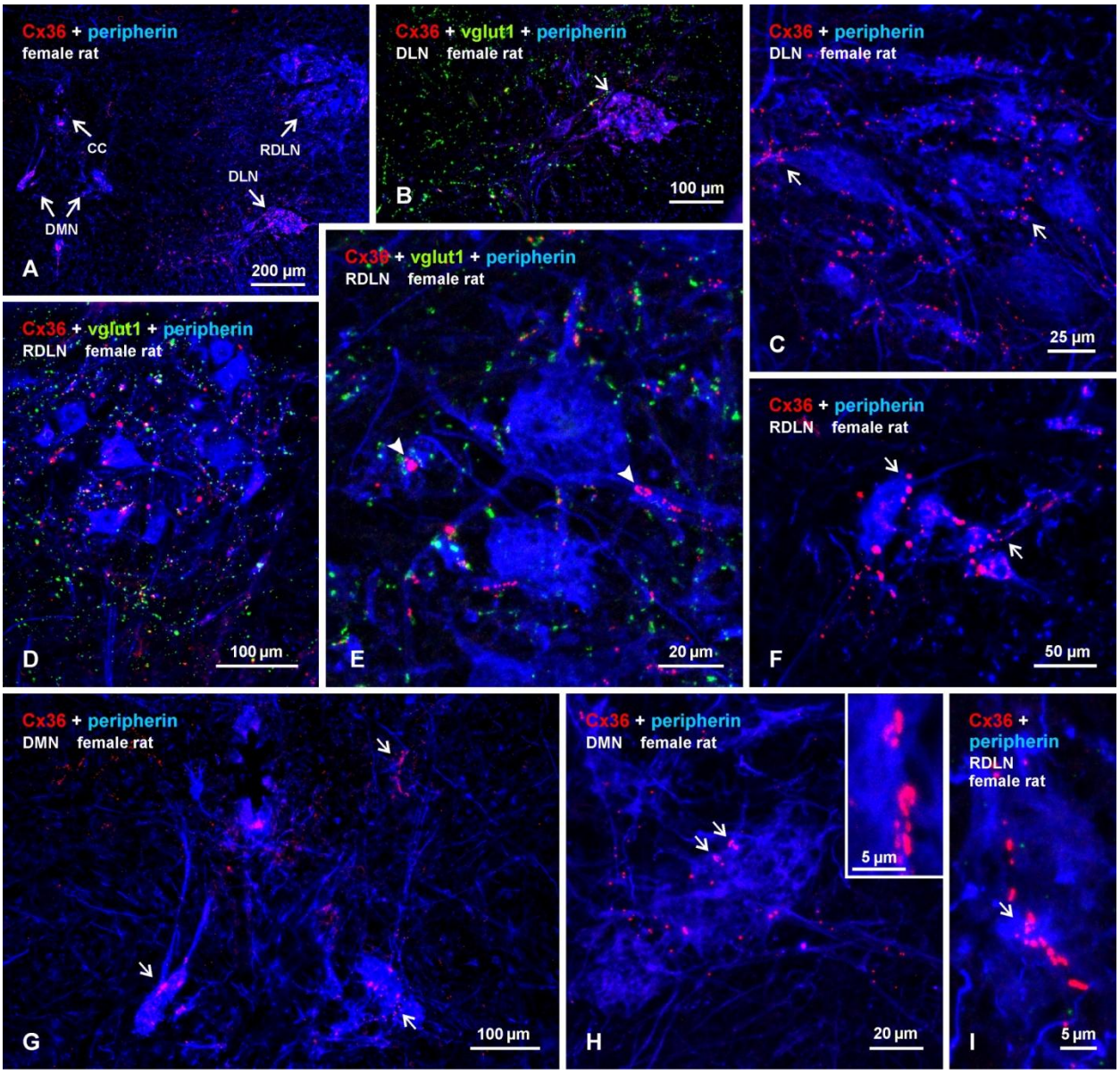
Cx36 + peripherin
female rat
CC
RDLN
DLN
DMN
A
200 µm
Cx36 + vglut1 + peripherin
DLN female rat
B
100 µm
Cx36 + peripherin
DLN female rat
C
25 µm
Cx36 + vglut1 + peripherin
RDLN female rat
D
100 µm
Cx36 + vglut1 + peripherin
RDLN female rat
E
20 µm
Cx36 + peripherin
RDLN female rat
F
50 µm
Cx36 + peripherin
DMN female rat
G
100 µm
Cx36 + peripherin
DMN female rat
H
20 µm
5 µm
Cx36 + peripherin
RDLN
female rat
I
5 µm

Figure 6

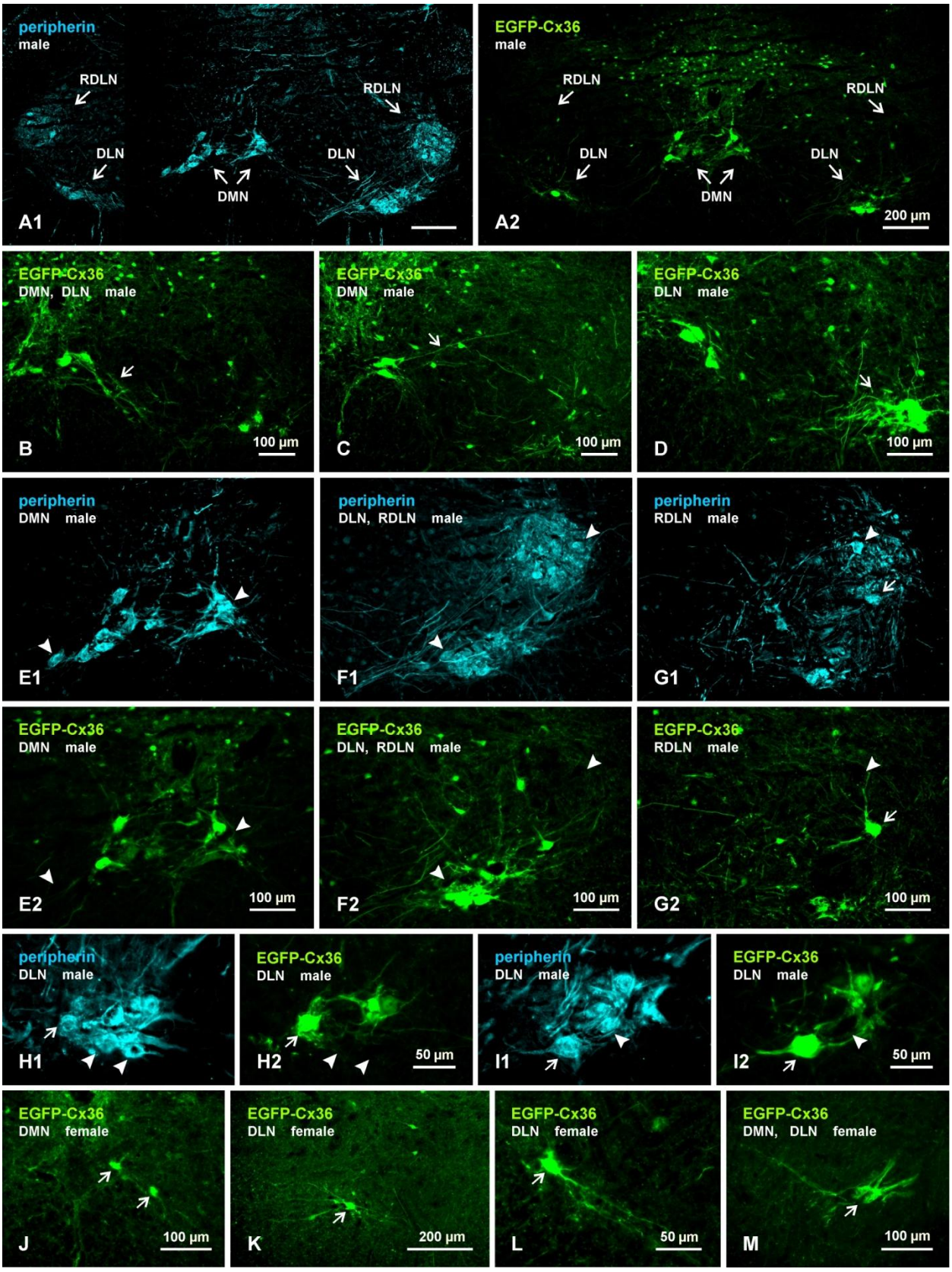
peripherin
male
RDLN
RDLN
DLN
DLN
DMN
A1
EGFP-Cx36
male
RDLN
RDLN
DLN
DLN
DMN
200 µm
A2
EGFP-Cx36
DMN, DLN male
B
100 µm
EGFP-Cx36
DMN male
C
100 µm
EGFP-Cx36
DLN male
D
100 µm
peripherin
DMN male
E1
peripherin
DLN, RDLN male
F1
peripherin
RDLN male
G1
EGFP-Cx36
DMN male
E2
100 µm
EGFP-Cx36
DLN, RDLN male
F2
100 µm
EGFP-Cx36
RDLN male
G2
100 µm
peripherin
DLN male
H1
EGFP-Cx36
DLN male
H2
50 µm
peripherin
DLN male
I1
EGFP-Cx36
DLN male
I2
50 µm
EGFP-Cx36
DMN female
J
100 µm
EGFP-Cx36
DLN female
K
200 µm
EGFP-Cx36
DLN female
L
50 µm
EGFP-Cx36
DMN, DLN female
M
100 µm

Fig S1 Movie

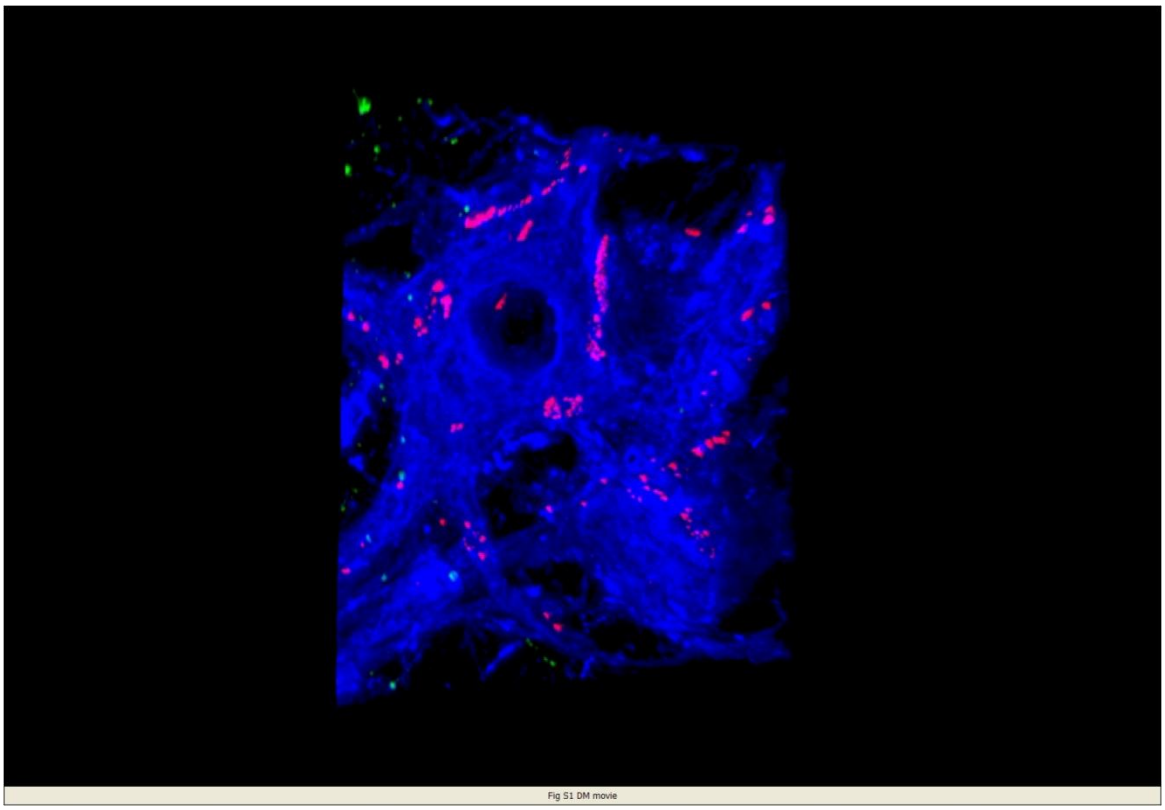

General discussion

The present thesis focuses in the demonstration of two novel ideas, the first one proposes that Cx36 containing gap junctions participate in the neuronal networks involved in presynaptic inhibition of the sensory reflexes in juvenile mice. The second one demonstrates the existence of mixed synapses between sensory afferents and motoneurones occurring mainly in the adult rat spinal cord, although at first instance these revealing results seemed rather contradictory to the idea that electrical synapses may enhance synchrony and efficacy of neuronal networks especially the ones containing inhibitory interneurones. Now we know that these results could be in fact complementary. Presynaptic inhibition of sensory reflexes occurs through a disynaptic pathway involving a population of gabaergic and glutamatergic interneurones that selectively decrease transmission in one set of primary afferents. Our results show that Ia afferents forming mixed synapses with motoneurones are subject to presynaptic inhibition, since we observed the presence of P boutons on these terminals. This suggests a dual mode to control motoneurone output once sensory information arrives, 1) involving the spread and distribution of the information to neighbour segments controlling output from several motor pools and 2) gating the speed of inhibition via neuronal gap junctions by propagating the depolarization caused by GABAA receptors in the presynaptic terminal towards the motoneurone postsynaptic membrane. Acting in similar mode as the trigeminal system where primary afferents are presumably acting as excitatory neurons(see introduction). This depolarization in theory would cause several effects in the motoneurone; one of them would be an overall increase of excitablility that leads to inactivation of voltage activated calcium and sodium channels that lead to a decrease in the size of the action potential. The depolarization wave propagated to the motoneurone would also trigger calcium entrance by glutamate receptors as it occurs after the activation of glutamate receptors triggered by an action potential, and will also prime the activation of NMDA receptors since these require depolarization to relieve Mg^{2+} blockade, taking the motoneurone to a state of lower threshold and allowing the recruitment of larger populations of motoneurones. This is in agreement with recent results that show that after deafferentation and removal of descending inputs to motoneurones in the adult rat results on a decrease in threshold, reduction of AHP and input resistance, (Button et al 2008) according to our results this will also eliminate mixed synapses on motoneurones. Then the fact that there is a change in the threshold could be attributed to the lack of mixed synapses between the afferents and the motoneurones, as we have

demonstrated in our results (section 2). In addition it has also been suggested that after the removal of all descending and afferent input a change of the intrinsic properties of fast motoneurones resemble the properties of the slow motoneurones (Button et al 2008). These evidences suggest that intrinsic motoneurone properties could potentially be influenced by the activation of mixed synapses.

The state of activation of these two modes of transmission would depend on the task and

the state of the reflexes; in this way they would serve as sensor mechanisms that determine,

depending in the sensory information provided by the afferents, if the duration of motoneurone

output should be decreased or enhanced.

Although the role of mixed synapses in the mammalian CNS has not been clearly defined, studies in non-mammalian systems show that mixed synapses have a role in enhancing the speed of chemical transmission as well as maintaining the synapse, in the Goldfish Mauthner cell mixed synapses enable plastic changes in the postsynaptic side such as LTP (Pereda et al, 2013).

The search for electrical interactions between presynaptic terminals and motoneurones started with the electrophysiological studies made in the cat spinal cord by Decima and Goldberg (1970) where antidromic stimulation of motneurones via ventral roots resulted in a early discharge in some dorsal root afferents. These authors refined their electrophysiological techniques and discovered that only a number of motoneurones in the whole segment needed to be activated in order to observe a dorsal root discharge in a single Ia afferent (Decima and Golberg 1973), with these studies these authors concluded that for this interaction to occur there is no requirement of massive activation of motoneurones nor synchronous conditioning stimulation indicating that these will only be activated during single events where motoneurones become active. This evidence became refuted at the time since subsequent studies (Gutnick et al, 1975) aimed to reproduce their findings, appareantly using similar conditions, showed no success. However these authors recognized that they were able to detect minor changes in excitability for both antidromical and ortodromical directions, in what they recalled surprising short latencies starting at 1ms and lasting 0.3 ms after ventral root volleys, however they concluded that the source could also be artefactual. A reboutal to this conclusion was released by Decima and Golberg

(1976) on the basis that both studies observed similar latencies for dorsal root discharges. According to these studies this depolarization could only be caused by the discharge produced in the motoneurones. These findings were later confirmed by Curtis (1981) that demonstrated backfiring of the Ia afferents produced at the same time as the Ia EPSP, this depolarization travel antidromically and produced an increase of PAD. Curtis (1979) revealed that the source of the electrical current passing to the afferents was not derived from the extracellular motoneurone activity, but instead was produced by the firing from the initial segment of motoneurones, according to these findings backfiring of motoneurones produced a 3-19% decrease on the threshold of the presynaptic terminals with a latency between 0.2-0.3 ms and a duration of 0.34 ms, these latencies seem to correspond to the earliest components of the antidromic action potential recorded intracellularly in the motoneurones (Curtis, 1979). Although no conclusive evidence yet exists, it has been suggested that this depolarization travelling antidromically could also produced an increase of PAD (Curtis, 1979). Remarkably, our anatomical findings in section 3 of this thesis show co-localization of P boutons in Vglut-1/Cx36 positive terminals, and provide the first morphological correlate for this proposal. This means that, mixed synapses are involved in PAD produced during presynaptic inhibition.

The studies by Decima and Goldberg (1970, 1973) proposed that an increase in the excitability of the presynaptic terminal is generated by membrane currents during the generation of the action potential, indicating that there is a local source of inward ion current flow making the motoneurone postsynaptic membrane to act as a source that would eventually lead to spread to the synaptic bouton resulting in a low resistance access to the extracellular space where if there is a node then outward current would be greater than the inward current at the apposition terminal allowing depolarization to be spread to the region of the outward current. The amount of depolarization can be influenced on the resistance of the presynaptic terminal and the postsynaptic terminal, as well as other anatomical factors such as total postsynaptic membrane area covered by presynaptic terminals from single afferents, their location, separate boutons arising from single afferents lectrically coupled in the preterminal network so that all of the boutons contribute to the depolarization if all are activated at the same time or if all of these undergo PAD during conditioning stimulation(Kuno,1964), then we would expect that only a few afferent motoneurone would be needed in order to produce depolarization of the afferent terminals.

Biophysical calculations using cable theory have also predicted that the large capacitance of the postsynaptic terminal makes any change created in the presynaptic terminal hardly detectable after an impulse invade the presynaptic bouton, nonetheless a number of solutions have addressed this problem and have come up with the calculation that if the specific resistivity of the postsynaptic membrane becomes 100 times lower than the average motoneurone resistivity in the rest of the motoneurone surface then this must imply the existence of junctional coupling or specializations at the synaptic cleft in these terminals (reviewed Redman 1979).

Regardless of the fact that concise electrophysiological evidence in rodent spinal cord does not yet exist, it is important to mention that one of the few examples where anatomical and electrophysiological evidence was first found in mammals for mixed synapses comes from the LVN of the adult rat (Korn et al 1973).

Although the role of mixed synapses in the mammalian CNS has not been clearly defined, studies in non-mammalian systems like the frog spinal cord showed that electrotonic dorsal root potentials are caused by antidromic invasion of motoneurones it has also been identified an electrical component preceding the motoneurone Ia EPSP (Carpenter and Rudomin 1973, Katz and Miledi, 1963; Shapovalov 1977). This electrotonic potential has not been found in adult mammalian preparations, however it has been suggested that this could be explained to the anatomical differences observed between these two species, frog motoneurones extend their dendrites quite dorsally reaching dorsal horn this is the site where these afferents terminals are located, meanwhile cat motoneurones extend their dendritic projections more ventral and medial perhaps reflecting the need for interneurone modulation in the cat whereas in the frog the afferents are serving as modulatory interneurones avoiding a synaptic delay needed for their fast responses. Other species where mixed synapses have a role in enhancing the speed of chemical transmission as well as maintaining the synapse is the case of the Goldfish Mauthner cell, here the electrical component of the EPSP occurs at a latency between 500 to 800 μs and is larger than the chemical component. Mixed synapses in this system enable LTP and plastic changes in the postsynaptic side (Pereda et al 2013). Due tothe absence of any evidence showing electrical component in motoneurone EPSP's in adult mammals, perhaps because the duration of the electrical component is close to a quarter of a milisecond, very few studies acknowledge the

possibility that an electrical interaction between motoneurones and primary afferents might even be functional, nonetheless we hope our study will contribute to the acceptance of previous evidence on this topic and provide with new insight for the future study of motoneurones and afferents.

Would the expression of PAD to motoneurones via gap junctions excite or inhibit motoneurone firing?

The outcome would depend on the onset and duration of PAD and the state of motoneurones at the time of PAD arrival. Activation of PAD at the primary afferent terminal if the gap junctions are open would cause that depolarization travel antidromically resulting in back propagated firing and further enhance on the reduction of neurotransmitter release by increasing PAD. If at the same time this depolarization travels orthodromically to the postsynaptic side at the motoneurones, this would result in an increase of excitability and increase in motoneurone firing annulating PAD and blocking presynaptic inhibition. The interplay and balance of critical factors such as the percentage of gap junctions open and also the state of both pre and postsynaptic terminals allow me to predict that at least 4 different outcomes can occur: 1) enhancement and prolongation of PAD, 2) cancelation of PAD when the amount of inhibition is equal to the excitation and 3) increased excitation and motoneurone firing when PAD is not active 4) motoneurone firing when PAD is active exceeding the blockade of neurotransmitter release, interestingly this outcome would allow motoneurones to fire even in conditions where synaptic transmission is blocked by PAD.

These four scenarios are likely to result from the influence of the intrinsic capacity for modifying transmission strength inherent to the IA-motoneurone synapse or be expressed after diverse conditions affecting gating of electrical synapses such peripheral nerve crush, axotomy, (Chang et al, 2000) denervation, chronic inflammation or spasticity (Yates et al, 2009) where a number

of injury signals in the terminals have been discovered (Kuno, 1995; Cope et al., 2001, Bichler et al 2007).

Mixed synapses formed by afferents in the spinal cord

Section 3 of this thesis also show that primary afferents ending in motoneurones. Previous studies (Alvarez et al 2004) looking at the distribution of Vglut-1 terminals shows that these are distributed in three main locations in the spinal cord: 1) dorsal horn lamina I and II o, 2) deep medial dorsal intermediate lamina V-VI, 3) medial lamina VI-VIII and LIX. Our results are in agreement with these studies and show that 40% of the total Cx36-positive puncta is co-distributed and co-localized in the regions of vglut1 terminal endings in laminae V-VI, lamina VII, VIII and IX. Remarkably we found that mixed synapses are also formed by Ia afferents vglut-1 positive terminals ending in motoneurones in lamina IX. In addition a group of interneurones with primary afferent terminals and mixed synapses were found to be distributed in clusters along the spinal cord in medial lamina VII (PACx domains), from C1 segment to S3 each cluster of interneurones followed the arborization pattern of primary afferents. Since these interneurones were negative for cholinergic or gabaergic markers and based on size, we assume that these interneurones with mixed synapses located in medial lamina VII are glutamatergic interneurones. Functional classification of these interneurones by their pattern of distribution and primary afferent contact would reveal that these are among a subset of propiospinal interneurones. However, further studies allowing *in vivo* recording of these interneurones and characterization of their input are needed in order to establish definitive conclusions.

Previous studies in the LVN propose that one of the reasons for mixed synapses to exist is to couple axon terminals of collaterals of the same afferent; this would allow spread of depolarization from one neuron to the other via axon terminals that are communicated with neurons (see Fig 3). In the cat HRP studies have demonstrated that Ia afferents form 10 to 50 collaterals that innervate 300 motoneurones (Brown and Fyffe 1978, Brown and Fyffe 1981). In a study by Mendell and Henneman 1971, EPSP's recorded in motoneurones from single Ia fibers show differences in amplitude, rise time and decay time depending on the location of the

terminals. This mode of transmission might allow coupling between motoneurones by their axon collateral terminals, increasing the rate of recruitment.

In our study vglut1 terminals ranged in size from 3.9 to 4.4 um in diameter, previous studies by Pierce and Mendell with HRP injection in Ia afferents in the cat show different size and shape modalities for the Ia boutons, these boutons are seen in ovoidal shape, and their sizes ranges from 0.7 to 7.2um in the long axis and 0.7 to 2.8 um along the short axis, with a mean area of 6.5um3. In our study we found heterogeneity in the shapes and volumes depending on the location, vglut1 terminals found closer to the soma were generally more flattened and ovoid, whereas vglut1 terminals approaching the distal dendrites appear rounded in shape. Our results are in agreement with differences in shape and size reported in Ia boutons located in Clarke's column (Nicol and Walmsley 1991), and motoneurones (Pierce and Mendell 1993).

According to previous ultrastructural studies by Pierce and Mendell (1993) the largest ovoidal shape terminals correspond to Ia boutons, these Ia boutons also presented P-butons on top arranged perpendicular to the postsynaptic membrane, according to these studies 63% of the Ia boutons contacting motoneurones were seen associated with more than one P bouton, one example shows one terminal having up to eight P boutons contacting one Ia terminal, 23 % were associated with one and 14% did not had P boutons. P boutons represent 0.5 – 18.5 % of the total surface area (Pierce and Mendell 1993). It has been estimated that the mean synaptic surface area of a Ia bouton is 6.8 um, representing an average of 31.8% of the total surface, meaning that at least 70% of the terminal is not on apposition to the postsynaptic membrane, the synaptic surface area contains also the active zones where the neurotransmission takes place. Our study demonstrates that the size of Cx36 positive puncta associated with Vglut1 terminals is in average of 0.2 to 0.4 um. Remarkably ultrastructure studies made in the HRP filled Ia terminals have also pointed out that some Ia boutons showed a gap in the center of the synaptic surface (0.18um wide), and in others small postsynaptic invaginations and knobs (0.2-0.4um) have been observed in the postsynaptic membrane, often associated with the active zones, this evidence overlaps with the size of the Cx36 positive puncta seen in the Vglut-1 terminals in our study, our confocal analyses of a Vglut-1 terminal associated with Cx36 positive puncta shows, in the 3-D rendering mode, a similar configuration to the one found by these studies, suggesting that this configuration of Ia terminals in the cat might correspond to spaces formed by gap junctions. We

estimate the presence of active zones in the vglut1 terminals associated with Cx36 positive puncta measured by the amount of basson (marker for active zones) positive puncta (not shown), the average of active zones per Ia terminal found in a study by Pierce and Mendell 1993 is 6.1 +- 4.8,where, symmetrical shapes counted for 79.5%, 17% show elongated shape and 2% and 1.5% were partially split and perforated, interestingly, the size of the perforation in the latter correspond to the mean size of Cx36 positive puncta, and the spaces between the partially split might correspond to a set of Cx36 positive puncta intermingled within the active zone area. However further ultrastructural studies need to be made in order to confirm the presence of neuronal gap junctions in cat motoneurones.

Although it is known that vesicle size also varies, these studies show vesicle size ranged from 60 – 80 nm. Terminal volume and vesicle number decreased in relation to the position of the arborization, being higher at the proximal sites and decreasing at more distal sites. This is certainly the case for the density of Vglut-1 terminals in central canal neurons where there is higher density of the terminals compared to motoneurones; this would be true assuming that they are being innervated by the same fiber.

Location of mixed synapses Ia synapses with respect to mixed synapses found on motoneurones

Mixed synapses were found at the intial somatodendritic compartment, although we are aware that vglut-1 positive terminals do not necessarily represent Ia terminals, since vglut-1 immunostaining does not distinguish between the different classes of afferents, we can only say that according to the size of the terminals, larger than 3.5 um, (Alvarez et al 2004) and their location on motoneurones, (Brown and Fyffe 1981) then we can assume that these terminals include Ia afferents. Nonetheless, definitive evidence would require a better marker for distal dendrites than the one used in our study since peripherin only labelled soma and proximal dendrites. Retrograde labelling using rhodamine or intracellular injection of HRP or biocityn combined with the double labelling for Cx36 and vglut1 would resolve this question.

Our results obtained with labelling of these terminals on peripherin positive motoneurone dendrites are in agreement with the extensive evidence demonstrating that Ia afferents terminals are located within the anatomical proximal somatodendritic compartment (Redman and Wamsley

1983) indicating that synaptic location calculated from cable properties agrees with anatomical synaptic location and the calculated time constant of 0.5 □ correspond to 250 to 400 □m distance from the soma in cat motoneurones (Redman and Walmsley 1983). Our results of mixed synapses located on rat lumbar motoneurones show distances in the range of 100-150 □m from the soma, time constants for these terminals have not been calculated in the rat. Proximity of these vglut-1 positive terminals to the first dendritic compartment is in support that these mixed synapses on motoneurones represent Ia terminals. Future studies using similar approaches used in cat are needed to answer this question in rat.

Electrophysiology of presynaptic inhibition in wild-type and Cx36 knockout mice

Several features associated with presynaptic inhibition in wild-type *in vitro* preparations of juvenile mice are similar to those in adult cat. These include the time course of the DRP, the long-lasting inhibition of the MSR, the occurrence of sensory-evoked PAD and the attenuation of the DRP and MSR inhibition by GABA antagonists. Although the DRP is strongly associated with GABAergic mediation of presynaptic inhibition (reviewed Rudomin and Schmidt, 1999; Rudomin, 2009), its attenuation by GABA antagonists ranges from partial (Rudomin *et al.* 1990; Thompson & Wall, 1996; Kremer & Lev-Tov, 1998; Wong *et al.* 2001; present results - Figs. 2*A*) to complete (Schreckengost *et al.* 2010). GABA antagonists can, however, very effectively attenuate the long-latency inhibition of the MSR evoked by conditioning stimulation (Fig. 3*B*; Eccles *et al.* 1963; Curtis *et al.* 1971). It remains an open question whether non-GABAergic mechanisms also contribute to presynaptic inhibition. Based on the similarities of the present results to those in the cat, it is reasonable to assume that MSR inhibition at the longer condition-test intervals in the mouse occurs predominately by a presynaptic mechanism. The inhibition at shorter condition test intervals (< 25 ms) likely includes a postsynaptic inhibitory component involving spinal reflex pathways (Bagust *et al.* 1981; Deshpande & Warnick, 1988; Wang *et al.* 2008).

Later components of the CDP are considered to reflect activity in dorsal horn interneurones and are correlated with activity in presynaptic inhibitory pathways (Enriquez *et al.* 1996, Rudomin *et al.* 1987). Although the shortest latency components of the CDP were qualitatively similar in wild-type and knockout mice, the later components were missing in knockouts. The absence of these components suggests a decrease in dorsal horn interneurone activity in these knockouts and

in turn a reduction in the activity of presynaptic inhibitory pathways. Consistent with this suggestion, DRP duration and amplitude were decreased substantially in mice lacking Cx36 compared to wild-types of the same age. Whereas bicuculline attenuated the long lasting DRP in wild-types, the remaining short-duration DRP observed in Cx36 knockout mice was not affected by GABAa antagonists. Presynaptic inhibition of transmitter release from large diameter primary afferent fibres in the mammalian spinal cord is mediated by GABA release at axo-axonic synapses (Rudomin, 2009), which causes a depolarization of intraspinal afferent fibre terminals, *i.e.*produces PAD. Consistent with the shortened and attenuated DRP in juvenile Cx36 knockoutmice, PAD could not be evoked in lumbar primary afferent terminals of these mice. In wildtypes, the ability of the gap junction blockers to antagonize MSR inhibition (Fig 5*A*) and reduce the DRP (Fig. 5*B, C*) provides further support for a critical involvement of neuronal gap junctions in presynaptic inhibition of large diameter sensory afferents.

Cx36 in juvenile and adult mice

There are a number of reports on electrical coupling between neurones in the spinal cord, but

there is little anatomical information available on the expression of Cx36 in the cord. Motoneurones in rat express Cx36 mRNA (Chang *et al.* 1999), and diffuse, intracellular labelling for Cx36 protein has been detected in these neurones (Marina *et al.* 2008). Here we demonstrate a much broader distribution of Cx36 in the spinal cord of both developing and adult mouse. Importantly, as elsewhere in the CNS (Li *et al.* 2004; Rash *et al.* 2004; Rash *et al.* 2007a,b), we found that specific immunofluorescence labelling for Cx36 in spinal cord (i.e., that which was absent in Cx36 knockout mice) consisted exclusively of Cx36-puncta.Presumably these puncta reflect localization of Cx36 to neuronal gap junctions that have been shown ultrastructurally to contain Cx36 (Rash *et al.* 2001a,b; Nagy *et al.* 2004).

Although spinal neurones may express other connexins (see Chang *et al.* 1999), the DRP and lasting inhibition of the MSR were severely affected by the absence of Cx36. It thus appears that Cx36-containing gap junctions are critically involved in the physiological processes examined here. In other CNS regions and in the spinal cord, developmental decreases in electrical coupling and down-regulation of Cx36 expression are well described (Walton and Navarrete, 1991; Kandler and Katz, 1995; Chang et al. 1999; Chang and Balice- Gordon, 2000; Meier and

Dermietzel, 2006). Present results show the persistence of moderate to dense levels of Cx36-puncta in both dorsal and ventral horn areas of adult spinal cord. This persistence is perhaps not surprising given the numerous brain structures where functional Cx36-containing electrical synapses are present in the adult (Connors and Long, 2004; Bennett and Zukin, 2004; Hormuzdi *et al.* 2004; Meier and Dermietzel, 2006). Particularly striking in adult cord was the widely distributed immunolabelling for Cx36 in laminae IV-VI, the labelling associated with a small subset of neurones scattered in laminae IV-VIII and dense collections of Cx36-puncta among a restricted set of neurones in lamina IX. Our anatomical observations suggest that Cx36-containing gap junctions continue to be

of importance in adult pools of spinal neurones and possibly in processes in addition to presynaptic inhibition. In this regard it is noteworthy that there is extensive electrical coupling between motoneurones in very young animals that is largely lost during the second week after birth (Walton and Navarrete, 1991). The re-distribution of Cx36-puncta on motoneurones observed during development presumably reflects changing physiological roles of electrical synapses associated with these cells in the adult; this event may be somehow related to the loss of coupling between these neurones during development. The demonstration of Cx36 puncta on motoneurones at P5, cells known to be electrically coupled, serves as a positive control for our techniques and supports our suggestion that spinal neurones in other regions are electrically coupled in the adult.

Because of the present interest in the process of presynaptic inhibition of large diameter primary afferents, dye-coupling between spinal interneurones was investigated only in regions known to contain neurones involved in this process, namely laminae V-VI. Theseregions contain the GABAergic interneurones that project to the ventral horn and form P boutons on muscle spindle afferents (Hughes *et al.* 2005; discussed below). As shown in Fig. 9, at P11 there is extensive dye-coupling between neurones in these laminae and extensive punctate labelling for Cx36 on dye-coupled neurones. The presence of functional Cx36-containing gap junctions between neurones in these areas is consistent with a role of electrical synapses in presynaptic inhibition. A full appreciation of the identity of dyecoupled neurones in relation to the localization and function of Cx36 in particular neuronal populations will require a more comprehensive analysis than was undertaken in the present study.

Role of gap junctions in presynaptic inhibition

Cx36-containing gap junctions might be involved in presynaptic inhibition of group Ia muscle spindle afferents making monosynaptic contacts on motoneurones. Presynaptic inhibition is believed to involve a three synapse, two neurones, pathway (Jankowska et al, 1981; but see Shreckengost et al, 2010) in which glutamatergic sensory afferents activate excitatory first order interneurones. The first order interneurones are thought to be glutamatergic because there is evidence that activation of excitatory glutamatergic interneurones occurs immediately before the onset of presynaptic inhibition (Rudomin,

2009). These neurones then activate a population of gabaergic interneurones that have axoaxonic

contacts on primary afferents (see Rudomin, 2009). There is strong electrophysiological and anatomical evidence that deep dorsal horn laminae are the principal locations of gabaergic interneurones mediating presynaptic inhibition of large diameter afferents in the cat and rodent spinal cord (Jankowska et al. 1981; Rudomin et al, 1987; Maxwell et al, 1990; Hughes et al, 2005; Betley et al. 2009). These interneurones may in part correspond to neurons in the medial laminae IV-VI where we found cells having the capacity for intercellular exchange of neurobiotin, and where neurobiotin-coupled cells were richly endowed with Cx36-puncta. Based on the foregoing, the hypothesis presented in section 1 of this thesis, is that gabaergic neurones in deep dorsal horn laminae are gap junctionally coupled and make axo-axonic contacts with large diameter primary afferents and, in particular, Ia spindle afferents. We propose that it is likely that gap junctions exist between excitatory first order interneurones that in turn activate second order presynaptic inhibitory pathways, but direct evidence for this is presently lacking. However, bearing on this point is that at least some components of the cord dorsum potential are related to activation of excitatory (presumably glutamatergic) interneurones in the dorsal horn (Rudomin, 2009). The depressed CDP observed in the Cx36 knockouts supports equally the possibility that, in the knockout mouse, glutamatergic interneurones lack synchronous robust activity conferred by gap junction coupling.

One of the most emphasised features of inter-neuronal gap junctions is their ability to function as low-pass filters, where longer duration, subthreshold, depolarizations, in contrast to spikes, are efficiently transmitted within a network of coupled neurons, allowing synchronization of spike

activity of near-threshold neurones (Bennett and Zukin 2004). Equally important, the behaviour of a coupled network will be dependent upon both the nature and duration of the afferent input as well as the intrinsic membrane properties of the coupled neurones (Mann-Metzer *et al.* 1999; Dugué *et al.* 2009; Curti *et al.* 2012). Gap junctions could serve to trigger intrinsic oscillatory currents in coupled neurones, to temporally synchronize action potentials with the onset of afferent input, to prolong activity in the population as the afferent input decays, or to help select a sub-population of coupled interneurones within a larger population of spinal neurones with similar afferent input. A

facilitation of activity within the gap junction coupled networks would presumably result in a concerted expression of presynaptic inhibition of primary afferents. This idea is in accord with the suggestion (see Rudomin, 2009) that synchronous activity of subpopulations of interneurones involved in presynaptic inhibition can distribute primary afferent depolarization to selected collaterals of afferents in different spinal locations. It is also in accord with the suggestion that when afferents contact multiple spinal pathways, activity in those displaying synchronous interneuronal activity, e.g. those in presynaptic inhibitory networks, would be promoted over reflex effects mediated through other, unsynchronized, networks (Chavez *et al.* 2012. Accordingly, gap junction coupling may be extensive within subsets of interneurones organized into functionally discrete groups. Based on these considerations, it might be predicted that pharmacological uncoupling of gap junctions in wild-type mice or the loss of Cx36 in transgenic mice, would compromise a concerted action of these interneurones on transmission at primary afferents. This proposed mechanism for an essential role of electrical connections between neurones in sensory-evoked presynaptic inhibition is supported by the loss of long-latency inhibition of the MSR in spinal cord preparations from Cx36 knockouts and following bath application of gap junction blockers in cords from wild-type mice. These observations provide strong evidence for the involvement of Cx36-containing gap junctions in the presynaptic control of the synapse between Ia muscle spindle afferents and lumbar motoneurones. The abundance of Cx36 puncta in spinal laminae IV-VI also suggests a role of electrical synapses in the presynaptic control of other segmental reflexes, for example, those from tendon organs and spindle secondary afferents. It is noteworthy that gap junctions may also be involved in the presynaptic control of sensory input to dorsal spinocerebellar tract neurones which shares several features of the presynaptic inhibition of Ia terminals on motoneurones. This includes axo-axonic

synapses (Walmsley, 1991), sensory-evoked PAD of group I afferent input (Jankowska and Padel, 1984) and gabaergic control of afferent input to dorsal spinocerebellar tract neurones (Hantman and Jessell, 2010).

Interestingly, some previously described laminae V-VI interneurones (Hughes *et al*. 2005) are GAD65-positive and make P-bouton (axo-axonic) contacts with primary afferent terminals in the ventral horn. Since Ia muscle spindle afferents are the only sensory afferents with extensive monosynaptic connections on motoneurones, present results on MSR inhibition raise the likelihood that at least some of the interneurones described by Hughes *et*

al. (2005) are coupled by electrical synapses. Recent reports, however, suggest that at least in

very young animals these spinal regions also contain populations of GABAergic interneurones not involved in presynaptic inhibition (Wilson *et al.* 2010). There is also strong physiological evidence that some GABAergic interneurones may be involved in both presynaptic inhibition of afferent transmission and postsynaptic inhibition of motoneurones (Rudomin *et al.* 1990; see Rudomin, 2009). Full identification of GABAergic interneurone populations in these laminae and the organization of gap junctionally coupled networks among them remains to be determined.

Presynaptic inhibition of large diameter muscle and cutaneous afferents in the spinal cord is a regulatory process in which sensory afferent activity results in reduced transmitter release from the same and other afferents and is an integral component of reflex control during locomotion and other movements (Rossignol *et al.* 2006; Rudomin 2009). Studies during locomotion, however, indicate the existence of an additional source of presynaptic inhibition that arises from the operation of central pattern generating circuitry and can occur without sensory stimulation (discussed in Gosgnach *et al.* 2000). It remains an attractive possibility that electrical synapses play a similar role in this centrally-evoked presynaptic inhibition as the one described here in sensory-evoked presynaptic inhibition. Dysregulation of presynaptic inhibition is believed to be one of the major factors in human spasticity arising from spinal cord injury, and drugs that augment presynaptic inhibition, such as baclofen, are a mainstay in treatment of spasticity (Simon and Yelnick, 2010). Recently, it has been suggested that injury-induced changes in connexin36 expression in spinal cord contribute to spasticity (Yates *et al.* 2011). The present

results directly linking Cx36 to presynaptic inhibition, a process known to malfunction in human spasticity, raises the possibility that this condition arises in part from dysfunction of gap junctionally coupled networks involved in presynaptic inhibition.

Connexin expression in spinal motoneurones during development and adulthood

Our observations from studying the expression of connexins previously reported as candidates to form neuronal gap junctions revealed that only two of them are indeed located at the plasma membrane of motneurones, a detail analysis of Cx37, Cx40, Cx43, Cx32, Cx36 and Cx45 expression in spina cord depicted that only Cx36 and Cx43 are located at apposition with the plasma membrane. The analysis of these connexins in early postnatal life

at P5 also revealed that there are differences in the pattern of expression of Cx36 and Cx43, being more widely dispersed and abundant at these earlier stages of development and appearing more restricted in adult motoneurones. Despite the fact that coupling among motoneurones have been recognized for many years, little effort has been made in order to describe the class of connexin responsible for forming electrical synapses in motoneurones. Although the results described in section 3 of this thesis are merely descriptive, these provide the key to understand and discern how many connexins could potentially form neuronal gap junctions. However we recognize that more direct evidence is needed to support these findings, which could be demonstrated by recording pairs of motoneurones at early postnatal ages in Cx36 knockout mice. The absence of electrical coupling or dye coupling will be a confirmation that Cx36-containing gap junctions form functional electrical synapses. Shedding light on the potential connexins involved in forming neuronal gap junctions may also help to decipher the reason for the lack of motor deficit or locomotor impairment in adult Cx36 knockouts, where the lack of Cx36 in motoneurones seem to be compensated by other connexins or replaced by an additional mechanism that do not involve neuronal gap junctions.

Cx36 forming purely electrical synapses on lower lumbar and sacral motoneurones

We show evidence that Cx36-puncta was present in both groups belonging to the sexually dimorphic nuclei: ischiocavernousus and bulbospongious. They are both segregated to different groups, the former being located in the DL group whereas the latter is mainly localized in the rostral DM group. These motoneurones are classified as sexually dimorphic motoneurones.

Previous studies have demonstrated that these motor groups belong to a class of motoneurones where dendrite arbor growth and number is modulated by androgen levels (Arnold & Sengelaub 1981). Dye coupling have been demonstrated for these set of motoneurones, however androgen modulation have not been shown to be correlated with the presence and amount of dye coupling (Coleman & Sengelaub 2001). Our findings are in agreement with previous anatomical descriptions of these nuclei in rat showing columns arrangements, with thick dendrites laying perpendicular to the soma.

Since the discovery of dye-coupling on these motoneurones very few studies have addressed on the type or the class of junctions present. One study using mRNA in situ hybridization has shown that these motoneurones are positive for Cx32mRNA message (Matsumoto *et al* 1992). However, our evidence shows that Cx32 is only present between the oligodendrocytes, which is restricted to Schwann cells on myelinated fibers and oligodendrocytes as it has been previously described by others (Lynn et al 2011).

Gap-junctions between sexually dimorphic motoneurones have been described by Coleman and Sengelaub (2002); however, demonstration of the type of connexin involved has only been approached by in situ hybridization (Matsumoto *et al* 1992).Our results are the first to characterize Cx36 as the neuronal connexin between these motor nuclei as well as other nuclei in the vicinity, such as external urethral sphincter and anal external sphincter motoneurones. Cx36-puncta were found between motoneurones in DM, DL in male rats as well as in groups V and RDL. Our confocal analyses shows at least four different configurations for Cx36: soma-somatic, dendrosomatic, dendrodendritic and axodendritic. All of these configurations were found in all of these nuclei, yet soma-somatic seem to be more abundant in DM and DL within the bulbospongious motor group, anal external sphincter and the external urethral sphincter motoneurones.

External sphincter motoneurones and anal sphincter motoneurones are considered to be non-sexually dimorphic since the number and size of these motoneurones does not vary between males and females (McKenna and Nadelhaft 1986). Our results evidence that Cx36- puncta is present in both sexually dimorphic and non-sexually dimorphic motoneurones contained in L5 and upper sacral cord. Therefore it is likely that Cx36 puncta appearance occurs prior to the development of motoneurones by androgens.

The groups V and DL are also more numerous in males than in females. Previous studies have found that bulbospongious motoneurones are also found in this nuclei, Shroder (1998) has suggested that these motorneurones innervate the pelvic diaphragm in the female, in the male previous studies have shown a common embryologic origin with the DL and DM, and related functions (Sengelaub & Arnold 1984), although gap junctions do not appear to be involved in the bilateral co-activation of these muscles, but rather they may serve increase gain activity (Coleman 2001).

Our results showing abundant Cx36-puncta at the dendritic intersections projecting contralateral.Anatomical evidence of bilateral crossings have also been described, however the function of these crossings have not yet elucidated. Our findings showing Cx36 at the crossing sites might indicate that both motor pools could display a certain degree of synchronization needed to produce bilateral pudendal reflexes.

In contrast, RDL group contains motoneurones that innervate the plantar muscles of the foot in the rat and mice (Nicolopoulos-Stournaras & Iles 1983; McHanwell and Biscoe 1981). These motoneurones are labeled after retrograde injections of the L6-S1 trunk, and therefore are always included in the classification of lower lumbar motoneurones located in L6 –S1. Interestingly we show that Cx36-puncta is also present among those nuclei, consistent with previous findings (Sengealub and Coleman 2002). We also noted that this motoneuron group consisted of two portions one dorsal and rostral and another caudal and ventral. A difference between these was that the dorsal part presented more vglut-1 terminals in axosomatic synapses forming mixed synapses, whereas the ventral part mostly received pure Cx36- puncta throughout the proximal dendritic regions. Innervation of these motoneurones comes from group I muscle spindles as well as cutaneous afferents contained in the sural nerve, the plantar muscles play a key role in the plantar extension and contraction of the foot (Nicolopoulos-Stournaras & Iles 1983; McHanwell and Biscoe 1981).

External urethral sphincter motoneurones and anal sphincter motoneurones belong to a special group of somatic motoneurones because these are under by voluntary control but are also highly modulated by sympathetic and parasympathetic inflow. External urethral sphincter motoneurones in the rat are located in the DL nuclei. In the male EUS motoneurones are segregated to the medial side of the DL, whereas in the female EUS these are more spread in the DL, since there

are very few ischiocavernousus motoneurones. Interestingly in the earliest anatomical search of the features of these particular classes of motoneurones in the cat and dog, EM and light microscopy studies found dendro-dendritic appositions (Mathews et al 1971; Scheibel and Scheibel 1970; Takahashi & Yamamoto 1979), however the scarce amount of examples found in the several studies at the time concluded that these appositions were forming desmosomes instead of gap junctions. The search of gap junction on these nuclei started due to the evidence showing that these motoneurones could be easily distinguished from the rest of somatic motoneurones due to their pattern of innervation, soma size and distribution in the nuclei with close appositions found between somas and dendrites (Mathews *et al* 1971; Sotelo *et al* 1974). A study performed by Takahashi & Yamamoto 1979 in the cat showed the presence of desmosome like structures by EM between the dendrites on the Onuf nucleus in the cat. Further studies in human (Feirabend *et al* 1997) appear to have identified gap junction structures between these motoneurones. Our study shows that Cx36-puncta forms neuronal gap junctions in external urethral sphincter motoneurones in the rat and Onuf nuclei in mice. These motoneurones displayed abundant Cx36-puncta, forming plaques and patches in soma-somatic, somadendritic and dendro-dendritic configurations. These results might suggest that the tonic activity produced in this muscle could originate from the synchronized activity occurring through electrical coupling.

EUS motoneurones receive scarce primary afferent input (DeGroat *et al* 1978, Jankowska *et al* 1978). Accordingly, our results show a paucity of vglut-1 terminals in both EUS and anal sphincter motoneurones. Tonic activation of these motoneurones originates from segmental or descending polysynaptic pathways from viscera and perineal afferents ending primarily in the distal dendrites (Pullan, 1988); however our study only shows scarce vglut1 terminals and even very low amount of c-terminals. We speculate that Cx36-containing gap junctions could be critical in order to activate the motor pool and maintain the tonus since there is almost no afferent input at the soma and proximal dendrites. Anal sphincter motoneurones were also found to have abundant Cx36-puncta among them. These motoneurones, located in the DM group in upper sacral segments, had similar configurations of Cx36 appositions. Interestingly previous reports have demonstrated that at rest these have tonic firing ranging from 8-21Hz. The tonus has been proposed to arise from hyperpolarization of the Vth and plateau potentials, and this tonus is required to maintain continency (Pachasky and Shefchick, 2000). Our findings showing the

presence of neuronal gap junctions among this group of motoneurones allow us to suggest that this tonus could emerge or be maintained through electrical coupling.

References

Achilles K, Okabe A, Ikeda M, Shimizu-Okabe C, Yamada J, Fukuda A, Luhmann HJ, Kilb W. (2007) Kinetic properties of Cl^- uptake mediated by Na+-dependent K+-2Cl cotransport in immature rat neocortical neurons. J Neurosci. 27:8616-27.

Alvarez FJ, Villalba RM, Zerda R, Schneider SP. (2004) Vesicular glutamate transporters in the spinal cord, with special reference to sensory primary afferent synapses. J Comp Neurol. 472:257-80

Alvarez-Leefmans FJ, Cruzblanca H, Gamiño SM, Altamirano J, Nani A, Reuss L. (1994) Transmembrane ion movements elicited by sodium pump inhibition in Helix aspersa neurons. J Neurophysiol. 71:1787-96.

Alvarez-Leefmans FJ, León-Olea M, Mendoza-Sotelo J, Alvarez FJ, Antón B, Garduño R. (2001) Immunolocalization of the Na(+)-K(+)-2Cl(-) cotransporter in peripheral nervous tissue of vertebrates. Neuroscience.;104(2):569-82.

Alvarez FJ, Kavookjian AM, Light AR. (1992) Synaptic interactions between GABA-immunoreactive profiles and the terminals of functionally defined myelinated nociceptors in the monkey and cat spinal cord. J Neurosci.12:2901-17.

Aoyama M, Hongo T, Kudo N. (1988) Sensory input to cells of origin of uncrossedspinocerebellar tract located below Clarke's column in the cat. J Physiol. 398:233-57.

Armett CJ, Gray JA, Hunsperger RW, Lal S. (1962) The transmission of information in primary receptor neurones and second-order neurones of a phasic system. J Physiol. 164:395-421

Awiszus F, Feistner H. (1993) The relationship between estimates of Ia-EPSP amplitude and conduction velocity in human soleus motoneurons. Exp Brain Res. 95:365-70.

Baldissera F, Campadelli P, Piccinelli L. (1982) Neural encoding of input transients investigated by intracellular injection of ramp currents in cat alpha-motoneurones. J Physiol; 328:73-86.

Bai L, Xu H, Collins JF, Ghishan FK. (2001) Molecular and functional analysis of a novel neuronal vesicular glutamate transporter. J Biol Chem. ;276:36764-9.

Ballanyi K, Grafe P. An intracellular analysis of gamma-aminobutyric-acid-associated ion movements in rat sympathetic neurones. J Physiol. 1985 365:41-58.

Bannatyne BA, Liu TT, Hammar I, Stecina K, Jankowska E, Maxwell DJ. (2009) Excitatory and inhibitory intermediate zone interneurons in pathways from feline group I and II afferents: differences in axonal projections and input. J Physiol. 587(Pt 2):379-99.

Barbaresi P, Rustioni A, Cuénod M. (1985) Retrograde labeling of dorsal root ganglion neurons after injection of tritiated amino acids in the spinal cord of rats and cats. Somatosens Res. 3:57-74.

Barber RP, Vaughn JE, Saito K, McLaughlin BJ, Roberts E. (1978) GABAergic terminals are presynaptic to primary afferent terminals in the substantia gelatinosa of the rat spinal cord. Brain Res. 141:35-55.

Barker D, Scott JJ, Stacey MJ. (1986) Reinnervation and recovery of cat muscle receptors after long-term denervation. Exp Neurol. 94:184-202

Barron DH, Matthews BH. Intermittent conduction in the spinal cord. J Physiol. (1935) 85:73-103.

Battaglia G, Rustioni A (1988). Coexistence of glutamate and substance P in dorsal root ganglion neurons of the rat and monkey. J Comp Neurol. ;277:302-12.

Beierlein, M., Gibson, J. R. & Connors, B. W. (2000). A network of electrically coupled interneurons drives synchronized inhibition in neocortex. Nature Neurosci. 3, 904–910

Bellocchio EE, Hu H, Pohorille A, Chan J, Pickel VM, Edwards RH. (1998) The localization of the brain-specific inorganic phosphate transporter suggests a specific presynaptic role in glutamatergic transmission. J Neurosci. 18:8648-59.

Bennett, M. V. L. (1966). Physiology of electrotonic junctions. *Ann.* N. Y. *Acad. Sci. 137:509-539.*

Bennett, M. V. L, Pappas, G. D., Aljure, E., Nakajima, Y (1967b). Physiology and ultrastructure of electrotonic junctions. II. Spinal and medullary electromotor nuclei in *mormyrid* fish.]. *Neurophysiol. 30:180-208.*

Bennett MV. (2000) Electrical synapses, a personal perspective (or history). Brain Res Rev. 32:16-28.

Bos R, Brocard F, Vinay L. (2011) Primary afferent terminals acting as excitatory interneurons contribute to spontaneous motor activities in the immature spinal cord. J.Neurosci.; 31(28):10184-8

Bos R, Sadlaoud K, Boulenguez P, Buttigieg D, Liabeuf S, Brocard C, Haase G, Bras H, Vinay L. (2013) Activation of 5-HT2A receptors upregulates the function of the neuronal K-Cl cotransporter KCC2. Proc Natl Acad Sci U S A. 110:348-53.

Brigant JL, Mallart A. (1982) Presynaptic currents in mouse motor endings. J Physiol; 333:619-36.

Briggs I, Barnes JC. (1987) Actions of opioids on the dorsal root potential of the isolated spinal cord preparation of the neonate rat. Neuropharmacology; 26:469-75.

Brown AG, Fyffe RE. (1978)[a] The morphology of group Ia afferent fibre collaterals in the spinal cord of the cat. J Physiol; 274:111-27.

Brown AG, Fyffe RE. (1978)[b] Synaptic contacts made by identified Ia afferent fibres upon motoneurones [proceedings]. J Physiol; 284:43P-44P.

Broman J, Anderson S, Ottersen OP. (1993) Enrichment of glutamate-likeimmunoreactivity in primary afferent terminals throughout the spinal cord dorsal horn. Eur J Neurosci. 5:1050-61.

Burke RE, Levine DN, Zajac FE (1971) 3rd. Mammalian motor units: physiological-histochemical correlation in three types in cat gastrocnemius. Science. 174(4010):709-12.

Burke RE, Walmsley B, Hodgson JA. HRP (1979) anatomy of group Ia afferent contacts on alpha motoneurones. Brain Res.160:347-52.

Burke RE, Glenn LL. (1996) Horseradish peroxidase study of the spatial and electrotonic distribution of group Ia synapses on type-identified ankle extensor motoneurons in the cat. J Comp Neurol. 372:465-85.

Cameron AA, Pover CM, Willis WD, Coggeshall RE. (1992) Evidence that fine primary afferent axons innervate a wider territory in the superficial dorsal horn following peripheral axotomy. Brain Res. 575:151-4.

Campbell V, Berrow NS, Fitzgerald EM, Brickley K, Dolphin AC (1995). Inhibition of the interaction of G protein G(o) with calcium channels by the calcium channel beta-subunit in rat neurones. J Physiol. 485 (Pt 2):365-72

Carlton SM, Zhou S, Coggeshall RE. (1999) Peripheral GABA(A) receptors: evidence for peripheral primary afferent depolarization. Neuroscience.;93:713-22.

Castro A, Aguilar J, Elias D, Felix R, Delgado-Lezama R. (2007) G-protein-coupled GABAB receptors inhibit Ca2+ channels and modulate transmitter release in descending turtle spinal cord terminal synapsing motoneurons. J Comp Neurol. 503:642-54.

Cervero F, Iggo A, Molony V (1979). Segmental and intersegmental organization of neurones in the Substantia Gelatinosa Rolandi of the cat's spinal cord. Q J Exp Physiol Cogn Med Sci. 64:315-26.

Cervero F, Connell LA. (1984) Distribution of somatic and visceral primary afferent fibres within the thoracic spinal cord of the cat. J Comp Neurol. 230:88-98.

Chang Q, Gonzalez M, Pinter MJ, Balice-Gordon RJ. (1999) Gap junctional coupling and patterns of connexin expression among neonatal rat lumbar spinal motor neurons. J Neurosci. 19:10813-28.

Chapman RJ, Lall VK, Maxeiner S, Willecke K, Deuchars J, King AE. (2013) Localization of neurones expressing the gap junction protein Connexin45 within the adult spinal dorsal horn: a study using Cx45-eGFP reporter mice. Brain Struct Funct. 218:751-65

Chaudhry FA, Lehre KP, van Lookeren Campagne M, Ottersen OP, Danbolt NC, Storm-Mathisen J. (1995) Glutamate transporters in glial plasma membranes: highly differentiated localizations revealed by quantitative ultrastructural immunocytochemistry. Neuron. 15:711-20.

Clayton GH, Owens GC, Wolff JS, Smith RL. (1998) Ontogeny of cation-Cl- cotransporter expression in rat neocortex. Brain Res Dev Brain Res. 109:281-92.

Craig AD, Mense S. (1983) The distribution of afferent fibers from the gastrocnemius-soleus muscle in the dorsal horn of the cat, as revealed by the transport of horseradish peroxidase. Neurosci Lett 41:233-8.

Condorelli DF, Parenti R, Spinella F, Trovato Salinaro A, Belluardo N, Cardile V, Cicirata F. (1998) Cloning of a new gap junction gene (Cx36) highly expressed in mammalian brain neurons. Eur J Neurosci. 10:1202-8.

Conradi S. (1969) Ultrastructure of dorsal root boutons on lumbosacral motoneurons of the adult cat, as revealed by dorsal root section. Acta Physiol Scand Suppl.332:85-115.

Cook WA Jr, Cangiano A. (1970) Presynaptic inhibition of spinal motoneurons. Brain Res. 24:521-4.

Coull JA, Boudreau D, Bachand K, Prescott SA, Nault F, Sík A, De Koninck P, De Koninck Y. (2003) Trans-synaptic shift in anion gradient in spinal lamina I neurons as a mechanism of neuropathic pain. Nature. 424(6951):938-42

Cunningham MO, Roopun A, Schofield IS, Whittaker RG, Duncan R, Russell A,

Jenkins A, Nicholson C, Whittington MA, Traub RD. (2012) Glissandi: transient fast

electrocorticographic oscillations of steadily increasing frequency, explained by

temporally increasing gap junction conductance. Epilepsia. 53:1205-14.

Curtis DR, Eccles JC, Eccles RM. (1957) Pharmacological studies on spinal reflexes. J Physiol. 136:420-34.

Curtis DR, Lacey G. (1994) GABA-B receptor-mediated spinal inhibition. Neuroreport. 5:540-2.

Curtis DR, Lacey G (1998) Prolonged $GABA_B$ receptor-mediated synaptic inhibition in the cat spinal cord: an in vivo study. Exp. Brain Res. 121:319-333.

Curti S, Pereda AE. (2004)Voltage-dependent enhancement of electrical coupling by a subthreshold sodium current. J Neurosci. 24:3999-4010.

Czarkowska J, Jankowska E, Sybirska E. (1981) Common interneurones in reflex pathways from group 1a and 1b afferents of knee flexors and extensors in the cat. J Physiol. 310:367-80

Deans MR, Gibson JR, Sellitto C, Connors BW, Paul DL. (2001) Synchronous activity of inhibitory networks in neocortex requires electrical synapses containing

connexin36. Neuron. 31:477-85.

De Biasi S, Rustioni A. (1988) Glutamate and substance P coexist in primary afferent terminals in the superficial laminae of spinal cord. Proc Natl Acad Sci U S A. 85:7820-4.

De Biasi S, Rustioni A. (1990) Ultrastructural immunocytochemical localization of excitatory amino acids in the somatosensory system. J Histochem Cytochem. 38:1745-54.

De-Doncker L, Picquet F, Petit J, Falempin M. (2003) Characterization of spindle afferents in rat soleus muscle using ramp-and-hold and sinusoidal stretches. J Neurophysiol. 89:442-9.

Dermietzel, R. & Spray, D. C. (1993) Gap junctions in the brain: where, what type, how many and why? Trends Neurosci.16, 186–192

Devor, A., Yarom, Y., (2002). Electrotonic coupling in the inferior olivary nucleus revealed by simultaneous double patch recordings. J. Neurophysiol. 87, 3048–3058.

Djouhri L, Lawson SN. (2001) Differences in the size of the somatic action potential overshoot between nociceptive and non-nociceptive dorsal root ganglion neurones in the guinea-pig. Neuroscience.108:479-91.

Draguhn A, Traub RD, Schmitz D, Jefferys JG. (1998) Electrical coupling underlies high-frequency oscillations in the hippocampus in vitro. Nature. 394:189-92.

Duchen MR. (1986) Excitation of mouse motoneurones by GABA-mediated primary afferent depolarization. Brain Res. 379:182-7.

Duenas SH, Loeb GE, Marks WB. (1990) Monosynaptic and dorsal root reflexes during locomotion in normal and thalamic cats. J Neurophysiol. 63:1467-76.

Eccles,]. C., O'Connor, W.]. (1939). Responses which nerve impulses evoke in mammalian striated muscles.] Physiol. 97:44-102.

Eccles,]. C., Katz, B., Kuffler, S. W. (1941). Nature of the "endplate potential" in curarized muscle.] NeurophysioL 4:362-387.

Eccles JC, Eccles RM, Lundberg A. (1957) The convergence of monosynaptic excitatory afferents on to many different species of alpha motoneurones. J Physiol. 137:22-50.

Eccles RM, Lundberg A. (1959) Supraspinal control of interneurones mediating spinal reflexes. J Physiol.147:565-84.

Eccles JC, Krnjevic K. (1959) Potential changes recorded inside primary afferent fibres within the spinal cord. J Physiol. 149:250-73.

Eccles JC, Eccles RM, Iggo A, Lundberg A. (1961) Electrophysiological investigations on Renshaw cells. J Physiol.159,461-78

Eccles JC, Eccles RM, Iggo A, Ito M. (1961) Distribution of recurrent inhibition among motoneurones. J Physiol. 159,479-99

Eccles JC, Kozak W, Magni F. (1961) Dorsal root reflexes of muscle group I afferent fibres. J Physiol. 159, 128-46

Eccles JC, Eccles RM, Magni F. (1961) Central inhibitory action attributable to presynaptic depolarization produced by muscle afferent volleys. J Physiol. 159, 147-66

Eccles JC, Oscarsson O, Willis WD. (1961) Synaptic action of group I and II afferent fibres of muscle on the cells of the dorsal spinocerebellar tract. J Physiol. 158, 517-43

Eccles JC, Hubbard JI, Oscarsson O. (1961) Intracellular recording from cells of the ventral spinocerebellar tract. J Physiol. 158, 486-516.

Eccles JC. (1961) Membrane time constants of cat motoneurons and time courses of synaptic action. Exp Neurol. 4:1-22.

Eccles JC, Magni F, Willis WD. (1962) Depolarization of central terminals of Group I

afferent fibres from muscle. J Physiol. 160:62-93.

Eccles JC, Schmidt RF, Willis WD. (1962) Presynaptic inhibition of the spinal monosynaptic reflex pathway. J Physiol. 161:282-97.

Eccles JC, Schmidt R & Willis WD (1963). Pharmacological studies on presynaptic inhibition. J Physiol 168: 500-530.

Eccles JC. (1964) Ionic mechanism of postsynaptic inhibition. Science. 145(3637):1140-7.

Edgley SA, Jankowska E. (1987) An interneuronal relay for group I and II muscle afferents in the midlumbar segments of the cat spinal cord. J Physiol. 389:647-74.

Edgley SA, Grant GM. (1991) Inputs to spinocerebellar tract neurones located in stilling's nucleus in the sacral segments of the rat spinal cord. J Comp Neurol. 305:130-8.

Eide E, Lundberg A, Voorhoeve P. (1961) Monosynaptically evoked inhibitory post-synaptic potentials in motoneurones. Acta Physiol Scand. 53:185-95.

Fan, R., Marin-Burgin, A., French, K., Otto Friesen, W., (2005). A dye mixture (Neurobiotin and Alexa 488) reveals extensive dye-coupling among neurons in leeches; physiology confirms the connections. J. Comp. Physiol. A: Sensory, Neural, and Behavioral Physiology 191, 1157–1171.

Fetz EE, Jankowska E, Johannisson T, Lipski J. (1979) Autogenetic inhibition of motoneurones by impulses in group Ia muscle spindle afferents. J Physiol. 293:173-95.

Fischer J, Bancila V, Mailly P, Masson J, Hamon M, El Mestikawy S, Conrath M. (1999) Immunocytochemical evidence of vesicular localization of the orphan transporter RXT1 in the rat spinal cord. Neuroscience. 92:729-43

Forsythe ID. (1994) Direct patch recording from identified presynaptic terminals mediating glutamatergic EPSCs in the rat CNS, in vitro. J Physiol. 479 (Pt 3):381-7.

Franz M, Mense S. (1975) Muscle receptors with group IV afferent fibres responding to application of bradykinin. Brain Res. 92:369-83.

Frank, K., Fuortes, M. (1957). Presynaptic and postsynaptic inhibition of monasynaptic reflexes. Fed. Proc. 16:39-40.

Frank E. (2009) A new class of spinal interneurons: the origin and function of C boutons is solved. Neuron. 64:593-5

Fremeau RT Jr, Troyer MD, Pahner I, Nygaard GO, Tran CH, Reimer RJ, Bellocchio EE, Fortin D, Storm-Mathisen J, Edwards RH. (2001) The expression of vesicular glutamate transporters defines two classes of excitatory synapse. Neuron. 31:247-60.

Fricker D, Miles R. (2001) Interneurons, spike timing, and perception. Neuron.

32:771-4. Review.

Fujimoto K. (1995) Freeze-fracture replica electron microscopy combined with SDS digestion for cytochemical labeling of integral membrane proteins. Application to the immunogold labeling of intercellular junctional complexes. J Cell Sci. 108 (Pt 11):3443-9

Fujiyama F, Furuta T, Kaneko T. (2001) Immunocytochemical localization of candidates for vesicular glutamate transporters in the rat cerebral cortex. J Comp Neurol. ;435:379-87.

Fukuda, T. & Kosaka, T. (2000) Gap junctions linking the dendritic network of GABAergic interneurons in the hippocampus. J. Neurosci. 20, 1519–1528

Fuortes MG, Frank K, Becker MC. (1957) Steps in the production of motoneuron spikes. J Gen Physiol. 40:735-52.

Furshpan, E. j., Potter, D. D. (1957). Mechanism of nerve impulse transmission at a crayfish synapse. *Nature 180:342-343.*

Furukawa, T., Furshpan, E. j. (1964). Two inhibitory mechanisms in the Mauthner neurons of goldfish.]. *Neurophysiol. 26:140-176.*

Galarreta M, Hestrin S. (2001) Spike transmission and synchrony detection in networks of GABAergic interneurons. Science. 292(5525):2295-9

Gerke MB, Plenderleith MB. (2004) Ultrastructural analysis of the central terminals of primary sensory neurones labelled by transganglionic transport of bandeiraea simplicifolia I-isolectin B4. Neuroscience.127:165-75.

Gibson, J. R., Beierlein, M. & Connors, B. W. (1999). Two networks of electrically coupled inhibitory neurons in neocortex. Nature 402, 75–79

Gopfert, H., Schaefer, H. (1938). Uber den direkt und inderekt errgten Aktionsstrom und die Funktion der motorischen Endplatte. Pflugers Arch. Ges. Physiol. 239:597-619.

Gogan P, Gueritaud JP, Horcholle-Bossavit G & Tyc-Dumont S (1977). Direct excitatory interactions between spinal motoneurones of the cat. J Physiol 272: 755-67.

Gosgnach S, Quevedo J, Fedirchuk B & McCrea DA (2000). Depression of group Ia monosynaptic EPSPs in cat hindlimb motoneurones during fictive locomotion. J Physiol 526: 639-52.

Graham B, Redman S. A (1994) simulation of action potentials in synaptic boutons during presynaptic inhibition. J Neurophysiol. 71:538-49.

Grant G, Ygge J. (1981) Somatotopic organization of the thoracic spinal nerve in the dorsal horn demonstrated with transganglionic degeneration. J Comp Neurol.,202:357-64.

Gray, E. G. (1962). A morphological basis for presynaptic inhibition? Nature 193: 82-83.

Hantman AW & Jessell TM (2010). Clarke's column neurons as the focus of a corticospinal corollary circuit. Nat Neurosci 13:1233-1237

Harrison PJ, Jankowska E. (1985) Organization of input to the interneurones mediating group I non-reciprocal inhibition of motoneurones in the cat. J Physiol. 361:403-18.

Harrison PJ, Jankowska E, Zytnicki D. (1986) Lamina VIII interneurones interposed in crossed reflex pathways in the cat. J Physiol. 371:147-66.

Hayward L, Wesselmann U, Rymer WZ. (1991) Effects of muscle fatigue on mechanically sensitive afferents of slow conduction velocity in the cat triceps surae. J Neurophysiol. 65:360-70.

Hestrin S, Galarreta M. (2005) Synchronous versus asynchronous transmitter release: a tale of two types of inhibitory neurons. Nat Neurosci. 8:1283-4.

Herzog E, Bellenchi GC, Gras C, Bernard V, Ravassard P, Bedet C, Gasnier B, Giros B, El Mestikawy S. (2001) The existence of a second vesicular glutamate transporter specifies subpopulations of glutamatergic neurons. J Neurosci. 21:RC181.

.

Hisano S, Hoshi K, Ikeda Y, Maruyama D, Kanemoto M, Ichijo H, Kojima I, Takeda J, Nogami H. (2000) Regional expression of a gene encoding a neuron-specific Na(+)-dependent inorganic phosphate cotransporter (DNPI) in the rat forebrain. Brain Res Mol Brain Res. 83:34-43.

Hochman S, Shreckengost J, Kimura H, Quevedo J. (2010) Presynaptic inhibition of primary afferents by depolarization: observations supporting non-traditional mechanisms. Ann N Y Acad Sci. 1198:140-52.

Hongo T, Jankowska E, Lundberg A. (1969) The rubrospinal tract. I. Effects onalpha-motoneurones innervating hindlimb muscles in cats. Exp Brain Res.7:344-64.

Hongo T, Ishizuka N, Mannen H, Sasaki S. (1978)Axonal trajectory of single group Ia and Ib fibers in the cat spinal cord. Neurosci Lett. 8:321-8

Hoffman P (1918) Uber die Beriehungen der Sehnenreflexe zur willkurlichen Bewegun und zum Tonus. Zeitschrift fur Biologie,68:351-70.

Hughes DI, Mackie M, Nagy GG, Riddell JS, Maxwell DJ, Szabo G, Erdelyi F, Veress G, Szucs P, Antal M, Todd AJ (2005) P boutons in lamina IX of the rodent spinal cord express high levels of glutamic acid decarboxylase-65 and originate from cells in deep medial dorsal horn. Proc Natl Acad Sci U S A 102:9038-9043

Hulliger M. (1984) The mammalian muscle spindle and its central control. Rev Physiol Biochem Pharmacol.101:1-110.

Hunt CC, Kuffler SW. (1954) Motor innervation of skeletal muscle: multiple innervation of individual muscle fibres and motor unit function. J Physiol. 126:293-303.

Hunt CC. (1990) Mammalian muscle spindle: peripheral mechanisms. Physiol Rev. 70:643-63.

Iles JF. (1976) Central terminations of muscle afferents on motoneurones in the cat spinal cord. J Physiol. 262:91-117.

Ishizuka N, Mannen H, Hongo T, Sasaki S. (1979)Trajectory of group Ia afferent fibers stained with horseradish peroxidase in the lumbosacral spinal cord of the cat: three dimensional reconstructions from serial sections. J Comp Neurol. 186:189-211.

Jack JJ, Roberts RC. (1978) The role of muscle spindle afferents in stretch and vibration reflexes of the soleus muscle of the decerebrate cat. Brain Res. 146:366-72.

Jack JJ, Redman SJ, Wong K. (1981) Modifications to synaptic transmission at group Ia synapses on cat spinal motoneurones by 4-aminopyridine. J Physiol. 321:111-26.

Jack JJ, Redman SJ, Wong K. (1981) The components of synaptic potentials evoked in cat spinal motoneurones by impulses in single group Ia afferents. J Physiol. 321:65-96.

Jackson MB. (1993) Passive current flow and morphology in the terminal arborizations

of the posterior pituitary. J Neurophysiol. 69:692-702.

Jancsó G, Király E. (1980) Distribution of chemosensitive primary sensory afferents in the central nervous system of the rat. J Comp Neurol. 190:781-92.

Jankowska E, Lindström S. (1972) Morphology of interneurones mediating Ia reciprocal inhibition of motoneurones in the spinal cord of the cat. J Physiol. 226:805-23.

Jankowska E, Roberts WJ. (1972) Synaptic actions of single interneurones mediating reciprocal Ia inhibition of motoneurones. J Physiol. 222:623-42.

Jankowska E, Fu TC, (1975) Lundberg A. Reciprocal La inhibition during the late reflexes evoked from the flexor reflex afferents after DOPA. Brain Res. 85:99-102.

Jankowska E, Lundberg A, Rudomin P, Sykova E. (1977) Effects of 4-aminopyridine on transmission in excitatory and inhibitory synapses in the spinal cord. Brain Res. 136:387-92.

Jankowska E, McCrea D, Rudomín P, Sykova E. (1981) Observations on neuronal pathways subserving primary afferent depolarization. J Neurophysiol. 46:506-16.

Jankowska E, Johannisson T, Lipski J. (1981) Common interneurones in reflex pathways from group 1a and 1b afferents of ankle extensors in the cat. J Physiol. 310:381-402.

Jankowska E, McCrea D, Mackel R. (1981) Pattern of 'non-reciprocal' inhibition of motoneurones by impulses in group Ia muscle spindle afferents in the cat. J Physiol. 316:393-409.

Jankowska E. (1992) Interneuronal relay in spinal pathways from proprioceptors. Prog Neurobiol.38:335-78. Review

Jankowska E, Bichler E, Hammar I. (2000) Areas of operation of interneurons mediating presynaptic inhibition in sacral spinal segments. Exp Brain Res. 133:402-6.

Jankowska E, Edgley SA, Krutki P, Hammar I. (2005) Functional differentiation and organization of feline midlumbar commissural interneurones. J Physiol. 565(Pt 2):645-58.

Jankowska E, Puczynska A. (2008) Interneuronal activity in reflex pathways from group II muscle afferents is monitored by dorsal spinocerebellar tract neurons in the cat. J Neurosci. 28:3615-22.

Jankowska E, Edgley SA. (2010) Functional subdivision of feline spinal interneurons in reflex pathways from group Ib and II muscle afferents; an update. Eur J Neurosci. 32:881-93. Review.

Jefferys, J. G., Traub, R. D. & Whittington, M. A. (1996) Neuronal networks for induced ‘40 Hz’ rhythms. Trends Neurosci. 19,202–208

Jones SR, Pinto DJ, Kaper TJ, Kopell N. (2000) Alpha-frequency rhythms desynchronize over long cortical distances: a modeling study. J Comput Neurosci. 9:271-91

Kanaka C, Ohno K, Okabe A, Kuriyama K, Itoh T, Fukuda A, Sato K. (2001) The differential expression patterns of messenger RNAs encoding K-Cl cotransporters (KCC1,2) and Na-K-2Cl cotransporter (NKCC1) in the rat nervous system. Neuroscience. 104:933-46.

Kaneko T, Fujiyama F. (2002) Complementary distribution of vesicular glutamate transporters in the central nervous system. Neurosci Res. 42:243-50. Review.

Kaufman MP, Longhurst JC, Rybicki KJ, Wallach JH, Mitchell JH. (1983) Effects of static muscular contraction on impulse activity of groups III and IV afferents in cats. J Appl Physiol. 55:105-12

Kellerth JO, Szumski AJ. (1966) Effects of picrotoxin on stretch-activatedpost-synaptic inhibitions in spinal motoneurones. Acta Physiol Scand. 66:146-56.

Kenagy J, VanCleave J, Pazdernik L, Orr JA. (1997) Stimulation of group III and IV afferent nerves from the hindlimb by thromboxane A_2. Brain Res. 744:175-8.

Korn H, Sotelo C, Crepel F. (1973) Electronic coupling between neurons in the rat lateral vestibular nucleus. Exp Brain Res.16:255-75.

Kremer E, Lev-Tov A. (1998) GABA-receptor-independent dorsal root afferents depolarization in the neonatal rat spinal cord. J Neurophysiol. 79:2581-92.

Kumazawa T, Mizumura K. (1977) Thin-fibre receptors responding to mechanical, chemical, and thermal stimulation in the skeletal muscle of the dog. J Physiol. 273:179-94.

Ladisman, C. E., Beierlein, M., Connors, B. W. (2000). Electrical synapses between thalamic reticular neurons. Soc. Neurosci. Abstr. 26, 819

Laporte Y, Lloyd DP. (1952) Nature and significance of the reflex connections established by large afferent fibers of muscular origin. Am J Physiol. 169:609-21.

Levavi-Sivan, B., Bloch, C., Gutnick, M., Fleidervish, I., (2005). Electrotonic coupling in the anterior pituitary of a teleost fish. Endocrinology. 2005 146:1048-52.

Lidierth M, Wall PD. (1996) Synchronous inherent oscillations of potentials within the rat lumbar spinal cord. Neurosci Lett. 220:25-8.

Llinas, R., Blinks,j. R., Nicholson, C. (1972). Calcium transient in presynaptic terminal of squid giant synapse: detection with aequorin. *Science* 176: 11271129

Lloyd, D. P. C. (1941). The spinal mechanism of the pyramidal system in cats. J. Neurophysiol. 4, 525-546.

Logan SD, Pickering AE, Gibson IC, Nolan MF, Spanswick D. (1996) Electrotonic coupling between rat sympathetic preganglionic neurones in vitro. J Physiol. 495 (Pt 2):491-502.

Lundberg A, Malmgren K, Schomburg ED. (1987) Reflex pathways from group II muscle afferents. 1. Distribution and linkage of reflex actions to alpha-motoneurones. Exp Brain Res.65:271-81.

MacVicar BA, Dudek FE. (1981) Electrotonic coupling between pyramidal cells: a direct demonstration in rat hippocampal slices. Science.213:782-5.

Mackie M, Hughes DI, Maxwell DJ, Tillakaratne NJ, Todd AJ. (2003) Distribution and colocalisation of glutamate decarboxylase isoforms in the rat spinal cord. Neuroscience.119:461-72.

Malcangio M, Bowery NG. (1996) GABA and its receptors in the spinal cord. Trends Pharmacol Sci. 17:457-62. Review.

Mann-Metzer P, Yarom Y. (1999) Electrotonic coupling interacts with intrinsic properties to generate synchronized activity in cerebellar networks of inhibitory interneurons. J Neurosci. 19:3298-306.

Martina M, Vida I, Jonas P. (2000) Distal initiation and active propagation of action potentials in interneuron dendrites. Science. 287(5451):295-300.

Maslany S, Crockett DP, Egger MD. (1992) Organization of cutaneous primary afferent fibers projecting to the dorsal horn in the rat: WGA-HRP versus B-HRP. Brain Res. 569:123-35.

Matthews PB. (1963) The response of de-efferented muscle spindle receptors to stretching at different velocities. J Physiol. 168:660-78.

Matthews MA, Willis WD, Williams V. (1971) Dendrite bundles in lamina IX of cat spinal cord: a possible source for electrical interaction between motoneurons? Anat Rec. 171:313-27.

Maxwell DJ, Noble R. (1987) Relationships between hair-follicle afferent terminations and glutamic acid decarboxylase-containing boutons in the cat's spinal cord. Brain Res. 408:308-12.

Maxwell DJ, Christie WM, Short AD, Brown AG (1990) Direct observations of synapses between GABA-immunoreactive boutons and muscle afferent terminals in lamina VI of the cat's spinal cord. Brain Res 530:215-222.

McCrea DA. (1986) Spinal cord circuitry and motor reflexes. Exerc Sport Sci Rev.;14:105-41. Review.

McCrea DA, Shefchyk SJ, Carlen P.C. (1990) Large reductions in composite EPSP amplitude following conditioning stimulation are not accounted for by increased conductances in motoneurons. Neurosci. Let. 109:117-122

Ménard A, Leblond H, Gossard JP. (2003) Modulation of monosynaptic transmission by presynaptic inhibition during fictive locomotion in the cat. Brain Res. 964:67-82.

Mendell LM, Henneman E. (1971) Terminals of single Ia fibers: location, density, and distribution within a pool of 300 homonymous motoneurons. J Neurophysiol. 34:171-87.

Mense S, Stahnke M. (1983) Responses in muscle afferent fibres of slow conduction velocity to contractions and ischaemia in the cat. J Physiol. 342:383-97.

Michelson, H. B. & Wong, R. K. Synchronization of inhibitory neurones in the guinea-pig hippocampus in vitro. J. Physiol.477, 35–45 (1994).

Mizumura K, Sugiura Y, Kumazawa T. (1993) Spinal termination patterns of canine identified A-delta and C spermatic polymodal receptors traced by intracellular labeling with Phaseolus vulgaris-leucoagglutinin. J Comp Neurol. 335:460-8

Morales-Aza BM, Chillingworth NL, Payne JA, Donaldson LF. (2004) Inflammation alteration chloride cotransporter expression in sensory neurons. Neurobiol Dis. 17:62-9.

Munson JB, Sypert GW. (1979) Properties of single central Ia afferent fibres projecting to motoneurones. J Physiol. 296:315-27.

Munson JB, Sypert GW, Zengel JE, Lofton SA, Fleshman JW. (1982) Monosynaptic projections of individual spindle group II afferents to type-identified medial gastrocnemius motoneurons in the cat. J Neurophysiol. 48:1164-74.

Nagy JI, Hunt SP. (1983) The termination of primary afferents within the rat dorsal horn: evidence for rearrangement following capsaicin treatment. J Comp Neurol.

218:145-58.

Nelson SG, Mendell LM. (1978) Projection of single knee flexor Ia fibers to homonymous and heteronymous motoneurons. J Neurophysiol.41:778-87.

Nicoll RA, Alger BE. (1979) Presynaptic inhibition: transmitter and ionic mechanisms. Int Rev Neurobiol.;21:217-58. Review.

Nolan, M.F., Logan, S.D., Spanswick, D. (1999) Electrophysiological properties of electrical synapses between rat sympathetic preganglionic neurones in vitro. J. Physiol. 519, 753–764

Paintal AS. (1960) Functional analysis of group III afferent fibres of mammalian muscles. J Physiol. 152:250-70.

Pappas, G. D., Waxman, S. G. (972). Synaptic fine structure-morphological correlates of chemical and electrotonic transmission. In *Structure and Function ofSynapses,* Pappas, G. D., Purpura, D. P., eds. New York: Raven Press. pp.1-43.

Payne AN. (1996) Inflammatory mechanisms in the CNS: targets for therapeutic intervention. Inflamm Res.45:575-8.

Pereda A, O'Brien J, Nagy JI, Bukauskas F, Davidson KG, Kamasawa N, Yasumura T, Rash JE. (2003) Connexin35 mediates electrical transmission at mixed synapses on Mauthner cells. J Neurosci. 23:7489-503.

Perreault MC, Enriquez-Denton M, Hultborn H. (1999) Proprioceptive control of extensor activity during fictive scratching and weight support compared to fictive locomotion. J Neurosci. 19:10966-76.

Pierce JP, Mendell LM. (1993) Quantitative ultrastructure of Ia boutons in the ventral horn: scaling and positional relationships. J Neurosci. 13:4748-63.

Plotkin MD, Snyder EY, Hebert SC, Delpire E. (1997) Expression of the Na-K-2Cl cotransporter is developmentally regulated in postnatal rat brains: a possible mechanism underlying GABA's excitatory role in immature brain. J Neurobiol. 33:781-95.

Popratiloff A, Valtschanoff JG, Rustioni A, Weinberg RJ. (1996) Colocalization of GABA and glycine in the rat dorsal column nuclei. Brain Res. 706:308-12.

Popratiloff A, Weinberg RJ, Rustioni A. (1998) AMPA receptors at primary afferent synapses in substantia gelatinosa after sciatic nerve section. Eur J Neurosci. 10:3220-30.

Puskár Z, Polgár E, Todd AJ. (2001) A population of large lamina I projection neurons with selective inhibitory input in rat spinal cord. Neuroscience.102:167-76.

Rack PM, Westbury DR. (1966) The effects of suxamethonium and acetylcholine on the behaviour of cat muscle spindles during dynamics stretching, and during fusimotor stimulation. J Physiol. 186:698-713.

Ralston HJ (1979) The fine structure of laminae I, II and III of the macaque spinal cord. J Comp Neurol. 184:619-42.

Ramón y Cajal, S.R. (1907) Regeneración de los Nervios. [Translation and edited by J. Bresler (1908) Studien über Nervenregeneration, JohannAmbrosius Barth]

Rash JE, Dillman RK, Bilhartz BL, Duffy HS, Whalen LR, Yasumura T. (1996) Mixed synapses discovered and mapped throughout mammalian spinal cord. Proc Natl Acad Sci U S A. 93:4235-9.

Redman S, Walmsley B. (1983) Amplitude fluctuations in synaptic potentials evoked in cat spinal motoneurones at identified group Ia synapses. J Physiol. 343:135-45.

Renshaw B. (1940) Activity in the simplest spinal reflex pathways.J Neurophysiol, 3:373-387.

Riddell JS, Jankowska E, Eide E. (1993) Depolarization of group II muscle afferents by stimuli applied in the locus coeruleus and raphe nuclei of the cat. J Physiol. 461:723-41.

Riddell JS, Jankowska E, Huber J. (1995) Organization of neuronal systems mediating presynaptic inhibition of group II muscle afferents in the cat. J Physiol. 483:443-60

Rivera C, Voipio J, Payne JA, Ruusuvuori E, Lahtinen H, Lamsa K, Pirvola U, Saarma M, Kaila K. (1999) The K+/Cl- co-transporter KCC2 renders GABA hyperpolarizing during neuronal maturation. Nature. 397:251-5.

Rossignol S, Dubuc R, Gossard JP (2006) Dynamic sensorimotor interactions in locomotion. Physiol Rev 86:89-154.

Rudomin P, Dutton H, Munoz-Martinez J. (1969) Changes in correlation between monosynaptic reflexes produced by conditioning afferent volleys. J Neurophysiol. 32:759-72.

Rudomin P, Solodkin M, Jimenez I (1987) Synaptic potentials of primary afferent fibers and motoneurons evoked by single intermediate nucleus interneurons in the cat spinal cord. J. Neurophysiol. 57:1288-1313.

Rudomin P, Jimenez I, Quevedo J, Solodkin M (1990) Pharmacologic analysis of inhibition produced by last-order intermediate nucleus interneurons mediating nonreciprocal inhibition of motoneurons in cat spinal cord. J Neurophysiol 63:147-160.

Rudomin P, Schmidt RF (1999) Presynaptic inhibition in the vertebrate spinal cord revisited. Exp. Brain Res. 129:1-37.

Rudomin P. (2009) In search of lost presynaptic inhibition. Exp Brain Res. 196:139-51. Review.

Sakata-Haga H, Kanemoto M, Maruyama D, Hoshi K, Mogi K, Narita M, Okado N, Ikeda Y, Nogami H, Fukui Y, Kojima I, Takeda J, Hisano S. (2001) Differential localization and colocalization of two neuron-types of sodium-dependent inorganic phosphate cotransporters in rat forebrain. Brain Res. 902:143-55.

Scheibel ME, Scheibel AB. (1969) Terminal patterns in cat spinal cord. 3. Primary afferent collaterals. Brain Res. 13:417-43.

Schomburg ED, Steffens H. (1998) Comparative analysis of L-DOPA actions on nociceptive and non-nociceptive spinal reflex pathways in the cat. Neurosci Res. 31:307-16.

Schouenborg J. (1984) Functional and topographical properties of field potentials evoked in rat dorsal horn by cutaneous C-fibre stimulation. *J Physiol.* 356,169-92

Serve G, Endres W, Grafe P. (1988) Continuous electrophysiological measurements of changes in cell volume of motoneurons in the isolated frog spinal cord. Pflugers Arch. 411:410-5.

Shakya Shrestha S, Bannatyne BA, Jankowska E, Hammar I, Nilsson E, Maxwell DJ. (2012)Inhibitory inputs to four types of spinocerebellar tract neurons in the cat spinal cord. Neuroscience. 226:253-69.

Shreckengost J, Calvo J, Quevedo J & Hochman S (2010). Bicuculline-sensitive primary afferent depolarization remains after greatly restricting synaptic transmission in the mammalian spinal cord. J Neurosci 30, 5283-8.

Shupliakov O, Atwood HL, Ottersen OP, Storm-Mathisen J, Brodin L. (1995) Presynaptic glutamate levels in tonic and phasic motor axons correlate with properties of synaptic release. J Neurosci. 15:7168-80.

Singer, W. & Gray, C. M. (1995) Visual feature integration and the temporal correlation hypothesis. Annu. Rev. Neurosci. 18, 555–586

Sinoway LI, Hill JM, Pickar JG, Kaufman MP. (1993) Effects of contraction and lactic acid on the discharge of group III muscle afferents in cats. J Neurophysiol. 69:1053-9

Smith CL. (1983) The development and postnatal organization of primary afferent projections to the rat thoracic spinal cord. J Comp Neurol. 220:29-43.

Stil A, Liabeuf S, Jean-Xavier C, Brocard C, Viemari JC, Vinay L. (2009) Developmental up-regulation of the potassium-chloride cotransporter type 2 in the rat lumbar spinal cord. Neuroscience. 164:809-21.

Simon O, Yelnik AP. (2010) Managing spasticity with drugs. Eur J Phys Rehabil Med. 46:401-10.

Snow PJ, Rose PK, Brown AG. (1976) Tracing axons and axon collaterals of spinal neurons using intracellular injection of horseradish peroxidase. Science. 191:312-3

Soghomonian JJ, Martin DL. (1998) Two isoforms of glutamate decarboxylase: why? Trends Pharmacol Sci. 19:500-5. Review.

Sotelo C, Llinás R. (1972) Specialized membrane junctions between neurons in the vertebrate cerebellar cortex. J Cell Biol. 53:271-89.

Steffens H, Schomburg ED. (2011) Spinal motor actions of the μ-opioid receptor agonist DAMGO in the cat. Neurosci Res. 2011.70:44-54.

Stein V, Hermans-Borgmeyer I, Jentsch TJ, Hübner CA. (2004) Expression of the KCl cotransporter KCC2 parallels neuronal maturation and the emergence of low intracellular chloride. J Comp Neurol. 468:57-64.

Sugiura Y, Terui N, Hosoya Y. (1989) Difference in distribution of central terminals between visceral and somatic unmyelinated (C) primary afferent fibers. J Neurophysiol. 62:834-40

Sugiura Y, Terui N, Hosoya Y, Tonosaki Y, Nishiyama K, Honda T. (1993) Quantitative analysis of central terminal projections of visceral and somatic unmyelinated (C) primary afferent fibers in the guinea pig. J Comp Neurol. 332:315-25.

Sun D, Murali SG. (1999) Na+-K+-2Cl- co-transporter in immature cortical neurons: A role in intracellular Cl- regulation. J Neurophysiol. 81:1939-48.

Sunnerhagen KS, Olver J, Francisco GE. (2013) Assessing and treating functional impairment in poststroke spasticity. Neurology.80:S35-44.

Suzue T, Jessell T. (1980) Opiate analgesics and endorphins inhibit rat dorsal root potential in vitro. Neurosci Lett. 16:161-6.

Szabadics, J., Lorincz, A., Tamas, G., (2001) Beta and gamma frequency synchroniza- tion by dendritic gabaergic synapses and gap junctions in a network of cortical interneurons. J. Neurosci. 21: 5824–5831.

Szentagothai J. (1964) Neuronal and synaptic arrangement in the substantia gelatinosa rolandi. J Comp Neurol.122:219-39.

Szucs P, Luz LL, Pinho R, Aguiar P, Antal Z, Tiong SY, Todd AJ, Safronov BV. (2013) Axon diversity of lamina I local-circuit neurons in the lumbar spinal cord. J Comp Neurol.

Takamori S, Rhee JS, Rosenmund C, Jahn R. (2000) Identification of a vesicular glutamate transporter that defines a glutamatergic phenotype in neurons. Nature. 407:189-94.

Takamori S, Rhee JS, Rosenmund C, Jahn R. (2001) Identification of differentiation-associated brain-specific phosphate transporter as a second vesicular glutamate transporter (VGLUT2). J Neurosci.21:RC182.

Tamás G, Buhl EH, Lörincz A, Somogyi P. (2000) Proximally targeted GABAergic synapses and gap junctions synchronize cortical interneurons. Nat Neurosci. 3:366-71.

Thimm F, Baum K. (1987) Response of chemosensitive nerve fibers of group III and IV to metabolic changes in rat muscles. Pflugers Arch. 410:143-52

Thompson SW & Wall PD (1996). The effect of GABA and 5-HT receptor antagonists on rat dorsal root potentials. *Neurosci Lett* **217**, 153-156.

Thompson SW, Bennett DL, Kerr BJ, Bradbury EJ, McMahon SB. (1999) Brain-derived neurotrophic factor is an endogenous modulator of nociceptive responses in the spinal cord. Proc Natl Acad Sci U S A. 96:7714-8. Review.

Todd AJ, Lochhead V. (1990) GABA-like immunoreactivity in type I glomeruli of rat substantia gelatinosa. Brain Res. 514:171-4.

Todd AJ, Sullivan AC. (1990) Light microscope study of the coexistence of GABA-like and glycine-like immunoreactivities in the spinal cord of the rat. J Comp Neurol. 296:496-505.

Todd AJ, Spike RC. (1993) The localization of classical transmitters and neuropeptides within neurons in laminae I-III of the mammalian spinal dorsal horn. Prog Neurobiol. 41:609-45. Review.

Todd AJ, Spike RC, Brodbelt AR, Price RF, Shehab SA. (1994) Some inhibitory neurons in the spinal cord develop c-fos-immunoreactivity after noxious stimulation. Neuroscience. 63:805-16.

Toyoda H, Yamada J, Ueno S, Okabe A, Kato H, Sato K, Hashimoto K, Fukuda A.(2005) Differential functional expression of cation-Cl- cotransporter mRNAs (KCC1, KCC2, and NKCC1) in rat trigeminal nervous system. Brain Res Mol Brain Res. 133:12-8.

Tresch MC, Kiehn O. (2000) Motor coordination without action potentials in the mammalian spinal cord. Nat Neurosci. 3:593-9.

Varoqui H, Erickson JD. (1997) Vesicular neurotransmitter transporters. Potential sites for the regulation of synaptic function. Mol Neurobiol. 15:165-91. Review.

Varoqui H, Zhu H, Yao D, Ming H, Erickson JD. (2000) Cloning and functional identification of a neuronal glutamine transporter. J Biol Chem. 275:4049-54

Valtschanoff JG, Phend KD, Bernardi PS, Weinberg RJ, Rustioni A. (1994) Amino acid immunocytochemistry of primary afferent terminals in the rat dorsal horn. J Comp Neurol. 346:237-52.

Venance L, Rozov A, Blatow M, Burnashev N, Feldmeyer D, Monyer H. (2000) Connexin expression in electrically coupled postnatal rat brain neurons. Proc Natl Acad Sci U S A. 97:10260-5.

Venance L, Glowinski J, Giaume C. (2004) Electrical and chemical transmission between striatal GABAergic output neurones in rat brain slices. J Physiol. 559:215-30.

Vera PL, Nadelhaft I. (1990) Conduction velocity distribution of afferent fibers innervating the rat urinary bladder. Brain Res. 520:83-9.

Verdier D, Lund JP, Kolta A. (2004) Synaptic inputs to trigeminal primary afferent neurons cause firing and modulate intrinsic oscillatory activity. J Neurophysiol.92:2444-55.

Vervaeke K, Lorincz A, Gleeson P, Farinella M, Nusser Z, Silver RA. (2010) Rapid desynchronization of an electrically coupled interneuron network with sparse excitatory synaptic input. Neuron; 67:435-51.

Wall PD, Bennett DL. (1994) Postsynaptic effects of long-range afferents in distant segments caudal to their entry point in rat spinal cord under the influence of picrotoxin or strychnine. J Neurophysiol. 72:2703-13.

Walmsley B. (1991) Central synaptic transmission: studies at the connection between primary afferent fibres and dorsal spinocerebellar tract (DSCT) neurones in Clarke's column of the spinal cord. Prog Neurobiol.36:391-423.

Watt DG, Stauffer EK, Taylor A, Reinking RM, Stuart DG. (1976) Analysis of muscle receptor connections by spike-triggered averaging. 1. Spindle primary and tendon organ afferents. J Neurophysiol.;39:1375-92.

Willis WD Jr. (1999) Dorsal root potentials and dorsal root reflexes: a double-edged sword. Exp Brain Res. 124:395-421. Review.

Willis WD. (2001) Role of neurotransmitters in sensitization of pain responses. Ann N Y Acad Sci.;933:142-56. Review.

Willis WD. (2006) John Eccles' studies of spinal cord presynaptic inhibition. Prog Neurobiol. 78:189-214.

Whittington, M. A., Traub, R. D. & Jefferys, J. G. (1995) Synchronized oscillations in interneuron networks driven by metabotropic glutamate receptor activation. Nature 373,

612–615

Woolf CJ, King AE. (1987) Physiology and morphology of multireceptive neurons with C-afferent fiber inputs in the deep dorsal horn of the rat lumbar spinal cord. J Neurophysiol. 58:460-79

Yates CC, Charlesworth A, Reese NB, Ishida K, Skinner RD, Garcia-Rill E. (2009) Modafinil normalized hyperreflexia after spinal transection in adult rats. Spinal Cord. 47:481-5.

Yates C, Garrison K, Reese NB, Charlesworth A, Garcia-Rill E. Chapter

11--novel mechanism for hyperreflexia and spasticity. (2011) Prog Brain Res. 188:167-80.

Ygge J, Grant G. (1983) The organization of the thoracic spinal nerve projection in the rat dorsal horn demonstrated with transganglionic transport of horseradish peroxidase. J Comp Neurol.216:1-9.

Zhang SJ, Jackson MB. (1995) GABAA receptor activation and the excitability of nerve terminals in the rat posterior pituitary. J Physiol.483:583-95.

Zhang Y, Narayan S, Geiman E, Lanuza GM, Velasquez T, Shanks B, Akay T, Dyck J, Pearson K, Gosgnach S, Fan CM, Goulding M. (2008) V3 spinal neurons establish a robust and balanced locomotor rhythm during walking. Neuron.;60:84-96.

Zhang L, Warren RA. (2008) Postnatal development of excitatory postsynaptic currents in nucleus accumbens medium spiny neurons. Neuroscience. 154:1440-9.

Ziegler DR, Cullinan WE, Herman JP. (2002) Distribution of vesicular glutamate transporter mRNA in rat hypothalamus. J Comp Neurol.;448:217-29.